The role of iron in rheumatoid arthritis

Averill, Andrew

Award date:
2008

Awarding institution:
University of Bath

The role of Iron in Rheumatoid Arthritis

Abdullah Al-Qenaei

A thesis submitted for the degree of Doctor of Philosophy
University of Bath
Department of Pharmacy and Pharmacology
August 2008

To my family …

TABLE OF CONTENTS

ACKNOWLEDGEMENTS

I am extremely grateful to Dr. Charareh Pourzand for giving me the opportunity to work under her supervision. I would like to thank her for the endless support, encouragement, and guidance. I am also very grateful to Dr. Nicolas Hall for his supervision, constant advice, and fruitful support – It was a pleasure working with them both.

I am very thankful and appreciative to Professor Rex Tyrrell for his highly valued advice and criticism. I would also like to thank Dr. Olivier Reelfs for sharing his knowledge and experience. I am particularly grateful to Dr. Anthie Yiakouvaki for her advice and training input. Many thanks to all members of laboratories 5W 2.20 and 5W 2.14, both past and present, for their support and friendly chats.

I am very grateful to Professor Sonia Levi and all her laboratory members especially Dr. Paolo Santambrogio for their continuous help, hospitality, and kindness during my visit to Milan. I would like to thank Professor Susan Wannacott and Dr. Jane Dickinson from the Department of Biology and Biochemistry (University of Bath) for their practical help. I would also like to thank Dr. Adrian Rogers from the Bioimaging suite for his help and advice.

I would like to thank my grandfather for his enthusiasm and his financial support of this project. I am also very grateful to my parents for their constant encouragements and support. And I am grateful for my dear wife for her love, patience and support. And I must not forget my two lovely daughters for their inspiration with their interesting talk and babbles during work at home. Last but not least, I would like to thank all my respected friends and all members of my family for their enthusiasm and encouragements.

I wouldn’t have made it without you all !

PUBLICATIONS

1. Yiakouvaki A, Savovic J, **Al-Qenaei A**, Dowden J, Pourzand. Caged-iron chelators a novel approach towards protecting skin cells against UVA-induced necrotic cell death. *Journal of Investigative Dermatology.* 2006 Oct;126(10):2287-95.

2. Collins CA, Fry FH, Holme AL, Yiakouvaki A, **Al-Qenaei A**, Pourzand C, Jacob C. Towards multifunctional antioxidants: synthesis, electrochemistry, in vitro and cell culture evaluation of compounds with ligand/catalytic properties. *Organic & biomolecular chemistry*. 2005 Apr 21;3(8):1541-6.

3. **Al-Qenaei, A.,** Yiakouvaki, A., Hall, N. D., Pourzand, C. The role of lysosomal labile iron pool in differential sensitivity of Jurkat T cell lines to hydrogen peroxide *American Journal of Hematology*. 82 (6): 565-565 JUN 2007.

ABSTRACT

Iron plays a potential role in oxidative stress-mediated injuries and pathologies e.g. rheumatoid arthritis (RA). Four decades ago it was suggested that iron may have a crucial role in the progression of inflammation in RA. Indeed, free radicals generated by iron can cause damage to lipids, proteins, carbohydrates, and DNA. It is this destructive process that is believed to occur in rheumatoid joints. However, none had differentiated between the role of iron in both acute and chronic phases of the disease and the origin of this 'labile' iron. Since RA cells are chronically exposed to oxidative stress, we have therefore chosen Jurkat cells to be our cell model. We used the parental (J16) cell line was used to mimic the acute phase of oxidative stress and the H_2O_2-resistant (HJ16) cells to mimic the chronic phase. By using hydrogen peroxide (H_2O_2) as the oxidising agent, we aim to study the role of iron in acute and chronic phase of oxidative stress and to know its origin. In the present study, we found that both antioxidants and H_2O_2-induced labile iron are modulated when cells are chronically exposed to H_2O_2. HJ16 cells contain higher total intracellular glutathione levels and glutathione peroxidase activity than J16 cells while the superoxide dismutase and catalase activity are similar. Haem oxygenase-1 (HO-1) was not detectable nor was it induced in these cell lines; HO-2 on the other hand was expressed but not induced. Although they had the same 'basal' LIP and L-Ft levels, J16 cells contain more than 7-fold higher H-Ft levels than in HJ16 cells. It was also found that H_2O_2-induced labile iron is directly correlated with necrotic cell death. These results are consistent with the conclusion that both antioxidant defence mechanism and labile iron status are modulated in cells chronically exposed to H_2O_2. We have also shown that the 'basal' and 'H_2O_2-induced' NFκB activation was higher in the HJ16 cells. We have also provided a link between labile iron release, lysosomal membrane damage and the ensuing necrotic cell death following H_2O_2 treatment.

ABBREVIATIONS

AA	Adjuvant Arthritis
ADP	Adenosine 5'-diphosphate
AI	Anaemia of inflammation
ARD	Ankyrin repeat domain
ATP	Adenosine 5'-triphosphate
BSO	Buthionine-[S,R]sulfoximine
CA	Calcein
CA-AM	Calcein-acetoxymethyl ester
CIA	Collagen induced arthritis
CM	Condition media
CO	Carbon Monoxide
DFO	Desferrioxamine
DMEM	Dulbecco's Modified Eagle's Medium
DMSO	Dimethyl Sulphoxide
DMT1	Divalent metal transporter 1
DNA	Deoxyribonucleic acid
DTT	Dithiothreitol
EDTA	Ethylenediaminetetraacetic acid
EGTA	Ethylene gycol-bis[β-aminoethylether]-N,N,N'N'tetraacetic acid
EMEM	Earle's modified minimum essential medium
EMSA	Electrophorectic mobility shift assay
FAD	Flavin adenine dinucleotide
Fe^{2+}	Ferrous iron
Fe^{3+}	Ferric iron
Ft	Ferritin
GPx	Glutathione peroxidase
GR	Glutathione disulphide reductase
GSH	Glutathione (reduced)
GSSG	Glutathione disulphide (oxidised)

GSH/GSSG	Total intracellular glutathione
H	Hour / Hours
H-Ft	H-chain of Ferritin
H_2O_2	Hydrogen peroxide
HCP-1	Haem carrier protein-1
HEPES	N-[2-hydroxyethyl]piperazine-N'-[2-ethanesulfonic acid]
HO-1	Haem oxygenase 1
HO-2	Haem oxygenase 2
IL-1β	Interleukin-1β
IRE	Iron-responsive element
IRP	Iron regulatory protein
RNS	Reactive nitrogen species
ROS	Reactive oxygen species
RT	Room temperature
$L^{\bullet}$	Fatty acid radical
LDL	Low density lipoprotein
L-Ft	L-chain of Ferritin
LIP	Labile iron pool
LI	Labile iron
$LOO^{\bullet}$	Fatty acid peroxyl radical
LOOH	Lipid hydroperoxide
LPI	Labile plasma iron
MnSOD	Manganese superoxide dismutase
Mt-Ft	Mitochondrial ferritin
NADP	Nicotinamide adenine dinucleotide phosphate
NADPH	Nicotinamide adenine dinucleotide phosphate (reduced)
NBTI	Non-transferrin bound iron
NF-κB	Nuclear Factor kappa B
NLS	Nuclear localization sequence
NO	Nitric oxide
NO_2	Nitrogen dioxide
NP-40	Nonidet P-40
NR	Neutral red

OA	Osteoarthritis
O_2	Oxygen
$^1O_2$	Singlet oxygen
$O_2^{\bullet-}$	Superoxide anion
$OH^{\bullet}$	Hydroxyl radical
PBS	Phosphate buffered saline
Pi	Inorganic Phosphate
PI	Propidium Iodide
PL	Picoliter
PMSF	Phenylmethanesulfonyl fluoride
PUFA	Polyunsaturated fatty acids
RA	Rheumatoid Arthritis
RHD	Rel-homology domain
ROS	Reactive oxygen species
RT	Room temperature
SDS	Sodium dodecyl sulphate
SF	Synovial fluid
SFM	Serum free media
SIH	Salicylaldehyde isonicotinoyl hydrazone
SOD	Superoxide dismutase
TCA	Trichloroacetic acid
Tf	Transferrin
TfR	Transferrin receptor
TNF	Tumor necrosis factor
TRx	Thioredoxin
UTR	Untranslated region
UV	Ultraviolet
V	Volts

CHAPTER ONE

INTRODUCTION

1.1 Inflammation

Inflammation has long been recognised both in clinical practice and in research laboratories (McCarty, 1989). The Roman physician Celsus (30 BC - 38 AD) described the classical signs of inflammation as 'redness' and 'swelling' with 'heat' and 'pain' *(rubor et tumor cum calore et dolore)*. A century later, Galen (130-200 AD) added 'loss of function' *(function laesa)* to be the fifth sign of inflammation (Bonta *et al*, 1985 and Junqueira *et al,* 1986). Many of the classical features of inflammation were described as early as 1600 BC in Egyptian papyrus writings (Goldsby *et al,* 2003).

1.1.1 General overview

Inflammation is a term used to illustrate the body's complex physiological response, whether acute or chronic, to tissue injury (Underwood, 1996). It is a vascular and cellular defence reaction against foreign bodies; mainly pathogenic bacteria or chemical substances (Junqueira *et al,* 1986). This response is not a single event but rather a sequence of events to that particular injury (Bonta *et al*, 1985).

Injuries can be classified into three types: (i) physical injury, (ii) chemical injury, and (iii) pathogenic organisms. Physical injuries are those injuries that are related to trauma, radiation, heat, or cold. Chemical injuries are due to acid, alkalis, phenols etc, and pathogenic organisms such as bacteria, viruses or fungi can also cause injury to the exposed tissue (Mulvihill *et al,* 2001). In 1940, it was postulated that the endogenous release of substances was responsible for the characteristic changes seen in inflammation (Menken, 1940). Many years later, in a study performed by Spector and Willoughby (1957), it was shown that the first substance to be released was histamine in acute inflammation. After this discovery, other mediators have been postulated to be responsible for the initiation of inflammation, e.g. 5-hydroxytryptamine, bradykinin, and prostaglandins (Di rosa *et al,* 1971).

Depending on the duration of inflammation, it may be subdivided into acute and chronic inflammation. The transition from the acute to the chronic phase may be the result of three different factors (Bonta *et al*, 1985 and Goldsby *et al,* 2003) : (a) the persistence of the initiating inflammatory irritant (e.g. poorly degradable substance i.e. microoganisms possessing cell wall components that enable them to resist phagocytosis), (b) the presence of an endogenous antigen (e.g. modified protein is important in the development of adjuvant arthritis), or (c) various endogenous factors which alter the cell type and their function (e.g. mitogenic factors).

1.1.2 Acute inflammation

Acute inflammation is evident when the response of the microcirculation to tissue injury is a brief vasoconstriction of the arteriolar vessels which is then followed by vasodilatation (Bonta *et al*, 1985). Due to the release of histamine from mast cells, during acute inflammation, increased blood flow and capillary permeability occur along with the accumulation of fluid, leukocytes, and inflammatory mediators such as cytokines (Feghali and Wright, 1997). This produces oedema and in turn causes pressure on the nerves resulting in pain and loss of function. The role of this acute response is to clear dead cells from the site of the injury, to protect the site against any pathogens, and to permit the immune system to gain access to the site of inflammation (Junqueira *et al,* 1986).

Neutrophils predominate during this initial or acute phase, since they were principally present in acute inflammatory lesions (Stevens and Lowe, 1995). Acute inflammation usually begins within two hours of the injury and lasts for a couple of days. IL-1, IL-6, and TNF-α are cytokines which play a crucial role in the development of local and systemic features of the acute response (Goldsby *et al,* 2003).

Reactions to the skin from a burn or an insect bite, acute epiglottitis, acute meningitis, and acute hepatitis are various examples of acute inflammation.

1.1.3 Chronic inflammation

It is crucial that inflammatory reactions are self-limited upon e.g. elimination of the triggering factors, if not, they do perpetuate to chronic inflammation (Schett, 2008). The transition between the acute phase and the chronic phase is largely dependent on the persistence of the inflammatory cause. When the cause persists,

chronic inflammation follows, which may last for a prolonged duration of time - weeks, months, or even indefinitely, and subsequently the cell population changes (Feghali and Wright, 1997). Chronic inflammation can occur in three different scenarios: (1) when phagocytes are unable to degrade the microoganisms, (2) in an autoimmune disease in which self-antigens continually activate T cells, or (3) in cancer where the inflammation contributes to tissue damage (Goldsby *et al,* 2003).

Lymphocytes and macrophages are the predominant cells in chronic inflammation (Junqueira *et al,* 1986; Underwood, 1996; and Stevens and Lowe, 1999). In the inflamed area, these cells engulf the remains of cells and fibres and participate in the production of antibodies against invading microoganisms (Junqueira *et al,* 1986). Lymphocytes are the key components in the onset and exacerbation of autoimmune diseases and the cytokines produced by them have a great impact on disease progression (Horwood, 2008). Large numbers of activated macrophages release hydrolytic enzymes and reactive oxygen and nitrogen species which are responsible for the tissue damage observed in chronic inflammation (Goldsby *et al,* 2003). Cytokines released by activated macrophages are known to stimulate fibroblast proliferation and collagen production. IFN-γ and TNF-α, are the two central cytokines which play a central role in the initiation of this chronic response; IFN-γ is produced primarily by T cells whereas TNF-α is mainly produced by macrophages.

Examples of chronic inflammation would be: implanted foreign body in a wound, tuberculosis, inflammatory bowel disease (Crohn's disease and ulcerative colitis), and rheumatoid arthritis.

1.1.3.1 Rheumatoid arthritis

Rheumatoid arthritis (RA) is a chronic inflammatory and a systemic autoimmune disease of unknown aetiology, affecting 1-1.5 % of the world's population and involves all racial and ethnic groups (McCarty, 1989 and Khurana and Berney, 2005). It is an illness with significant mortality and morbidity rates due to organ damage and failure. The ratio of female to male patients is approximately 2-4:1, the basis of this difference is unknown (Khurana and Berney, 2005). Symmetric inflammation of synovial joints leading to progressive erosion of both articular cartilage and periarticular bone is its main characteristic (Doan and Massarotti, 2005 and Lipsky, 2007). Symptoms such as weight loss, fatigue, and malaise also occur in rheumatoid arthritic patients in addition to the articular manifestations (Khurana and

Berney, 2005). Rheumatoid arthritis is therefore a disease which combines chronic inflammation and bone loss; growing evidence shows that inflammation *per se* is a major precipitator for skeletal destruction (Schett, 2006).

Although the aetiology of RA is not known, it is believed to be related to a complex of genetic, endogenous (e.g. hormonal, endocrine, or metabolic factors), and exogenous factors (e.g. geographic, infectious agents, or occupational factors) (McCarty, 1989 and Doan and Massarotti, 2005). All have been shown to be implicated in the progress of RA but none is shown to be its primarily cause.

Evidence coming from different experimental approaches (Panayi *et al,* 2001) strongly supports the hypothesis that RA is a disease initiated and driven by T cells irrespective of its cause. Macrophages, fibroblasts, and T lymphocytes are three cell populations which are found abundantly in the rheumatoid arthritic synovium (Tran *et al,* 2005); T-cells represent 40% of the synovial cellular infiltrate (Ling and Miossec, 2007). These cells are shown to play a substantial role in the development and the progression of RA (Cope, 2002). Stimulation of monocytes, macrophages, and synovial fibroblasts, by T-cells, leads to the secretion of a number of mediators including enzymes which are involved in the erosion and degradation of bone and cartilage. Along with this, these cells produce antibodies and proinflammatory cytokines (notably IL-1, IL-6 and TNF-α) that drive the chronic inflammation in RA (Doan and Massarotti, 2005 and Lipsky, 2007).

1.1.3.2 Osteoarthritis

Osteoarthritis (Weiland *et al,* 2005) is one of the most common musculo-skeletal diseases and as in RA, the aetiology is largely unknown. It is characterised by the gradual development of pain, stiffness, and limitation of motion and these symptoms are localized in the joints (McCarty, 1989). It is therefore a painful and disabling disease that affects millions of patients around the globe i.e. every 1.5 minutes, a joint is replaced due to osteoarthritis (OA) in Europe. It mostly affects people above the age of 65, and inflammation can occur in OA but is more like a wear process, where the cartilage in the joint can't tolerate the load which has been placed on it. In RA by comparison, this process is a complication that only occurs later. Figure 1.1 shows an illustration of the cross section of a normal, RA, and OA knee joint.

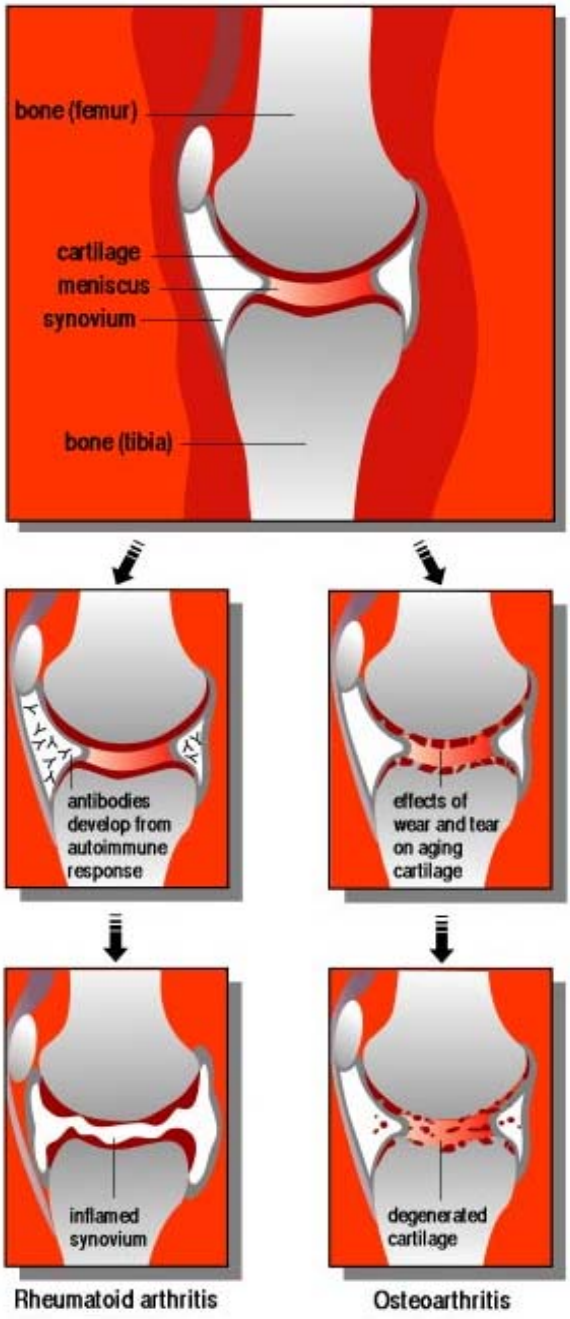

Figure 1.1 :
Cross section of a normal, RA, and OA knee joint.

The topmost illustration shows the cross section of a normal knee joint: a crescent-shaped disk held in place by ligaments (the meniscus) reduces friction during joint movement, while the membrane surrounding movable joints (the synovium) secretes a lubricating fluid.

Below that, the two illustrations on the left show the effect of rheumatoid arthritis, and the two illustrations on the right show the effects of osteoarthritis.

FDA Consumer Health Information; used with permission.

1.2 Iron

The chemical symbol for iron, Fe, comes from the Latin word for iron – *ferrum*. Iron, with an atomic number of 26, is the second most abundant metal in the Earth's crust (aluminium is the most abundant metal).

1.2.1 General aspects

Iron is an essential element for nearly all living organisms by participating in a wide variety of important metabolic processes, such as oxygen transport (binding and release of haemoglobin), DNA synthesis, electron transport, lipid metabolism, photosynthesis and gene regulation (Lieu *et al,* 2001 and Cairo *et al,* 2006). Therefore, iron is indispensable for the living species. Under aerobic conditions, ferrous iron (Fe^{2+}) is readily oxidised in solution to give ferric iron (Fe^{3+}) which is insoluble at neutral physiological pH. As a result of this, iron has limited bioavailability (Papanikolaou and Pantopoulus, 2005) since environmental iron is in the ferric state (Syed *et al,* 2006).

Iron, in mammals, is a component of an iron storage protein (e.g. myoglobin and ferritin) and iron transport protein (e.g. haemoglobin and transferrin) (reviewed in Ganz and Nemeth, 2006) and the majority is present in the haemoglobin in erythrocytes (reviewed in Dunn *et al,* 2007). In humans, iron represents around 50 mg/kg in an adult man and because of increased blood loss during menstruation and child birth, around 40 mg/kg of total body weight in an adult woman (Worwood, 2005). Figure 1.2 shows a diagrammatic representation of iron distribution in the body (75kg man). Iron in circulating haemoglobin accounts for the largest component (nearly 80%). The remainder is mostly contained in ferritin and haemosiderin. Haemosiderin is the insoluble product of ferritin proteolysis in lysosomes (Halliwell and Gutteridge, 1999). Iron in myoglobin represents around 10%, with 1.3% in cytochromes and iron-sulphur proteins, and 0.1% in transferrin.

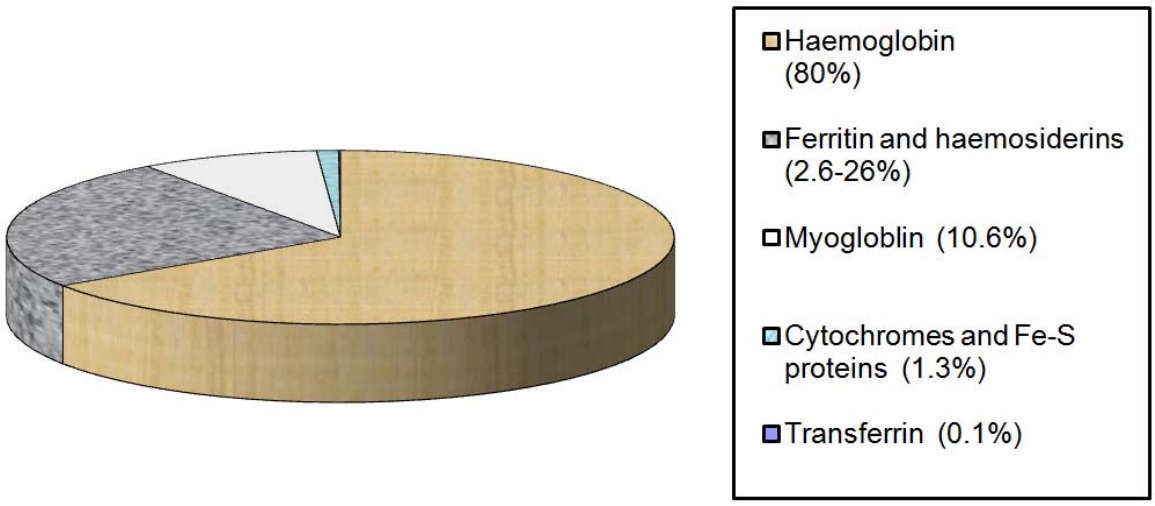

Figure 1.2:

Diagrammatic representation of iron distribution in the body

1.2.2 Iron Absorption

Due to epithelial shedding in the gastrointestinal tract and the skin and because of blood loss in women, around 1-2 mg of iron is lost on a daily basis. This loss is usually compensated by the absorption of iron through the diet which contains approximately 10-20 mg of iron of which 1-2 mg is absorbed under normal circumstances. This absorption is increased several fold when iron levels are low (e.g. in anaemia and hypoxia) and decreased when the iron stores are replete (e.g. in iron overload conditions and inflammation) (Andrews, 2005 and Ganz, 2007).

Dietary iron is absorbed in the duodenum by the duodenal enterocytes absorptive lining close to the gastro-duodenal junction (Andrews, 2000 and Miret *et al,* 2003). It consists of two components, haem and non-haem iron. Haem iron is exclusively present in animal tissues (e.g. in red meat), and is highly bioavailable and readily absorbed. Haem is a molecule that consists of protoporphyrin ring that binds ferrous iron. It results from the breakdown of haemoglobin and myoglobin found in meat products. Non-haem iron which is present in e.g. cereals and vegetables (and also in meat) is either in the reduced ferrous (Fe^{2+}) or mostly, in the oxidised ferric state (Fe^{3+}). Low pH in the gastric efflux facilitates iron absorption as it releases iron from ligands in food.

Haem enters the cell (see figure 1.3) via the haem carrier protein 1 (HCP-1) (Shayeghi *et al,* 2005) which is expressed in the apical membrane of duodenal epithelial cells, and inside the cell haem is degraded by haem oxygenase to yield ferrous iron (see section 1.4.2.4). The enterocytes of the luminal brush border contain an enzymatic ferric reductase activity, called Dcytb (the cytochrome *b*-like protein) (McKie *et al,* 2002), to ensure that non-haem iron is in the ferrous (Fe^{2+}) state since the bioavailability of iron is reduced when it is in the ferric state (Fe^{3+}). Along with the Dcytb, the presence of dietary reducing agents, such as ascorbate and small peptides containing cysteinyl and histidyl residues aid this reduction (Sharp, 2005). Divalent metal transporter 1 (DMT1, also known as Nramp2 and DCT1) is the apical major ferrous transporter, which is responsible for transporting iron into the cell. Other divalent metals such as Mn^{2+}, Cu^{2+} and Zn^{2+} are also transported by DMT1 (reviewed in Donovan and Andrews, 2004).

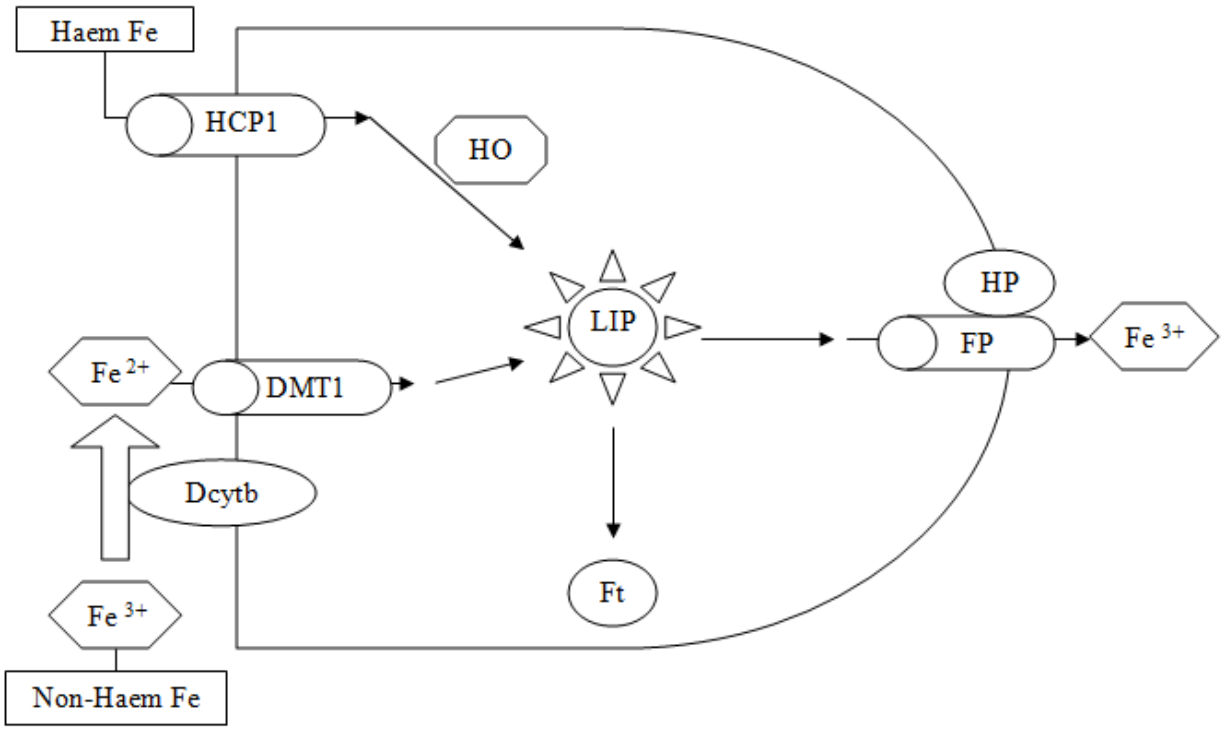

Figure 1.3:

The absorption of dietary iron by duodenal enterocytes.

Molecular pathways of haem and non haem iron absorption in the duodenum (Modified from Sharp, 2005 and Syed *et al,* 2006)

Haem enters the cell via the HCP-1 which is expressed in the apical membrane of duodenal epithelial cells, and it is degraded by haem oxygenase to yield ferrous iron inside the cell. Iron enters the LIP where it may be then stored in Ft or transferred to the plasma and tissues by FP aided by HP, which exhibits a ferroxidase activity. The enterocytes of the luminal brush border contain an enzymatic ferric reductase activity, apparently the cytochrome *b*-like protein Dcytb, to ensure that non-haem iron is in the ferrous state since the bioavailability of iron is reduced when it's in the ferric state. DMT1 is the apical major ferrous transporter, which is responsible for transporting iron into the cell.

Abbreviation used: Dcytb, cytochrome *b*-like protein; DMT1, Divalent metal transporter 1; FP, ferroportin; Ft, ferritin; HCP1, haem carrier protein 1; HP, hephaestin; HO, Haem oxygenase; LIP; Labile iron pool.

Identified in 2000 by three groups (Abboud and Haile, 2000; Donovan *et al,* 2000; McKie *et al,* 2000), ferroportin (also known as IREG1 and MTP1) is a distinct transporter which is an excellent candidate for the basolateral transfer of iron to the plasma and tissues, although little is known how it transports iron (Ganz, 2007). Iron exports from intestinal cells appear to be aided by hephaestin, which exhibits a ferroxidase activity (i.e. converts Fe^{2+} to Fe^{3+}) required for such export (reviewed in Ganz and Nemeth, 2006) and ceruloplasmin is involved in iron export from non-intestinal cells. This notion is supported by the fact that hephaestin deficiency results in severe iron-deficiency anaemia (Anderson *et al,* 2002) and the deficiency of ceruloplasmin leads to iron accumulation in macrophages, hepatocytes, and cells of the central nervous system (Xu *et al,* 2004).

1.2.3 Iron homeostasis and metabolism

Although iron is indispensable for living organisms from bacteria to mammals (see 1.2.1), the tight control of this abundant transition metal metabolism is critical since disease is associated with both iron overload and deficiency (Andrews, 2000). Firm control of iron uptake, storage, and export is essential for cellular iron homeostasis (Hentze *et al,* 2004). It is normally controlled by the coordinate regulation of the expression of two proteins i.e. Ferritin (Ft) and transferrin receptor (TfR) (Harford and Klausner, 1990).

The presence of non-transferrin bound iron (NBTI) in the plasma of patients with iron overload disorders (e.g. thalassemia and haemochromatosis) and also in patients undergoing chemotherapy was first reported in 1975 (Hershko, 1975). However, still very little is known about its chemical nature. Following its receptor mediated uptake, NTBI causes organ dysfunction (Syed *et al,* 2006). Nevertheless, the majority of iron in the blood plasma of normal individuals and in the intestinal fluid is bound and transported by transferrin (Tf) (Klausner *et al,* 1993), that is an 80 kDa serum glycoprotein capable of binding a maximum of two atoms of ferric iron (Aisen and Listowsky, 1980). Plasma diferric Tf binds to the cell surface TfR, which is located on the surface of plasma membrane. The latter is a homodimer of 95 kDa that is capable of binding to two molecules of Tf. The Tf-TfR complex is then internalised by endocytosis. The endosome is then acidified and iron is exported to the cytosol via DMT1 (reviewed in Muckentahler *et al,* 2008), this results in the

release of ferric iron from the Tf and its subsequent reduction to ferrous iron. Iron is then utilised for the synthesis of iron-containing proteins and the excess is stored in the 440 kDa iron storage protein, ferritin. Cytosolic iron is stored in Ft in the ferric state but the mechanism of delivery is unknown. Recently, Shi *et al,* (2008) proposed that human poly (rC)-binding protein (PCBP1) can act as cytosolic iron chaperone in the delivery of iron to Ft. The remaining fraction of cytosolic iron usually stays in the cytosol weakly bound to low molecular weight 'chelates' such as citrate, ATP, pyrophosphates, and ascorbate. This fraction is accessible to iron chelators and therefore it is referred to as 'chelatable iron'. The chelatable iron, which is in both ionic forms (Fe^{2+} and Fe^{3+}), is also known as the "labile iron pool" (LIP) (Jacobs, 1977 and Kakhlon and Cabantchik, 2002). The LIP, at normal levels, represents less than 5 % of the total cellular iron (Kakhlon and Cabantchik, 2002 and Andrews, 2004), but this portion changes with the iron status of the cell (reviewed in Arredondo and Nunez, 2005). The LIP reflects the iron status of the cell since it contains the cells' metabolically and catalytically reactive iron, therefore it is a marker of total iron content in the cells. The balanced movement of iron from extracellular and intracellular sources maintains the LIP. The Calcein (CA) assay is a simple and non-invasive fluorescent technique that is capable of measuring LIP in living cells (Epsztejn *et al,* 1997).

Transferrin has three major functions: (1) It allows ferric iron to remain soluble i.e. in aqueous and pH neutral plasma environment, (2) It allows iron to circulate in the safe form, and (3) It facilitates the cellular import of iron (Heeney and Andrews, 2004).

Ferritin (see section 1.4.1.3) is the principal site for iron storage and detoxification in microbial, plants, and animal species (Kuhn, 1994 and Aisen *et al,* 1999). In addition to its storage capacity, it serves as an iron source for haem synthesis and iron containing proteins, and it replenishes the LIP (Meyron-Holtz *et al,* 1999). The mammalian Ft is a heteropolymer of a combination of heavy (H) and light (L) chains of around 21 kDa and 19 kDa, respectively (Theil, 1987) which co-assemble to form a protein shell of 24 subunits. It can hold up to 4,500 iron atoms in its iron core that it surrounded by the shell, but usually has fewer. To store iron in Ft, several steps are required: (1) Fe^{2+} binding and migration to the ferroxidase site, (2) Fe^{2+} oxidation, (3) Fe^{3+} hydrolysis, and finally (4) nucleation and the core formation (reviewed in Harrison and Arosio, 1996 and Yang *et al,* 1998). The H-chain has a

ferroxidase capacity which is responsible for the rapid oxidation of ferrous iron to ferric iron and its incorporation. Therefore, the H-Ft has been proposed to be a regulator of the intracellular labile iron pool and a possible attenuator of oxidative stress in cells (Epsztejn *et al,* 1999). The L-chain contributes to the overall protein stability and is responsible for iron hydrolysis, nucleation, and the core formation (Lawson *et al,* 1989; Levi *et al,* 1992; Santambrogio *et al,* 1993; reviewed in Harrison and Arosio, 1996; Yang *et al,* 1998). Unlike H-Ft, L-Ft does not seem to have a major role in iron metabolism since subjects with genetic hyperferritinaemia-cataract syndrome have nearly 10-fold higher L-Ft than normal with no obvious abnormalities in iron metabolism (Beaumont *et al,* 1995 and Girelli *et al,* 1995).

Several studies have shown that the levels of iron co-ordinately control the levels of TfR and Ft. For example, during iron deficiency; the synthesis of Ft (L and H chain) will be brought to an end while the TfR expression is increased in mammalian cells therefore a higher number of TfRs will be present on their cell surface for internalisation. The opposite is true when iron is raised in culture medium; TfR is down regulated, whereas Ft synthesis is increased to remove excess iron (Kuhn, 1994 and reviewed in Cairo and Pietrangelo, 2000).

Levels of Ft and TfR are controlled by two mammalian iron regulatory proteins (IRP1 and IRP2), which are also the sensors of cytoplasmic labile iron (reviewed in Cairo and Pietrangelo, 2000). To ensure that the cells always contain sufficient iron for essential metabolic needs without exceeding the threshold of toxicity, intensive regulation of these proteins is essential (reviewed in Cairo *et al,* 2002). Adjustment of the intracellular iron concentration to normal and standard levels is mainly achieved by the use of these proteins at post-transcriptional levels, IRP-2 being the major sensor and modulator of iron metabolism (Recalcati *et al,* 2006). Iron-responsive elements (IRE) are stem loop structures with special base sequence in the mRNA of the Ft and TfR proteins (Theil 1990 and Eisenstein, 2000). In both H and L subunit of Ft, there is one IRE situated in the 5'- untranslated region (UTR), whereas TfR has five IRE motifs in its 3' UTR (Thomson *et al,* 1999). In iron-deficient cells, IRP-1 is activated by the removal of an attached iron-sulphur cluster and IRP-2's half life is prolonged which causes them to bind to the Ft's and TfR's IRE (Samaniego *et al,* 1994). The consequences of this binding complex are (1) inhibition of Ft mRNA translation and (2) the increase of the stability of TfR mRNA from nucleolytic degradation, therefore more protein is made. This will also increase the

translation of DMT1 and decrease ferroportin (reviewed in Muckentahler *et al,* 2008). Conversely, in iron replete cells, IRP-1 will be inactivated by its conversion to cytosolic aconitase (its physiological importance remains to be defined) and IRP-2 will be degraded subsequent to oxidation and ubiquitination (Iwai *et al,* 1998). This will cause (1) translation of mRNA encoding H and L Fts and (2) degradation of TfR mRNA. The lack of IRP binding activity will also decrease the translation of DMT1 and increase ferroportin (reviewed in Muckentahler *et al,* 2008). Thus, the IRP/IRE system (see figure 1.4) plays an important role for the regulation of Ft and TfR proteins (Eisenstein, 2000) and it has been suggested that this regulation is via the cytosolic LIP (Meyron-Holtz *et al,* 1999).

1.2.4 Iron and inflammation

During inflammation, T cells and macrophages produce a number of cytokines which influence the metabolism of iron; affecting its cellular uptake, transport, storage, as well as its absorption (Weiss, 2005). The induction of iron sequestration in macrophages and the decrease in iron absorption in the small intestine was shown in infections and inflammatory diseases. This results in the development of anaemia, termed 'anaemia of inflammation' (AI), formerly known as 'anaemia of chronic disease' (ACD).

The AI is a most common condition that is noticeable in patients suffering from inflammatory disorders (e.g. rheumatic diseases) (Konijn, 1994). It is characterised by low to normal serum iron levels (i.e. hypoferremia), low serum iron binding capacity, and normal to elevated ferritin concentrations. Several proinflammatory cytokines, such as IL-1β and TNF-α, have been shown to contribute to the development of AI by the induction of hypoferremia. These cytokines cause a significant decrease in the low serum iron via the induction of Ft biosynthesis in macrophages (Alvarez-Hernandez *et al,* 1989 and Brock and Alvarez-Hernandez*,* 1989). They were also found to down-regulate TfR expression (Weiss, 2002) and to decrease Tf levels in patients with active RA and AI (Jongen-Lavernic *et al,* 1995). The up-regulation of DMT1 expression and the increase of iron influx into activated macrophages were shown by IFN-γ, LPS, and TNF- α. (Ludwiczek *et al,* 2003).

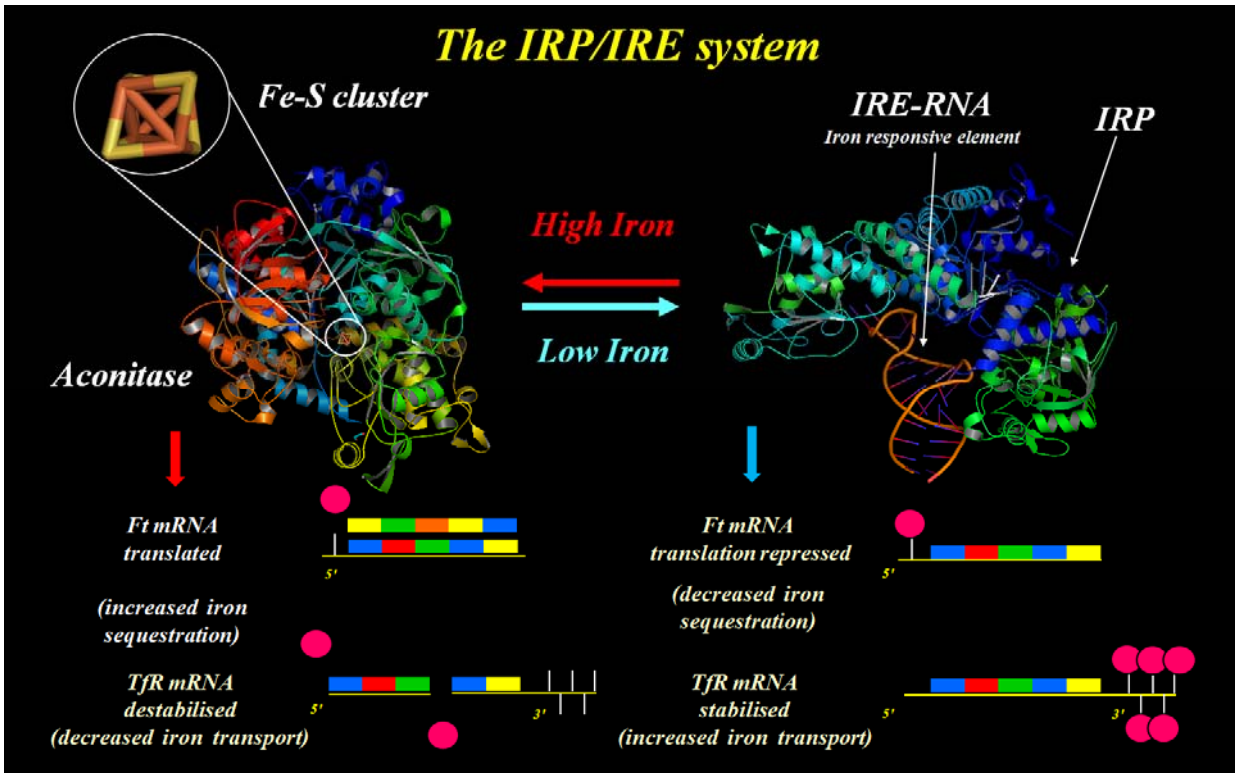

Figure 1.4 :

Illustration of the Iron regulatory proteins / Iron responsive elements system.

On the right, is a ribbon diagram of aconitase and on the left is a ribbon diagram of IRP bound to IRE. The pink circles on the right and the left represent the aconitase and IRP, respectively. The small white vertical lines on the 5' or the 3' region represent the IRE.

In iron deficiency, IRP binds to the IRE motifs of H- and L-Ft and TfR and therefore represses the translation of H- and L-Ft and stabilises TfR mRNA; leading to increased protein expression. Under iron excess conditions, IRP has low affinity for the IRE and instead has aconitase activity. This in turn leads to the translation of Ft and the destabilisation of TfR mRNA.

Reproduced and modified from Dr. James Dowden (University of Nottingham, UK); used with permission.

Rheumatoid arthritic patients with anaemia had significantly higher serum levels of TNF- α, IL-1 and IL-6, when compared to non-anaemic RA patients (Voulgari et al, 1999). When macrophages were stimulated by IFN-γ and lipopolysaccharide (LPS), this induced nitric oxide (NO) synthesis and activated the IRP/IRE binding system (Weiss *et al,* 1993). Lipopolysaccharide, an endotoxin, is a component of the outer membrane of gram negative bacteria. Low intracellular iron is correlated with the production of NO which in turn decreases Ft synthesis and subsequently produces an increase in free iron (Weiss *et al,* 1994). It was recently demonstrated that T cells from RA patients produce > 2.5 times more NO than healthy donor T cells (Nagy *et al,* 2008). Since TNF-α increases NO production *in vitro* (e.g. in Jurkat cells), this indicates that the TNF-α induced NO production may contribute to RA disease progression.

Nemeth *et al,* (2004[a]) showed that hypoferremia of inflammation is mediated by IL-6 inducing the synthesis of hepcidin, an iron-regulatory hormone. Hepcidin is a 25 amino acid polypeptide, with an antimicrobial action, produced mainly by hepatocytes, distributed in plasma and first isolated from the urine (reviewed in Ganz, 2003). During inflammation and infections, hepcidin is markedly induced causing the sequestration of iron in macrophages, hepatocytes and enterocytes (Ganz, 2005). It acts by inhibiting iron release from macrophages and from hepatic stores, and by inhibiting intestinal iron absorption. Hepcidin exerts its action by directly binding to ferroportin (FP) ; this binding causes the internalisation of FP and its and degradation in the lysosomes (Nemeth *et al,* 2004[b]). The loss of ferroportin from the cell membrane prevents cellular iron export. Acute and chronic inflammation and iron overload were shown to induce hepcidin synthesis, whereas anaemia and hypoxia suppress it (Pigeon *et al,* 2001 and Nicolas *et al,* 2002).

1.2.5 Rheumatoid arthritis and Iron

The potential role of iron in rheumatoid arthritis is well documented for the past four decades. *In vitro* studies revealed that ferrous ions in trace amounts were very active in the depolymerisation of purified hyaluronic acid and this is correlated with the low viscosity of synovial fluid (SF) of patients with RA. Spectrographic studies showed that SF from patients with RA contained elevated concentration of iron (Niedermeier *et al,* 1962). By emission spectrometric analysis, the mean concentration of iron was higher in the SF of RA patients than normal subjects

(Niedermeier and Griggs, 1971). Muirden and Senator (1968) were one of the first to suggest the critical role that iron could play in the pathogenesis of RA. In this study, their intention was to demonstrate the distribution of iron, using Prussian blue staining, in both normal and joint disease synovia. The staining occurred in all but one of the 23 rheumatoid arthritic synovia. On the other hand, all of the normal synovia showed a negative reaction with Prussian blue staining.

Proinflammatory cytokines such as TNF-α, IL-1, IL-6, and INF-γ, were shown to increase Tf and non-Tf bound iron uptake into human monocytes and increase Tf-bound iron uptake by synovial fibroblasts isolated from rheumatoid arthritic synovium (Telfer and Brock, 2004). This suggests that cytokines present in the rheumatoid arthritic synovium may lead to the accumulation of iron which contributes to the pathogenesis of the disease. Interestingly, TNF-α, IL-1, and IL-6 were also responsible for the induction of Ft synthesis in a hepatic cell line (reviewed in Torti and Torti, 2002).

Iron, mainly bound to Ft, is present in both the rheumatoid synovial membrane and fluid (Blake *et al,* 1981). In rheumatoid arthritic and osteoarthritic patients, iron concentration in the synovial tissue was significantly elevated (Ogilvie–Harris and Fornaiser, 1980). In RA, anaemia is the most frequent extra-articular manifestation of the disease. Its frequency in patients ranges from 15% to 80%, depending on the inflammatory condition. Nine of the eleven rheumatoid arthritic patients receiving iron dextran for the treatment of anaemia showed an exacerbation of synovitis (Blake *et al,* 1985). *In vitro*, iron dextran stimulates lipid peroxidation. As a result of this lipid peroxidation, it was suggested that iron dextran worsens synovial inflammation. Administration of desferrioxamine (DFO) to a chronic inflammatory animal model significantly decreased the chronic inflammatory phase (Blake *et al,* 1983). Desferrioxamine (DFO) is a chelating agent that has a high binding affinity for iron, it complexes one molecule of Fe^{3+} per molecule of DFO. Its advantage is in its capacity to chelate the 'free iron' inside the cell. It was therefore suggested that effective iron chelation and its removal may modify the inflammatory process in man. Desferrioxamine is also a weak scavenger of superoxide anion but a powerful one of hydroxyl radical and therefore it efficiently inhibits lipid peroxidation and protects cells against oxidative damage (Halliwell and Gutteridge, 1986). Also, when adjuvant arthritic rats were treated with DFO, the incidence and severity of joint inflammation was reduced (Andrews *et al,* 1987[a]). It was also reported that mild iron deficiency

significantly reduces the severity of adjuvant induced joint chronic inflammation (Andrews *et al,* 1987[b]). Taken together, these results suggest a potential role for iron in inflammatory joint disease notably rheumatoid arthritis.

1.3 Oxidative Stress

Oxygen is an element that exists in the atmosphere at the percentage of 21%, existing as a diatomic molecule, O_2, which is referred to as dioxygen. Oxygen has a pivotal role in all animals, plants, and bacteria, since it is essential for the production of energy by the use of the O_2 dependent electron transport. Experiments have shown that the O_2 will cause toxicity if given at a concentration higher than normal (Martinez-Cayueta, 1995).

1.3.1 General overview

"Oxidative stress" is a term introduced to illustrate the imbalance within the cells between the production of prooxidants and antioxidant defences in favour of the former. It occurs either from the increased production of reactive oxygen species (ROS) or reactive nitrogen species (RNS), or a deficiency in the antioxidant defence systems (Halliwell and Gutteridge, 1999 and Morel and Barouki, 1999).

1.3.2 Free Radicals

Any atom, molecule, or complex possessing an unpaired electron(s) and capable of independent existence is defined as a "free radical" (Cadogan, 1973). They can exist in either the gaseous or the liquid phase.

Free radicals can be formed by three independent methods:

(a) Addition of a single electron: $A + e^- \longrightarrow A^{\bullet -}$

(b) Loss of a single electron: $A \longrightarrow A^{\bullet +} + e^-$

(c) Homolytic fission of a covalent bond where each pair possesses one of the unpaired electron: $A : B \longrightarrow A^{\bullet} + B^{\bullet}$

The primary source of the production of free radicals within the cells is the leakage of electrons, in the mitochondria and the endoplasmic reticulum, from the electron transport chain. Additionally free radicals are also produced by activated phagocytes (i.e. macrophages, monocytes, and lymphocytes) during inflammation (Cheeseman and Slater, 1993). In addition to these intracellular sources, there are

also exogenous sources such as ionizing radiation, tobacco smoking, and pollutants (Martinez-Cayueta, 1995).

1.3.3 Reactive oxygen species (ROS)

Reactive oxygen species (ROS) is a term used to include oxygen radicals and non-radical derivatives of oxygen. Superoxide anion radical ($O_2^{\bullet-}$) and hydroxyl radical ($OH^{\bullet}$) are examples of oxygen radicals, whereas hydrogen peroxide (H_2O_2) and singlet oxygen ($^1O_2$) are examples of non-radicals.

Superoxide anion ($O_2^{\bullet-}$) is formed by the addition of a single electron to a dioxygen molecule, from about 1-3 % of the oxygen we breath in (Halliwell, 1994). The protonated form of the reduction of molecular dioxygen by two electrons is H_2O_2. Both $O_2^{\bullet-}$ and H_2O_2 are produced by the NADPH oxidase which is located in the cell membrane. Singlet Oxygen ($^1O_2$) is produced by a process which involves the input of energy to turn the two parallel spinning electrons into antiparallel spinning. The major source of the $OH^{\bullet}$ is formed via the metal catalyzed Haber-Weiss or the Fenton reaction: Superoxide anion radical ($O_2^{\bullet-}$) converts ferric iron to ferrous ions and then ferrous ions react with H_2O_2 to produce $OH^{\bullet}$:

$$O_2^{\bullet-} + Fe^{3+} \longrightarrow O_2 + Fe^{2+}$$

$$Fe^{2+} + H_2O_2 \longrightarrow Fe^{3+} + OH^- + OH^{\bullet} \quad \text{(Fenton reaction)}$$

$$\text{Net : } O_2^{\bullet-} + H_2O_2 \xrightarrow{\text{metal catalyst}} O_2 + OH^- + OH^{\bullet} \quad \text{(Haber-Weiss reaction)}$$

The most potent catalysts of $OH^{\bullet}$ formation under normal physiological conditions are iron and copper ions (Halliwell and Gutteridge, 1999). The hydroxyl radical is more reactive than $O_2^{\bullet-}$ and H_2O_2, possessing a short half life, while $O_2^{\bullet-}$ and H_2O_2 have longer half lives but are less reactive (Martinez-Cayueta, 1995).

All major cellular components may be injured by ROS. The cell membrane and the membrane of cell organelles (e.g. mitochondria, lysosomes, and peroxisomes) are rich in polyunsaturated fatty acids (PUFAs). Polyunsaturated fatty acids contain two or more carbon-carbon double bonds. The oxidative damage of PUFAs will result in lipid peroxidation; a free radical chain reaction that will generate fatty acid radical ($L^{\bullet}$) and consequently fatty acid peroxyl radical ($LOO^{\bullet}$), and aldehydes (Cheeseman and Slater, 1993). In addition to rupturing the membrane and causing cell death, lipid peroxidation products can inhibit protein synthesis and block macrophage action (Winrow *et al*, 1993). Furthermore ROS can cause disturbances in proteins since they could react with amino acids such as histidine and cysteine.

Reactive oxygen species can also cause a cellular ion imbalance by attacking the proteins responsible for the maintenance of such balance (Halliwell and Gutteridge, 1999). In addition, DNA strand breakage has been demonstrated when cells were exposed to ROS, since $OH^{\bullet}$ can damage sugars, purines, and pyrimidines. Carbohydrate damage has also been noticed in view of the fact that $OH^{\bullet}$ in the presence of iron is responsible for the depolymerization of hyaluronic acid in vitro studies (Wong *et al,* 1981). The viscosity of synovial fluid within the joints is maintained by hyaluronic acid since it has lubricating properties.

1.3.4 Reactive nitrogen species (RNS)

Oxides of nitrogen such as nitric oxide ($NO^{\bullet}$) and nitrogen dioxide ($NO_2^{\bullet}$) are also free radicals which have the term 'reactive nitrogen species'. Nitric oxide ($NO^{\bullet}$) is formed *in vivo* from the amino acid L-arginine by three different NO-synthases (NOS) while $NO_2^{\bullet}$ is made when $NO^{\bullet}$ reacts with oxygen. They are both found in polluted air and smoke from the burning of organic material e.g. cigarette smoking. Peroxynitrite ($ONOO^-$) is often regarded as both a ROS and RNS, it is the reaction product of $O_2^{\bullet-}$ and $NO^{\bullet}$ (Halliwell and Gutteridge, 1999) which are both produced from cells of the immune system during inflammation (Valko *et al,* 2007). Peroxynitrite ($ONOO^-$) is considered to be a potent oxidant and a major cytotoxic agent that can cause DNA fragmentation and lipid oxidation (Mladenka *et al,* 2006). In addition to $ONOO^-$, nitrous acid (HNO_2) and dinitrogen trioxide (N_2O_3) are examples of non-radical RNS.

1.3.5 Oxidative stress in Rheumatoid arthritis

Oxidative stress has been implicated in several physiological and pathological conditions (Vendemiale *et al,* 1999), such as atherosclerosis, diabetes, aging, rheumatoid arthritis, osteoarthritis, cancer, inflammatory bowel disease, and many more (Halliwell and Gutteridge, 1999 and Martinez-Cayueta, 1995). It is important to mention that the oxidative stress in many human diseases is a consequence and not a cause. In principle, disease-associated oxidative stress could result from either (or both): (1) decreased amount of enzymatic and non-enzymatic antioxidants (see section 1.4) and (2) increased production of ROS/RNS (see sections 1.3.3 and 1.3.4). For example during inflammatory processes, oxidative burst occurs (Halliwell *et al,* 1992) that is characterised by the massive production of ROS/RNS in that

environment which play a key role in defending cells against pathogens. The consequent increase in ROS/RNS leads to changes in signal transduction and gene expression; a common phenomenon seen in disease. Signal transduction (also called, cell signalling) is a process enabling information to be transmitted from outside the cell to various functional elements inside the cell and it is also the mechanism by which cells communicate with each other. Tissues often respond to mild oxidative stress by producing extra antioxidants, but severe oxidative stress can cause tissue injury and consequently cell death (Halliwell, 1994).

Several lines of evidence are in agreement with the concept that an 'oxidative stress' contributes to the pathogenesis of RA. Several studies have been suggesting that the rheumatoid synovium is relatively ischemic and that ischemia-reperfusion has been implicated to be major factor in the injury occurring in RA (Han *et al,* 2003). As ischemia-reperfusion occurs in the inflamed joint upon rest and movement, the authors suggest that it could be a potential target for the treatment of RA. During the isolation and stimulation of cells which are present in the inflamed joint (e.g. macrophages, neutrophils, and lymphocytes), the ability to produce ROS was noticed (Merry et al, 1989). T cell stimulation leads to the production of ROS and cytokines (reviewed in MacKenzie, 2006). Interestingly, also cytokines such as TNF-α and IL-1 lead to oxidant production (Finkel, 2003). In rheumatoid arthritic synovial lymphocytes, Remans *et al,* (2005) found intracellular ROS production. Hydrogen peroxide appears to be one of the ROS involved, since the addition of catalase (see 1.4.2.3) suppressed the intracellular ROS production. It was concluded that chronic oxidative stress observed in synovial T lymphocytes originates from intracellular ROS production. In other studies, Malondialdehyde (MDA) was measured as a marker of lipid peroxidation in rheumatoid arthritic patients and control subjects. The levels of plasma (Kamanli *et al,* 2004) and serum (Ozkan *et al,* 2007) MDA were significantly higher in patients with RA compared to the control. Recently Altindag *et al,* (2007) also demonstrated that DNA damage and total oxidative status was higher in patients with RA than in healthy controls and that total antioxidant status was lower in the same patients. It was therefore concluded in this study that the increase in lymphocyte DNA damage increase in patients with RA may be related to the increased oxidative stress and decreased antioxidant capacity.

1.3.6 Oxidative stress and the regulation of iron

Iron is an important element believed to generate oxidative stress i.e. an increase in the steady state concentration of prooxidants (e.g. by the formation of $OH^{\bullet}$) that damage membranes and DNA (Meneghini, 1997). The higher the LIP in the cells, the higher levels of ROS are noticed. Therefore, the LIP is not only a marker of the total Fe content in the cells but also determines the redox state of it.

Oxidative stress in the form of ultraviolet (UV) light has been shown to accumulate iron. Ultraviolet (UV) B radiation was shown to increase the skin level of non-haem iron (Bissett *et al,* 1991) and UVA radiation caused an immediate increase in 'free' iron in fibroblasts (Pourzand *et al,* 1999). When rat livers were exposed to oxidative stress in the form of phorone (a glutathione depleting drug), data suggests that there was an early increase in the levels of free iron pool (Cairo *et al,* 1995). Breuer *et al,* (1997) also showed that H_2O_2 induced a significant increase in LIP levels in cultured K562 cells. Iron deficiency is compensated by increased IRP activity which consequently results in the induction of TfR levels and reduced Ft synthesis, and therefore increases LIP levels (reviewed in Hentze and Kuhn, 1996). Stimulation of IRP activity by exposure of cells to H_2O_2 was shown in a number of studies (Pantopoulos and Hentze, 1995; Martins *et al,* 1995; Pantopoulos *et al,* 1996; Pantopoulos *et al,* 1997; Mueller *et al,* 2001). On the contrary, incubation of rat liver lysates with xanthine oxidase (which generates both superoxide anions and H_2O_2) revealed that a combined action of both H_2O_2 and $O_2^{\bullet-}$ were responsible to induce a reversible inactivation of IRP (Cairo *et al,* 1996 and Cairo *et al,* 1998). IRP inactivation by H_2O_2 and $O_2^{\bullet-}$ combination may serve as a protective mechanism against oxidative damage since it diminishes LIP before it converts H_2O_2 and $O_2^{\bullet-}$ into a potent oxidant. It has been demonstrated that H_2O_2 and $O_2^{\bullet-}$ can release iron from Ft (Rudeck *et al,* 2000 and Agrawal *et al,* 2001). Menadione-induced oxidative stress in B6 fibroblasts caused a post-translational inactivation of IRP (Gehring *et al,* 1999). IRP inactivity was also observed in rat subjected to ischemia-reperfusion, a process accompanied by a burst of ROS (Tacchini *et al,* 1997). There is therefore substantial evidence to conclude that the IRP proteins are targeted under conditions of oxidative stress in the cells (reviewed in Cairo *et al,* 2002). In a recent study, Andriopoulos *et al,* (2007) showed that sustained low levels of H_2O_2 up-regulated TfR1, leading to increased transferrin-mediated iron uptake and iron accumulation in the cells. Since IRP-1 was only partially and temporarily activated (likely because of H_2O_2 signalling)

the authors suggested that this effect is independent of IRP/IRE system. The lower biological reactivity of H_2O_2 (compared to many ROS) with its capacity to cross membranes makes H_2O_2 an ideal signaling molecule (Hampton and Orrenius, 1997). Indeed, it has been proposed that extracellular H_2O_2 seem to act through a membrane-transduced signaling process (reviewed in Cairo and Pietrangelo, 2000). Activation of IRP by H_2O_2 has been seen in intact cells but not in lysates (Mueller, 2005). Taken together, it seems that IRP responds in a different way to a variety of oxidative stress stimuli (Gehring *et al,* 1999).

1.4 Antioxidant defence systems

As previously mentioned, free radicals have been implicated in several physiological and pathological conditions. In addition they can cause protein oxidation, lipid peroxidation, carbohydrate damage, and DNA damage. Fortunately, our bodies acquire several defence mechanisms intended to prevent the damage or at least to minimize it.

Antioxidants are one of the major defence systems the body has acquired. An antioxidant is defined as "a substance that when present at low concentration compared to those of an oxidisable substrate significantly delays or prevents oxidation of that substrate" (Sies, 1997). There are considerable data to show their beneficial effects in animal models and clinical trials in the treatment of RA (Kunsch *et al,* 2005). Antioxidants can be divided into two categories; enzymatic and non-enzymatic antioxidants which can be found in both aqueous and membrane compartments within the cells.

1.4.1 Non-enzymatic antioxidants

1.4.1.1 Glutathione

Glutathione (L-γ-glutamyl-L-cysteinyl-glycine) is a tripeptide molecule that is found in animals, plants, and many aerobic bacteria. In mammalian cells it is present in a millimolar range (Meister and Anderson, 1983) and it is the major cellular antioxidant. It is highly abundant in the cytosol (1-11 mM), nucleus (3-15 mM), and mitochondria (5-11 mM). It is synthesised by two steps (Halliwell and Gutteridge,

1999) as detailed below: First, the dipeptide formation is catalysed by γ-glutamylcysteine synthetase:

L-glutamate + L-cysteine + ATP → L-γ-glutamyl-L-cysteine + ADP + Pi

Then GSH is produced by glutathione synthetase:

L-γ-glutamyl-L-cysteine + glycine + ATP → GSH + ADP + Pi

Glutathione is present in two forms, the reduced form (GSH) and the oxidised form (GSSG) where it redox-cycles between them, but the vast majority (95-99%) is in the reduced form (Dethmers and Meister, 1981 and Meister and Anderson, 1983). In the cytosol and mitochondrial matrix, mammalian cells contain approximately 10 mM GSH and 0.5 mM GSSG (Droge *et al,* 1994). GSSG is synthesised by the addition of two GSH molecules with the oxidation of the –SH groups in cysteine to form a disulphide bridge (-S-S-) (Halliwell and Gutteridge, 1999).

The glutathione system within the cells acts as a major homeostatic redox buffer and represents a primary antioxidant defence considering that it depends on the relative amounts of GSH/GSSG. Intracellular glutathione acts as an antioxidant in several ways. It can reduce peroxides to form H_2O (Martinez-Cayueta, 1995) or scavenge directly ROS (Cuzzocrea *et al,* 2004). It can also act as a chelator of Cu^{2+} and reduces its activity to generate ROS (Halliwell and Gutteridge, 1999). Glutathione, in yeasts, was found to play a major role in the maturation of cytosolic iron-sulphur proteins (Sipos *et al,* 2002).

Oxidative stress in the form of UVA radiation (oxidising component of sunlight, 320 - 380 nm) or H_2O_2 has been found to deplete intracellular glutathione (Lautier *et al,* 1992 ; Brunk *et al,* 1995[a] ; Hempel *et al,* 1996). Treatments of Wistar rats with phorone, a glutathione depleting drug that amplifies the effects of ROS, induced Ft synthesis 6-fold in liver slices as a late response (Cairo *et al,* 1995). Recently, it was found that homocysteic acid, a glutathione depleting drug, increased the levels of H- and L-Ft mRNA (by nearly 2-fold) in HT22 murine hippocampal cells (Morozova *et al,* 2007). Exposure of mouse nerve cell line to glutamate blocks cysteine uptake and therefore depletes GSH, this leads to the accumulation of ROS and ultimately apoptotic cell death (Sagara *et al,* 1998). Several studies have shown that the depletion of intracellular glutathione sensitises cell populations to several circumstances such as aerobic ionising radiation, cytotoxic drugs, and H_2O_2. Indeed, glutathione depletion (by buthionine-[S,R]sulfoximine, BSO) sensitises cultured

human lymphoid cells against γ radiation (Dethmers and Meister, 1981), therefore it is regarded as a major protective agent.

1.4.1.2 Thioredoxin (TRx)

Thioredoxin is a thiol-polypeptide molecule that is present in mammalian cells. It is generally concentrated in the endoplasmic reticulum and also can be found on the cell surface. In addition to glutathione, TRx is also a major carrier of redox potential within cells (Kontou *et al,* 2004). They both maintain signalling components in a reduced state and are counterbalanced in signalling by oxidative stress, typically ROS (Jones *et al,* 2004). The term redox signalling is used to describe a regulatory process in which a signal is delivered through redox reactions (Valko *et al,* 2007). TRx has two –SH groups (reduced form) that is converted to an oxidised TRx with a disulphide (-S-S-). It undergoes redox reactions in the presence of proteins (Halliwell and Gutteridge, 1999).

$$TRx—(SH)_2 + protein—S_2 \rightleftharpoons TRx—S_2 + protein—(SH)_2$$

Thioredoxin exerts its antioxidant activity by different pathways. It has been shown to possess a radical-scavenging activity (Schenk *et al,* 1994). It has been also involved in DNA repair, since it acts as a hydrogen donor for ribonucleotide reductase, which is an enzyme that is involved in the production of deoxyribonucleosides. It is also implicated in protein repair since it supplies methionine sulphoxide reductase with electrons. Methionine sulphoxide reductase repairs oxidative damage to methionine residues (Halliwell and Gutteridge, 1999). Thioredoxin levels in the synovial fluid and the synovial tissue of rheumatoid arthritic patients were elevated when compared with other joint diseases (Maurice *et al,* 1999). This observation suggests that synovial TRx may be a potential biomarker for RA (Kunsch *et al,* 2005).

1.4.1.3 Ferritin (Ft)

The ferritin molecule is a hollow protein shell (outside diameter around 13 nm, inside diameter around 8 nm), composed as mentioned in section 1.2.3, of heavy (H) and light (L) chains which co-assemble to form a protein shell of 24 subunits. Ratios of H-and L-Fts broadly differ from $H^{24}L^{0}$ to $H^{0}L^{24}$, these change in various diseases and under certain conditions (Halliwell and Gutteridge, 1999 and Theil,

2003). H-Ft is ubiquitous and contains a ferroxidase site, whereas L-Ft is catalytically inactive and unique to animals. Most intracellular iron is stored in Ft; it can store up to 4500 ion of iron (Halliwell and Gutteridge, 1999). In addition to iron, traces of other metals can be found in Ft including copper (Halliwell and Gutteridge, 1999).

Cairo *et al* (1995) have suggested that liver Ft can act as a pro- or an anti-oxidant in a time dependent manner. An early decrease in Ft has been shown after Wistar rats were treated with phorone, a glutathione depleting drug that amplifies the effects of ROS. Interestingly, 6-fold induction of Ft synthesis was shown as a late response. Treatment of skin fibroblasts with UVA lead to a total degradation of Ft (Pourzand *et al,* 1999). Six hours following UVA treatment, Ft levels returned to normal and increased up to 3-fold 24-48 hours following UVA treatment (Vile and Tyrrell, 1993). In endothelial cells, iron loading for 1 h significantly increased the cytotoxicity of H_2O_2 or oxidants from activated inflammatory cells (Balla *et al,* 1992 and Balla *et al,* 1993). Interestingly, at 16 h the cells became highly resistant to oxidative-mediated injury. This was correlated with 50-fold and 10-fold increase in haem oxygenase (HO) and Ft, respectively. The same phenomenon has also been seen in murine L1210 lymphocytic leukaemia cells using various types of oxidative insults (Lin and Girotti, 1997). Long exposure (i.e. 20-24 h) to hemin increased significantly the resistance of cells against H_2O_2- and $^1O_2$-mediated toxicity. This resistance was correlated with 12- to 15-fold increase in H-Ft; L-Ft, on the other hand, was not modified. Iron loading of J774 macrophages increased the lysosomal iron content and their sensitivity to H_2O_2-induced (0.25 mM for 30 minutes) oxidative damage (Garner *et al,* 1998). However, after 24-72 hours, the cells were desensitised to the cytotoxic effects of H_2O_2. The resistance observed was linked to the lysosomal iron exocytosis and Ft synthesis. Therefore, it seems from the above studies that: in the early stages of oxidative challenge, Ft might act as a pro-oxidant molecule since its degradation could be a potential source of iron involved in the exacerbating the oxidative damage occurred in cells as a result of oxidative insult.

The evidence for Ft acting as an antioxidant molecule is also overwhelming (reviewed in Arosio and Levi, 2002). Various studies have reported that different forms of oxidative challenge have demonstrated an increase in Ft levels, conferring resistance to the subsequent insult. It was demonstrated that the ferroxidase sites in H-Ft significantly reduces the production of $OH^{\bullet}$ from the Fenton reaction (Zhao *et al,* 2006). Induction of HO-1 by UVA radiation increases the Ft levels up to 3-fold 24-48

hours post-UVA radiation in human skin fibroblasts (Vile and Tyrrell 1993 and Vile *et al,* 1994). UV radiation has been shown to increase the Ft levels in both the epidermal and dermal tissue allowing increased protection against oxidative stress (Applegate et al, 1998). Hela cells, exposed to H_2O_2 treatment, increased the synthesis of H- and L-Ft and this overexpression in turn reduced the accumulation of ROS (Orino *et al,* 2001). It was suggested that Ft has an active role in regulating LIP levels and attenuating ROS generation in human erythroleukemia cells (Kakhlon *et al,* 2001). *In vivo* and *in vitro* studies, acute UVA exposure increased the expression Ft levels in basal epidermal cells (Siete *et al,* 2004). When human HL-60 leukaemia cells were pre-treated with hemin, they became more resistant to H_2O_2 and $^1O_2$ toxicity (Lin and Girotti, 1998). This was correlated with 4 to 12-fold increase in Ft protein levels over a period of 24 hours. Bovine artery endothelial cells became sensitive to photodynamic therapy after 1 h treatment with hemin, but after 23 h they became more resistant (Lin *et al,* 1998). The hyperresistance to photodynamic therapy was correlated with the induction of H-Ft by hemin in these cells. The authors suggested that the enhanced oxidant resistance observed is due to the ability of Ft to rapidly sequester redox-active iron. Doxorubicin is an anticancer drug that generates ROS in H9c2 cardiomyocytes (embryonic rat heart-derived cell line) and promotes iron-catalysed oxidative damage (Corna *et al,* 2004). Through the action of ROS, it has also been shown that it increased H-Ft levels in these cells, and this has been correlated with the resistance to iron-mediated damage. Oxidised low density lipoprotein (LDL), an oxidant, dramatically stimulated L-Ft in the THP-1 macrophage line but failed to induce either H- or L-Ft in other studies (reviewed in Torti and Torti, 2002). L-Ft has been suggested to have an important role in the protection against oxidative damage due to the presence of antioxidant-responsive element (ARE) in the human L-Ft gene, which was positively regulated by hemin (Hintze and Theil, 2005). The ARE increases the expression of a diverse set of proteins involved in redox homeostasis such as TRx, HO and glutathione.

Levi *et al,* (2001) have described a gene that encodes a mitochondrial ferritin (MtF) located inside the matrix of the human mitochondria. Unlike other mammalian Fts, human MtF is a homodimer of 24 subunits that has a ferroxidase activity significantly lower than the H-chain cytosolic Ft (Bou-Abdallah *et al,* 2005). Iron is transported to the mitochondria for several metabolic processes, specifically haem and [Fe-S] cluster synthesis. Mitochondrial ferritin can efficiently store large

amounts of iron (1) to prevent its participation in Fenton reaction and (2) to protect the cell from iron being escaped during haem and [Fe-S] cluster synthesis. Since mitochondrial chelatable iron has been linked to several human diseases (e.g. Friedreich ataxia, Parkinson's and Alzheimer's disease), a new fluorescent indicator to determine this iron pool was synthesised (Petrat *et al,* 2002). During sideroblastic anaemia, large quantities of iron (due to the blockage of haem synthesis) and high levels of this new ferritin (MtF) appear to be present in the mitochondria. This suggests that MtF is responsible for the detoxification and the trafficking of iron in the mitochondria (reviewed in Arosio and Levi, 2002).

1.4.1.4 Vitamins

Antioxidant protection can also be achieved by vitamins that are available in our diet. Vitamin C (ascorbic acid) exerts its antioxidant levels by scavenging ROS i.e. $O_2^{\bullet-}$ and $OH^{\bullet}$. On the contrary, *in vitro* studies have shown that it has prooxidant properties as it acts as an iron reductant to produce $OH^{\bullet}$, but it has no major physiological relevance as any excess is simply excreted from the body (Halliwell and Gutteridge, 1999). The levels of vitamin C in human plasma were found to be around 10-100 μM (Halliwell and Gutteridge, 1999). Good sources of vitamin C in our diet are vegetables and fresh fruits, especially tomatoes. It has very important roles in the body, in addition of functioning as an antioxidant, it regenerates vitamin E. In lipid peroxidation, vitamin E (a fat soluble vitamin) acts as an inhibitor of the free-radical reaction. Vitamin E has 8 members in its family, the best characterised is α-tocopherol. α-tocopherol, as well as inhibiting lipid peroxidation, it also acts as a scavenger of lipid peroxyl radicals (Cheeseman and Slater, 1993). Vitamin E may also act as a hydrogen donor to ROS, resulting in a less reactive species (Martinez-Cayueta, 1995). Green vegetables and cereal grains are excellent sources of vitamin E. α-tocopherol succinate pre-treatment protected cardiac myocytes against H_2O_2- and $O_2^{\bullet-}$-induced lysosomal damage (Roberg and Öllinger, 1998). α-tocopherol acetate was also involved in preventing UVA-mediated activation of NF-κB that appeared to cause membrane damage to human skin fibroblasts (Vile *et al,* 1995 and Reelfs *et al,* 2004).

1.4.2 Enzymatic antioxidants

1.4.2.1 Glutathione peroxidase (GPx) / Glutathione reductase (GR)

Glutathione peroxidase (GPx) and Glutathione reductase (GR) are present at high concentration in some parts of the human body i.e. liver, kidney, and whole blood. Glutathione peroxidase, first discovered in 1957, can be found in the cytoplasm and the mitochondria. It has four selenium atoms (Se), on its four protein subunits, which are responsible for its activity. Glutathione peroxidase catalyses the reduction of H_2O_2 yielding oxidised glutathione (GSSG):

$$H_2O_2 + 2GSH \xrightarrow{GPx} GSSG + 2H_2O$$

It also catalyses the reduction of lipid hydroperoxides (Martinez-Cayueta, 1995):

$$LOOH + 2GSH \xrightarrow{GPx} GSSG + H_2O + LOH$$

On the other hand GR contains flavin adenine dinucleotide (FAD), as its active site, on its two protein subunits. It is a cytosolic protein. Whilst the conversion of GSH to GSSG is high in normal cells (Halliwell and Gutteridge, 1999), GR acts by reducing oxidised glutathione to GSH.

$$GSSG + NADPH + H^+ \xrightarrow{GR} 2GSH + NADP^+$$

1.4.2.2 Superoxide dismutase (SOD)

SOD exerts its activity to produce H_2O_2 and O_2 from the dismutation of $O_2^{\bullet-}$ (Martinez-Cayueta, 1995).

$$O_2^{\bullet-} + O_2^{\bullet-} + 2H^+ \xrightarrow{SOD} H_2O_2 + O_2$$

In mammalian cells three SODs are present: SOD1, SOD2 and SOD3 (Raha and Robinson, 2000). SOD1 is the cytosolic copper-zinc (CuZn) containing superoxide dismutase (or alternatively CuZnSOD), SOD2 is the intramitochondrial manganese (Mn) superoxide dismutase (or alternatively MnSOD), and SOD3 is the extracellular CuZn superoxide dismutase. Whereas SOD2 (MnSOD) is mostly present in the mitochondria, it is also present in the cytosol at a very low concentration (Halliwell and Gutteridge, 1999).

1.4.2.3 Catalase

Catalase is composed of four protein subunits, each of which have a ferric (Fe^{3+}) haem group bound to its active site (Halliwell and Gutteridge, 1999). It is present in all major body organs and at high concentrations in the liver. Catalase is

mainly located in the peroxisome, a cellular organelle found in the cytoplasm bound by a single membrane. As mentioned in the previous section, H_2O_2 is the product of the dismutation of $O_2^{\bullet-}$. Catalase removes the harmful effects of H_2O_2 (see section 1.3.3) by the following reaction (Martinez-Cayueta, 1995) :

$$2\ H_2O_2 \xrightarrow{\text{catalase}} 2\ H_2O + O_2$$

1.4.2.4 Haem Oxygenase (HO)

Haem oxygenase (HO) is the rate limiting enzyme, found in the endoplasmic reticulum, that catalyses the degradation of haem (a pro-oxidant) and the formation of biliverdin and carbon monoxide (CO), and the release of ferrous iron ions (Halliwell and Gutteridge, 1999):

$$\text{Heam} \xrightarrow{\text{HO}} \text{Biliverdin} + CO + Fe^{2+}$$

Biliverdin is then reduced, by biliverdin reductase, to produce bilirubin (an antioxidant). With a decrease in the pH, the potency of bilirubin as a free radical scavenger is increased (Winrow *et al,* 1993). All three discrete products (i.e. Fe^{2+}, CO, and biliverdin-bilirubin) have vital physiological roles which may be complementary (Snyder and Baranano, 2001). Depending on the cellular redox potential and the metabolic fate of haem iron, HO may have both pro- and antioxidant properties (Ryter and Tyrrell, 2000).

To date, three haem oxygenase isozymes have been identified: HO-1, HO-2 and finally HO-3. HO-1 (the inducible form) and HO-2 (in general; the constitutive form) isozymes are both known to be haem catalyst (Maines *et al,* 1986), HO-3 has a poor haem catalyst activity (Wunder and Potter, 2003). Out of the three, HO-3 is less understood; it is thought to serve primarily as a haem-binding protein (McCoubrey *et al,* 1997 and Weng *et al*, 2003).

While HO-2 is believed to be the constitutive form of HO, HO-1 is a stress-induced enzyme (Keyse and Tyrrell, 1989) which is activated by a number of stimuli such as UV radiation and H_2O_2 in human skin fibroblasts. Since HO-1 mRNA is strongly induced by ROS, this makes it a potential marker for cellular oxidative stress at the mRNA level. It has been proposed that H_2O_2 formation during mitochondrial respiratory chain deficiency (a pro-oxidant state) leads to the overexpression of antioxidant enzymes; GPx activity, GPx and HO-1 mRNAs (Brambilla *et al,* 1997). Glutathione depletion by BSO treatment of human skin fibroblasts lead to a

significant increase in the level of HO mRNA (Lautier *et al,* 1992). It was also 10-fold higher 24 h after either UVA or H_2O_2 treatment. Synthesis of HO-1 but not HO-2 was shown to be induced by glutathione depletion in Chinese hamster ovary cells (Saunders *et al,* 1991). Glutathione depletion also induced HO-1 protein and mRNA in rat brain (Ewing and Maines, 1993). Interestingly, HO-1 was most expressed in the lesions of synovial tissue of patients with RA than in those from the other patient groups (osteoarthritis, and patients with noninflammatory joint disease). Both hemin and auranofin (a disease-modifying antirheumatic drug) induced HO-1 and reduced expression of TNF-α mRNA, LPS-induced secretion of IL-6 and IL-8, and expression of cyclooxygenase 2 in the synovial cell lines (Kobayashi *et al,* 2006).

As mentioned earlier (see section 1.4.1.3), induction of HO-1 by UVA radiation increases the Ft levels up to 3-fold 24-48 hours post-UVA treatment in human skin fibroblasts (Vile and Tyrrell 1993 and Vile *et al,* 1994). The photoimmunoprotective activity of UVA radiation seen in mice has been attributed to the HO induction (Reeve and Tyrrell, 1999). A strong relationship between HO induction and photoimmunoprotection by UVA has been established (Reeve and Domanski, 2002). Cells overexpressing HO have shown hypersensitivity to UVA shortly after hemin treatment (Kvam *et al,* 2000). These cells were no longer hypersensitive to UVA, 24 hours post-hemin treatment. It has also been found that HO-1 is linked to the efflux of iron from the cells, therefore it was suggested that its induction prevents cell damage and death by regulating cellular iron (Ferris *et al,* 1999). Therefore, the HO system has been implicated in antioxidant, anti-inflammatory, and cytoprotective events (Taramelli *et al,* 2000; Ryter and Tyrrell, 2000; Tranter and Jones, 2008).

1.5 Lysosome

Lysosomes were first isolated by Christian de Duve and colleagues in rat liver, later they were found to exist in a variety of cells and tissue (De Duve and Wattiaux, 1966) including animal and plant cells. They are membrane bound organelles filled with around 40 types of hydrolytic enzymes, including cathepsins, proteases, nucleases, lipases, and phospholipases. These enzymes are active under acidic condition (pH around 5.0) and this is maintained by an ATP driven H+ pump located in the lysosomal membrane (Alberts *et al,* 2002). Lysosomes mainly serve as sites for

degradation in the cell and a centre for normal turnover of organelles; it is also the major site of intracellular catabolic processes (Sriram *et al,* 2006).

1.5.1 The role of lysosomal iron in oxidative stress

In animal cells, Ft is consistently found in the cytosol and lysosomes (reviewed in Harrison and Arosio, 1996). The lysosomal degradation of metalloproteins (e.g. cytochromes) and ferruginous material (e.g. Ft) ensures the intralysosomal availability of redox-active low-molecular-weight chelatable iron i.e. LIP (Ciechanover, 2005). By laser scanning microscopic study, chelatable iron was found to be 2-3 fold higher in the endosomal/lysosomal apparatus than in the cytosol of isolated rat hepatocytes and rat liver endothelial cells (Petrat *et al,* 2001). Therefore a major part of the LIP might be present in the lysosomes (Kakhlon and Cabantchik, 2002). This, along with the $OH^{\bullet}$ produced by Fenton reaction, accounts for the sensitivity of lysosomes to oxidative stress. Also, since the lysosomal environment is acidic it facilitates the release of iron from proteins and it enhances its reduction to ferrous iron, therefore the oxidative damage is enhanced.

Treatment of macrophage–like J-774 cells with a bolus dose of 0.5 mM H_2O_2 caused lysosomal damage and plasma membrane blebbing as an early sign of damage (Brunk *et al,* 1995[b]). These effects were prevented by pre-treatment with DFO, which is taken up by endocytosis and stored intralysosomally. DFO, being a hydrophilic compound, has limited cellular penetration (Rice-Evans *et al,* 1989 and Link *et al,* 2003) therefore it enters the cells by endocytosis and finally accumulates in the lysosomes (Lloyd *et al,* 1991 and Cable and Lloyd, 1999). When the cells are not exposed to the drug anymore, DFO can then slowly leave the lysosomal compartment, reaching the cytosol and subsequently the extracellular fluid. The protective effects of DFO were prevented by the inhibition of its endocytosis. Lipid peroxidation, destabilisation of lysosomes, and eventually cell death were seen when rat hepatocytes were treated with naphthazarin, a redox-cycling drug which mainly exerts its toxicity through oxidative stress (Öllinger and Brunk, 1995). Pre-treatment with DFO protected the cells from lysosomal destabilisation and cell death. Exposure to a low steady state of H_2O_2 (25 μM) in Jurkat T cells induces apoptosis, which is consequence of lysosomal rupture (Antunes *et al,* 2001). Pre-exposure to DFO preserved lysosomal stability and consequently protected the cells from apoptosis. Ogawa *et al,* (2004) have shown that ROS formation was augmented in the

mitochondria and the lysosomes of irradiated T cells in the presence of a low concentration of H_2O_2 (0.1 mM) when compared with those treated only with irradiation. Both lysosomal and cellular damage were prevented when cells were pre-treated with the lipophilic chelator salicylaldehyde isonicotinoyl hydrazone (SIH) and/or DFO prior to their exposure to H_2O_2, since LIP was efficiently decreased (Kurz *et al,* 2006).

When human fibroblasts were irradiated with a moderate dose of blue light, this (moderate) stress of photo-oxidation resulted in apoptosis (Brunk *et al,* 1997). The blue light-mediated damage appears to be accompanied by leakage of lysosomal contents including hydrolytic enzymes, such as cathepsin D (CATH D) (Roberg and Öllinger, 1998). Severe photo-oxidation, on the other hand, results in severe lysosomal damage and consequently cellular necrosis, therefore the cascade of events is dependent on the magnitude of the insult. Treatment of macrophages with oxidised LDL induced lysosomal destabilisation, relocation of CATH D to the cytosol, and increased cathepsin L (CATH L) cytosolic activity (Li *et al,* 1998). During lysosomal membrane permeabilisation, cathepsin B (CATH B) and CATH D have been documented to be released from the lysosomes (Erdal *et al,* 2005). Treatment of human skin fibroblasts with UVA radiation (320 – 380 nm) lead to an immediate release of iron via the proteolysis of Ft (Pourzand *et al,* 1999). This study provided the first evidence that UVA-mediated Ft degradation originates from the destabilization of lysosomal membranes and the subsequent leakage of proteolytic enzymes. Chymotrypsin, a lysosomal protease that is responsible for the degradation of Ft molecules in lysosomes, was around 3-fold higher in the cytosolic fraction of UVA-treated cells when compared with unirradiated controls. The degradation of Ft was prevented when cells were pretreated with Chymotrypsin-specific lysosomal protease inhibitors (i.e. Chymostatin and Leupeptin). Delocalisation of CATH B from the lysosomal compartment to the cytosol was observed after UVA radiation in human skin fibroblasts (Basu-Modak *et al,* 2006). When human skin fibroblasts were pre-treated with catechins (flavonoid constituents with protective properties predominantly against oxidative stress) prior to UVA-radiation; iron release was prevented (Basu-Modak *et al,* 2006). Based on measurements of lysosomal integrity (Lysosensor assay and CATH B immunocytochemistry), the data strongly indicate that catechins protect against lysosomal damage induced by UVA. 40 Gy radiation of radio-resistant lymphoma (J774) cells increased the 'loose' iron by nearly 5-fold

(Persson *et al,* 2005). This increase was correlated with lysosomal rupture and consequent cell death following a second dose of 20 Gy. Addition of DFO before the first or second radiation stabilised the lysosomal membrane and largely prevented cell death. Cytochemical analysis from this study revealed that the most redox-active iron lies within the lysosomes. Unless catalytically active iron is present, neither superoxide radicals nor H_2O_2 induced any lysosomal damage by themselves in lysosome-enriched mitochondrial fraction of a rat liver homogenate (Zdolsek and Svensson, 1993). Overall, these results support the idea that oxidative stress *per se* is not injurious but it requires the presence of intralysosomal redox active iron (reviewed in Terman *et al,* 2006).

1.5.2 The role of lysosomal iron in rheumatoid arthritis

Lysosomes are abundant in the lining cells of the synovial membrane. There is a considerable amount of evidence to support that lysosomal membrane damage is linked to acute and chronic inflammation in joints. The lysosomal membrane contains large amount of PUFAs (see section 1.3.3) that are susceptible to lipid peroxidation. When lipid peroxidation occurs the membrane is disrupted and this releases hydrolytic enzymes which will potentiate inflammation (Blake *et al,* 1981). Increased lysosomal enzyme activity has been found in the synovial fluid and membrane in RA. It is evident that materials in lysosomes can provoke inflammation, tissue injury and breakdown of connective tissue (Weissmann, 1972).

It was concluded that the extensive tissue breakdown in adjuvant arthritis is due to the release and degradative action of lysosomal enzymes on connective tissue components (Anderson, 1970). Administration of two non-steroidal anti-inflammatory was found to increase the lysosomal stability in adjuvant arthritic rats (Reddy and Dhar, 1987). Oral administration of several anti-inflammatory drugs such as phenlybutazone and hydrocortisone decreased both the enzymatic activity and oedema. The study concluded that these drugs may act by inhibiting lysosomal enzyme, stabilising cell or lysosomal membrane, or decreasing influx of leucocytes. In patients with RA, high enzyme levels were found and this was correlated with damage to the joints (Muirden, 1972). In all patients with RA, elevated cysteine protease CATH B, dipeptidyl peptidases I, asparate protease CATH D and two glycosidases were found (Sohar *et al,* 2002). The magnitude of the increased activity was correlated with duration of the disease.

Recently, *Cleome gynandra* was found to markedly decrease lysosomal enzymes in both the plasma and the liver of adjuvant-induced arthritic rats (Narendhirakannan *et al,* 2007). *Cleome gynandra*, a common weed which grows in tropical countries, is commonly used to treat rheumatism. It was proposed that *Cleome gynandra* might exert its anti-inflammatory actions by stabilizing the lysosomal membrane and thereby preventing the release of lysosomal enzymes. The above findings support the concept that lysosomal enzymes are involved in connective tissue damage and that lysosomes play a crucial role in the pathogenesis of RA.

1.6 The NF-κB transcription factor

Nuclear Factor κB (NF-κB) is a transcription factor that was first discovered in 1986, as a nuclear factor that binds to a site in the immunoglobulin κ light chain enhancer in B cells only, hence its name (Sen and Baltimore, 1986). Within a few years, it was found that NF-κB is present virtually in all cell types. The NF-κB regulates the transcription of many genes involved in immune and inflammatory responses, and apoptosis (Ghosh and Karin, 2002). The activation of NF-κB has been implicated in various diseases (Baldwin, 2001) e.g. rheumatoid arthritis, cancer, AIDS, inflammatory bowel disease etc. The NF-κB is a dimer of proteins that belongs to the NF-κB/Rel family.

1.6.1 The NF-κB/Rel family

In mammalian cells the NF-κB/Rel family consists of 5 members; RelA (p65), RelB, c-Rel, p50 (NF-κB 1), and p52 (NF-κB 2). The first three are produced within the cells as transcriptionally active proteins, whereas p50 and p52 are generated from p105 and p100, respectively, by proteolytical degradation (Mercurio and Manning, 1999). They can form homo- and hetero-dimers with each other but certain dimers do not exist i.e. RelB can only hetero-dimerise with p50 or p52 (Ryseck *et al,* 1995). The "classical" NF-κB dimer is RelA/p50 given that it is the most abundant and biologically active within the cells, and it was also the first form to be identified (Huxford *et al,* 1998 and Karin and Ben-Neriah, 2000).

This family possesses an N terminal region of around 300 amino acids called the Rel-homology domain (RHD), hence the family's name. The RHD is responsible

for dimerisation with other member of the same family, nuclear translocation since it has a nuclear localization sequence (NLS), DNA binding, and the interactive domains of the inhibitory IκB proteins (Siebenlist *et al,* 1994).

1.6.2 The IκB family

Members of this family include IκBα, IκBβ, IκBγ, IκBε, p100, p105, and Bcl-3. They contain six to eight ankyrin repeat domains (ARD) which are 33 amino acids in length (Siebenlist *et al,* 1994). These ARDs regulate the binding to RHD and shield the NLS of NF-κB (Karin and Ben-Neriah, 2000). The protein that is best characterised and the first cloned is IκBα. In spite of the fact that the main function of IκBα is to bind to NF-κB proteins to maintain them in the cytoplasm, it is also involved in the removal of NF-κB from the nucleus (reviewed by Yamamoto and Gaynor, 2004). Free IκBα has a very short half-life ranging from 70 seconds to less that 1 hour depending on the cell line (Ginn-Pease and Whisler, 1998).

1.6.3 The IκB kinase (IKK) complex

The IKK complex is a very high molecular weight protein complex composed of several polypeptides (DiDonato *et al,* 1997). It consists of three IKK polypeptides; IKKα (IKK1), IKKβ (IKK2), and IKKγ. IKKα and IKKβ are catalytic subunits whereas IKKγ is regulatory (reviewed by Karin, 1999). It was revealed that IKK activity is dependent on its phosphorylation and this is achieved by NF-κB inducing kinase (NIK) (Malinin *et al,* 1997). NIK is a member of the mitogen-activating protein kinase kinase kinase (MAPK3) family which phosphorylates IKKα specifically at Ser-176 (Ling *et al,* 1998).

1.6.3 NF-κB activation pathways

In most cells NF-κB is present in a latent state retained in the cytoplasm, sequestered to IκBα. IκBα degradation has been observed with all NF-κB inducers tested (Thanos and Maniatis, 1995). Activation of NF-κB has been shown with a variety of stimuli including inflammatory cytokines, bacterial products, bacteria, viruses, and oxidative stress (Pahl, 1999). Its activation can be divided into two pathways, the ‘classical’ and the ‘alternative’ pathway (Senftleben *et al,* 2001).

1.6.3.1 The 'classical' pathway

After cell stimulation, the IKK complex is activated by the phosphorylation of particular serine residues within the activation loop of IKKα and IKKβ (reviewed by Yamamoto and Gaynor, 2004). Then the IκB protein gets phosphorylated, at Ser 32 and Ser 36 in IκBα and Ser 19 and Ser 23 in IκBβ (Chen *et al,* 1995 and DiDonato *et al,* 1996), by the IKK complex. This phosphorylation marks the protein for polyubiquitination (Maniatis, 1999 and Sun and Chen, 2004) by an ubiquitin containing complex at two lysines, Lys-21 and Lys-22 (Scherer *et al,* 1995). Roff *et al,* (1996) emphasised the importance of the degradation of IκB in the activation of NF-κB, IκB is then selectively degraded by 26S proteasome. Next the NLS will be exposed and this causes nuclear translocation of NF-κB to the nucleus. The NF-κB would then bind to the *cis*-acting κB sites (5'-GGGPuNNPyPyCC-3') in the DNA to initiate transcription (Pahl, 1999) of the target genes. This pathway is suggested to be involved in the innate immunity whereas the 'alternative' pathway is involved in the adaptive immunity (Bonizzi and Karin, 2004).

The involvement of IKK complex in NF-κB activation does not occur in two cases. One of these is the activation of NF-κB by short-wavelength ultraviolet C (UVC) light accompanying the degradation of IκBα. In UVC treated cells, neither IKK activation nor IκBα phosphorylation was observed (Li and Karin, 1998). The second exception was tyrosine (Tyr-42) phosphorylation of IκBα (Imbert *et al,* 1996) which was observed during the treatment of cells with tyrosine phosphatase inhibitor (pervanadate), hypoxia (Koong *et al,* 1994), upon reoxygenation of hypoxic cells, or after H_2O_2 treatment (Schoonbroodt *et al,* 2000). This led to the dissociation of IκBα from NF-κB. The degradation of IκB by different pathways is dependent on the cell-type and the kind of stimulus.

Under specific circumstances, such as nutrient deprivation, other proteolytic systems have been implicated such as lysosomal degradation. In Chinese hamster ovary cells, the increase in IκB degradation has been completely inhibited by lysosomal inhibitors (Cuervo *et al,* 1998) and the half-life of IκBα pool in the lysosomes has been significantly increased by the presence of antioxidants, suggesting that intracellular ROS mediates IκBα degradation in the lysosomes. This results in an increase in the NF-κB activity.

1.6.3.2 The 'alternative' pathway

Several years ago an 'alternative' pathway leading to NF-κB activation was reported that occurs specifically in B cells (Senftleben *et al,* 2001 and reviewed in Simmonds and Foxwell, 2008). Unlike the classical pathway, this pathway is dependent only on IKKα, and not IKKβ nor IKKγ. RelB/p100 is the target molecule of the IKKα homodimers in this pathway. Following cell stimulation, the IKKα homodimers get phosphorylated at two C-terminal sites. This generates the polyubiquitination and proteasomal degradation of only the inhibitory C-terminal half of p100, and not the whole protein. This would cause the processing of p52 from p100 (see section 1.6.1). Subsequently this would result in the nuclear translocation of RelB/p52 dimer to induce gene expression (reviewed in Yamamoto and Gaynor, 2004).

1.6.4 Redox regulation of NF-κB

*Red*uction-*ox*idation or "Redox" is a term introduced to classify the oxidation and reduction reactions that have occurred. Oxidation is the loss of electrons while reduction is the gain of electrons (Langrehr, 1971). The intracellular redox within the cells is pivotal for various biological events to occur i.e. enzyme activation, DNA synthesis, cell cycle regulation, and transcriptional activation of several genes (Arrigo, 1999). Recently, much interest has been seen with regard to the redox regulation of transcription factors, including NF-κB**.**

Glutathione acts as a homeostatic redox buffer (see section 1.4.1.1). It was reported that partial depletion of intracellular glutathione in human T cell line inhibits activation and nuclear translocation of NF-κB whereas the administration of extracellular cysteine inhibits the DNA-binding activity of the NF-κB complex. This inhibition is suggested to be caused by the elevation of GSSG levels (Mihm *et al,* 1995). Therefore, it was proposed that GSSG was necessary for NF-κB activation in the cytoplasm, while GSH was required for the NF-κB DNA binding (Droge *et al,* 1994). Treatment of human promonocytic (U937) cells with BSO significantly decreased GSH, increased ROS production and activated NF-κB as a survival cell response against oxidative stress (Filomeni *et al,* 2005).

In addition to these observations, TRx overexpression in the cytoplasm suppresses the degradation of IκBα (Hirota *et al,* 1999). Therefore an oxidizing

environment is required in the cytoplasm for the activation of NF-κB (Ginn-Pease and Whisler, 1998). On the other hand a reducing environment was shown to be necessary in the nucleus. The reduction of the cysteine residue at position 62 (Cys-62) in the NF-κB is essential for its DNA binding. This is thought to be achieved by TRx which regulates the NF-κB binding by reducing Cys-62 (Matthews *et al,* 1992). It was also demonstrated that TRx translocates from the cytoplasm to the nucleus in response to UVB radiation and TNF-α (Hirota *et al,* 1999), which are both stimuli of NF-κB activation. It is important to mention that the oxidation of Cys-62 resulted in the inhibition of DNA binding (Arrigo, 1999).

1.6.5 Oxidative stress and NF-κB activation

NF-κB was the first transcription factor shown to be regulated by oxidative stress. Several lines of evidence support this hypothesis. The majority of the agents that induce NF-κB activity may be involved in ROS synthesis (Schreck *et al,* 1991). Furthermore, NF-κB activation has been shown to be induced directly by ROS i.e. H_2O_2 and by SOD overexpression, and interestingly was prevented by catalase overexpression (Schmidt *et al,* 1995). Finally, antioxidants were shown to be effective in the blockage of NF-κB activation (reviewed in Schreck *et al,* 1992).

The IκBα phosphorylation and degradation was shown to be responsive to oxidative stress and blocked by antioxidants (Li and Karin, 1999). It was proposed that ROS generated would induce NF-κB activation by activating IKK which consequently leads to the dissociation of IκBα (Sen *et al,* 2004). In several cell lines NF-κB activation was induced by ROS in the form of H_2O_2 (Byun *et al,* 2002 and Li and Karin, 1999). UVC (200 – 290 nm), UVB (290 – 320 nm), and for the first time UVA (320 – 380 nm) via oxidative stress was able to active NF-κB in human skin fibroblasts (Vile *et al,* 1995). Labile-iron release by UVA was found to be a key regulator of UVA-induced NF-κB activation (Reelfs *et al,* 2004). Specific membrane antioxidants (butylated hydroxytoluene and α-tocopherol) that inhibit lipid peroxidation, have inhibited UVA radiation-dependent activation of NF-κB. Antioxidants may act to prevent IκBα phosphorylation and degradation by (i) scavenging radicals, (ii) chelating metal ions to prevent Fenton reaction (see section 1.3.3), (iii) maintaining the activity of other antioxidative enzymes, or (iv) inhibiting the activity of oxidising enzymes (Schreck and Baeuerle, 1992). However it was proven that a number of other cell lines were not sensitive to H_2O_2 treatment,

including monocytic cells, astrocytoma, standard Jurkats except at high concentration, J. Jhan lymphoblastoid T cells, and some other cell lines (Bowie and O'Neill, 2000). Interestingly Lahdenpohja *et al* (1998) have reported that the ROS-forming capacity is weaker after chronic oxidative stress to Jurkat cell lines, and subsequently this has lead to the decreased NF-κB transcription since IκBα is not effectively phosphorylated and degraded.

1.6.6 NF-κB and rheumatoid arthritis

NF-κB has been proposed to have a central role in inflammation (Tak and Firestein, 2001). Several studies have shown the link between the activation of NF-κB and a number of inflammatory diseases. Indeed, the NF-κB complex was found to be highly activated in patients with chronic inflammatory conditions such as rheumatoid arthritis (Handel *et al,* 1995; Asahara *et al,* 1995; Marok *et al,* 1996; Gilston *et al,* 1997 and Han *et al,* 1998). It was also markedly increased in murine collagen-induced arthritis (CIA) (Han *et al,* 1998), and in adjuvant arthritis in rats and in carrageenan rat air pouch model of inflammation (Ellis *et al,* 2000). It is not surprising to know that target genes for NF-κB include many genes that are involved in the inflammatory response, such as IL-1, TNF-α, IL-6, and inducible nitric oxide synthase (Baeuerle and Henkel, 1994).

The activation of NF-κB protected animal models of RA against apoptosis and provided a potential link between inflammation and hyperplasia (Miagkov *et al,* 1998). Inhibition of NF-κB in T cells resulted in reducing the NF-κB regulated gene expression (Gerlag *et al,* 2000) and decreasing CIA (Seethraman *et al,* 1999 and Gerlag *et al,* 2000). IMD-0506, an inhibitor of IKK, suppressed the nuclear translocation of NF-κB and the phosphorylation of IκBα induced by TNF-α in fibroblast-like synoviocytes (Okazaki *et al,* 2005). This also suppressed the production of inflammatory cytokines. Spontaneous production of TNF-α and other pro-inflammatory cytokines is NF-κB dependent in rheumatoid synovial tissue (Bondeson *et al,* 1999). Treatment with dexamethasone resulted in reducing the number of cells stained for activated NF-κB in carrageenan rat air pouch model of inflammation (Ellis *et al,* 2000).

Several drugs that are used for treating RA are either inhibitors of NF-κB activation (e.g. sulfasalazine and gold compounds), or they block IκB kinase (e.g. aspirin and sodium salicylate), or they increase IκBα (e.g. glucocorticoids) (Jue *et al,*

1999). Therefore several papers have proposed that the blockage of NF-κB activation would be a good therapeutic target for both acute and chronic inflammation (Lee *et al,* 1998; Epinat and Gilmore, 1999; Feldmann *et al,* 2002; Wang *et al,* 2006; Tergaonkar, 2006). However, because of its central role in many normal biological processes, global inhibition may not be therapeutically viable (Aya *et al,* 2005). Indeed, inhibition of the NF-κB activation can result in exacerbation of inflammation if TNF-α production by macrophages is not controlled (reviewed in Simmonds and Foxwell, 2008).

1.6.7 The role of iron in NF-κB activation

In synovial cells, the NF-κB is activated and this activation was correlated with increased IRP activity (Guillén *et al,* 1998). The addition of iron in the lungs of rat demonstrated Ft induction, oxidative stress, elevated IL-1 levels, as well as NF-κB activation (Zhou *et al,* 2003). Immediate labile-iron release by UVA is a key regulator of UVA-induced NF-κB activation in human skin fibroblasts (Reelfs *et al,* 2004). Studies using liver macrophages and rat brain microglia in cell culture have provided evidence to support the direct participation of chelatable iron in NF-κB activation and its prevention with iron chelators such as DFO (Youdim *et al,* 1999). Increase in the intracellular labile iron leads to IKK and NF-κB activation in response to LPS or TNF-α in macrophages, and iron chelators abrogated this response (Xiong *et al,* 2003). It was therefore proposed that iron is responsible for the NF-κB activation in hepatic macrophages (Xiong *et al,* 2004). Ferritin (heavy chain) was shown to be rapidly induced by NF-κB activation, which had an antiapoptotic activity, in response to TNF-α treatment (Pham *et al,* 2004). This induction suppressed the accumulation of ROS which is achieved through iron sequestration. This study suggests that H-Ft to be an essential mediator of antioxidant and protective activities of NF-κB. Recently, Tacchini *et al,* (2008) have demonstrated that the upregulation of NF-κB by inflammatory signals induces a rapid activation of the transcription factor hypoxia-inducible factor 1 (HIF-1)-dependent TfR1 expression and iron uptake in macrophages.

1.7 Aims and objectives of the project

The synovial fluid and tissue of patients suffering from RA contain high levels of free 'labile' iron but its origin has not been properly investigated. Furthermore because of the phenomenon of ischemia-reperfusion, synovial cells' components are chronically exposed to ROS. We therefore sought to investigate the mechanism underlying the adaptation of synovial T cells to H_2O_2 by evaluating changes in antioxidant molecules and enzymes, intracellular labile iron, and NF-κB activation. Several studies have also shown a role for iron in the progression of inflammatory diseases such as RA (see section 1.2.4 and 1.2.5); but none, to our knowledge, had differentiated between the role of iron in both acute and chronic phases of the disease. Therefore, to investigate the role of iron in both acute and chronic oxidative conditions was necessary.

To achieve our aims, we have extensively studied two cell lines which were Jurkat cells, human T-cell leukaemia cell line. One of them was the parental cell line (J16 cell line) and the other was derived from the parental cell line and gradually adapted to be resistant to H_2O_2 (HJ16 cell line). In established RA, T cells represent the most abundant inflammatory cells in the joint (Aya *et al,* 2005 and Deng and Lenardo, 2006). Experimental and clinical evidence for T cell involvement in the pathology of RA is compelling. Indeed, activated synovial T cells are key initiators and orchestrators of inflammation in RA, and therefore they represent key cellular targets for therapy (Cope *et al,* 2007). Jurkat cells are widely used in the study of T-cell activation processes (Schreck *et al,* 1991) and they are considered as critical determinants of the extent and chronicity of an inflammatory response. The Jurkat T cell lines composed of 'parental J16' and 'H_2O_2 resistant HJ16' provide a good model to study the differential response of cells to both acute and chronic exposure. We have used the parental cell line to mimic the acute condition after relevant treatments of H_2O_2 and the resistant cell line to mimic the chronic condition. The HJ16 cell line that was established following the gradual adaptation of the J16 cell line to increasing concentrations of oxidising agent H_2O_2, provides us with a useful model to mimic the chronic exposure of T cells in synovium to ROS that is almost certainly involved in the pathology of RA.

We used H_2O_2 as an oxidising agent, since this is commonly used to study the effect of ROS in biochemical pathways. Furthermore it is likely that H_2O_2 is produced in the synovial membrane during the ischemia-reperfusion cycles. Tissues,

in different pathological conditions, are confronted with elevated H_2O_2 concentrations derived either extra- or intracellularly. Hydrogen peroxide is generated during normal metabolism and produced in large amounts by phagocytic cells during inflammation (Hampton and Orrenius, 1997). Because it is uncharged and soluble in both aqueous and lipid phases, H_2O_2 would be expected to distribute rapidly between cellular compartments (Hyslop *et al,* 1995).

In addition to UVA (Morliere *et al,* 1997 and Pourzand *et al,* 1999) and visible light irradiation (Ohishi *et al,* 2005), it has already been shown that the exposure of cells to H_2O_2 (see section 1.3.6) provokes an increase in the LIP that correlates with cell damage and necrotic cell death, although the mechanisms involved has not yet been fully understood. To understand this phenomenon, we have investigated the role of LIP, Ft, and HO (i.e. HO-1 and HO-2) in our cell model. The lysosomal compartment seems to contain the major important cellular pool of labile iron (Petrat *et al,* 2001 and Persson *et al,* 2003) since the degradation of many macromolecules that are rich in iron (e.g. ferritin and mitochondrial electron-transport complexes) occurs in the lysosomes (Radisky and Kaplan, 1998 and Kurz *et al,* 2007) making these organelles vulnerable to oxidative stress (Persson *et al,* 2005). Therefore, understanding the link between lysosomal membrane damage and the above parameters may define pathological mechanisms associated with oxidative stress and lysosomal activity.

The potentially harmful free 'labile' iron is recognised as an important promoter of oxidative stress through aiding the production of ROS and thus a potential mediator of the inflammatory process in RA. Previous studies carried out by A. Yiakouvaki in this laboratory (PhD Thesis, 2003 – University of Bath) have provided us with a link between the amount of H_2O_2-induced labile iron release and the extent of oxidative damage and cell death in Jurkat T cells. Furthermore, the study has shown that adaptation of Jurkat T cells to H_2O_2 can influence the basal level of antioxidant enzymes that is likely to contribute to the resistance of the HJ16 cells to H_2O_2 insult. This thesis has continued the study of Yiakouvaki (2003) by further characterising the differential response of parental J16 and H_2O_2-adapted/resistant HJ16 Jurkat T cells to H_2O_2 insult with special focus on (1) The role of antioxidant systems (e.g. GSH/GSSG, HO, and Ft); (2) The role of NF-κB activation; (3) The role of iron; and (4) The role of lysosomes.

In addition to the Jurkat cells, we have performed preliminary studies on a

series of primary human and rat fibroblasts. The human fibroblasts were developed and cultured in our laboratory from human synovial tissues; normal (HN-1), rheumatoid arthritic (HRA-1) and osteoarthritic patients (HOA-1). In addition to the human cells, two primary rat synoviocytes were kindly provided by Dr. Vivienne Winrow (School for Health, University of Bath, UK) for the purpose of our study. The latter were isolated from normal Wistar rats (VW-1) and Wistar rats with adjuvant arthritis (AAVW-1). To gain insight into levels of synovial intracellular iron levels, the labile plasma iron was also measured on a series of normal, RA and OA synovial fluid.

CHAPTER TWO

MATERIALS AND METHODS

2.1 Chemicals and Reagents

Cell culture materials were obtained from Gibco (Germany) except for fetal bovine serum (PAA Laboratories, Austria) and RPMI-1640 medium (Promocell, Germany). All chemicals were from Sigma-Aldrich Chemical (Poole, UK) unless otherwise indicated. Protease inhibitors cocktail tablets, Annexin-V-FLUOS, Klenow enzyme, and Bovine Serum Albumin (BSA) were supplied from Roche (Mannheim, Germany). Glutathione reductase, Hydrogen peroxide solution, and Mowiol® 4-88 were obtained from Calbiochem (CN Biosciences LTD, Nottingham). Dimethyl sulphoxide and Nonident P-40 was purchased from VWR International Ltd (Leicestershire, England). Antibodies for immunocytochemistry (p65, Cathepsin-B and Oct-1) were purchased from Santa Cruz Biotechnology, Inc. (Santa Cruz, California). CA-AM (Calcein-acetoxymethyl ester) and LysoSensor™ Green DND-153 were purchased from Molecular Probes (Leiden, Netherlands). Desferrioxamine mesylate Ph. Eur. (DFO) was purchased from Ciba-Geigy laboratories (Basel, Switzerland). [α^{32}P]-dATP was obtained from Amersham Biosciences UK Limited (Buckinghamshire, England). Stock solutions (100 mM) of deoxynucleotide triphosphates (dNTPs) such as dCTP, dGTP, and dTTP were purchased from Promega (Madison, USA).

2.2 Cell Culture

The Jurkat J16 cells are a human T-cell leukaemia cell line. The HJ16 cells are a polyclonal H_2O_2 resistant cell line which were derived from the J16 cell line after gradual adaptation to 3mM H_2O_2. In this process, HJ16 cells were treated with increasing concentration of H_2O_2 (i.e. from 0.1 mM to 3 mM) at weekly to fortnightly intervals. After each treatment the surviving cells were allowed to recover normal growth characteristics before further exposure to a higher concentration of

H_2O_2. Following this adaptation, stocks of HJ16 cells were stored in Liquid Nitrogen to ensure their resistance to H_2O_2. The J16 and HJ16 cell lines were kindly provided by Dr. N.D Hall (Pharmacy and Pharmacology, University of Bath, UK). Since in an independent study from our laboratory (i.e. Yiakouvaki, 2003) it was found that HJ16 cells had 3.4-fold higher cell volume than J16 cells (i.e. J16 cells: 0.47 ± 0.08 pl and HJ16: 1.6 ± 0.19 pl), where applicable, normalisation of the data in this thesis was always performed to protein concentration and not to the cell number/cell volume.

Both cell lines were cultured routinely in RPMI-1640 medium supplemented with 10% v/v heat inactivated fetal bovine serum (FBS), L-Glutamine (2 mM), Penicillin/Streptomycin (50 IU/ml each) and 2.7% v/v sodium bicarbonate. They were incubated at 37°C in a humidified atmosphere with 5% CO_2.

2.3 Treatments

2.3.1 Hydrogen peroxide (H_2O_2) treatment

Stock solution: 176mM in phosphate buffered saline (PBS)

Hydrogen peroxide (H_2O_2) solutions were freshly prepared from a 30% stock solution. Treatments were performed in serum free media (SFM) to prevent the degradation of H_2O_2 by the catalase present in the serum. Cells were incubated with the relevant concentration of H_2O_2 for 30 minutes. After centrifugation, they were resuspended and incubated in the conditioned media for the times indicated in the Results section (see Chapter Three). The J16 and HJ16 cell lines were both tested routinely during the experimental work to demonstrate their differential sensitivity to H_2O_2 treatment.

2.3.2 Buthionine-[S,R]sulfoximine (BSO) treatment

Stock solution: 50mM in phosphate buffered saline (PBS)

Unless otherwise stated, cells were incubated with 25 μM BSO for 18 h at 37°C in the conditioned media prior to experimentation.

2.3.3 DFO treatment

Stock solution: 150 mM in H_2O

Unless otherwise stated, cells were treated with 100 µM of DFO for 18 h at 37°C prior to experimentation.

2.3.4 Hemin treatment

Stock solution: 20 mM in dimethyl sulphoxide.

Unless otherwise stated, cells were treated with 20 µM of hemin for 18 h at 37°C prior to experimentation.

2.4 MTT Assay

The MTT assay is widely used in cell proliferation and cytotoxicity assays (Berridge *et al,* 1996). It is a sensitive colorimetric assay (Mosmann, 1983 and Doyle and Griffiths, 1998) that was performed to determine the viability of cells after relevant treatments. Cellular and mitochondrial dehydrogenase enzyme converts MTT [3-(4,5-dimethylthiazol-2-yl)-2,5-diphenyl tetrazolium bromide], a yellow water-soluble substrate, into a dark blue formazan product that is insoluble in water. The amount of formazan produced is directly proportional to the viable cell number.

The MTT stock solution of 5mg/ml in PBS was filtered through a 0.2 µm filter (Ministart®, Germany) for sterilisation and stored at –20ºC. On the day of the experiment and after the relevant treatments, the pellets were resuspended in SFM containing MTT stock solution at a final concentration of 0.5mg/ml. From this solution, 100-200 µl were placed, in triplicate, into a 96 well microplate. The 96-well microplate was then incubated for 3h at 37ºC. Then the MTT / SFM solution was aspirated and 50-200 µl of dimethyl sulphoxide (DMSO) was added to each well. Finally, the plate was swirled for 3 minutes by a 3D rocking platform (Stuart Scientific, UK) and the absorbance was read by VERSAmax™ (Molecular devices, California) at 550 nm.

2.5 Flow Cytometric Analysis

Quantification of apoptotic, necrotic, and live cells were evaluated by flow cytometry. Apoptotic lymphocytes were shown to express phosphatidylserine (PS) on the outer layer of the plasma membrane (Fadok *et al,* 1992). In the early stages of apoptosis, PS translocates from the inner part of the plasma membrane to the outer layer. Annexin-V-FLUOS is a phospholipid binding protein with a high affinity for PS. Therefore it is suitable for the detection of apoptotic cells. On the other hand, necrotic cells that lose cell membrane integrity are stained with both Annexin-V-FLUOS and Propidium Iodide (PI). Therefore, Annexin-V-FLUOS and PI double-staining can differentiate between necrotic and apoptotic cells.

After relevant treatments and incubation periods, cells were collected and washed with PBS. Cells were then resuspended in 100 µl of incubation buffer (10 mM Hepes/NaOH pH 7.4, 140 mM NaCl, 5 mM $CaCl_2$) containing Annexin-V-FLUOS (20µl/ml) and PI (20µl/ml). Samples were then transferred to a 5ml polystyrene round-bottom tube and incubated for 10-15 minutes at room temperature (RT) in a dark place. Data analysis was performed using CellQuest software (Becton-Dickinson, Erembodegem, Belgium).

2.6 Protein Measurements

Protein concentrations were measured according to the method of Bradford (1976) with slight modification. This modification was performed to enable the measurements of the protein content to be carried out in the 96-well plate to decrease the amount of protein extract used. To calibrate the standard curve, bovine serum albumin (BSA, 2 mg/ml) was first diluted (1:1) with MilliQ water (i.e. to 1 mg/ml) and used at final concentrations of 0, 1, 2, 4, 6, 10, 15, and 20 mg/ml. The total volume of cellular extract (1-5 µl) or BSA (0-20 µl) with MilliQ water used in the each well was 160 µl, done in duplicates. 40 µl of Bio-rad Protein Reagent (Bio-rad, 500-0006) was finally added, and the solution was thoroughly mixed with a pipette (preferably, a multichannel pipette). The absorbance was read by VERSAmax™ (Molecular devices, California) at 595 nm filter.

2.7 Glutathione Measurements

Total intracellular glutathione was measured according to the spectrophotometric method developed by Tietze (1969). It is an enzymatic recycling procedure which offers a high sensitivity rate. Glutathione is assayed by a system in which it is readily oxidised by 5,5'-dithiobis(2-nitrobenzoic acid) DTNB and reduced by NADPH in the presence of glutathione reductase (GR). The rate of 2-nitro-5-thiobenzoic acid formation is monitored and the glutathione is determined by the comparison of the result with a standard curve with the known amounts of glutathione (Griffith, 1980 and Pourzand *et al,* 2000).

The standard curve consists of GSSG stock solution diluted in [5% TCA in 2 mM EDTA] in a range of 0.01 – 2 μM. Cells (1.0×10^6) were incubated with BSO for 18 h (see section 2.3.2). After the incubation period, the pellets were resuspended in cold PBS and then extracted in a freshly prepared mixture of [5% TCA in 2 mM EDTA] in order to give 500μL per 1.0×10^6 of cells.

100 μl samples from either the stock solution (0.01 – 2 μM) or the treated cells were transferred to an eppendorf tube containing 1ml of phosphate buffer, 50 μl of NADPH (5 mM in 0.5% $NaHCO_3$), and 20 μl of freshly prepared DTNB (1.5 mg/ml in 0.5% $NaHCO_3$). The eppendorf tube was then placed in a 25°C water bath for 10 minutes. Next, 100μl of GR (18 u/ml in phosphate buffer) was added to the mixture and change in absorbance was monitored by a Uvikon 922 spectrophotometer (Kontron instruments, Italy) for 6 minutes at 412 nm (25°C).

The total intracellular glutathione was then normalised by two determinations, cell count and total cellular protein. For this purpose, either the viability of cells were assessed using a haemocytometer and the cells were stained by Trypan blue (Doyle and Griffiths, 1998), or the cells were lysed and the total cellular protein was then measured via the Bradford assay (see section 2.6).

2.8 Electrophoretic Mobility Shift Assay (EMSA)

An adaptation of the protocol described by Schreiber *et al,* (1989) was used for the analysis of the activation of NF-κB by EMSA. Typically, 0.5×10^6 cells from four 6 cm plates of specified treatments were used. Cells were then washed with 2ml ice-cold PBS and pelleted by centrifugation at 1500 rpm (400 x*g*, Falcon 6/300 -

MSE) at 4ºC. The pellet was resuspended with 80 µl of Buffer A [10 mM HEPES (pH 7.9), 10 mM KCl, 0.1 mM EDTA, 0.1 mM EGTA] with a fresh supplementation of DTT (1 mM) and Protease inhibitors cocktail tablets (20x), and allowed to swell for 15 minutes on ice. 0.5% of 10% w/v NP-40 was added and the eppendorf was vigorously vortexed for 10 seconds. The lysates were then centrifuged for 30 seconds at 13,000 rpm (9000 xg, Micro Centaur – MSE). The supernatant which contained the cytoplasmic proteins was collected and flash-frozen on dry-ice. It was stored at -80ºC. The nuclear pellet was then resuspended in buffer C [20 mM HEPES (pH 7.9), 0.4 M NaCl, 1 mM EDTA, 1 mM EGTA] with a fresh supplementation of DTT (1 mM) and Protease inhibitors cocktail tablets (20x). The Eppendorf was vigorously rocked for 15 minutes at 4ºC on a shaking platform. The nuclear extract was then centrifuged for 5 minutes at 13,000 rpm (9000 x*g*) in a Biofuge 13 centrifuge (Heraeus Instruments) in a cold room (4ºC). The supernatant (nuclear proteins) was collected and flash-frozen on dry-ice. It was stored at -80ºC. Protein concentration was measured (see section 2.6) in duplicates on 3 µl aliquots of the extracts and the mean was taken.

2.8.1 Annealing and purification of the oligonucleotides

The annealing and purification of the oligonucleotides were kindly developed and performed by Dr. Olivier Reelfs through the following protocol:

The oligonucleotides possess *Hind*III and *Sal*I linker sites on their 5' and 3' end, respectively (Zabel *et al,* 1991). The sequence of the "κB" oligonucleotides used as a radioactive DNA was as follows:

5'- AGCTTCAGAGGGGACTTTCCGAGAGG - 3'

3' – AGTCTCCCCTGAAAGGCTCTCCAGCT – 5'

Equal amounts of each oligonucleotide and its complementary strand were mixed in a buffer containing 100 mM Tris (pH 7.6), 100 mM $MgCl_2$, boiled for 3 minutes and the mixture was left to be cooled at RT. Proper annealing was first verified on a 20% polyacrylamide gel, and then purified on a 20% polyacrylamide preparative gel in a 0.5x TBE buffer [44.4 mM Tris, 44.4 mM borate, 1 mM EDTA (pH 8.0)]. Elution of the band from the gel was performed by electroelution (Biotrap; Schleicher & Schuell, Switzerland), the oligonucleotides were ethanol precipitated, resuspended in TE buffer [10 mM Tris (pH 7.6), 1 mM EDTA (pH 8.0)] and aliquoted at -20ºC.

2.8.2 Preparation of the probe

100 ng of the annealed oligonucleotide was labelled by end-filling using the Klenow enzyme in the presence of 50μCi [α^{32}P]-dATP, 0.033 mM of cold dCTP, dGTP, dTTP, and 3μl of 10x polymerase buffer [0.5 M Tris (pH 7.5), 0.1 M $MgCl_2$, 10mM DTT, 0.5 mg/ml BSA].

2.8.3 Binding reactions

For detecting NF-κB binding activity after relevant treatments of both J16 and HJ16 cell lines: First, 6 μg of the nuclear extract was incubated for 10 minutes at RT in a freshly prepared buffer composed of 20 mM HEPES (pH 7.9), 12% glycerol, 0.2 mM EDTA, 0.2 mM PMSF, 0.5 mM DTT, 5 mM $MgCl_2$, 3mM ATP, and 100 μg poly [(dI)-(dC)]. Salt concentration was adjusted to 100 mM in each sample. After the 10 minutes incubation period, 0.3 ng of the labelled oligonucleotide was added to the mixture and incubated for 30 minutes at RT.

2.8.4 Running and processing the gel

The reaction mixtures were loaded on a 5 % polyacrylamide gel and electrophoresed at 140V in 0.4x TBE buffer at RT for 2-3 h. Next the gel was fixed in a mixture of methanol: acetic acid: water (at propositions of 10: 10: 80) for 20-30 minutes and then it was vacuum-dried for 1.5 h (in high mode). Results were shown as autoradiograms using high performance chemiluminescence films (Amersham Biosciences UK Limited, England) developed by Fuji X-ray Film Processor (Fuji Photo Film Co, Japan). The bands were scanned and the quantification was assessed using LabImage software - Version 2.7.2 (Kapelan Bio-Imaging Solutions, Germany).

2.9 Western blot analysis

Whole cell extracts were prepared by the lysis of the cells with 0.1% Triton X-100 lysis buffer [20mM TrisHCl (pH 8), 0.1% Triton X-100, 10% glycerol, 2mM EDTA, 137mM NaCl, 100mM PMSF, Protease inhibitors cocktail (20x)]. Protein measurements were then determined by Bradford's assay (see section 2.6). Equal amounts of protein (40 μg) were diluted with 4x loading buffer [180 mM Tris (pH

6.8), 3% SDS, 150 mM DTT, 30% glycerol, 0.0015% bromophenol blue, 0.53 ml Milli Q water] and then boiled for 5 minutes at 95°C. They were then resolved by Polyacrylamide (10% acrylamide) gel electrophoresis (SDS-PAGE) for ~ 1.75 h at 150 volts (V) in running buffer (1.5 % w/v Tris, 7.2 % w/v glycine, 0.5 % SDS) and transferred to nitrocellulose membranes (Amersham Biosciences, UK) at 4°C or 1.5 h at 100 V in a transfer buffer (3% w/v Tris, 14.4 % w/v glycine, 20 % v/v methanol). The transfer was verified by the colouration of the membrane with Ponceau S solution for 1-2 minutes and then rinsed several times with a small amount of Milli Q water to reveal the bands. The membrane was then thoroughly washed with 0.5% Tween-20 (Acros Organics, Belgium) PBS (PBST) and blocked for 1 h in 5% w/v milk powder in 0.05% PBST, placed on a rocking platform (Stuart Scientific, UK). Next, the membrane was washed once with 0.5% PBST and incubated with one of the following primary antibodies in 5% w/v milk in 0.05% PBST overnight at 4ºC with; 1:50 anti-HO-1 mouse monoclonal antibody (OSA-110, Stressgen Bioreagents), 1:200 anti-HO-2 rabbit polyclonal antibody (kindly provided by Prof. Rex Tyrrell, University of Bath), or 1:500 anti-actin mouse monoclonal antibody (Sigma, A4700). The membrane was then washed extensively with 0.5% PBST and incubated with (1:500 for HO-1 and 1:2000 for Actin) goat anti-mouse IgG peroxidase conjugated (Sigma, A4416) or (1:1500 for HO-2) anti-rabbit IgG (whole molecule)-Peroxidase (Sigma, A6154) in 5% w/v milk in 0.05% PBST for 1 h at RT on a rocking platform (Stuart Scientific, UK). The membrane was then washed extensively with 0.5% PBST, and the protein bands were finally detected using enhanced chemiluminescence (ECL) plus detection system according to manufacturer's instructions (Amersham Biosciences). *Re-blot Plus* (Strong Antibody Stripping Solution) was used in order to re-blot, according to manufacturer's instructions (Chemicon, 2504).

2.10 Ferritin ELISA

Enzyme-Linked ImmunoSorbent Assay (ELISA) is a biochemical technique used mainly in immunology to quantify the presence of an antibody or an antigen in a sample. Reagents for ferritin ELISA were kindly provided by Dr. Santambrogio (Milan, Italy), and the assay performed as described in Santambrogio *et al,* 2000 and 2007. Cytosolic ferritin concentrations were determined in cell lysates by

monoclonal antibodies specific for human H- and L- ferritin subunits (rH02, LF03), and mitochondrial ferritin concentrations in mitochondria enriched fractions by mouse polyclonal antibody specific for mitochondrial ferritin (MoαHuFtMt) by the means of ELISA, then normalised to protein concentration (see section 2.6).

For cell lysates: After relevant treatments, cells (10 x 10^6 cells / condition) were washed with ice cold PBS and the lysates were prepared as described in 2.9. The supernatant was then flash frozen on dry ice with ethanol and kept at -80°C until use. Microtiter plates were coated with 0.1 ml of 10µg/ml of rH02 or LF03 antibodies diluted in 50 mM Na carbonate buffer pH 9.5. Standard ferritins and samples were diluted in PBST with 1% BSA (0.05% Tween-20 in PBS-BSA) and 0.1 ml was added to the plates, incubated for 1 h at 37°C, washed three times with PBST (0.05% Tween-20 in PBS), and further incubated for 1 h at 37°C with the same HRP-labelled antibodies (LF03-HRP 1:3000 and rH02-HRP 1:15,000, in PBST + 1% BSA) to reveal the bound ferritin. The peroxidase activity was developed with *o*-phenylenediamine dihydrochloride (Sigma, P1526).

For mitochondria preparation (Smith, 1967 and Atorino *et al,* 2003) : After relevant treatments, cells (10 x 10^6 cells / condition) were washed with ice cold PBS and resuspended in ice cold-isotonic buffer (250 mM Sucrose, 5 mM tris-HCl pH 7.5, 0.1 mM PMSF) and homogenised using PowerGen 125 Homogenizer (Fisher Scientific, UK) for 30 seconds. This was then centrifuged at 600 x*g* for 15 minutes at 4°C in a Biofuge 13 centrifuge (Heraeus Instruments) to remove the nuclei and cell debris. Next, the supernatant was collected and centrifuged at 13,000 rpm (9000 x*g*) in a Biofuge 13 centrifuge (Heraeus Instruments) for 25 minutes at 4°C. The pellet was finally dissolved in the same buffer containing 1mM EDTA and centrifuged at 13,000 rpm (9000 x*g*) for 25 minutes at 4°C in a Biofuge 13 centrifuge (Heraeus Instruments). The mitochondrial pellet was flash frozen on dry ice with ethanol, and kept at -80°C until use. On the day of the assay, the pellet was resuspended in the ice cold-isotonic buffer. As above, microtiter plates were coated with 0.1 ml of 10µg/ml of MoαHuFtMt antibodies diluted in 50 mM Na carbonate buffer pH 9.5. Standard ferritins and samples were diluted in PBST with 1% BSA (0.05% Tween-20 in PBS-BSA) and 0.1 ml was added to the plates, incubated for 1 h at 37°C, washed three times with PBST (0.05% Tween-20 in PBS), and further incubated for 1 h at 37°C with the same HRP-labelled antibody (MoαHuFtMt-HRP 1:6000, in PBST + 1%

BSA) to reveal the bound ferritin. The peroxidase activity was developed with *o*-phenylenediamine dihydrochloride (Sigma, P1526).

2.11 Neutral red uptake assay

The neutral red (NR) uptake assay is a cell survival/viability assay, based on the ability of the viable cells to incorporate and bind NR. Neutral red is a relatively non-toxic, weakly cationic dye which was introduced as a vital stain in 1894 (Dietz *et al,* 1979). This dye enters the cells and accumulates in the lysosomes (since it has a low pH) and binds to its matrix by non-ionic diffusion, a mechanism by which weak acids and bases pass through lipid membranes in a non-ionised form (Anderson and Orci, 1988).

The neutral red stock solution was made by thoroughly dissolving 0.02g of NR powder in 5ml of Milli Q water. 500 µL of the stock solution was added to 39.5 ml of 10 % FCS-RPMI, this solution was stored overnight at 37°C to remove fine precipitates and dye crystals which form when NR is mixed with the medium (Borenfreund and Puerner, 1985). On the day of the assay, this solution was centrifuged for 10 minutes at 1200 rpm (120 x*g*) in a Jouan B 3.11 centrifuge and filtered through a 0.2 µm filter (Ministart®, Germany). The cells were centrifuged and washed once with PBS, resuspended in 2-3 ml of the filtered dye/media mixture, and then incubated at 37°C for 1.5 h. Next, they were centrifuged at 1500 rpm (300 x*g*) in a Falcon 6/300 MSE centrifuge and fixed with 500 µL of the fixing solution (40% formaldehyde + 10% $CaCl_2$) for a maximum of 1 minute since formaldehyde will result in the extraction of the dye. The cells were centrifuged again and lysed with 500 µL of lysis buffer (1% acetic acid + 50% ethanol). 150 µL of each sample was placed in duplicate in a 96-well plate and the absorbance was measured at 540 nm by VERSAmax™ (Molecular devices, California).

2.12 Lysosensor immunofluorescence

The LysoSensor™ Green DND-153 was used to monitor the integrity of the lysosomal membrane after relevant treatments. This probe is a fluorescent pH indicator that partitions into acidic organelles at the result of protonation.

Treatments were performed when cells were placed on sterilised glass coverslips laid on the bottom of 3cm^3 plates, done in duplicate. After relevant treatments, 500 µL of methanol (stored in -20°C) was placed on the plates for 5 minutes, to fix the cells on the coverslips. The methanol was then aspirated and the plates were kept at –20°C till use. On that day, 1 ml of PBS was added to the plates for 10 minutes to rehydrate the cells. The PBS was then aspirated and 500 µL of the 1 µM probe (stock) solution (freshly prepared in 10% FCS-RPMI) was placed on the cells and they were then incubated for 2 h at 37°C. Meanwhile, microscope slides were prepared and cleaned by soaking them in ethanol for 5 minutes, then with Milli Q water for 2 minutes and finally in acetone for 5 minutes. After the 2 h, the coverslips were drained, washed gently with PBS, and mounted overnight on the slides containing 20 µL of Mowiol® 4-88 mounting medium. Finally, the cells were analysed by LSM 510 Confocal Microscope (Carl Zeiss system, Germany) and the objective used was described as Plan-Apochromat 63 x / 1.40 oil DIC. The line of excitation used from the Argon laser was 488 nm and the emission was passed through a Long Pass 505 nm (LP 505) filter. Pictures were scanned at a resolution of 1024x1024 pixels; this is equivalent to an approximate resolution of 1.05 mega pixels.

2.13 Immunocytochemistry

Treatments were performed when cells were placed on sterilised glass coverslips laid on the bottom of 3cm^3 plates, done in duplicate. After relevant treatments, cells were fixed by methanol (stored in -20°C) for 5 minutes. The methanol was then aspirated and the plates were stored in –20°C till use. On that day, 1 ml of PBS was added in the plates for 10-15 minutes to rehydrate the cells. The PBS was aspirated and the non-specific sites were blocked by the addition of 150 µL of Buffer X (0.1 % TritonX100 + 2% BSA in PBS) at room temperature (RT) for 10 minutes. The primary antibodies used were Cathepsin B, NF-κB (p-65), and Oct-1 (C-21). The dilution was 1:100 in Buffer X and they were incubated for 1 h at RT placing parafilm on the top. After the 1 h passed, the cells were gently washed twice with PBS and were then incubated with the secondary antibody (dilution 1:100, in Buffer X) for another 1 h at RT. The secondary antibody used

was a FITC conjugated goat anti-rabbit IgG (Sigma, F9887). Meanwhile, microscope slides were prepared and cleaned by soaking them in ethanol for 5 minutes, then with Milli Q water for 2 minutes and finally in acetone for 5 minutes. After the 1 h incubation time, the coverslips were then drained, gently washed twice with PBS, and mounted overnight on the slides containing 20 µL of Mowiol® 4-88 mounting medium. Finally, the cells were analysed by LSM 510 Confocal Microscope (Carl Zeiss system, Germany) and the objective used was described as Plan-Apochromat 63 x / 1.40 oil DIC. The line of excitation used from the Argon laser was 488nm and the emission was passed through a Long Pass 505nm (LP 505) filter. Pictures were scanned at a resolution of 1024x1024 pixels; this is equivalent to an approximate resolution of 1.05 mega pixels.

2.14 Preliminary Clinical data

In collaboration with Dr. James Murray orthopaedic consultant (Frenchay and the Avon Orthopaedic Centre in Southmead, Bristol) and according to the South West Local Research Ethics committee approval BA 574 (2003/4), we have received synovial fluid and synovial tissue biopsies from normal, rheumatoid arthritic, and osteoarthritic patients (see table 2.1 for the statistics). The synovial fluid was centrifuged at 3000 rpm (1000 x*g*) in a Falcon 6/300 MSE centrifuge for 15 minutes to remove debris and any other unwanted particles. The supernatant was collected and stored at -80ºC. Before culturing fibroblasts from the biopsies, they were washed with 1ml Penicillin/Streptomycin (50 IU/ml each), they were then placed in 6 cm plates, sliced and sheared into small pieces. The biopsy was maintained in 15% v/v FBS-EMEM supplemented with an antibiotic mix [Penicillin G - 10^7 units (Sigma); Streptomycin sulphate – 10g (Sigma); Fungizone – 100 ml (Gibco)] prepared in our laboratory. The fibroblasts were then cultured and grown in 15% v/v FBS-EMEM supplemented with), L-Glutamine (2 mM), Penicillin/Streptomycin (50 IU/ml each) and 2.7% v/v sodium bicarbonate. They were incubated at 37°C in a humidified atmosphere with 5% CO_2.

In addition to the above, Dr Vivienne Winrow (School for Health, University of Bath) kindly supplied us with primary rat synoviocytes (fibroblasts), labelled VW-1 and adjuvant arthritic (AA) rat fibroblasts, labelled AAVW-l.

Synovial Fluid

Condition	Collected	Stored @ -80°C	Analysed
Normal	1	1	1
RA	6	6	2
OA	23	23	6

Synovial Biopsy

Condition	Collected	Cultured	Analysed
Normal	5	1	1
RA	17	2	1
OA	25	2	1

Table 2.1 :

Table listing the synovial fluid (top) and the synovial knee biopsies (bottom) received and analysed for either labile plasma iron (LPI) or labile iron pool (LIP), respectively.

Adjuvant arthritis is a chronic model and a standard procedure which has been used for many years (Pearson, 1956 ; Currey and Ziff, 1968 ; Andrews *et al,* 1987). It is a useful model for screening putative therapeutics for diseases such as human RA; it induces both soft inflammation and bone destruction (Ragno *et al,* 1996). Rats with AA share many characteristics with human RA such as genetic linkage, synovial $CD4^+$, and T cell dependence (Goodson *et al,* 2003). They were grown in 10% v/v FBS DMEM (1000 mg/L glucose; Pyruvate) supplemented with L-Glutamine (2 mM), Penicillin/Streptomycin (50 IU/ml each) and 2.7% v/v sodium bicarbonate (0.27%). They were incubated at 37°C in a humidified atmosphere with 5% CO_2. Since the human and the rat fibroblasts are not cell line (ie not immortalised), they will not passage indefinitely. Therefore, as Dr. Vivienne Winrow advised, functional studies were not performed beyond passage 12 (maximum).

2.15 LIP determination in 96 well-plates

The level of LIP was determined by an adaptation of the method developed by Epsztejn *et al*, 1997 and Petrat *et al,* 1999. The cytochemical calcein-acetoxymethyl ester (CA-AM) assay is well established as a technique for the assay of cellular LIP. The principle of this assay is that non-fluorescent lipophilic CA-AM that easily penetrates cellular membranes produces fluorescent CA when rapidly cleaved by unspecific cytosolic esterases. The fluorescent CA is a fluorochromic alcohol that chelates labile iron (Tenopoulou *et al,* 2007). The level of intracellular CA-Fe complexes was determined by the increase in fluorescence produced by the addition of the fast membrane permeable iron chelator, salicylaldehyde isonicotinoyl hydrazone (SIH). Salicylaldehyde isonicotinoyl hydrazone (kindly provided by Professor Ponka, Lady Davis Institute - Canada) is a lipophilic strong chelator that restores the fluorescence by removing the complexed iron (Glickstein *et al,* 2005).

Cells were grown for 48 h in dark 96-well plates (Costar, 3603) at a density of 6×10^4 cells / well (final density needed ~ 8×10^4 cells / well). After the 48 h, the conditioned media was aspirated and the cells were washed once with DPBS (Dulbecco's phosphate buffered saline with Ca and Mg – Cambrex, Belgium). After H_2O_2 treatments, cells were washed once with DPBS and loaded with 0.25 μM CA-AM in Earle's minimum essential media [containing 20 mM HEPES (pH 7.3) and

BSA 1 mg/ml] for 15 min at 37°C. The cells were then washed with DPBS, and the fixing solution [10 mM HEPES buffer containing 150mM NaCl and 2 mM diethyltriamine-pentaacetic acid (DTPA)] was added. The fluorescence (F1) was then measured (Excitation 485 – Emission 535) by a Fluoroskan Ascents microplate reader (Labsystems, OY). 200 μM of SIH was then added, and the plate was placed on a rocking platform (Stuart Scientific, UK) for 15 minutes to allow chelation. After the 15 minutes, the fluorescence (F2) was measured (Excitation 485nm – Emission 535nm). The fractional increase of fluorescence (ΔF = (F2-F1) / F2) was first determined by the calibration curve and then normalised to total cellular protein. This correlates with the LIP (μM/μg) within the cells (Duarte and Jones, 2007).

The calibration curve was prepared with ferrous ammonium sulphate (Petrat *et al,* 2000). It was initially diluted with DPBS to 1 mM and then to 1μM (final) and from it 1:1 serial dilutions were prepared, till 2.44 x 10^{-4} μM (total = 12 concentrations were used). 0.25 μM of CA (Sigma, C0875) was added to the 12 serial dilutions and the fluorescence (F1) was measured (Excitation 485 – Emission 535) by a Fluoroskan Ascents microplate reader (Labsystems, OY). 200 μM of SIH was then added to the serial dilutions, and the plate was placed on a rocking platform (Stuart Scientific, UK) for 15 minutes to allow chelation. After the 15 minutes, the fluorescence (F2) was measured (Excitation 485 – Emission 535). For the calibration curve (Darbari *et al,* 2003), the fractional increase of fluorescence (ΔF = (F2-F1) / F2) was plotted against the iron concentration used (y = 9.981x + 0.088, is the linear equation of the trendline).

2.16 Labile plasma iron (LPI) measurements

Labile plasma iron (LPI) represents the redox-active and chelatable component of non-transferrin-bound iron (NTBI) (Le Lan *et al,* 2005). It is capable of permeating into organs and inducing tissue iron overload (Cabantchick *et al,* 2005). The method of measuring LPI is based on its capacity to generate reactive oxygen radicals when prompted with ascorbate in a manner blockable by specific iron chelators such as DFO. Non fluorescent dihydrorhodamine (DHR) is converted by various oxidants, such as reactive oxygen radicals, to the fluorescent form.

As described by Esposito *et al,* (2003): Quadruplicates of 20 µL synovial fluid (SF) were placed in a clear-bottom 96 well plate. To two of the four wells, 180 µL iron-free HEPES buffered saline (HBS; HEPES 20mM, 60nM DFO, NaCl 150 mM, pH 7.4 – treated with 1g of 100ml^{-1} Chelex-100) containing 40 µM ascorbate and 50 µM DHR (= Test mix) was placed. 180 µL iron-free HBS containing 40 µM ascorbate, 50 µM DHR, and 50 µM DFO was added to the other two wells (= Reference mix). The kinetics of the fluorescence was measured with the excitation at 485 nm and the emission at 538 nm by a Fluoroskan Ascents microplate reader (Labsystems, OY). This was measured for 40 minutes, with readings every 2 minutes, immediately after the addition of the test and reference mix. The slopes (r) of DHR fluorescence intensity with time were calculated from measurements taken 15 and 40 minutes. The duplicate values of r in the presence and absence of DFO, r_{DFO} and r, respectively, were averaged, and the LPI concentration (µM) was determined from calibration curves relating the difference in slopes with and without DFO against Fe concentration: $LPI = \Delta r/r_{st} = (r - r_{DFO})/r_{st}$.

Calibration curves were obtained by spiking plasmalike medium (PLM) with Fe:NTA, 1:7 (mol/mol), followed by serial dilution in PLM and incubation for 30 minutes at 37°C to allow binding of the Fe. Plasmalike medium (PLM) contained 20 mM HEPES, 150 mM NaCl, 120 µM sodium citrate, 40 µM sodium ascorbate, 1.2 mM sodium phosphate dibasic, 10 mM sodium bicarbonate, and 40 mg/mL human serum albumin (pH 7.4). Fe^{3+}/NTA complexes were formed by mixing 70 mM nitrilotriacetic acid (NTA), titrated to pH 7.0 with NaOH, with 20 mM ferrous ammonium sulphate to produce a Fe/NTA molar ratio of 1:7 and allowing the Fe^{2+} to oxidise to Fe^{3+} in ambient air for 30 minutes. Quadruplicates of 20 µL of these samples were assayed for LPI as described in the previous paragraph.

2.17 Statistical analysis of data

Results were expressed as the mean ± standard deviation. Data were analysed using paired or unpaired Student's one-tailed *t*-test, as appropriate. The p value of < 0.05 was considered to indicate a significant difference between groups of data.

CHAPTER THREE

RESULTS

Background:

The response of cells to either an acute (single high dose) or chronic (repeated low doses) exposure to oxidising agents is quite different. Depending on the degree of the oxidising insult, acute exposure could trigger a series of intracellular antioxidant defence mechanisms that counteract the damage caused but if these are not sufficient, cells will die by either apoptosis or necrosis. In chronically exposed cells, the antioxidant defence mechanism is altered as exposure of cells to low doses of oxidants usually provokes the development of a distinct adaptive response that differs quite sharply from that following acute exposure. Because of such adaptive responses, cells may withstand high toxic doses of the oxidising agent that would otherwise be lethal. The study of the mechanisms underlying the adaptive responses of cells to oxidising agents provides clues to understand the promotion and progression of the chronic inflammatory process in diseases such as Rheumatoid Arthritis (RA). A potentially major factor influencing this process is that the rheumatoid synovium is relatively hypoxic, and is exposed to chronic cycles of hypoxia and reperfusion. This promotes oxidative stress, which has marked effects on many cell types, including enhanced production of pro-inflammatory cytokines by mononuclear cells.

The Jurkat T cell lines composed of 'parental J16' and 'H_2O_2 resistant HJ16' provide a good model to study the differential response of cells to both acute and chronic exposure. Furthermore the HJ16 cell line that was established following adaptation of J16 cell line to increasing concentrations of oxidising agent H_2O_2, provides us with a useful model to mimic the chronic exposure of T cells in synovium to ROS that are almost certainly involved in the pathology of RA.

The potentially harmful free 'labile' iron is recognised as an important promoter of oxidative stress through aiding the production of ROS and thus a potential mediator

of the inflammatory process in RA. Previous studies carried out by A. Yiakouvaki in this laboratory (PhD Thesis, 2003 – University of Bath) have provided us with a link between the amount of H_2O_2-induced labile iron release and the extent of oxidative damage and cell death in Jurkat T cells. Furthermore the study has shown that adaptation of Jurkat T cells to H_2O_2 can influence the basal level of antioxidant enzymes that is likely to contribute to resistance of HJ16 cells to H_2O_2 insult.

This thesis has continued the study of Yiakouvaki (PhD Thesis, 2003 – University of Bath) by further characterising the differential response of parental J16 and H_2O_2-adapted/resistant HJ16 Jurkat T cells to H_2O_2.

3.1 Determination of the sensitivity of J16 and HJ16 cell lines to H_2O_2

The accumulation of the damage caused by ROS, including H_2O_2, plays an important role in the aetiology and/or progression of a number of diseases (Moskovitz *et al*, 2002). In order to evaluate the cytotoxicity of H_2O_2 on J16 (parental) and HJ16 (H_2O_2-resistant**)** cell lines, both cell lines were treated with various concentrations of H_2O_2 (i.e. 0.1, 0.5, 1, and 3 mM) and two cytotoxicity assays were performed; MTT (see section 2.4) and flow cytometry (see section 2.5). These assays were performed 24 h following H_2O_2 treatment, since previous studies have revealed that the cytotoxicity of H_2O_2 towards these cell lines is only apparent from 18 h post-treatment time point (A.Yiakouvaki - PhD thesis, 2003). Epsztejn *et al*, (1999) have also reported that cell damage and death was only present 24 h-post H_2O_2 treatment.

3.1.1 MTT assay

According to MTT analysis that assesses cell viability, treatment of both cell lines with H_2O_2 resulted in a concentration-dependent decrease in cell viability (see figure 3.1). However J16 cells were more sensitive to H_2O_2 treatment than HJ16 cells. Indeed even a concentration of H_2O_2 as low as 0.1 mM was able to cause damage to the J16 cells as the intracellular dehydrogenase activity of H_2O_2-treated cells decreased to 57.4 ± 0.8 % of the control. On the other hand, the HJ16 cells were clearly resistant to H_2O_2 treatment up to 3 mM final concentration.

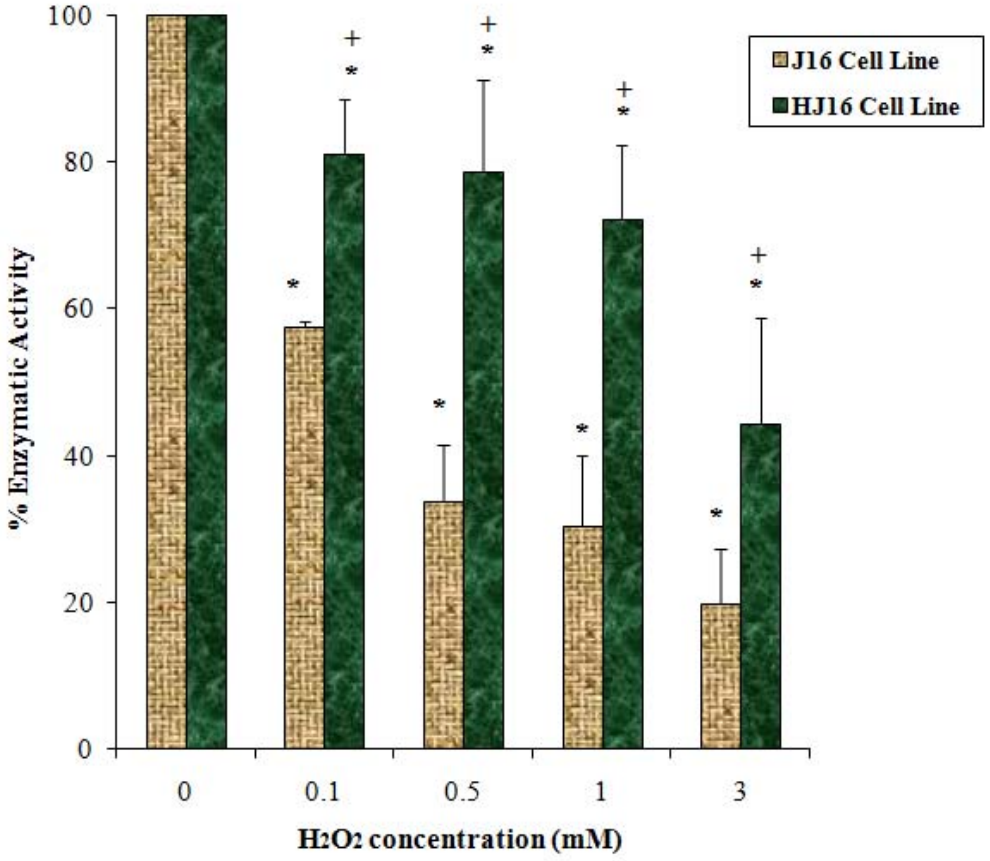

Figure 3.1 :

Effect of different concentrations of H_2O_2 treatment on the viable cells in J16 (parental) and HJ16 (H_2O_2-resistant) cell lines.

MTT analysis (see section 2.4) was performed 24 h following H_2O_2 treatment. These results are expressed as mean ± standard deviation (n=3)

* : $p < 0.05$ significantly different when compared with corresponding control of the same cell line.
+ : significantly different when compared with J16 cell line of the same treatment.

3.1.2 Flow cytometric analysis

Since two mechanisms of cell death occur within the cells, flow cytometric analysis was performed to distinguish between the two mechanisms. Cells either die by necrosis (accidental form of cell death) or alternatively by apoptosis (programmed form of cell death). The dual staining of the cells with Annexin-V / Propidium iodide (PI) will allow to gate the cells to determine the percentage of live, apoptotic, and necrotic cells.

An example of such analysis is illustrated in figure 3.2. In this example J16 and HJ16 cell lines were either untreated or treated with H_2O_2 concentrations of 0.5 and 3 mM. As displayed in figure 3.2, there are 4 compartments. The lower left quadrant indicates the total of live cells (i.e. Annexin-V negative - PI negative), whereas the lower right quadrant indicates apoptosis (i.e. Annexin-V positive - PI negative). The upper right (i.e. Annexin-V positive - PI positive) and upper left (i.e. Annexin-V negative - PI positive) quadrants indicate primary and secondary necrosis, respectively.

Flow cytometric analysis (see figure 3.3) carried out following dual Annexin-V / PI staining of both J16 and HJ16 cell lines 24 h after H_2O_2 treatment confirms our previous results determined with MTT analysis. Overall, the flow cytometric analysis revealed that neither J16 nor HJ16 cell lines undergo H_2O_2–mediated apoptotic cell death. Furthermore in both cell lines, H_2O_2 induced a concentration–dependent necrotic cell death. However the comparison of the percentage of necrotic cell death in both cell lines following H_2O_2 treatment clearly demonstrated that the HJ16 cell line has significantly higher resistance to the oxidising agent (i.e. up to 3 mM H_2O_2) than the J16 cell line. Indeed in the J16 cell line, the cytotoxicity of H_2O_2 was already apparent at a concentration as low as 0.5 mM, since the population of live cells was decreased from 90% to 50%. At a higher concentration of 3 mM H_2O_2, almost no live J16 cells were present in the flow cytometric chart. The dose-dependent decrease in live J16 cells following H_2O_2 treatment also coincided with a reciprocal increase in the percentage of necrotic cells, strongly suggesting that necrosis is the primary mode of cell death induced by H_2O_2 in this cell line.

In summary, the flow cytometric analysis was in agreement with the MTT analysis, as both assays confirmed that the HJ16 cell line possessed higher resistance to H_2O_2 than the parental J16 cell line.

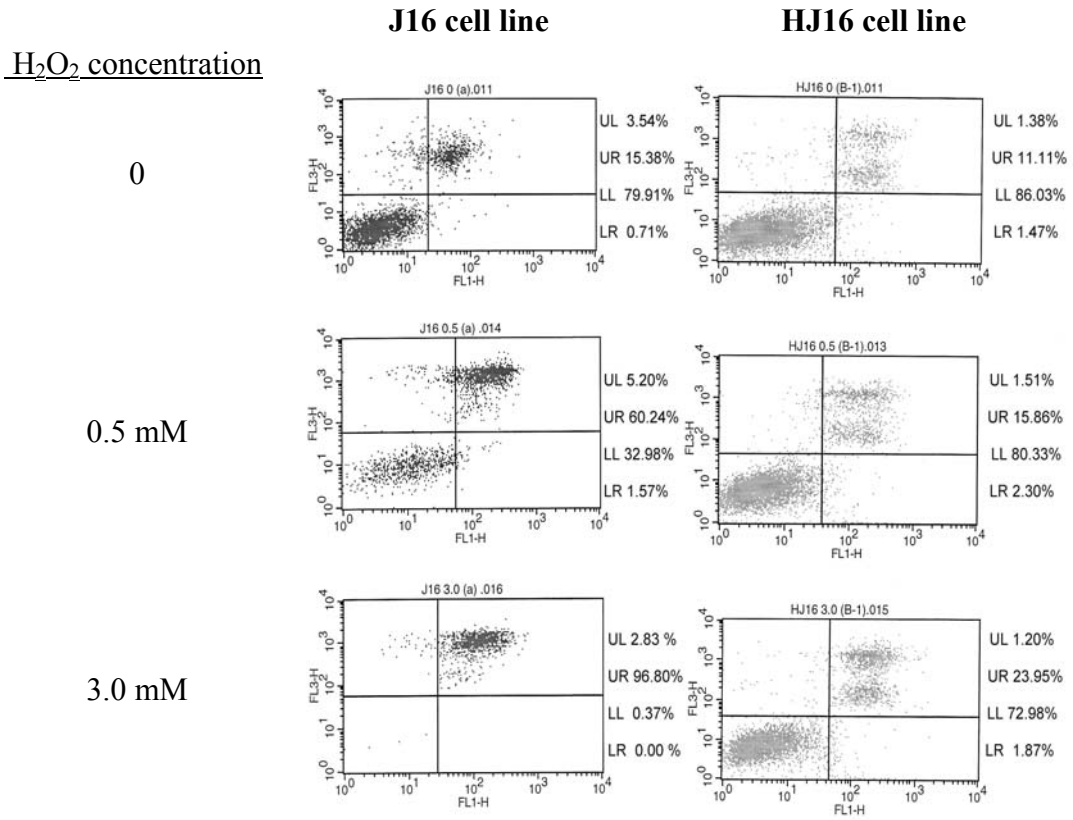

Figure 3.2 :

An example of the evaluation of flow cytometry analysis following H_2O_2 treatment (i.e. 0.5, and 3 mM) of J16 and HJ16 cell lines.

The analysis (see section 2.5) was performed 24 h after H_2O_2 treatment following dual Annexin-V/PI staining. Live cells are situated in the lower left quadrant (LL), whereas apoptotic cells are situated in the lower right quadrant (LR), and primary and secondary necrotic cells are situated in the upper right (UR) and upper left (UL) quadrant, respectively.

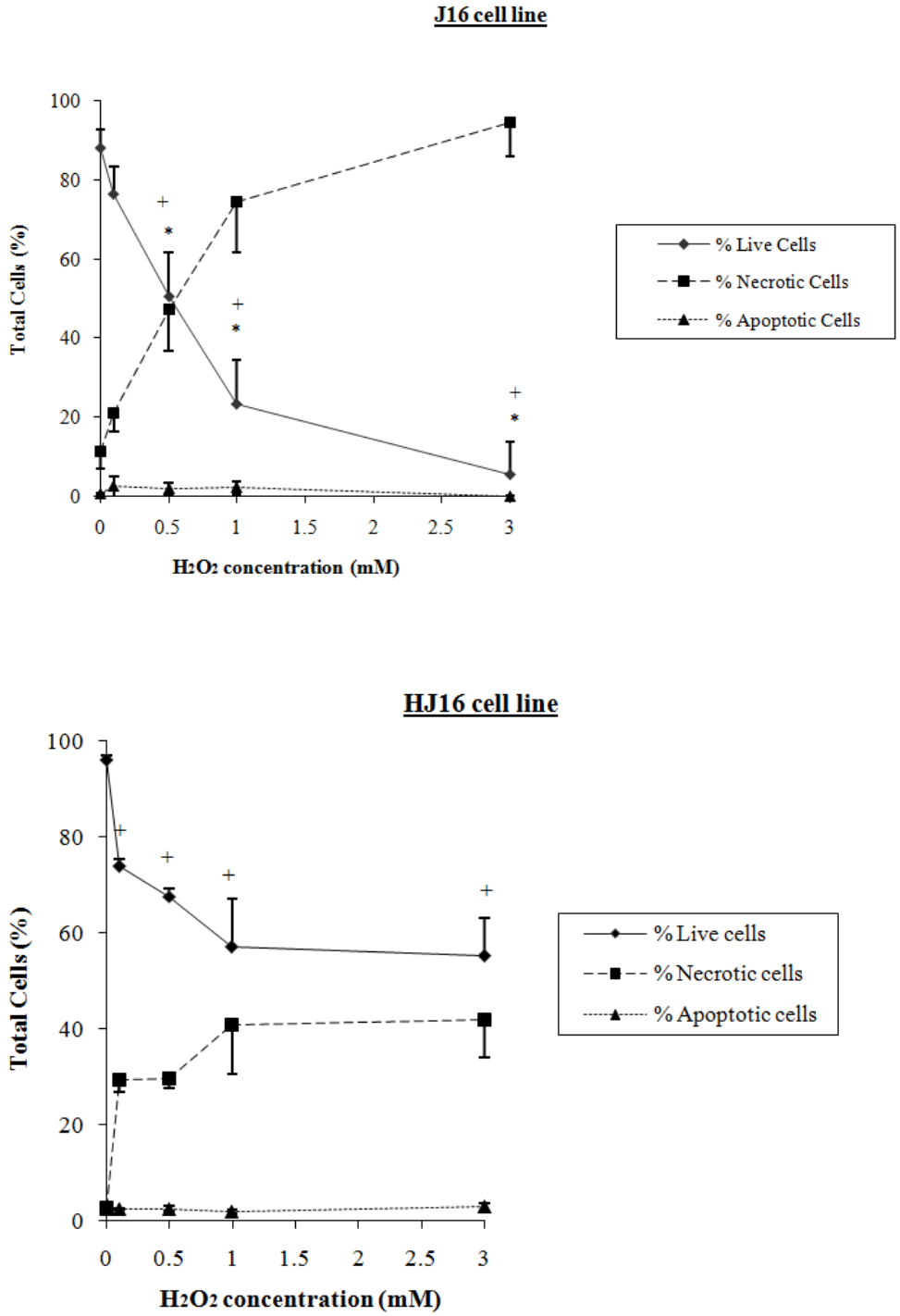

Figure 3.3 :

The effect of H_2O_2 on the percentage of live, necrosis, and apoptosis in J16 and HJ16 cell lines. Flow cytometric analysis (see section 2.5) was performed 24 h after H_2O_2 treatment following dual Annexin-V/PI staining. The results are expressed as mean ± standard deviation (n=3)

+ : $p < 0.05$ significantly different between treated and corresponding controls.
* : $p < 0.05$ significantly different from HJ16 cell line (Live cells).

3.2 The role of total intracellular glutathione

The total intracellular glutathione (GSH/GSSG) system acts as a homeostatic redox buffer (see section 1.4.1.1) providing a major constitutive defence against oxidants (Applegate *et al,* 1992). Yiakouvaki (2003) showed that while the basal level activity of GPx enzyme in the HJ16 cell line is 2-fold higher than in J16 cell line, catalase activity is only 1.2-fold higher in HJ16 cells (non-significant). The higher GPx activity is likely to contribute to higher resistance of the HJ16 to H_2O_2-mediated toxicity. To determine whether the total intracellular levels of glutathione play a role in increased resistance of HJ16 cell line to H_2O_2, the basal GSH/GSSG level was monitored in both parental (J16) and H_2O_2 – resistant (HJ16) cell lines. Furthermore an attempt was made to deplete GSH/GSSG in both cell lines (i.e. by BSO, see next section) to demonstrate the possible link between GSH/GSSG and susceptibility of both cell lines to H_2O_2–mediated cytotoxicity.

3.2.1 The effect of Buthionine-[S,R]sulfoximine (BSO) treatment on J16 and HJ16 cells

Buthionine-[S,R]sulfoximine (BSO) is known to be a relatively non-toxic compound whose effect is apparently restricted to the inhibition of γ-glutamylcysteine synthetase. *In vivo* studies have shown that the administration of BSO to mice for several weeks has no undesirable effects other than glutathione depletion (Dethmers and Meister, 1981).

To evaluate the toxicity of BSO in our cell lines, MTT analysis (see section 2.4) was performed. J16 and HJ16 cell lines were treated for 18 h with a range of BSO (see section 2.3.2) concentrations (i.e. 2, 5, 15, 25, 50, and 250 μM). The results (see figure 3.4) clearly showed that in both cell lines the compound has no toxicity towards the cells at concentrations up to 250 μM.

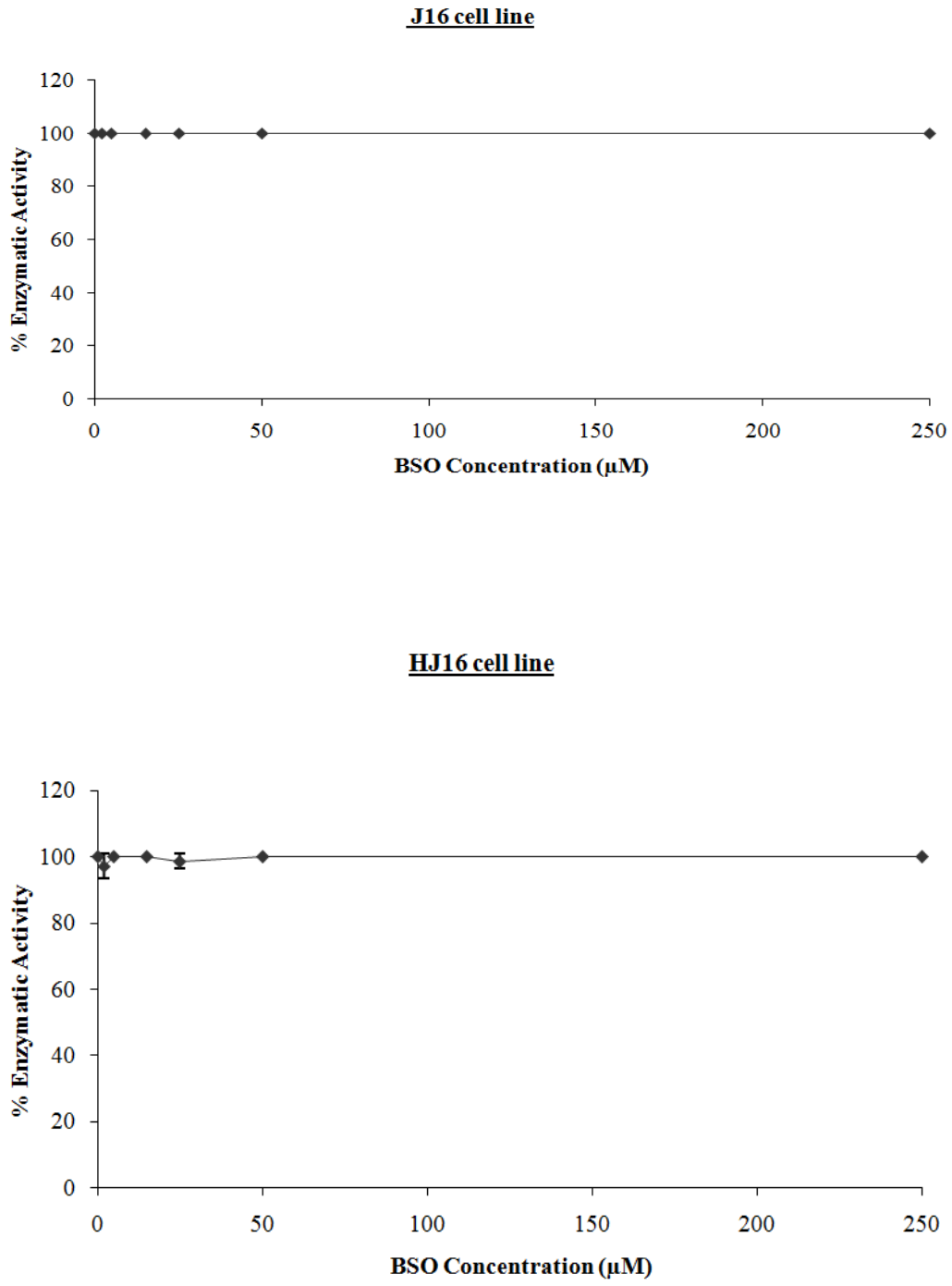

Figure 3.4 :

Effect of BSO on the viable cells in both J16 and HJ16 cell lines.

MTT analysis (see section 2.4) was performed 18 h following treatment of both cell lines with BSO at concentrations of 2, 5, 15, 25, 50, and 250 µM for 18 h. The results were expressed as mean ± standard deviation (n=3).

3.2.2 The effect of BSO on the total intracellular levels of glutathione in J16 and HJ16 cells

To study the modulation of GSH/GSSG by increasing concentrations of BSO, the GSH/GSSG was determined using Tietze's method (see section 2.7). Furthermore it was important to check the differences in basal intracellular glutathione levels that might contribute to the higher resistance of HJ16 cell line to H_2O_2 when compared to J16 cell lines. For this purpose both cell lines were treated with a range of concentrations of BSO (i.e. 2, 5, 15, 25, 50, and 250 μM) and then assayed by Tietze's method to evaluate the intracellular glutathione levels. The GSH/GSSG level was then normalised by two methods: cell count [per 10^6 cells] and protein concentration [per total protein (mg)]. The normalisation with both methods (see figure 3.5 and figure 3.6) showed that a dose of 25 μM of BSO was sufficient to deplete the GSH/GSSG level in both J16 and HJ16 cell lines.

3.2.3 Basal levels of the total intracellular glutathione in J16 and HJ16 cell lines

The basal level of the GSH/GSSG was assessed in both cell lines by using Tietze's method. The normalisation with cell count and with protein concentrations (see figure 3.5 and figure 3.6) revealed that HJ16 cells possess significantly higher levels of intracellular glutathione than J16 cells. Indeed, the measurement of the intracellular glutathione in the HJ16 cell line was found to be 3.4-fold higher than in the J16 cell line (see table 3.1). Since in an independent study from our laboratory (i.e. Yiakouvaki, 2003), it was found that these two cell lines had considerable difference in their cell volume (i.e. J16 cells: 0.47 ± 0.08 pl and HJ16: 1.6 ± 0.19 pl), it was therefore concluded that the normalisation with cell count is an inaccurate method for estimating the basal level of the GSH/GSSG in these cell lines, and that the data normalised with protein concentration should be used instead.

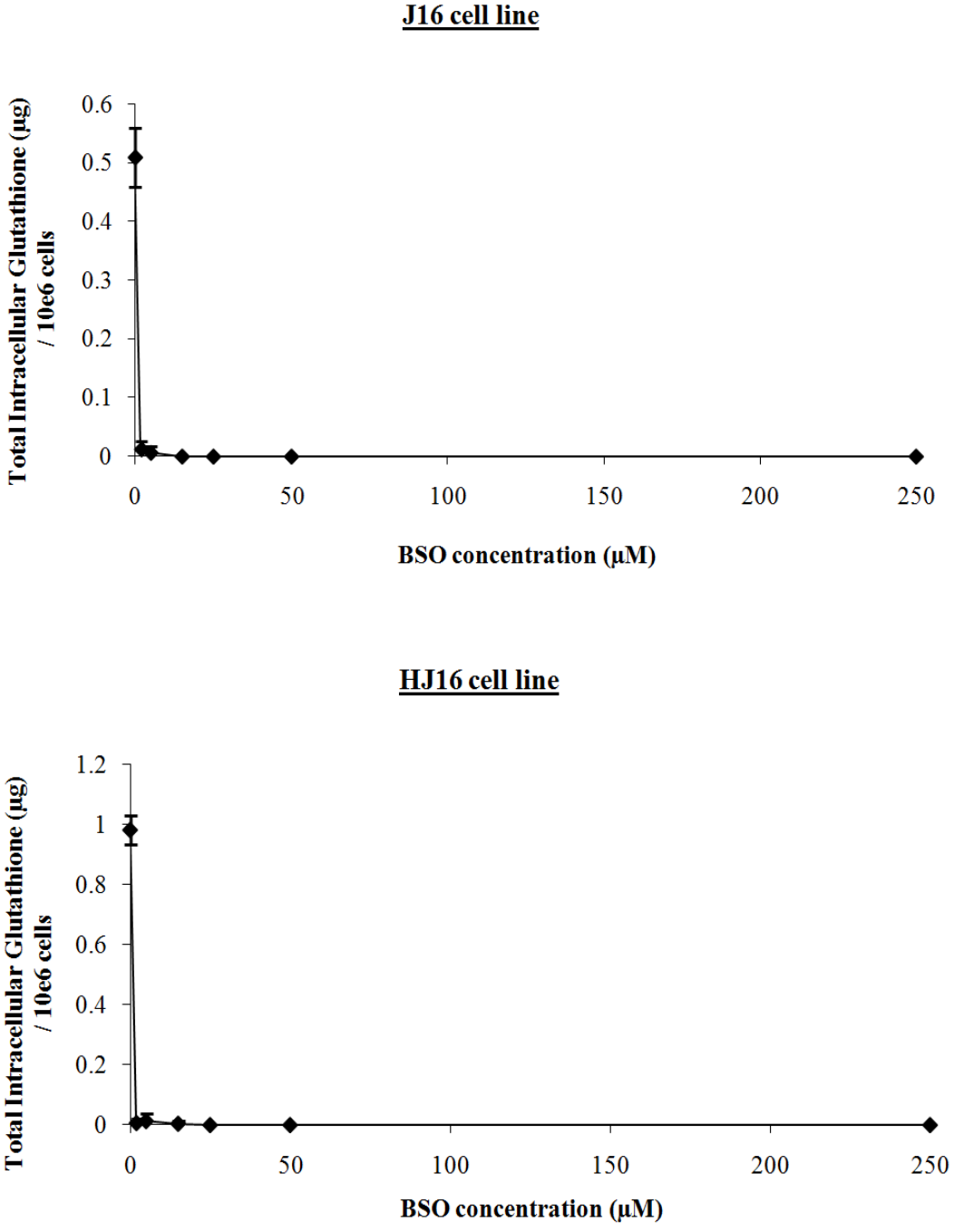

Figure 3.5 :

The normalisation of intracellular glutathione in J16 and HJ16 cell lines to cell count.

Both cell lines were treated with BSO for 18 h at concentration of 2, 5, 15, 25, 50, and 250 µM prior to intracellular glutathione measurements (see section 2.7). The results were expressed as mean ± standard deviation (n=3).

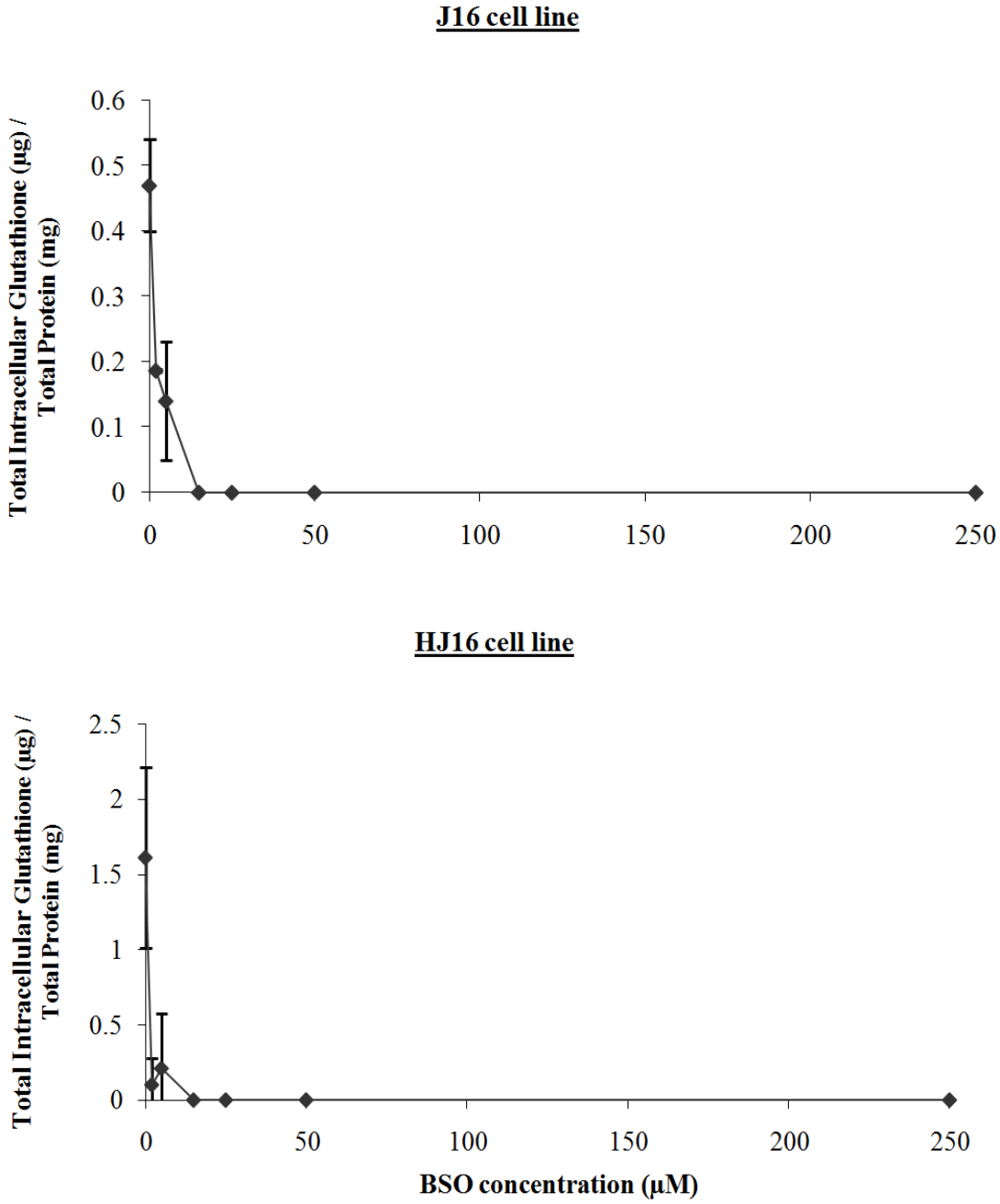

Figure 3.6 :

The normalisation of intracellular glutathione for J16 and HJ16 cell lines to total intracellular protein levels.

Both cell lines were treated with BSO for 18 h at concentration of 2, 5, 15, 25, 50, and 250 µM prior to intracellular glutathione measurements (see section 2.7). The results were expressed as mean ± standard deviation (n=3).

Table 3.1 :

Effect of BSO on the total intracellular glutathione content of J16 and HJ16 cell line.

Treatment	**J16 Cell Line** (μM glutathione / mg protein)	**HJ16 Cell Line** (μM glutathione / mg protein)
Control	0.47 ± 0.07	1.61 ± 0.67 *
25 μM BSO for 18 h	0	0

Cells were pre-treated with 25 μM BSO for 18 h as described in section 2.7. The total glutathione levels were assayed by Tietze's Method (see section 2.7) and normalised to total cellular protein . The results were expressed as mean ± standard deviation (n=4).

* : $p < 0.05$ significantly different when compared with J16 cell line.

3.2.4 The susceptibility of both cell lines to H_2O_2 following glutathione depletion by BSO

To investigate the susceptibility of both cell lines to H_2O_2 treatment following the depletion of the GSH/GSSG, J16 and HJ16 cell lines were first incubated for 18 h with 25 μM BSO and then treated with H_2O_2 at concentrations of 0.1, 0.5, 1.0, and 3 mM. The MTT analysis was then performed to determine the levels of cytotoxicity following these various treatments. The MTT results (see figure 3.7) showed that the susceptibility of the J16 cell line to a range of concentrations of H_2O_2 increases following the depletion of the GSH/GSSG by BSO. In HJ16 cells (see figure 3.7) the depletion of the GSH/GSSG also lead to enhanced cytotoxicity of the H_2O_2 treatment.

The MTT results were also confirmed by flow cytometric analysis using H_2O_2 doses up to 1 mM only, since the H_2O_2 dose of 3 mM was lethal to the J16 cell line. We have introduced to the treatments the H_2O_2 dose of 0.05 mM; therefore the concentrations of H_2O_2 used for flow cytometric analysis became 0.05, 0.1, 0.5, and 1.0 mM. The results obtained from flow cytometric analysis (see figure 3.8) confirmed the results shown by MTT analysis. Indeed in both cell lines, the susceptibility of cells to necrotic cell death increased after various doses of H_2O_2 following the depletion of the GSH/GSSG by 25 μM BSO. The cytotoxicity was significantly different in both the J16 and the HJ16 cell lines at all concentrations of H_2O_2 used.

3.2.5 Levels of total intracellular glutathione in J16 and HJ16 cell lines after the treatment of H_2O_2

The levels of total intracellular glutathione were determined following H_2O_2 treatment in J16 and HJ16 cell lines following the observation that the susceptibility of both cell lines to a range of concentrations of H_2O_2 increases following the depletion of the GSH/GSSG by BSO (see section 3.2.2). Our results (see figure 3.9) showed that H_2O_2 doses of higher than 0.1 mM depletes significantly the amount of total intracellular glutathione in the J16 cell line. However in HJ16 cells, H_2O_2 treatment only decreased to half the GSH/GSSG.

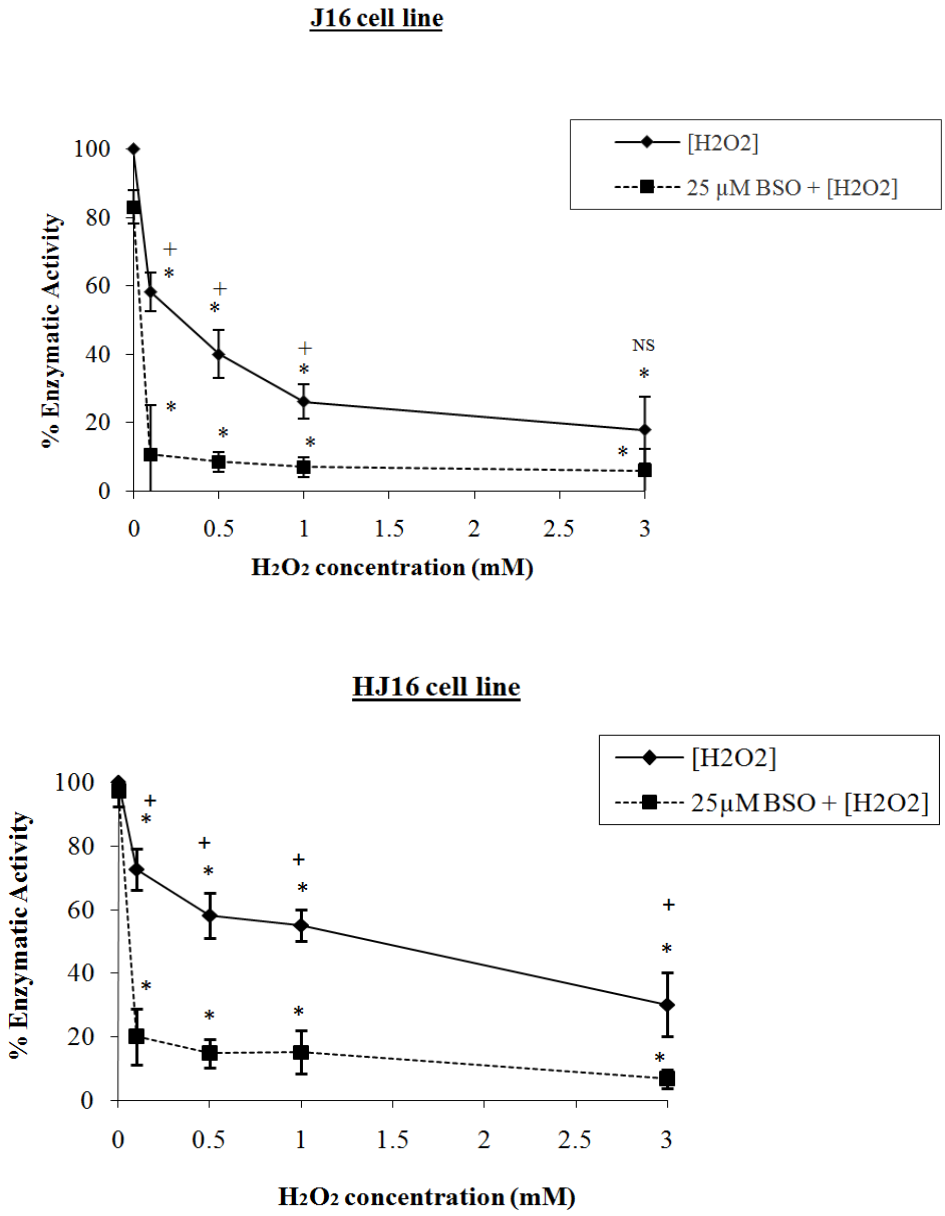

Figure 3.7 :
The evaluation of the susceptibility of J16 and HJ16 cell lines to H_2O_2 after the depletion of intracellular glutathione (Analysis : MTT).

Cells were treated overnight with BSO (25 µM) and then treated with various concentrations of H_2O_2 (0.1, 0.5, 1.0, and 3 mM). MTT analysis (see section 2.4) was performed 24 h following H_2O_2 treatment. The results are expressed as mean ± standard deviation (n=3).

* : $p < 0.05$ significantly different when compared with corresponding control of the same treatment.
+ : $p < 0.05$ significantly different when compared with cells treated with BSO prior to H_2O_2 treatment.
NS : non-significant different when compared with cells treated with BSO prior to H_2O_2 treatment

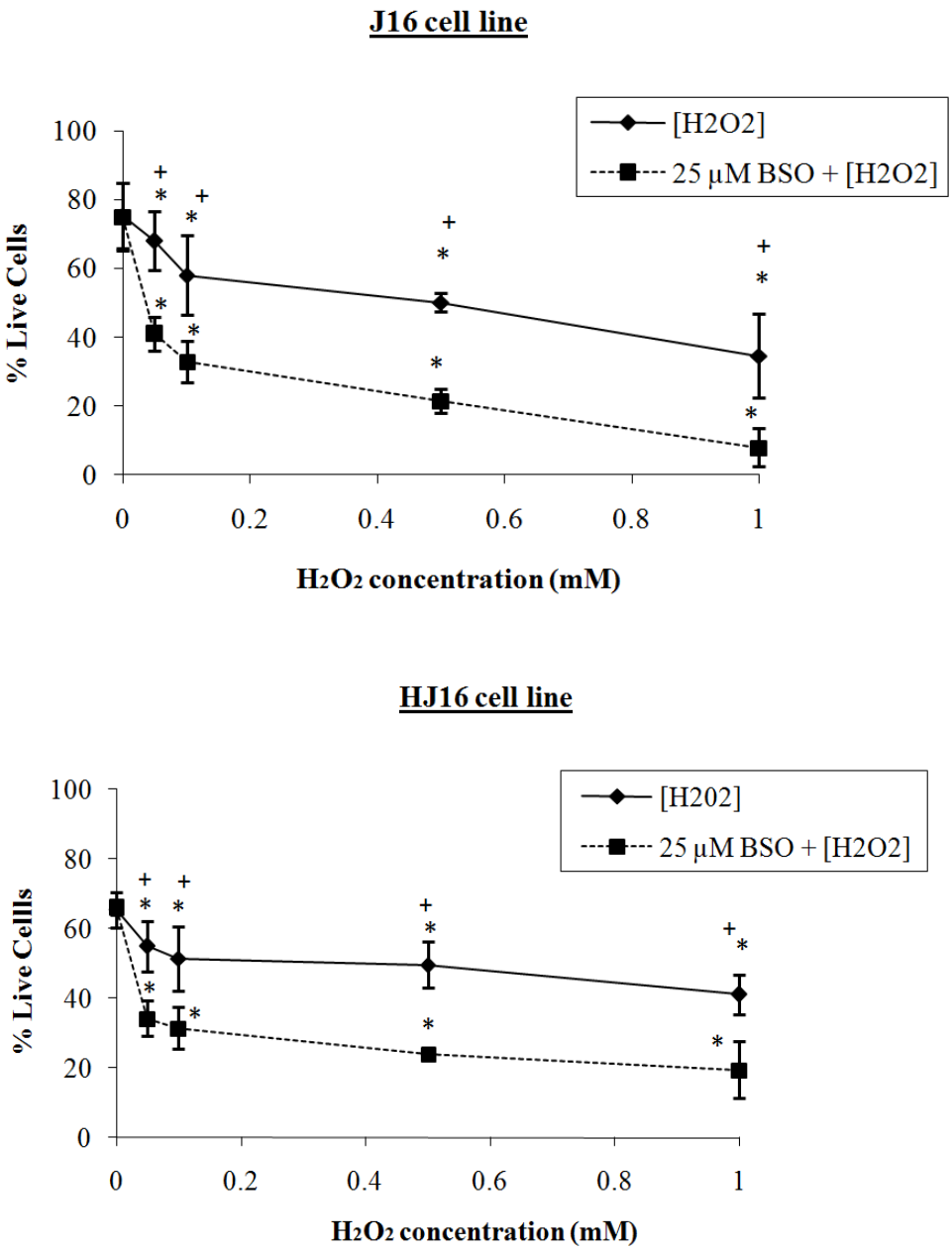

Figure 3.8 :
The determination of the susceptibility of J16 and HJ16 cell lines to H_2O_2 after the depletion of total intracellular glutathione (Flow cytometric analysis).

Cells were treated overnight with BSO (25 µM) and then treated with various concentrations of H_2O_2 (0.05, 0.1, 0.5, and 1.0 mM). Flow cytometry analysis (see section 2.5) was performed 24 h following H_2O_2 treatment. The results are expressed as mean ± standard deviation (n=3).

* : $p < 0.05$ significantly different when compared with corresponding control of the same treatment.
+ : $p < 0.05$ significantly different when compared with cells treated with BSO prior to H_2O_2 treatment.

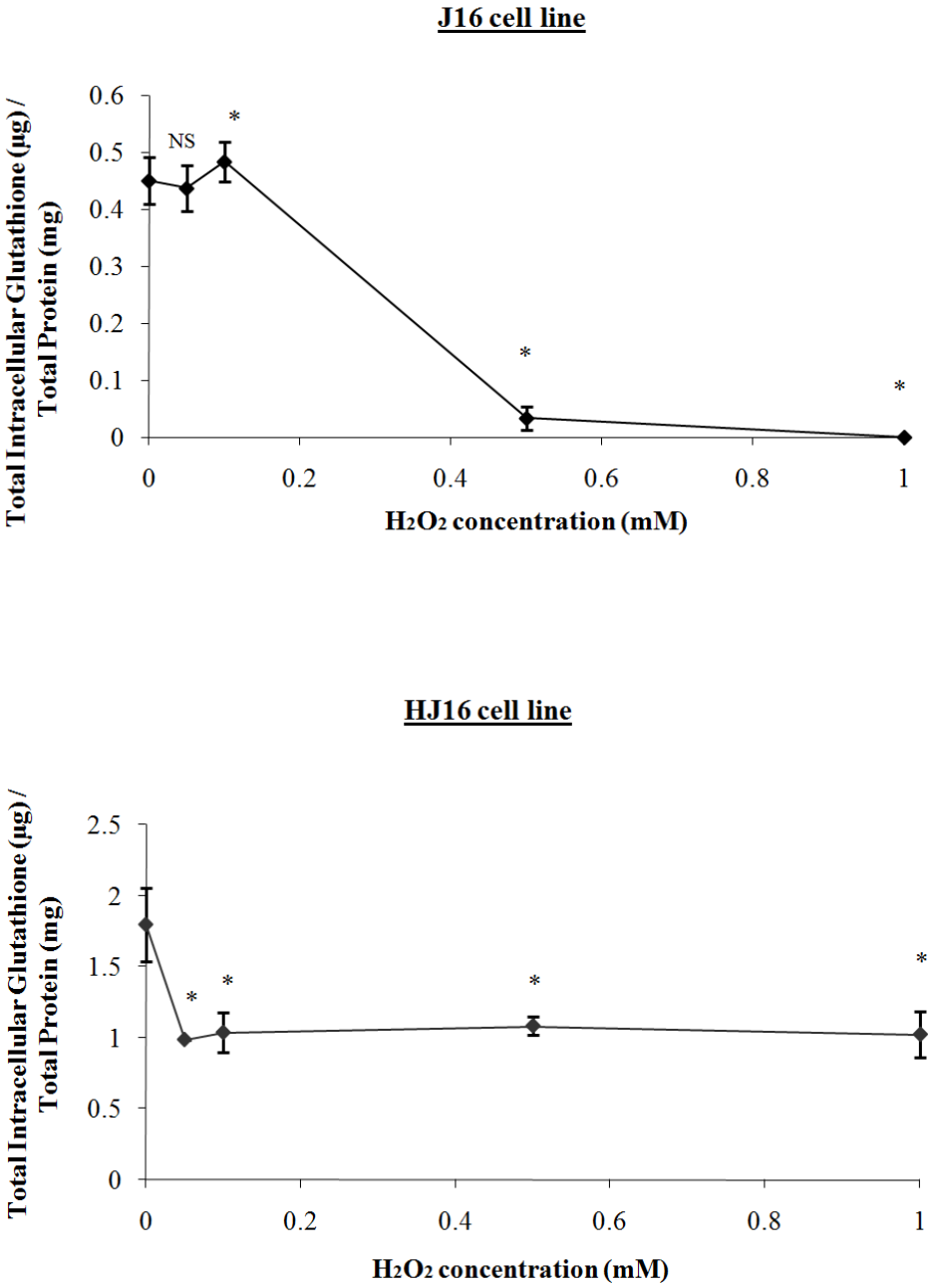

Figure 3.9 :

The determination of the levels of glutathione after the treatment with H_2O_2.

Cells were treated with H_2O_2 (0, 0.05, 0.1, 0.5, 1.0mM) as described in Materials and Methods and the total glutathione levels were assayed by Tietze's Method (see section 2.7) after the H_2O_2 treatment by 24 h. The results were expressed as mean ± standard deviation (n=3).

* : $p < 0.05$ significantly different between treated and the corresponding control.
NS : non-significant difference from the corresponding control.

The results suggest that chronic exposure of HJ16 cells to H_2O_2 provokes an adaptive mechanism preventing the total depletion of total intracellular glutathione in these cells. This will almost certainly contribute to the resistance of HJ16 cells to doses as high as 1mM H_2O_2.

3.3 Characterisation of the response of NF-κB to H_2O_2

As mentioned earlier (see section 1.6.5), the inducibility of the NF-κB complex in response to H_2O_2 is cell-specific. Furthermore it is not clear whether this response will be lost if cells are chronically adapted to H_2O_2 treatment, in the case of the HJ16 cell line. Therefore the inducibility of NF-κB complex, measured by Electrophoretic Mobility Shift Assay (EMSA) and immunocytochemistry was investigated in both J16 and HJ16 cell lines following H_2O_2 treatment.

3.3.1 The induction of NF-κB complex in the J16 and HJ16 cell lines

After the performance of supershift analysis it was found that the first complex (CI) is the classical NF-κB complex (RelA / p50), and the second complex (CII) appears to be p50 / p50 homodimer (A.Al-Qenaei MPhil Thesis, 2004 – University of Bath). This result was compatible with other studies that have been previously performed with other cell lines including Jurkat cells (Ginn-Pease and Whisler, 1996; Schoonbroodt *et al,* 2000; Gilston *et al,* 2001; Shin *et al,* 2004).

After 1 hour of various treatments of H_2O_2 (i.e. 0.5, and 1.0 mM), the induction of NF-κB complex binding was observed in J16 cell line (see figure 3.10). The induction of NF-κB in J16 cells appeared to be weak compared to HJ16 cell line. Nevertheless the NF-κB complex binding by H_2O_2 was dose-dependent in J16 cells, as shown by the quantification of the bands (see table 3.2). The HJ16 cell line was treated with the same concentrations of H_2O_2 (0.5, and 1.0 mM). The basal NF-κB complex binding was strongly induced in both concentration used (see figure 3.10 and table 3.2). These results confirm that NF-κB complex is present and induced by H_2O_2 in both J16 and HJ16 cells, although the induction was higher in HJ16 cells.

3.3.2 Characterisation of the response of NF-κB and Oct-1 to H_2O_2 treatment by immunocytochemistry

To confirm the previous results with EMSA, both J16 and HJ16 cells were treated with an intermediate dose, i.e. 0.5 mM H_2O_2, and subsequently the cells were incubated with 1, 6, and 24 h in condition medium and then immunocytochemistry of RelA (p65) and Oct-1 was performed (see section 2.10). The results shown in figure 3.11 and 3.12 reveal that p65 was situated in the cytoplasm, as expected.

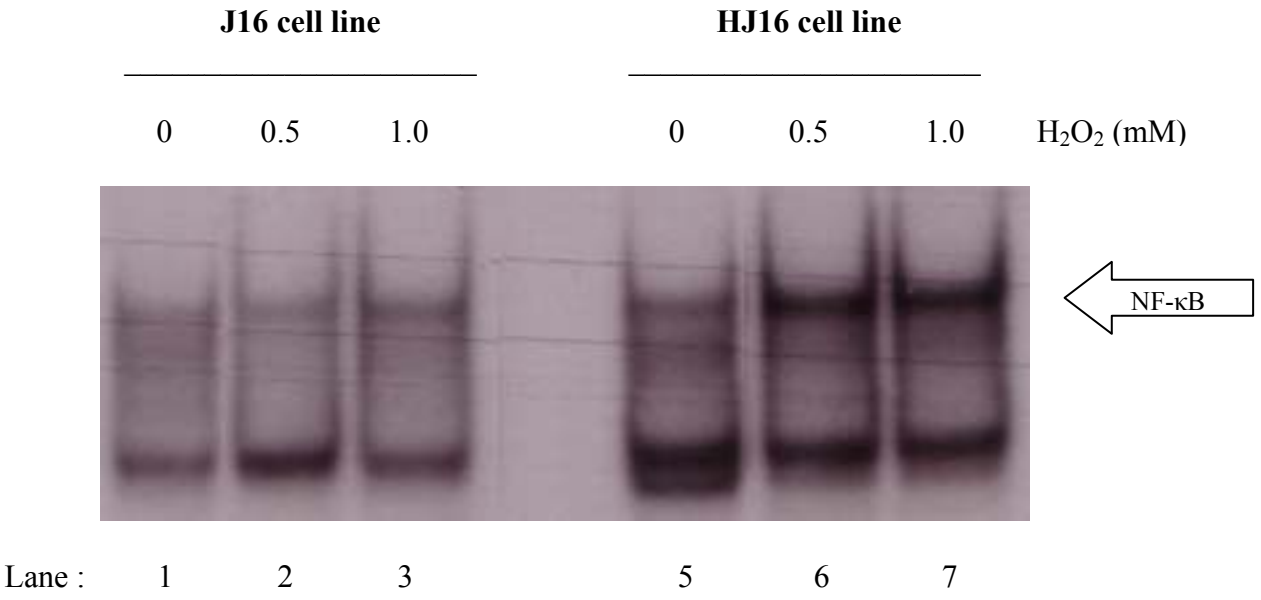

Figure 3.10 :

The induction of NF-κB activation in J16 and HJ16 cell lines 1 hour after H_2O_2 treatment.

[Analysed by electrophoretic mobility shift assay (EMSA) (see section 2.8)]

Lane 1 is the untreated J16 cell line (control), lanes 2 and 3 indicate the treatment of H_2O_2 (0.5 and 1.0 mM) respectively. Lane 5 is the untreated HJ16 cell line (control), lanes 6 and 7 indicate the treatment of H_2O_2 (0.5 and 1.0 mM) respectively.

The arrow indicates the position of the classical NF-κB complex (RelA / p50).

Table 3.2:

Numerical values of the quantification of the bands observed in Figure 3.11 (HJ16 and J16 cell line).

H_2O_2 Concentration (mM)	**J16 cell line**	**HJ16 cell line**
0	100 %	100 %
0.5	109 %	143 %
1.0	128 %	158 %

The bands were scanned and the quantification was assessed (see section 2.12.4) using LabImage software - Version 2.7.2 (Kapelan Bio-Imaging Solutions, Germany).

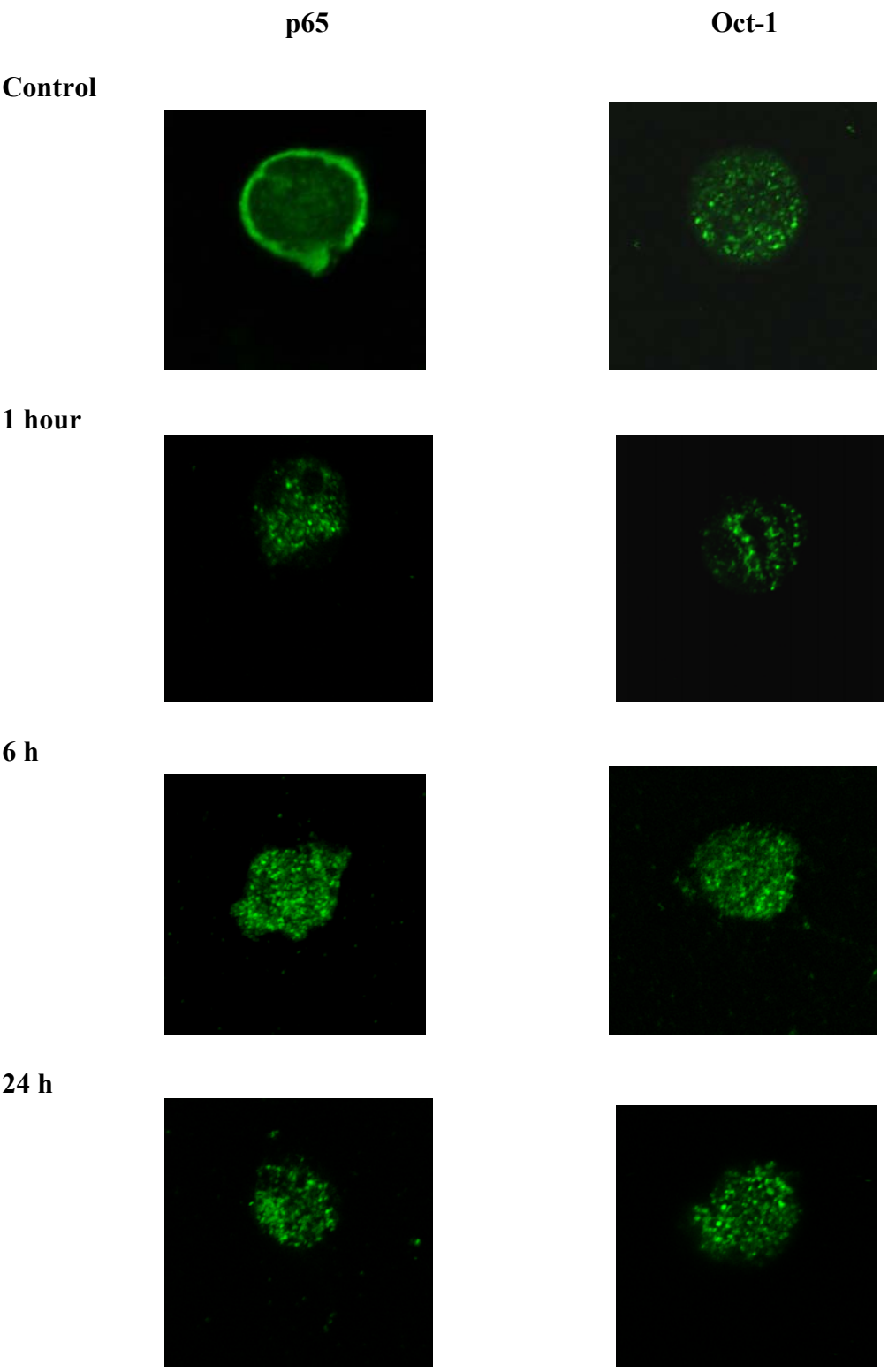

Figure 3.11 :
Localisation of RelA (p65) and Oct-1 following H_2O_2 treatment in J16 cell line.

J16 cells were treated with 0.5 mM of H_2O_2 and processed for immunochemistry (see section 2.13) at 1, 6, and 24 h post-treatment as described in section 2.13. The photographs are representative of three experiments.

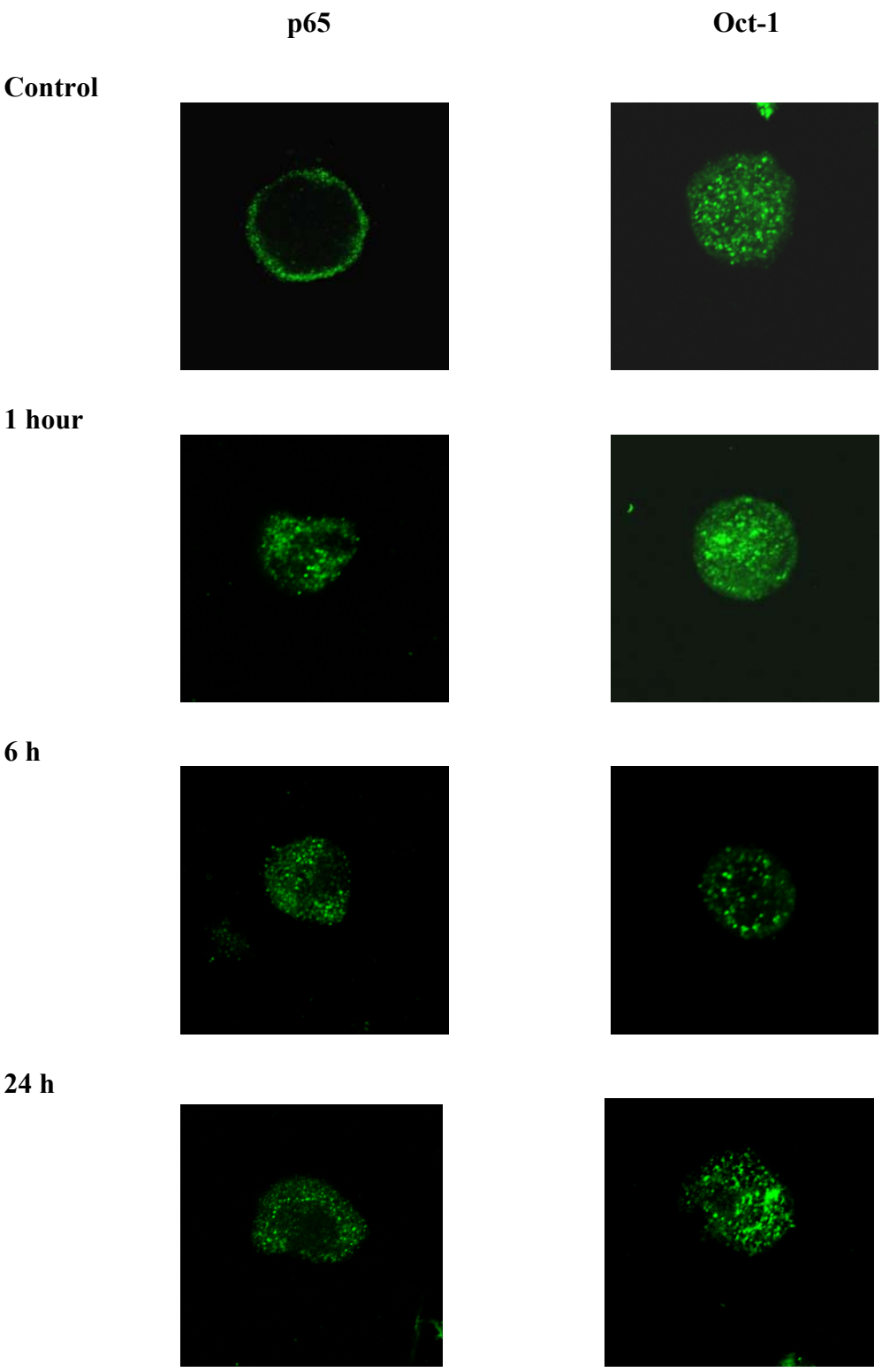

Figure 3.12 :

Localisation of RelA (p65) and Oct-1 following H_2O_2 treatment in HJ16 cell line.

HJ16 cells were treated with 0.5 mM of H_2O_2 and processed for immunochemistry (see section 2.13) at 1, 6, and 24 h post-treatment as described in section 2.13. The photographs are representative of three experiments.

Following H_2O_2 treatment, p65 translocated to the nucleus as early as 1 hour post-treatment and remained in the nucleus for at least 24 h after treatment. Studies with NF-κB and UVA in our laboratory have shown that UVA damages the nuclear membrane leading to the leakage of freshly translocated NF-κB to the cytosol. This was monitored by parallel leakage of nuclear Oct-1 to the cytosol (Reelfs *et al,* 2004). We therefore used Oct-1 in this study, to monitor possible damage to the nuclear membranes by H_2O_2. Our results demonstrated that Oct-1, the ubiquitous nuclear protein in mammalian cells, remained nuclear before and after H_2O_2 treatment in both cell lines in agreement with the notion that H_2O_2 does not damage the nuclear membrane. Taken together, the results showed that H_2O_2 activates the NF-κB translocation in both cell lines and confirmed the activation observed in EMSA.

3.4 The role of labile iron

Iron is a known catalyst of biological oxidation. Studies from this laboratory and others have demonstrated that both 'basal' and 'oxidant-induced' level of labile iron pool (LIP) could influence the susceptibility of cells to oxidative damage and cell death (e.g. Bissett *et al,* 1991; Zhong *et al,* 2004; Morliere *et al,* 1997).

For example in the case of acute exposure of skin to UVA, Zhong *et al,* (2004) from this laboratory, demonstrated that epidermal keratinocytes have higher resistance to UVA-induced oxidative damage and cell death than dermal fibroblasts presumably because both the 'basal' and 'UVA-induced' level of labile iron is dramatically lower in keratinocytes than fibroblasts. Furthermore the modulation of 'basal' and 'UVA-induced' level of LIP by either DFO (iron chelating) and/or hemin (iron loading) treatment significantly affected the extent of UVA-induced necrotic cell death in both cell lines and it was concluded that cellular susceptibility to UVA-induced necrotic cell death reflects the intracellular level of LIP.

The study carried out by Yiakouvaki (2003) using a Jurkat T cell model and H_2O_2, indicated that although cellular resistance to H_2O_2 is tightly associated with intracellular level of LIP, it is the 'H_2O_2-induced' rather than 'basal' level of LIP that is responsible for the increased susceptibility of cells to oxidative stress, although the underlying mechanism remained unclear. We therefore decided to further investigate this phenomenon in our cell lines.

3.4.1 The role of LIP in differential sensitivity of the J16 and HJ16 cells to H_2O_2 treatment

Figures 3.13 to 3.15 summarize the main finding of A. Yiakouvaki (PhD Thesis, 2003) that was repeated and confirmed and then complemented in the present study. The results demonstrated that the 'basal' level of LIP in both J16 and HJ16 cells are quite similar i.e. 3.08 μM ± 0.59 and 3.34 μM ± 0.87 respectively, but following H_2O_2 treatment (e.g. at a final concentration 0.5 mM), the 'H_2O_2-induced' level of LIP increases in both cell lines but to a lesser extent in HJ16 cells. The lower induction of H_2O_2-mediated LIP release in HJ16 cell line correlated with lower necrotic cell death (see table 3.3).

Table 3.3 :

The effect of H_2O_2-induced LIP on necrotic cell death in J16 and HJ16 cells.

Condition / Cell line	J16 cells	HJ16 cells
Basal LIP	3.08 μM ± 0.59	3.34 μM ± 0.87
H_2O_2-induced LIP	9.86 μM ± 0.15 *	5.27 μM ± 1.12 *+
Fold increase in H_2O_2-induced LIP	3.2-fold increase	1.6-fold increase
Percentage necrotic cell death post-H_2O_2	47 % ± 11	30 % ± 2 +

Note : Measurements of LIP were performed by CA-assay immediately after 0.5 mM of H_2O_2 treatment. The results are expressed as mean ± standard deviation (n=3-8). Flow cytometric analysis (see section 2.5) was performed 24 h after H_2O_2 treatment following dual Annexin-V/PI staining. The results are expressed as mean ± standard deviation (n=3)

* : $p < 0.05$ significantly different between treated and the corresponding control
+ : $p < 0.05$ significantly different from the corresponding J16 cell line.

To ascertain the importance of H_2O_2-induced labile iron release in modulating the susceptibility of cells to H_2O_2-induced necrotic cell death, both J16 and HJ16 were treated with DFO, a strong iron chelator or hemin (i.e. ferric haem) as a source of iron for 18 h prior to H_2O_2 treatment and then the level of LIP was measured following H_2O_2 treatment using the CA assay. The results demonstrated that DFO treatment abolishes both the 'basal' and 'H_2O_2-induced' LIP levels and necrotic cell death (see table 3.4a-b, figures 3.13 and 3.14) in both cell lines, consistent with the notion that iron chelation by DFO protects the cells against H_2O_2-induced necrotic cell death. In the case of hemin treatment, hemin alone (i.e. when not followed by H_2O_2 treatment) does not modulate the level of LIP in J16 cells but upon H_2O_2 treatment it causes a low increase in LIP that correlates with low necrosis (see table 3.4-a, figures 3.13 and 3.15). This is in agreement with previews studies by Balla and co-workers showing that the endothelium's susceptibility to H_2O_2-mediated insults decreases following exposure to hemin or haemoglobin (Balla *et al,* 1992 and 1993). On the other hand, hemin treatment modulated both the basal and H_2O_2-induced LIP levels in HJ16 cells. The accumulation of high levels of LIP in HJ16 cells following hemin treatment increased their susceptibility to H_2O_2-induced damage since the level of necrosis significantly increased upon hemin- H_2O_2 treatment (see table 3.4b, figures 3.13 and 3.15).

Further investigation with time course analysis revealed that in J16 cells, hemin treatment (20 μM) transiently increases the LIP levels within the first 4 h up to 2.2-fold, after which it returns to normal levels (see table 3.5a). In the HJ16 cells, hemin treatment provokes higher accumulation of LIP that is sustained at least for 18 h. The hemin-mediated increase in LIP appeared also to be concentration-dependent in the HJ16 cells (see figure 3.16). Since the high accumulation of LIP in HJ16 cells following hemin treatment increases the percentage of necrotic cell death, it was concluded that the intracellular level of LIP may play a key role in determining the level of sensitivity of these cells to H_2O_2-mediated necrotic cell death.

To further demonstrate the strict–dependence of H_2O_2-induced necrotic cell death to LIP level present in the cells, hemin treatment (20 μM) for 18 h was followed by an additional treatment with 1 mM DFO for 2h. The latter treatment was expected to lower the hemin-mediated increase in LIP, leading to decreased necrosis by H_2O_2.

Table 3.4 a: LIP measurements and the % of necrosis in J16 cell line.

Condition (J16 cell line)	**LIP (μM)**	**Percentage necrotic cell death**
Control (Basal)	3.08 μM ± 0.59	11 % ± 5
H_2O_2-0.5mM	9.86 μM ± 0.15 *	47 % ± 11 *
DFO-100μM – 18 h	0 *	0.53 % ± 0.12 *
DFO-100μM + H_2O_2-0.5mM	0 *	0.53 % ± 0.11 *
Hemin-20μM – 18 h	2.93 μM ± 0.73 ^{NS}	1.4 % ± 0.47 *
Hemin-20 μM + H_2O_2-0.5mM	4.02 μM ± 0.95 ^{NS}	27.2 % ± 0.8 *

Table 3.4 b: LIP measurements and the % of necrosis in HJ16 cell line.

Condition (HJ16 cell line)	**LIP (μM)**	**Percentage necrotic cell death**
Control (Basal)	3.34 μM ± 0.87	3 % ± 0.6
H_2O_2-0.5mM	5.27 μM ± 1.12 *$^{+}$	30 % ± 1.9 *$^{+}$
DFO-100μM -18 h	0 *	4.3 % ± 1.6 ^{NS}
DFO-100μM + H_2O_2-0.5mM	0 *	4.2 % ± 0.95 ^{NS}
Hemin-20μM – 18 h	7.2 μM ± 0.56 *$^{+}$	3 % ± 0.76 $^{NS+}$
Hemin-20 μM + H_2O_2-0.5mM	12.2 μM ± 0.34 *$^{+}$	43.2 % ± 3.1 $^{*+}$

Note: Measurements of LIP were performed by CA-assay immediately after the specified treatments (above). The results are expressed as mean ± standard deviation (n=3-8). Flow cytometric analysis (see section 2.5) was performed 24 h after H_2O_2 treatment following dual Annexin-V/PI staining. The results are expressed as mean ± standard deviation (n=3).

* : $p < 0.05$ significantly different between treated and the corresponding control
NS : non-significantly different from the corresponding control.
+ : $p < 0.05$ significantly different from the corresponding J16 cell line.

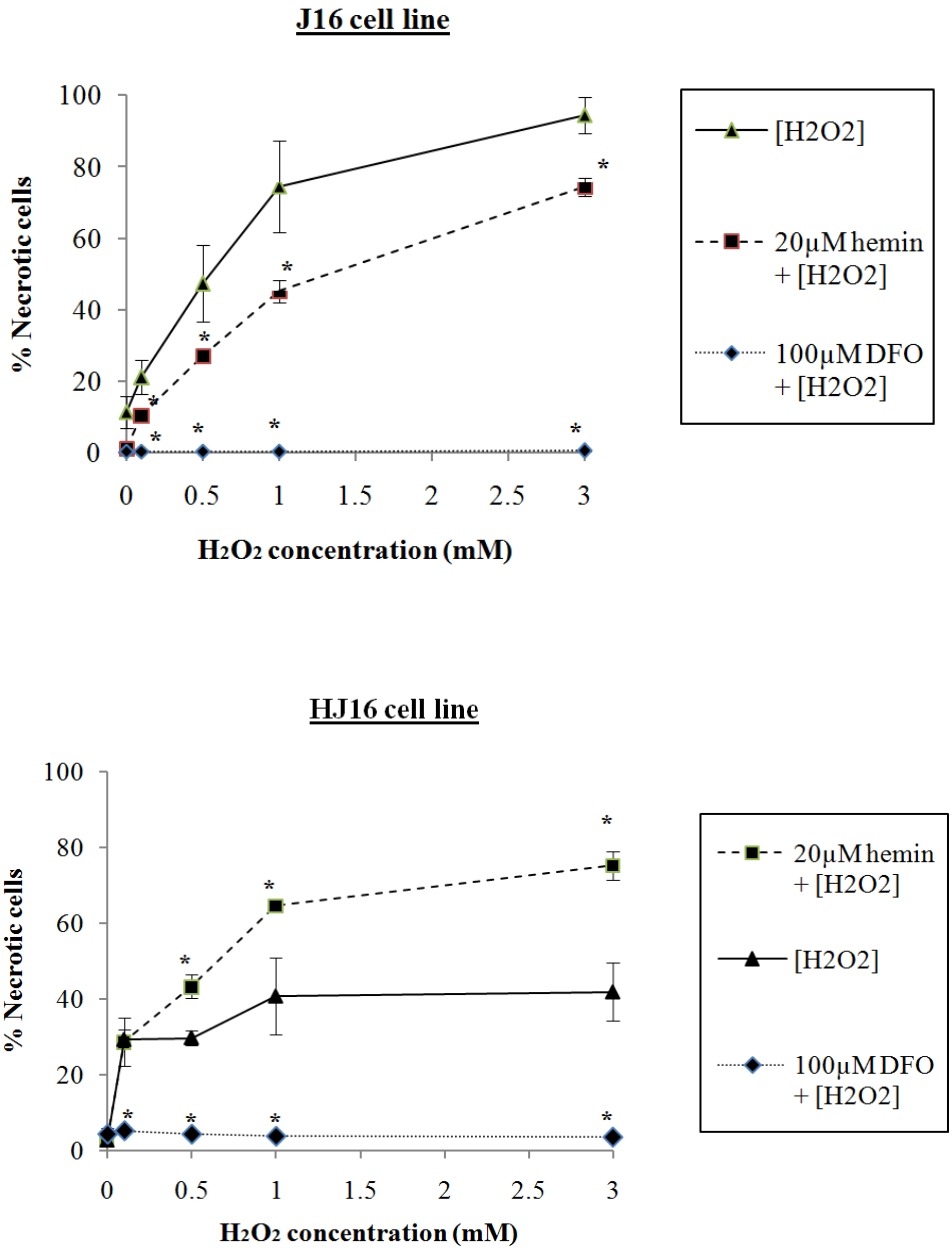

Figure 3.13 :

The evaluation of the susceptibility of J16 and HJ16 cell lines to iron chelation and loading prior to H_2O_2 treatment (Flow cytometric analysis).

Cells were pretreated with either 100 µM DFO or 20 µM hemin for 18 h before H_2O_2 treatment. Flow cytometric analysis (see section 2.5) was performed 24 h after H_2O_2 treatment following dual Annexin-V/PI staining. These results are expressed as mean ± standard deviation (n=3).

* : $p < 0.05$ significantly different from the cells treated with H_2O_2 treatment alone.
NS : non-significant different from the cells treated with H_2O_2 treatment alone.

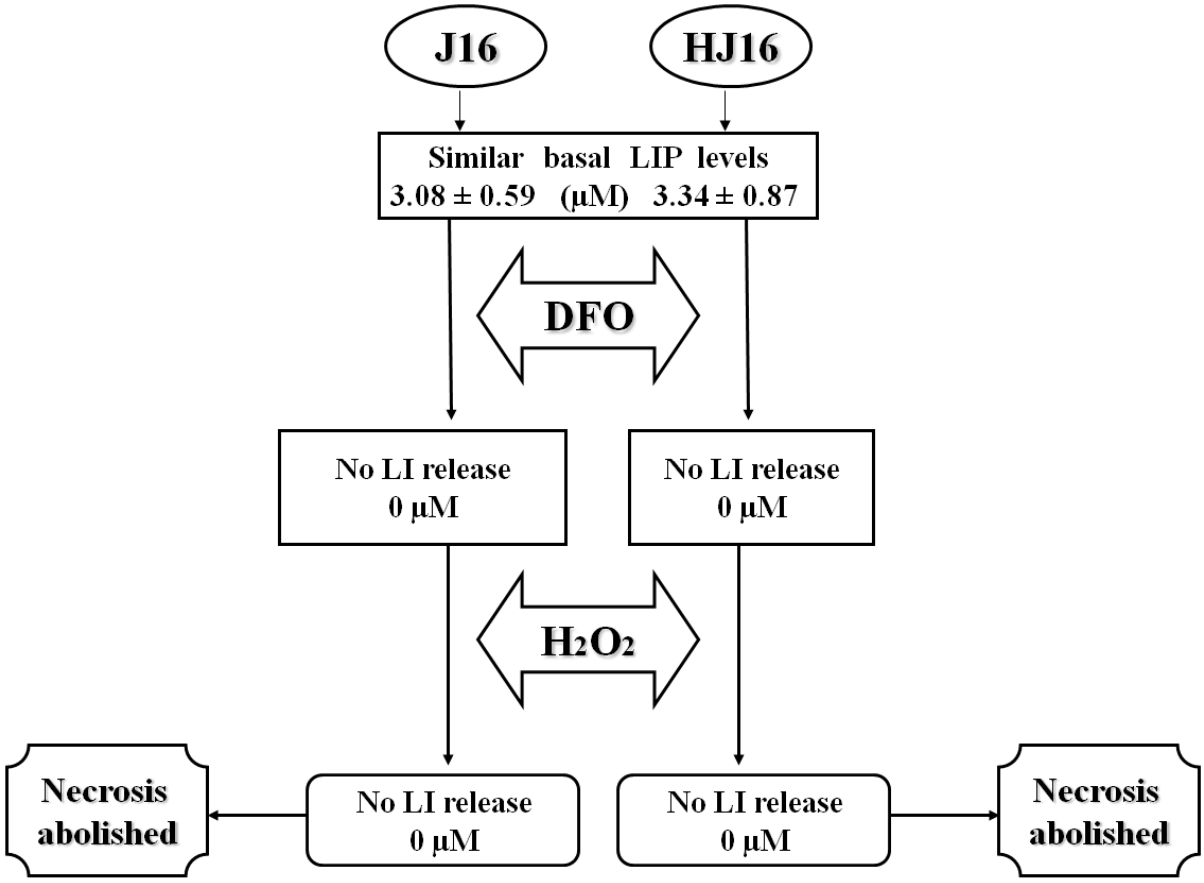

Figure 3.14:

Schematic representation of the effect of DFO ± H_2O_2 treatment on labile iron pool (LIP) and the viability of J16 and HJ16 cells.

Both cell lines were either treated overnight with 100 μM DFO alone or 100 μM DFO for 18 h prior an intermediate dose of H_2O_2 (i.e. 0.5mM). The levels of LIP was determined (Yiakovaki, 2003) by a modification of the method developed by Epsztejn *et al* (1997). The level of necrosis was determined by flow cytometric analysis (see section 2.5).

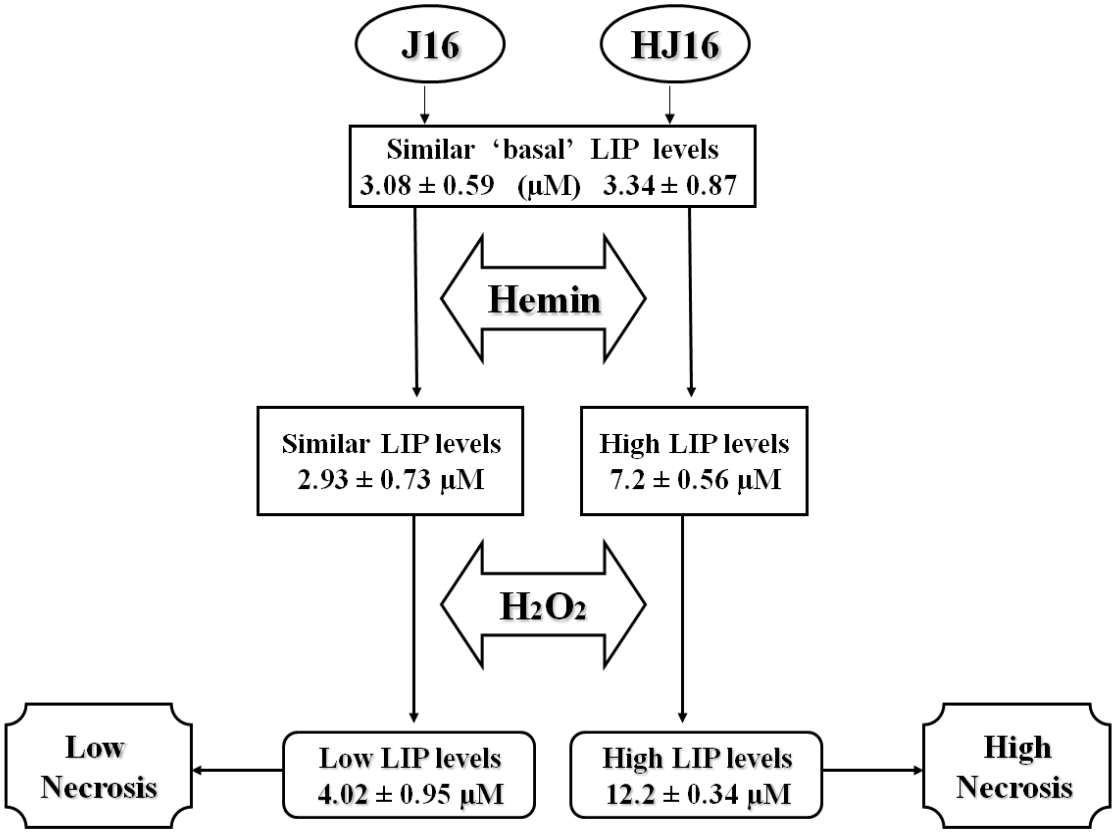

Figure 3.15:

Schematic representation of the effect of hemin ± H_2O_2 treatment on labile iron pool (LIP) and the viability of J16 and HJ16 cells.

Both cell lines were either treated overnight with 20 μM hemin alone or 20 μM hemin for 18 h prior an intermediate dose of H_2O_2 (i.e. 0.5mM). The levels of LIP was determined by a modification of the method developed by Epsztejn *et al* (1997). The level of necrosis was determined by flow cytometric analysis (see section 2.5).

Table 3.5a: Time course of LIP measurements and the fold increase of LIP after 20 μM hemin treatment of J16 cells.

Condition	LIP (μM)	Fold increase
Basal - 0 h	3.3 μM ± 0.87	1
2 h	6.8 μM ± 1.6 *	2-fold increase
4 h	7.4 μM ± 1.8 *	2.2-fold increase
6 h	3.1 μM ± 0.53	Non-significant
8 h	3.5 μM ± 0.38	Non-significant
18 h	2.6 μM ± 0.42	Non-significant

Table 3.5b: Time course of LIP measurements and the fold increase of LIP after 20 μM hemin treatment of HJ16 cells.

Condition	LIP (μM)	Fold increase
Basal - 0 h	3.34 μM ± 0.87	1
2 h	11.8 μM ± 1.8 *$^{+}$	3.5-fold increase
4 h	11.2 μM ± 1.7 *$^{+}$	3.4-fold increase
6 h	14.1 μM ± 0.93 *$^{+}$	4.2-fold increase
8 h	10.3 μM ± 0.41 *$^{+}$	3.1-fold increase
18 h	7.2 μM ± 0.56 *$^{+}$	2.2-fold increase

Note : The LIP was monitored by Calcein assay following the treatment of J16 and HJ16 cells with 20 μM hemin for various times (i.e. 2, 4, 6, 8 and 18 h). The results are expressed as mean ± standard deviation (n=6-8).

* : $p < 0.05$ significantly different between treated and the corresponding control
+ : $p < 0.05$ significantly different from the corresponding J16 cell line.

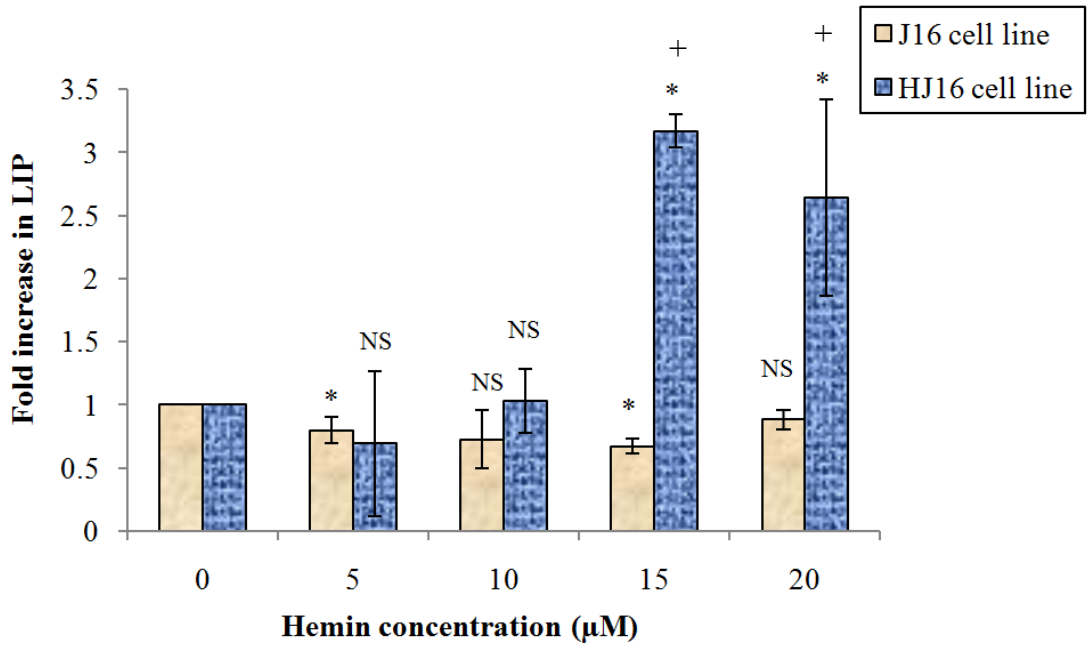

Figure 3.16:

Fold increase in LIP measurements after various concentrations of hemin.

LIP measurements were taken after J16 cell line and HJ16 cell line were treated with different concentration of hemin (i.e. 5, 10, 15, and 20 µM) for 18 h. These results are expressed as mean ± standard deviation (n=3).

* : $p < 0.05$ significant difference between untreated and treated cells.
NS : Non-significant difference between untreated and treated cells.
+ : $p < 0.05$ significant difference from the corresponding J16 cell line.

The results (see figure 3.17) showed that, in agreement with our hypothesis, in both cell lines, DFO treatment of cells pre-treated with hemin significantly decreased the levels of H_2O_2-induced necrotic cell death when compared to cells treated with hemin alone.

The source of iron in HJ16 cells following hemin treatment

The source of iron after overnight hemin treatment of the HJ16 cell line was an interesting point to investigate in this study. Hemin (ferric haem) is a known substrate of HO proteins (i.e. HO-1 and HO-2). Both the inducible form HO-1 and the constitutive HO-2 enzymes break down haem to release its iron (see section 1.4.2.4). This iron is then stored within the iron storage protein ferritin (Ft).

We hypothesised that the high accumulation of labile iron in HJ16 cells following hemin treatment could either be due to higher HO protein levels or lower intracellular Ft levels in HJ16 cells when compared to parental J16 cells. We therefore investigated the level of these proteins in both J16 and HJ16 cells following various treatments as detailed below.

3.4.2 The expression of HO-1 and HO-2 in Jurkat T cell lines

The higher expression of HO-1 and/or HO-2 in HJ16 cell line might contribute to accumulation of labile iron following hemin treatment. Previous analysis of the level of *ho-1* mRNA accumulation in J16 and HJ16 cells using the real-time PCR technique (Yiakouvaki, 2003) revealed that the basal level of *ho-1* cDNA is 2-fold higher in the H_2O_2-resistant HJ16 cells than in the parental J16 cells. Yiakouvaki (2003) also performed a series of Western blot analyses using a polyclonal HO-1 antibody. These Western blot analyses were not conclusive since the polyclonal antibody cross-reacted with a number of proteins in cell extracts resulting in high background and multiple bands that made the interpretation of results difficult. The study therefore moved on to use flow cytometry as a more trustworthy technique to study the expression of HO-1 in the Jurkat cells using a monoclonal antibody. The results revealed that in agreement with real-time PCR data, the basal level of HO-1 protein in H_2O_2 resistant cells was up to 2-fold higher than in parental cells.

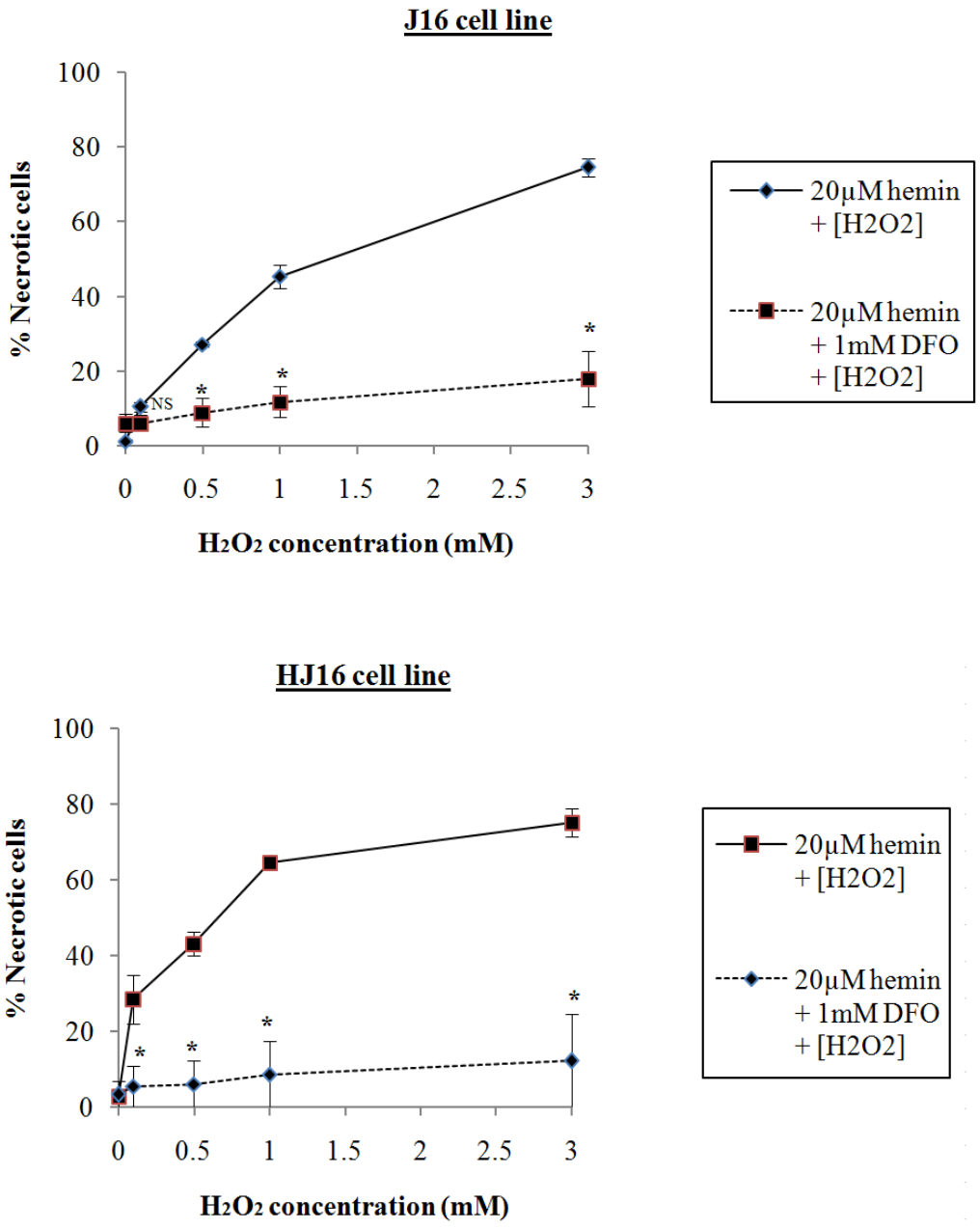

Figure 3.17:

The evaluation of the susceptibility of J16 and HJ16 cell lines after DFO treatment following iron loading prior to H_2O_2 treatment.

Cells were pretreated with either 20 µM Hemin for 18 h or 20 µM Hemin for 18 h and then 1mM DFO for 2 h before H_2O_2 treatment. Flow cytometric analysis (see section 2.5) was performed 24 h after H_2O_2 treatment following dual Annexin-V/PI staining. These results are expressed as mean ± standard deviation (n=3).

* : $p < 0.05$ significantly different between the hemin ($+H_2O_2$) treated cells.
NS: non-significantly different when compared with the hemin ($+H_2O_2$) treated cells.

So it was concluded, with the previous observations, that HO-1 expression should play a role in hemin-induced iron accumulation in HJ16 cells. Furthermore when both cell lines were treated with 20 μM hemin at various time points, a significant increase in HO-1 was only observed in the parental J16 cell line. Yiakouvaki (2003) concluded that HO-1 protein is not inducible in HJ16 cells presumably because gradual adaptation of cells to H_2O_2 has provoked a refractory response of HO-1 to hemin.

Since hemin is also a known substrate of HO-2 protein, it was important to check the level of its expression in Jurkat T cells. We therefore decided to carry out an in depth study of the expression of HO-1 and HO-2 at protein levels using Western blot analysis. For HO-2 analysis, we used the polyclonal antibody raised in R.M. Tyrrell's laboratory (Pourzand *et al,* 1999 and Kvam *et al,* 2000) as this antibody, unlike commercially available HO-2 antibodies, is known to be very specific. For HO-1, the Western blotting was carried out with a monoclonal antibody to avoid high background and cross-hybridisations. This antibody induced less background but still some cross hybridization was observed in the study. As a result one important positive control was added in each blot to identify the true HO-1 band in blots. That control was FEK4 cells (human fibroblast cell line) treated with a UVA dose of 250 kJ/m^2 and incubated in condition media (CM) for 8 h before it was collected.

Figures 3.18 to 3.21 compare the level of HO-1 and HO-2 in both J16 and HJ16 cells collected *immediately* (0 h) or left in CM for *24 h* (24 h) following hemin, DFO and/or H_2O_2 treatment. As can be seen, the basal level of HO-1 was very low in these cells and the difference in expression observed by Flow cytometry could not be visualized here. Furthermore neither overnight treatments with 20 μM hemin, 100 μM DFO, nor exposure to 0.5 mM H_2O_2 alone or combined with hemin or DFO treatment increased the level of HO-1 in these cell lines. The basal HO-2 level on the other hand was higher than HO-1 in both cell lines but it was not modulated by any of the above treatments.

To ascertain that HO protein levels were not modulated following hemin and/or H_2O_2, the HO-1 and HO-2 levels were followed in time course analysis from 0 to 18 and/or 24 h following hemin and/or H_2O_2 treatments. The results (see figures 3.22-3.27) revealed that neither HO-1 nor HO-2 levels are modulated by these treatments.

A.

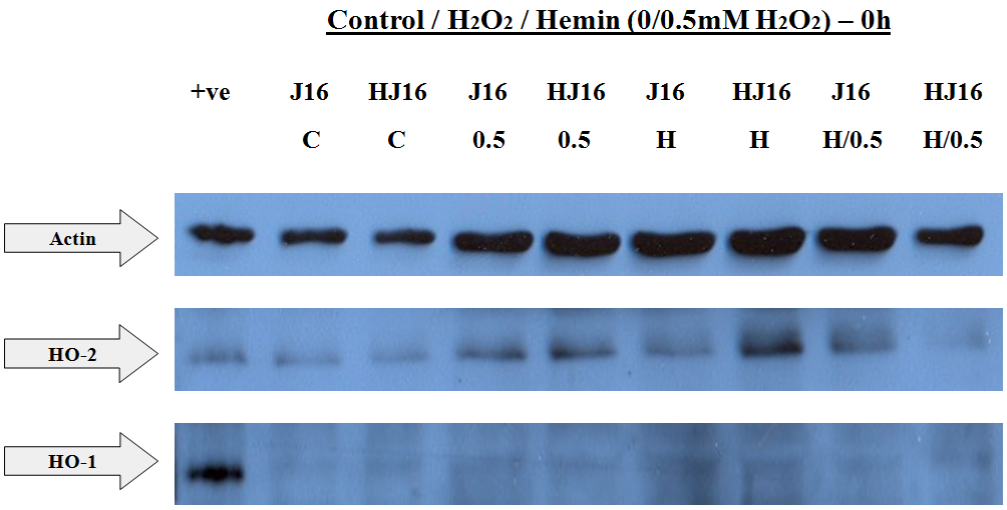

B.

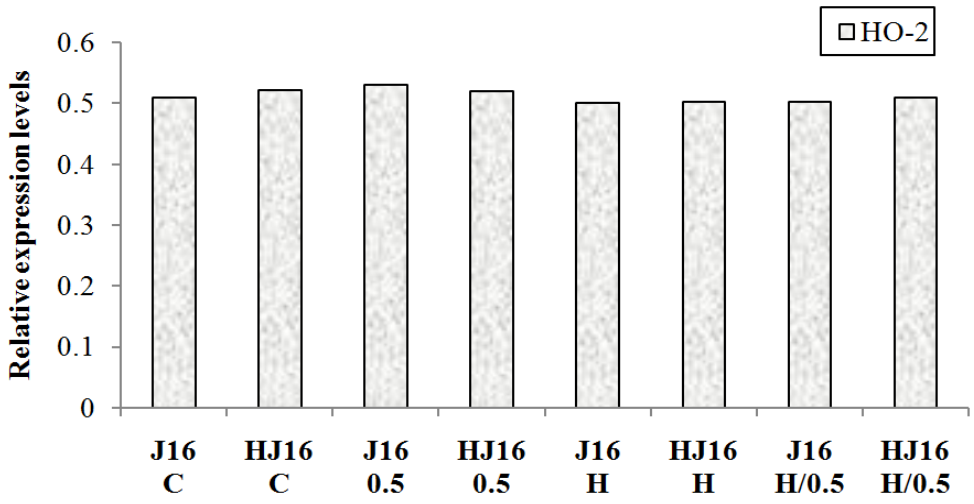

Figure 3.18:

The induction of HO-1 and HO-2 in J16 and HJ16 cell lines (0 h).

J16 and HJ16 (C) are the untreated cells (controls), J16 and HJ16 (0.5) are cells treated with 0.5mM H_2O_2, J16 and HJ16 (H) are cells treated with 20 µM hemin for 18 h, and J16 and HJ16 (H/0.5) are cells treated overnight with 20µM hemin and then with 0.5mM H_2O_2. Cells were collected *immediately* following the specified treatments and used to prepare whole cellular extracts for Western blot analysis (see section 2.9). The positive control (+ve) was FEK4 cells (human fibroblast cell line) treated with a UVA dose of 250 kJ/m^2 and collected after 8 h. (B) The relative expression levels of HO-2 were normalised with respect to the intensity of the actin signal.

The intensities of the bands were assessed using LabImage software - Version 2.7.2 (Kapelan Bio-Imaging Solutions, Germany).

A.

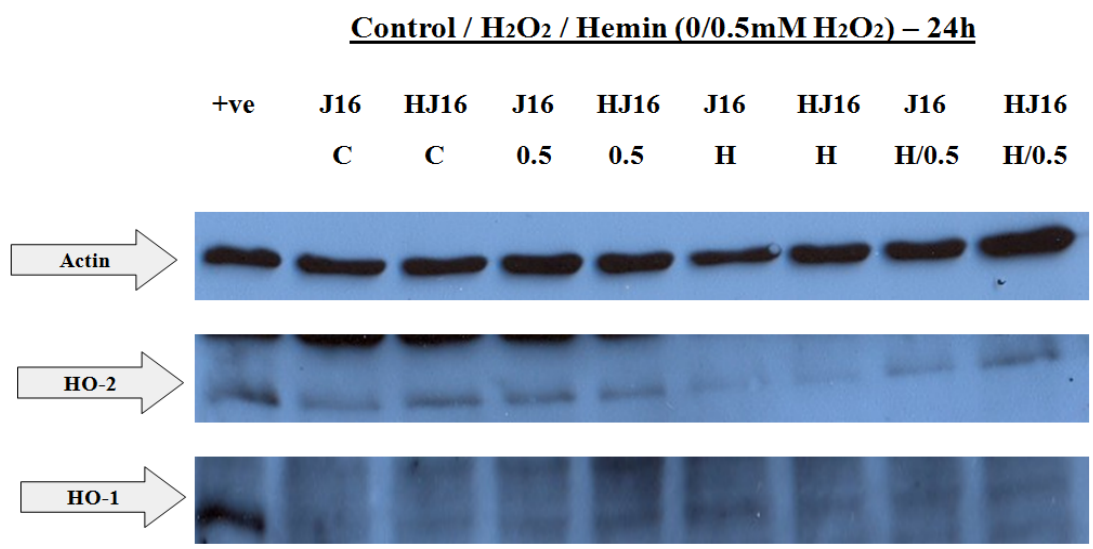

B.

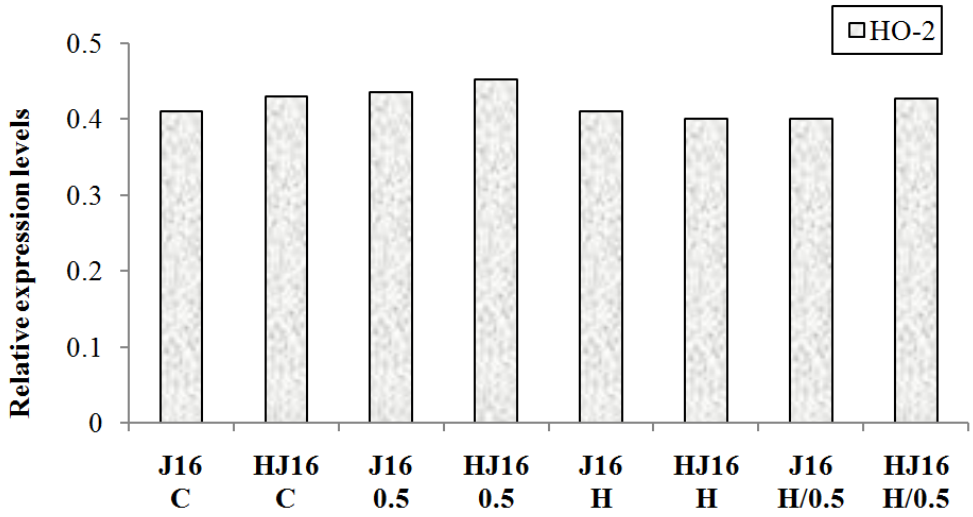

Figure 3.19:

The induction of HO-1 and HO-2 in J16 and HJ16 cell lines (24 h).

J16 and HJ16 (C) are the untreated cells (controls), J16 and HJ16 (0.5) are cells treated with 0.5mM H_2O_2, J16 and HJ16 (H) are cells treated with 20 µM hemin for 18 h, and J16 and HJ16 (H/0.5) are cells treated overnight with 20µM hemin and then with 0.5mM H_2O_2. Cells were collected *24 h* following the specified treatments and used to prepare whole cellular extracts for Western blot analysis (see section 2.9). The positive control (+ve) was FEK4 cells (human fibroblast cell line) treated with a UVA dose of 250 kJ/m^2 and collected after 8 h. (B) The relative expression levels of HO-2 were normalised with respect to the intensity of the actin signal.

The intensities of the bands were assessed using LabImage software - Version 2.7.2 (Kapelan Bio-Imaging Solutions, Germany).

A.

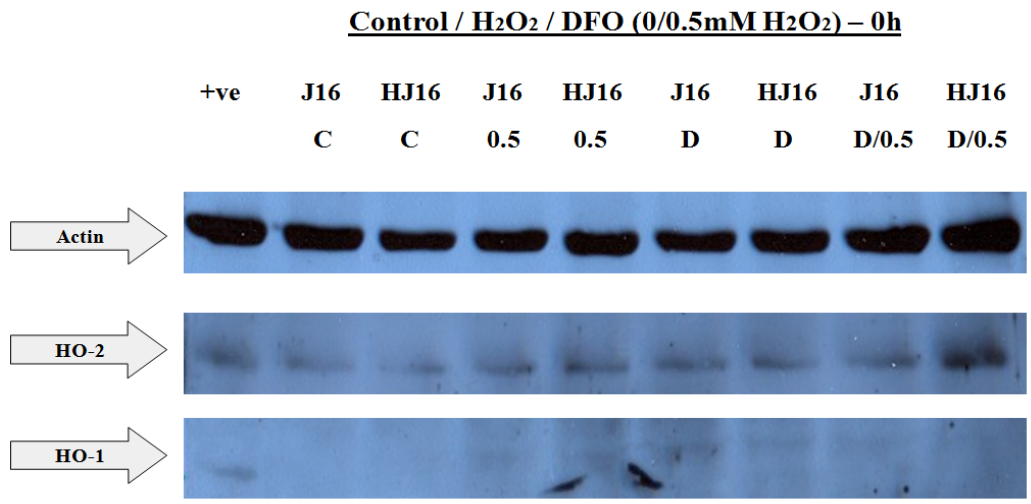

B.

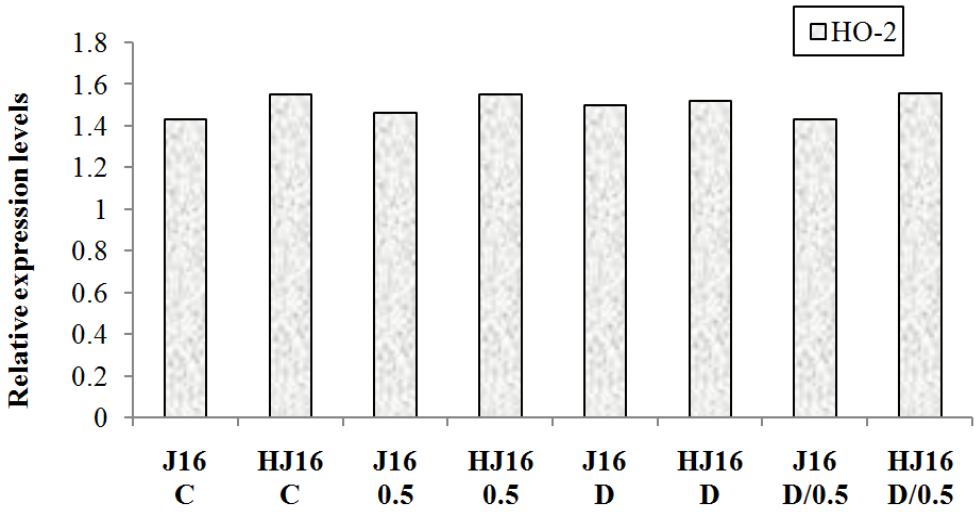

Figure 3.20:
The induction of HO-1 and HO-2 in J16 and HJ16 cell lines (0 h).

J16 and HJ16 (C) are the untreated cells (controls), J16 and HJ16 (0.5) are cells treated with 0.5mM H_2O_2, J16 and HJ16 (D) are cells treated with 100 µM DFO for 18 h, and J16 and HJ16 (D/0.5) are cells treated overnight with 100 µM DFO and then with 0.5mM H_2O_2. Cells were collected *immediately* following the specified treatments and used to prepare whole cellular extracts for Western blot analysis (see section 2.9). The positive control (+ve) was FEK4 cells (human fibroblast cell line) treated with a UVA dose of 250 kJ/m^2 and collected after 8 h. (B) The relative expression levels of HO-2 were normalised with respect to the intensity of the actin signal.

The intensities of the bands were assessed using LabImage software - Version 2.7.2 (Kapelan Bio-Imaging Solutions, Germany).

A.

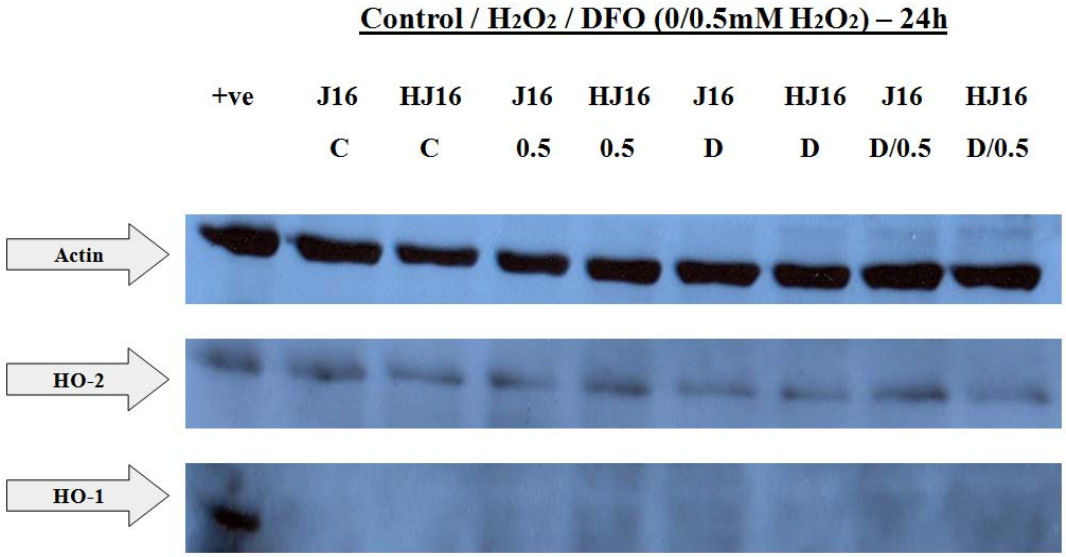

B.

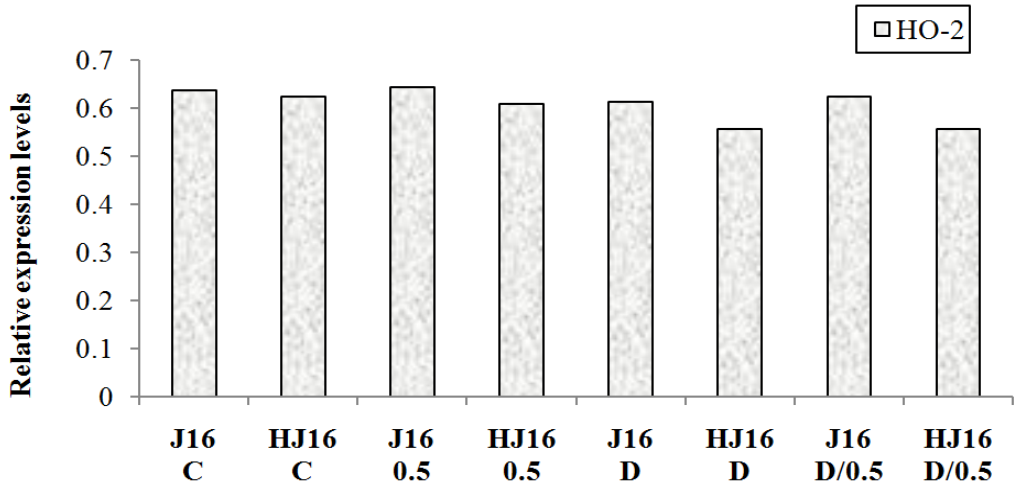

Figure 3.21:

The induction of HO-1 and HO-2 in J16 and HJ16 cell lines (24 h).

J16 and HJ16 (C) are the untreated cells (controls), J16 and HJ16 (0.5) are cells treated with 0.5mM H_2O_2, J16 and HJ16 (D) are cells treated with 100 µM DFO for 18 h, and J16 and HJ16 (D/0.5) are cells treated overnight with 100 µM DFO and then with 0.5mM H_2O_2. Cells were collected *24 h* following the specified treatments and used to prepare whole cellular extracts for Western blot analysis (see section 2.9). The positive control (+ve) was FEK4 cells (human fibroblast cell line) treated with a UVA dose of 250 kJ/m^2 and collected after 8 h. (B) The relative expression levels of HO-2 were normalised with respect to the intensity of the actin signal.

The intensities of the bands were assessed using LabImage software - Version 2.7.2 (Kapelan Bio-Imaging Solutions, Germany).

A.

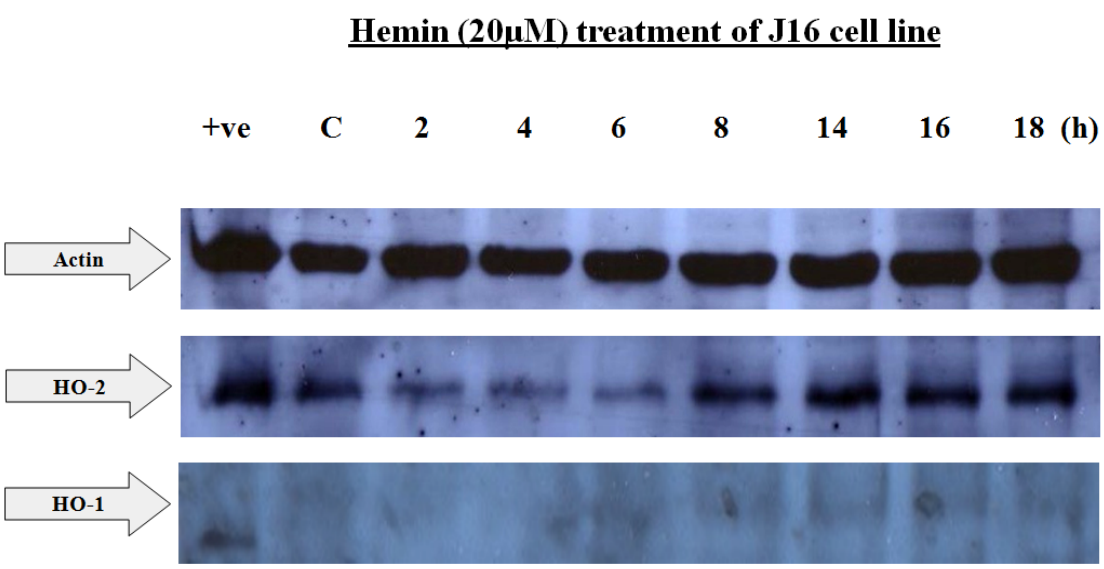

B.

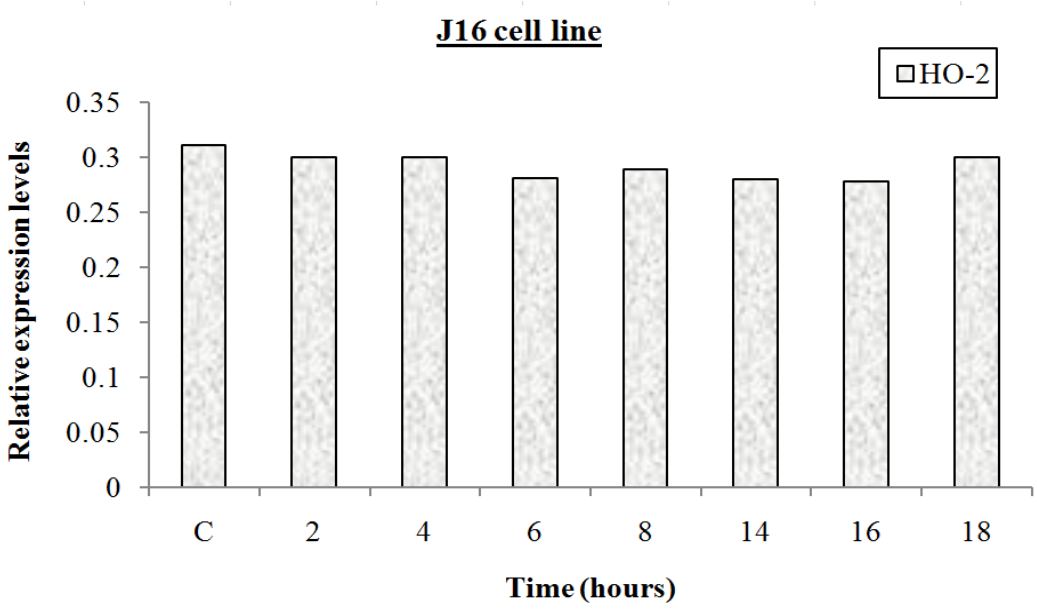

Figure 3.22 :
Time course induction of HO-1 and HO-2 in J16 cell line after 20 µM hemin.

(A) J16 cell line was treated with 20 µM hemin. Cells were collected at various times (i.e. 2, 4, 6, 8, 14, 16, and 18 h) and used to prepare whole cellular extracts for Western blot analysis (see section 2.9). The positive control (+ve) was FEK4 cells (human fibroblast cell line) treated with a UVA dose of 250 kJ/m^2 and collected after 8 h. (B) The relative expression levels of HO-2 were normalised with respect to the intensity of the actin signal.

The intensities of the bands were assessed using LabImage software - Version 2.7.2 (Kapelan Bio-Imaging Solutions, Germany).

A.

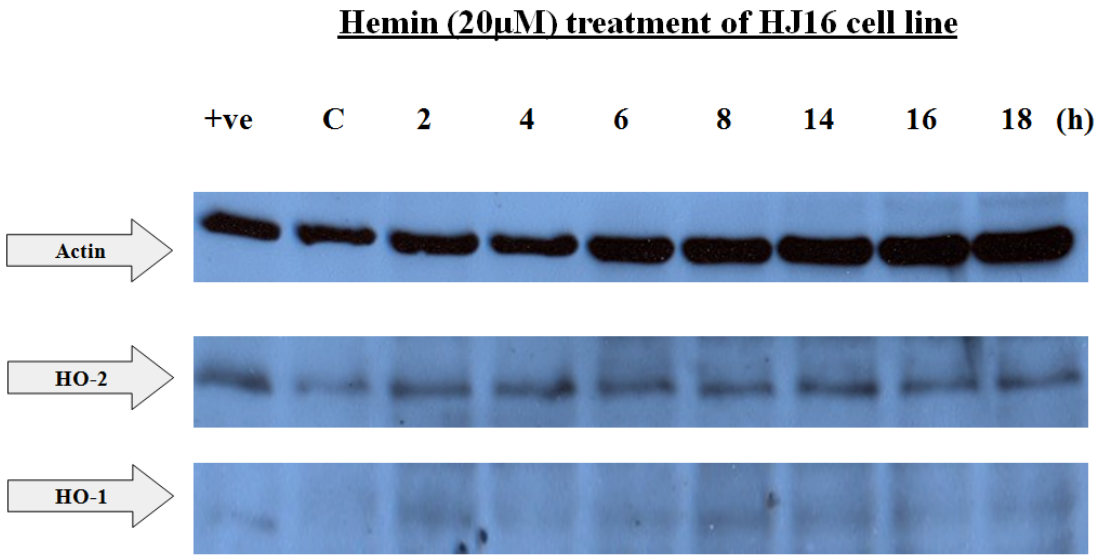

B.

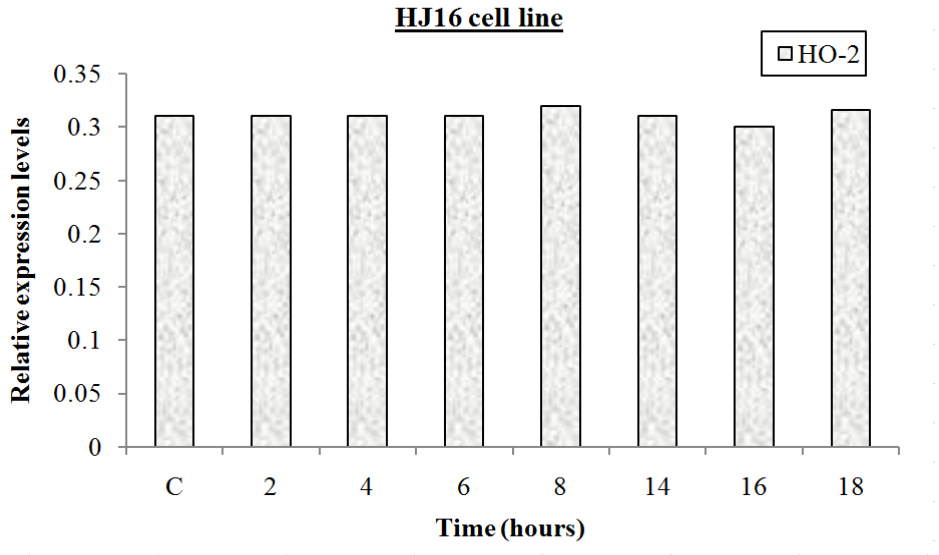

Figure 3.23 :

Time course induction of HO-1 and HO-2 in HJ16 cell line after 20 µM hemin.

(A) HJ16 cell line was treated with 20 µM hemin. Cells were collected at various times (i.e. 2, 4, 6, 8, 14, 16, and 18 h) and used to prepare whole cellular extracts for Western blot analysis (see section 2.9). The positive control (+ve) was FEK4 cells (human fibroblast cell line) treated with a UVA dose of 250 kJ/m^2 and collected after 8 h. (B) The relative expression levels of HO-2 were normalised with respect to the intensity of the actin signal.

The intensities of the bands were assessed using LabImage software - Version 2.7.2 (Kapelan Bio-Imaging Solutions, Germany).

A.

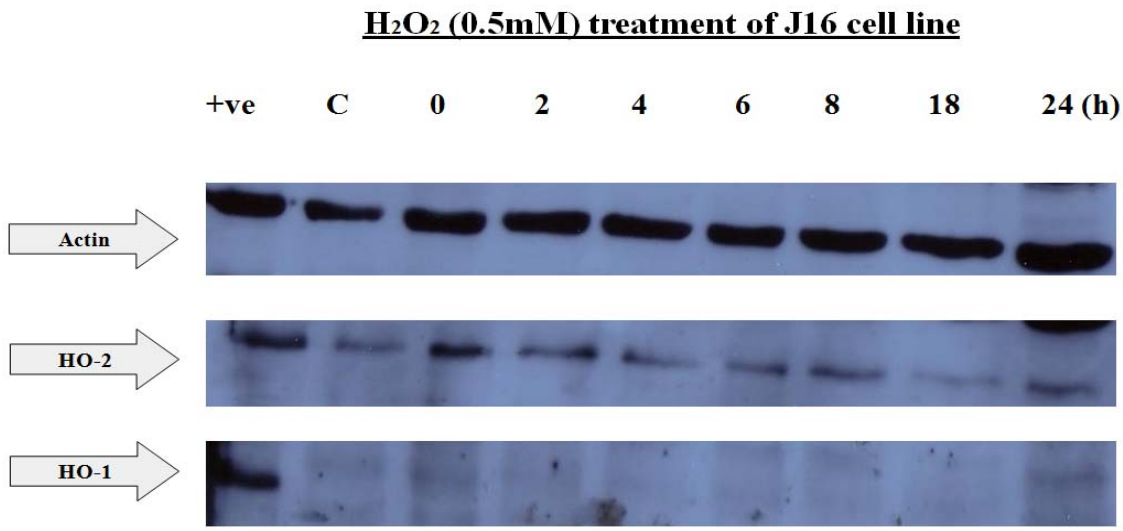

B.

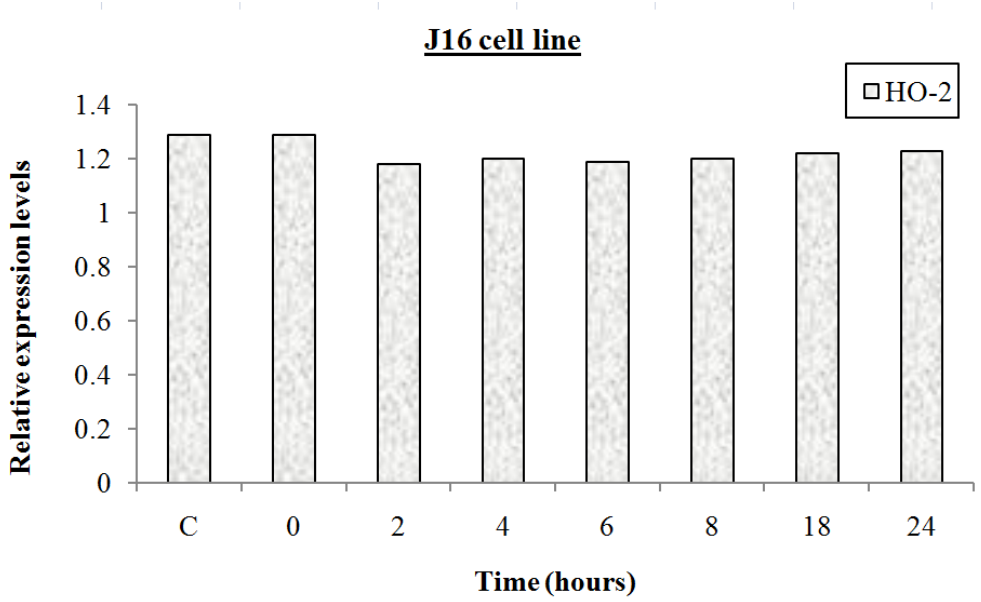

Figure 3.24 :

Time course induction of HO-1 and HO-2 in J16 cell line after 0.5 mM H_2O_2.

(A) J16 cell line was treated with an intermediate dose of H_2O_2 (i.e. 0.5 mM). Cells were collected at various times (i.e. 0, 2, 4, 6, 8, 18, and 24 h) and used to prepare whole cellular extracts for Western blot analysis (see section 2.9). The positive control (+ve) was FEK4 cells (human fibroblast cell line) treated with a UVA dose of 250 kJ/m^2 and collected after 8 h. (B) The relative expression levels of HO-2 were normalised with respect to the intensity of the actin signal.

The intensities of the bands were assessed using LabImage software - Version 2.7.2 (Kapelan Bio-Imaging Solutions, Germany).

A.

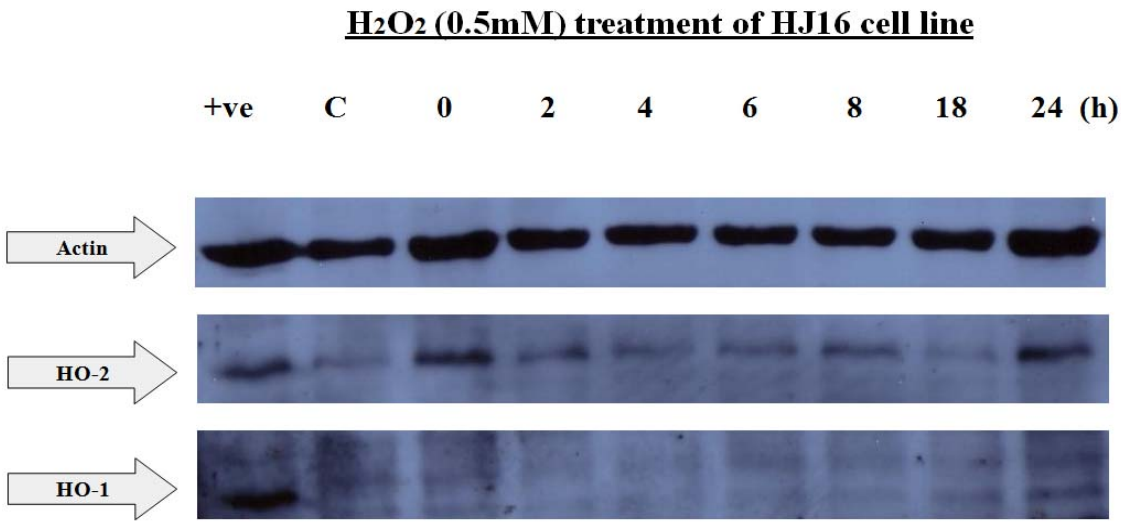

B.

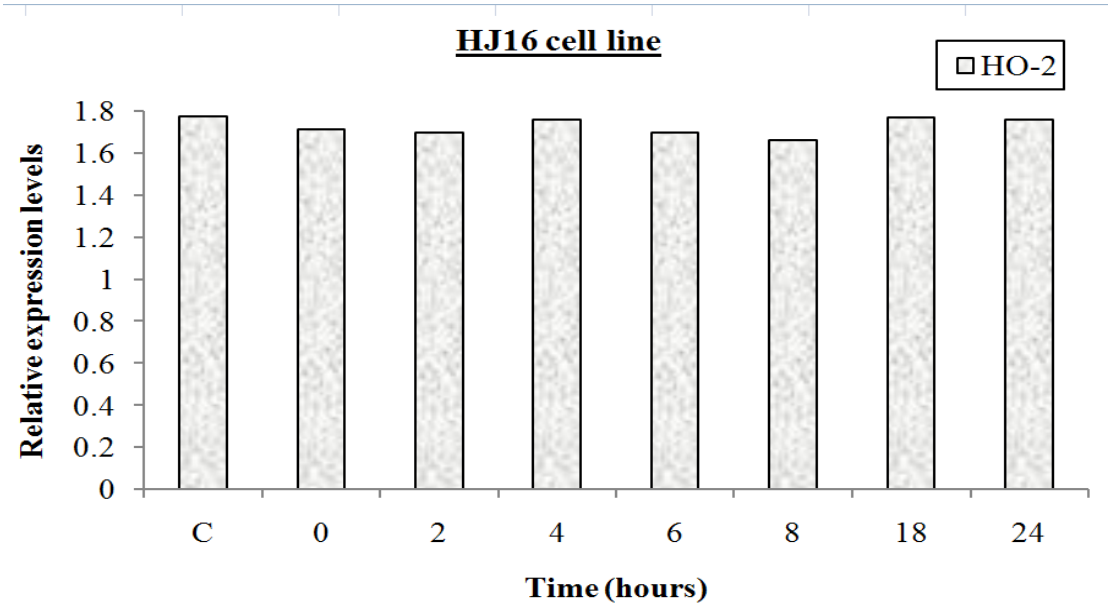

Figure 3.25 :

Time course induction of HO-1 and HO-2 in HJ16 cell line.

(A) HJ16 cell line was treated with an intermediate dose of H_2O_2 (i.e. 0.5 mM). Cells were collected at various times (i.e. 0, 2, 4, 6, 8, 18, and 24 h) and used to prepare whole cellular extracts for Western blot analysis (see section 2.9). The positive control (+ve) was FEK4 cells (human fibroblast cell line) treated with a UVA dose of 250 kJ/m^2 and collected after 8 h. (B) The relative expression levels of HO-2 were normalised with respect to the intensity of the actin signal.

The intensities of the bands were assessed using LabImage software - Version 2.7.2 (Kapelan Bio-Imaging Solutions, Germany).

A.

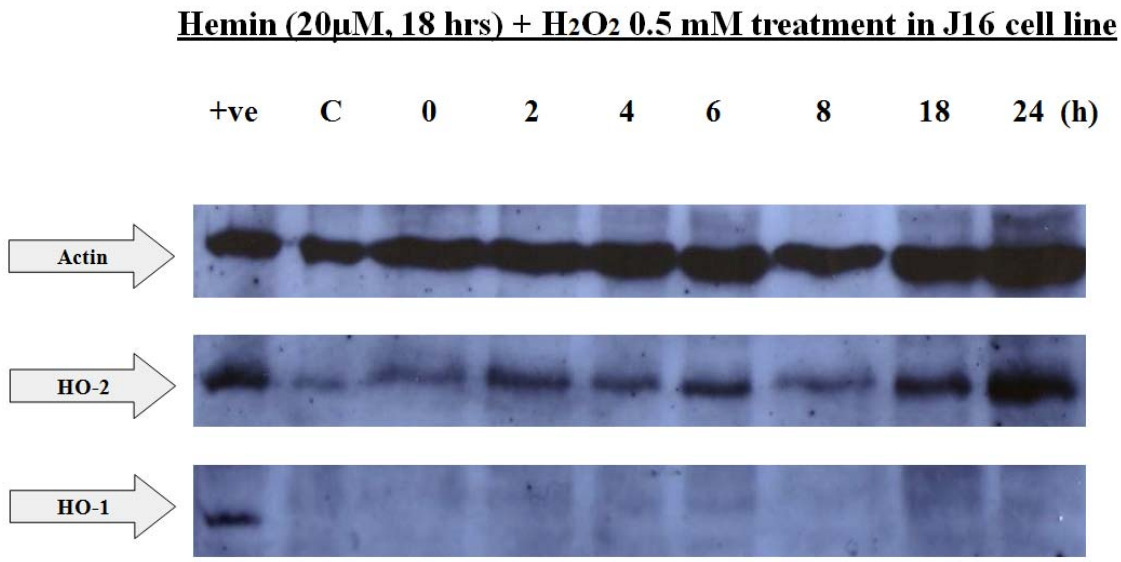

B.

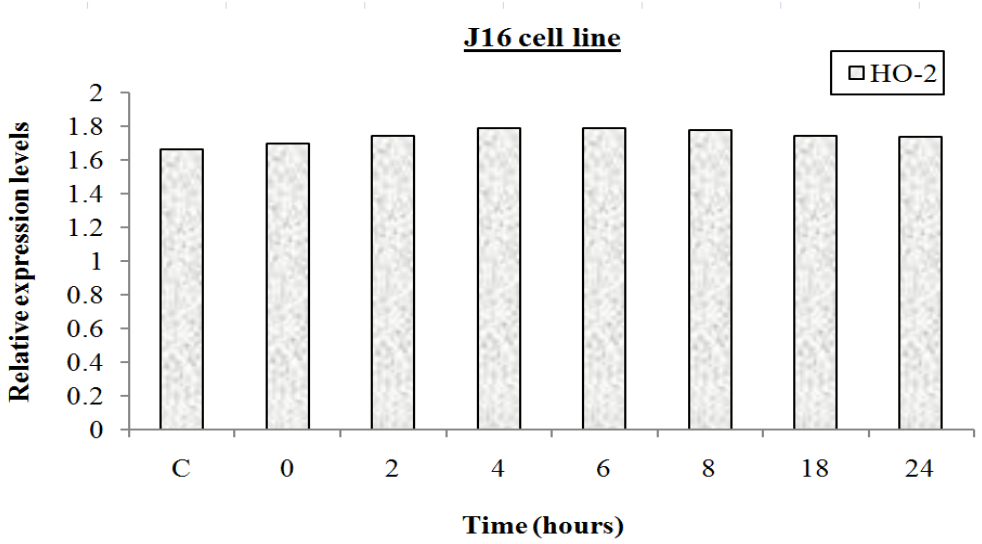

Figure 3.26 :
Time course induction of HO-1 and HO-2 in J16 cell line following overnight treatment of 20µM hemin followed by an intermediate dose of H_2O_2 (i.e. 0.5 mM)

(A) J16 cell line was treated overnight with 20µM hemin and then with an intermediate dose of H_2O_2 (i.e. 0.5 mM). Cells were collected at various times (i.e. 0, 2, 4, 6, 8, 18, and 24 h) and used to prepare whole cellular extracts for Western blot analysis (see section 2.9). The positive control (+ve) was FEK4 cells (human fibroblast cell line) treated with a UVA dose of 250 kJ/m^2 and collected after 8 h. (B) The relative expression levels of HO-2 were normalised with respect to the intensity of the actin signal.

The intensities of the bands were assessed using LabImage software - Version 2.7.2 (Kapelan Bio-Imaging Solutions, Germany).

A.

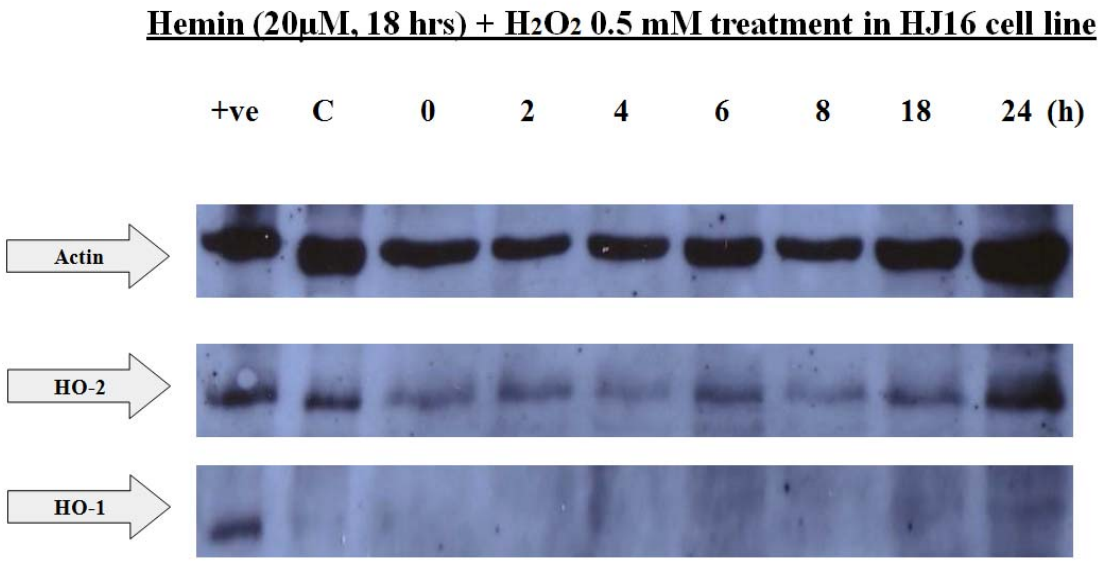

B.

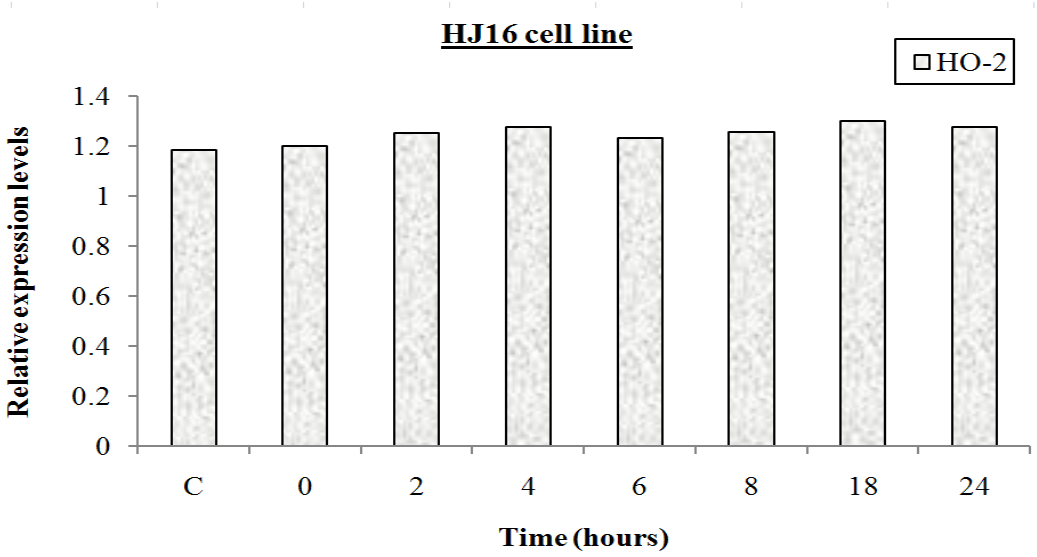

Figure 3.27:
Time course induction of HO-1 and HO-2 in HJ16 cell line following overnight treatment of 20µM hemin followed by an intermediate dose of H_2O_2 (i.e. 0.5 mM)

(A) HJ16 cell line was treated overnight with 20µM hemin and then with an intermediate dose of H_2O_2 (i.e. 0.5 mM). Cells were collected at various times (i.e. 0, 2, 4, 6, 8, 18, and 24 h) and used to prepare whole cellular extracts for Western blot analysis (see section 2.9). The positive control (+ve) was FEK4 cells (human fibroblast cell line) treated with a UVA dose of 250 kJ/m^2 and collected after 8 h. (B) The relative expression levels of HO-2 were normalised with respect to the intensity of the actin signal.

The intensities of the bands were assessed using LabImage software - Version 2.7.2 (Kapelan Bio-Imaging Solutions, Germany).

To complete the analysis, the level of HO-1 and HO-2 proteins were also checked after combined hemin (20 mM, 18 h) + DFO (1 mM, 2 h) and/or H_2O_2 (0.5 mM) treatment. Again here, no modulation in protein levels of HO-1 and HO-2 was observed (see figure 3.28). In summary, HO-1 expression was found to be very low and it was not induced with any of the above treatments (in both cell lines). On the other hand, HO-2 protein was present at higher levels than HO-1 in both cell lines but was not induced by any treatment used. Taken together these results showed that high iron accumulation after hemin treatment in HJ16 cells might not be related to differential expression of HO proteins in these cells.

3.4.3 The level of ferritin in Jurkat T cell lines

Ferritin sequesters the potentially harmful labile iron within its shells by H-Ft's ferroxidase activity so that iron can be stored in an inactive form. Several cellular studies have shown that in oxidative stress conditions Ft may have a protective effect against oxidative damage as it removes iron that acts as a catalyst in biological oxidation (reviewed in Arosio and Levi, 2002 and Torti and Torti, 2002).

In the case of UVA irradiation however, Ft when degraded has been identified as a potential source of harmful labile iron that triggers necrotic cell death in skin fibroblasts (Pourzand *et al,* 1999). Indeed UVA has been shown to promote the proteolytic degradation of Ft and the consequent release of potentially harmful labile iron in skin cells. The release of Ft's iron exacerbates the extent of UVA-induced peroxidative damage in the cell membrane as well as membranes of vital organelles, notably those of mitochondria and lysosomes, leading to necrotic cell death (Zhong *et al,* 2004). The proteolytic degradation of Ft occurs as a result of damage to lysosomal membranes leading to leakage of potentially harmful lysosomal proteases into the cytosol which in turn act to degrade cytosolic proteins, notably Ft.

Studies by Brunk and co-workers (Brunk *et al,* 1995[b]) have demonstrated that acute exposure of macrophage–like J-774 cells to H_2O_2 also triggers lysosomal damage. The irradiation of human fibroblasts with a moderate dose of blue light also resulted in oxidative apoptotic cell death as a result of damage to lysosomal organelles (Brunk *et al,* 1997).

A.

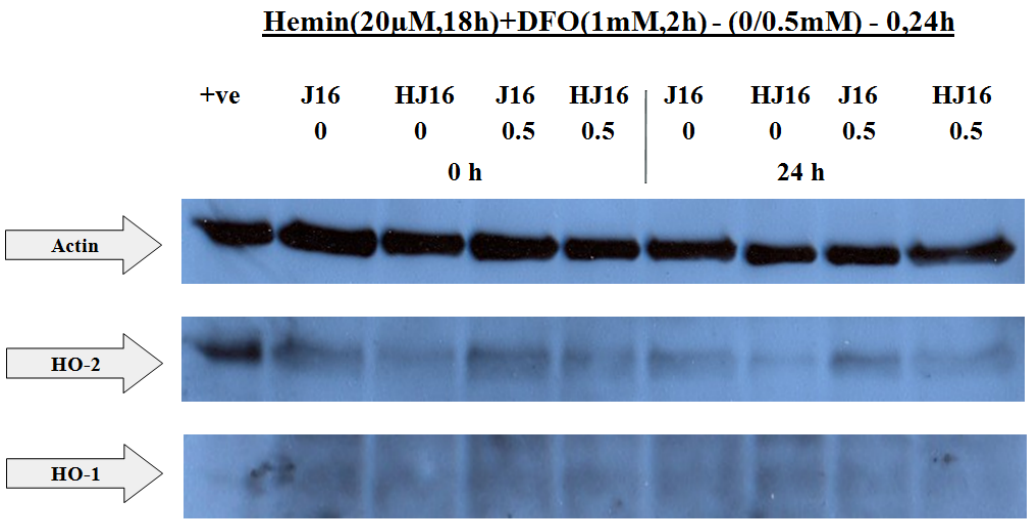

B.

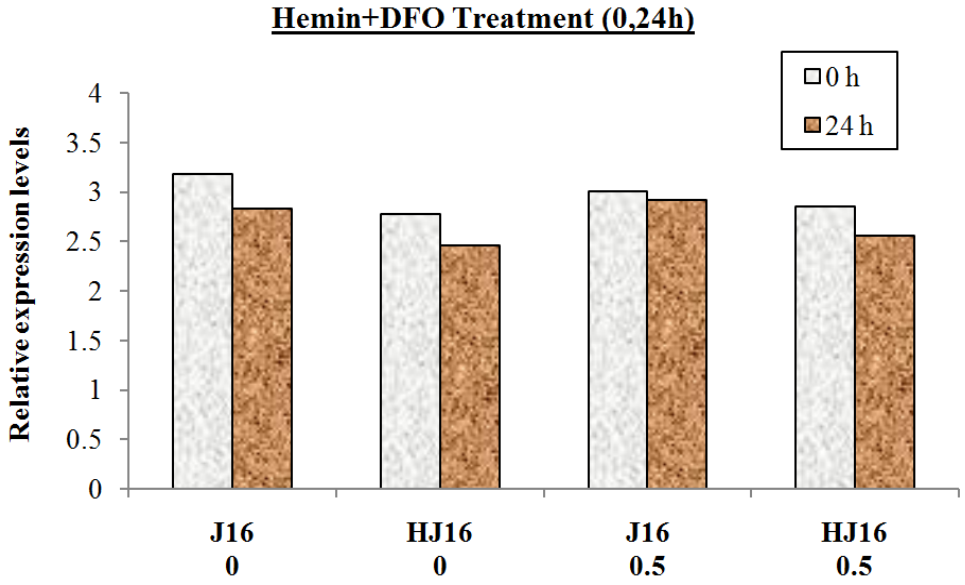

Figure 3.28 :

The induction of HO-1 and HO-2 in J16 and HJ16 cell lines (0,24 h)

(A) J16 and HJ16 (0) are cells treated with 20 µM hemin for 18 h and then with 1 mM DFO for 2 h, and J16 and HJ16 (0.5) are cells with 20 µM hemin for 18 h and then with 1 mM DFO for 2 h and finally with 0.5mM H_2O_2. Cells were collected at 0 and 24 h following the specified treatments mentioned above, and used to prepare whole cellular extracts for Western blot analysis (see section 2.9). The positive control (+ve) was FEK4 cells (human fibroblast cell line) treated with a UVA dose of 250 kJ/m^2 and collected after 8 h. (B) The relative expression levels of HO-2 were normalised with respect to the intensity of the actin signal.

The intensities of the bands were assessed using LabImage software - Version 2.7.2 Kapelan Bio-Imaging Solutions, Germany).

Damage to lysosomes was accompanied by leakage of lysosomal contents including hydrolytic enzymes, such as cathepsin D (CATH D) (Roberg and Öllinger, 1998) that should almost certainly lead to proteolytic degradation of Ft as well.

Interestingly epidermal skin keratinocytes that have low basal levels of Ft and LIP are naturally resistant to UVA-induced necrotic cell death but overnight hemin treatment renders these cells vulnerable to UVA-induced peroxidative damage and necrotic cell death (Zhong *et al,* 2004). This is because iron loading of cells with hemin increases strongly the level of intracellular Ft which in turn increases the level of UVA-induced LIP upon radiation-mediated proteolysis of Ft molecules.

Since HJ16 cells' resistance to H_2O_2 was abolished after hemin treatment presumably because of high accumulation of labile iron in these cells, it was important to investigate the role of Ft in this phenomenon. Ferritin level was first investigated by Western blot analysis (Yiakouvaki, 2003) but because the H- and L-Ft levels were not detectable, it was decided to do the analysis by ELISA that is a more sensitive assay to detect low protein levels in cellular studies. Tables 3.6 and 3.7 (a, b, c, and d), and figures 3.29-3.33 summarises the ELISA results in J16 and HJ16 cells following various treatments.

3.4.3.1 Basal levels of Ft in J16 and HJ16 cell line

As it can be seen in table 3.6-a, the 'basal' levels of H-Ft in J16 cell line (381.3 ± 53.6 ng/mg) were found to be more that 7 fold higher than in HJ16 cell line (51.6 ± 2 ng/mg). The lower H-Ft levels in HJ16 might be part of the adaptive response developed during gradual adaptation of these cells to H_2O_2. As for L-Ft they had the same 'basal' level; 10.2 ± 3 ng/mg in J16 cells and 9.2 ± 0.95 ng/mg in HJ16 cells.

3.4.3.2 Effect of H_2O_2 on the Ft levels

When cells were treated with 0.5 mM H_2O_2 and the Ft levels were measured *immediately* (see table 3.6-b) the H-Ft level decreased to 70 % of the control value in J16 cells but did not affect significantly the L-Ft. The H-Ft levels in HJ16 were not significantly affected by H_2O_2 treatment, L-Ft on the other hand increased up to 3-fold of the control value (see table 3.6-b).

Table 3.6 a: Basal H- & L-Ft measurements in J16 and HJ16 cell lines

Cell line	H-Ft (ng/mg)	%	L-Ft (ng/mg)	%
J16	381 ± 54	100	10 ± 3	100
HJ16	52 ± 2	100	9 ± 1	100

Table 3.6 b: H- & L-Ft measurements *immediately* following H_2O_2-0.5mM

Cell line	H-Ft (ng/mg)	%	L-Ft (ng/mg)	%
J16	263 ± 36	69	15 ± 6	Non-significant
HJ16	58 ± 8	Non-significant	26 ± 7	288

Table 3.6 c: H- & L-Ft measurements *immediately* following 100 µM DFO for 18 h

Cell line	H-Ft (ng/mg)	%	L-Ft (ng/mg)	%
J16	32 ± 8	8	3 ± 1	30
HJ16	20 ± 2	38	18 ± 4	200

Table 3.6 d: H- & L-Ft measurements *immediately* following 20 µM hemin for 18 h

Cell line	H-Ft (ng/mg)	%	L-Ft (ng/mg)	%
J16	965 ± 30	253	52 ± 8	520
HJ16	380 ± 11	730	20 ± 10	222

Note : H- and L-Ft measurements performed by ELISA (see section 2.10) *immediately* following the condition/treatments specified above. The percentage represents the significant difference of the corresponding basal levels. These results are expressed as mean ± standard deviation (n=3).

But when the cells were incubated for *24 h* in CM following H_2O_2 treatment (see table 3.7-b), the H-Ft decreased more in J16 cells (i.e. to 32 % of the control value) but there not a significant change in HJ16 cells. The L-Ft on the other hand, was not significantly affected in J16 cells, but was increased in HJ16 cells by 2.4-fold of the control value (see table 3.7-b).

The time course experiment (see figure 3.29) further revealed that following H_2O_2 treatment the levels of H-Ft decreased gradually in J16 cells at 6 h post treatment time point and then remained low up to 24 h following treatment. Hydrogen peroxide treatment of cultured fibroblasts and macrophages significantly inhibited the synthesis of Ft (Pantopoulos and Hentze, 1995 and Mehlhase *et al,* 2005, respectively). This is also shown when rat liver lysates were subjected to postischemic reperfusion (Tacchini *et al,* 1997). The L-Ft time course study following H_2O_2 treatment revealed that the L-Ft levels remain unchanged in J16 cells but slightly increase up to 2-fold control value in HJ16 cells at 6 h time point and then return to around control value at 24 h (see figure 3.29).

3.4.3.3 Effect of DFO ± H_2O_2 on the Ft levels

The treatment of cells with 100 μM DFO strongly reduced the level of H-Ft in J16 cells to 8 % of the control value (see table 3.6-c and figure 3.30-A1). In HJ16 cells, DFO treatment also decreased the level of H-Ft although to a lesser extent than in J16 cells (i.e. to 38 % of the control value). The decrease in H-Ft levels by DFO is consistent with previous observations showing that DFO diminishes Ft biosynthesis in B6 fibroblasts (Pantopoulos and Hentze, 1995) and reduces Ft levels in macrophages (Mehlhase *et al,* 2005). The L-Ft levels on the other hand decreased significantly in J16 but were strongly induced in HJ16 cells (see table 3.6-b and figure 3.30-A2). Following *24 h* incubation in CM after the DFO treatment (see table 3.7-c and figure 3.30-B1), H-Ft decreased significantly in J16 and HJ16 cells (i.e. to 6 % and 15 % of the control values, respectively). DFO treatment of HeLa cells demonstrated nearly a total repression of Ft (Cairo *et al,* 1985), as it also significantly decreased both subunits in K562 cells (Konijn *et al,* 1999). On the other hand, the L-Ft levels (see table 3.7-c and figure 3.30-B2) decreased significantly in J16 cells but there was a non-significant increase in HJ16 cells.

Table 3.7 a: Basal H- & L-Ft measurements in J16 and HJ16 cell lines

Cell line	H-Ft (ng/mg)	%	L-Ft (ng/mg)	%
J16	381 ± 54	100	10 ± 3	100
HJ16	52 ± 2	100	9 ± 1	100

Table 3.7 b: H- & L-Ft measurements *24 h* following H_2O_2-0.5mM

Cell line	H-Ft (ng/mg)	%	L-Ft (ng/mg)	%
J16	122 ± 51	32	14 ± 6	Non-significant
HJ16	42 ± 15	Non-significant	22 ± 8	244

Table 3.7 c: H- & L-Ft measurements *24 h* following 100 µM DFO for 18 h

Cell line	H-Ft (ng/mg)	Fold difference	L-Ft (ng/mg)	%
J16	23 ± 14	6	2 ± 1	20
HJ16	8 ± 3	15	12 ± 3	Non-significant

Table 3.7 d: H- & L-Ft measurements *24 h* following 20 µM hemin for 18 h

Cell line	H-Ft (ng/mg)	%	L-Ft (ng/mg)	%
J16	1443 ± 150	379	30 ± 10	300
HJ16	474 ± 49	912	69 ± 19	767

Note : H- and L-Ft measurements performed by ELISA (see section 2.10) *immediately* following the condition/treatments specified above. The percentage represents the significant difference of the corresponding basal levels. These results are expressed as mean ± standard deviation (n=3).

A.

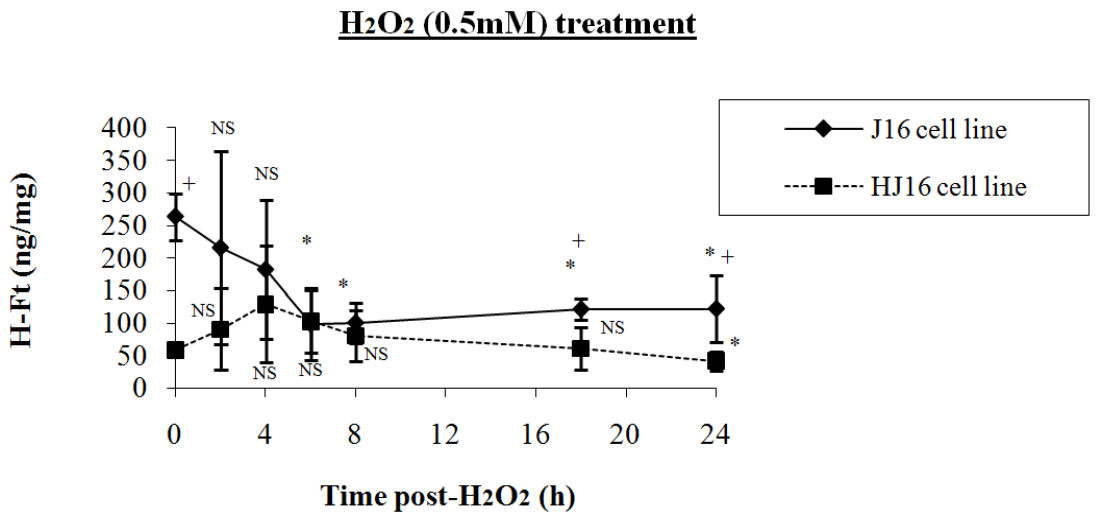

B.

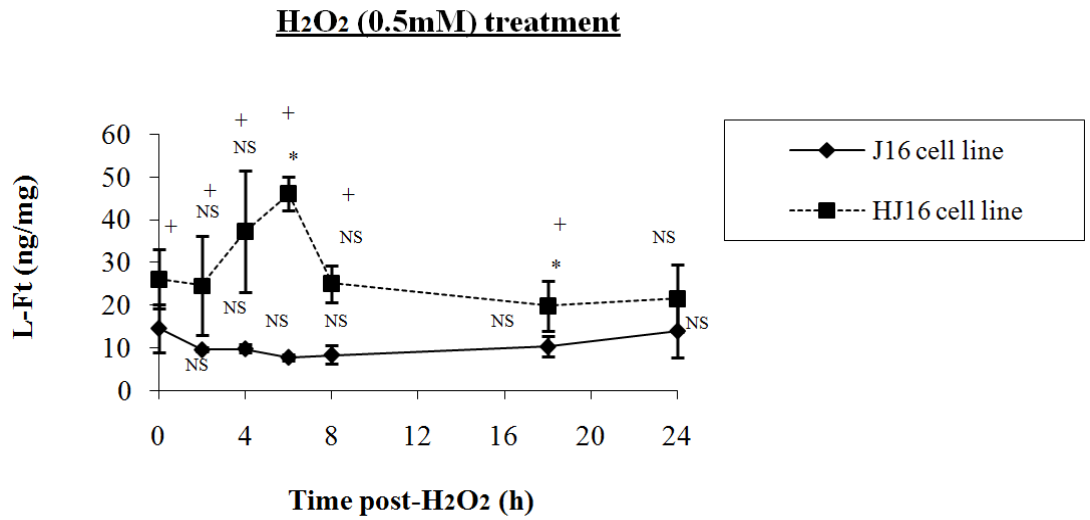

Figure 3.29:

Effect of 0.5 mM H_2O_2 on H and L-Ft in J16 and HJ16 cell lines.

J16 and HJ16 cell lines were treated with an intermediate dose of H_2O_2 (i.e. 0.5 mM) and were then collected at various times (i.e. 2, 4, 6, 8, 18, and 24 h). Whole cellular extracts were prepared for Ferritin ELISA (see section 2.10) to investigate the roles of H and L-Ft (A. and B., respectively). These results are expressed as mean ± standard deviation (n=3).

* : $p < 0.05$ significant difference between corresponding control.
NS : Non-significant difference between corresponding control.
+ : $p < 0.05$ significantly different when compared with the other cell line.

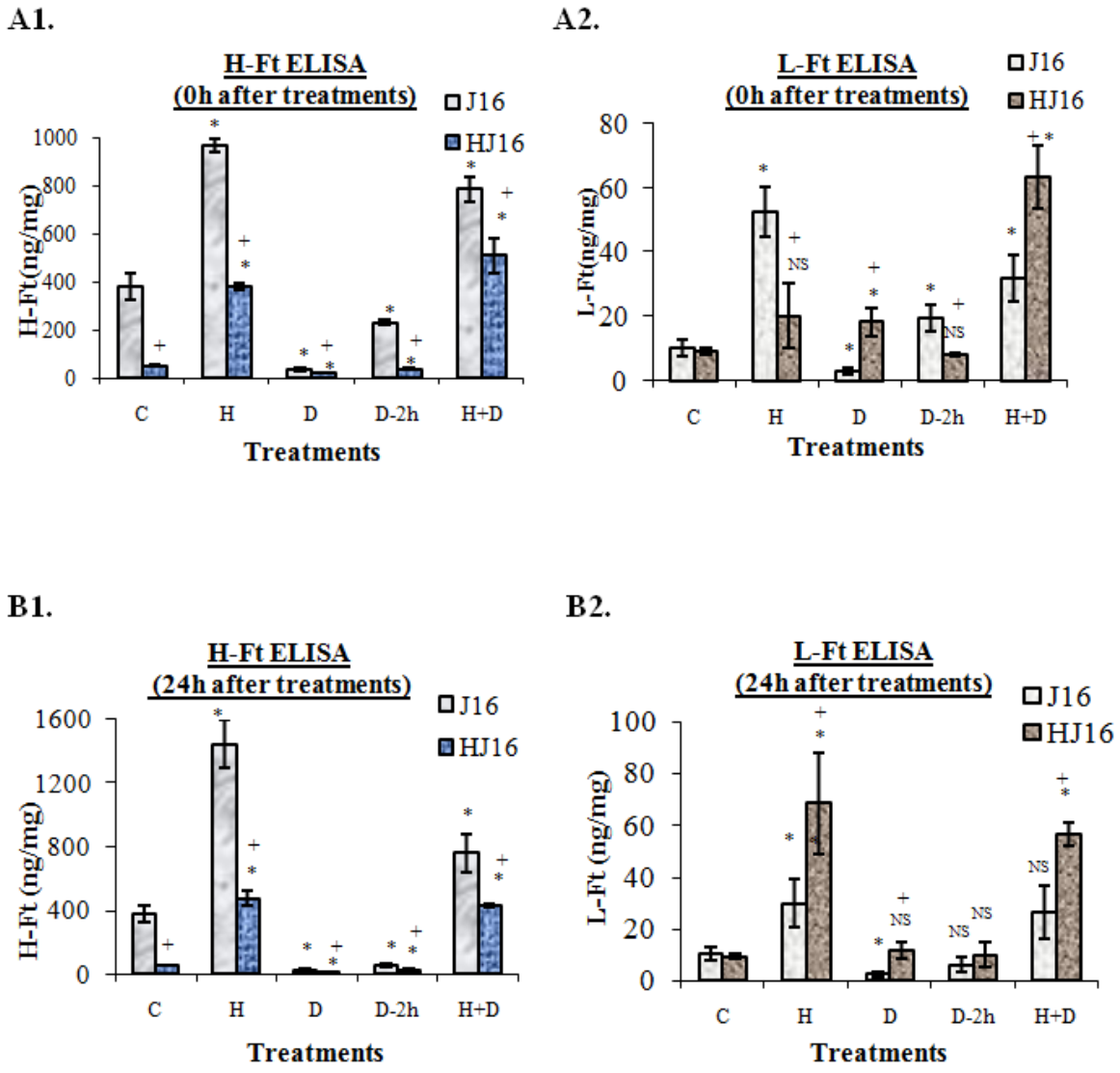

Figure 3.30:

Effect of hemin or/and DFO on H and L-Ft in J16 and HJ16 cell lines (0,24 h).

J16 and HJ16 cell lines were either treated overnight with 20µM hemin (H), 100 µM DFO (D), 1mM DFO for 2 h (D-2h), or with 20 µM hemin for 18 h and then with 1 mM DFO for 2 h (H+D). Cells were either collected *immediately* after the specified treatment (i.e. 0h, A1 and A2) or after incubating them in CM for *24 h* following the specified treatments (i.e. 24 h, B1 and B2) and used to prepare whole cellular extracts for Ferritin ELISA (see section 2.10) to investigate the roles of H and L-Ft (A1 – B1 and A2 – B2, respectively). These results are expressed as mean ± standard deviation (n=3).

* : $p < 0.05$ significant difference between corresponding control.
NS : Non-significant difference between corresponding control.
+ : $p < 0.05$ significantly different when compared with the corresponding J16 cells.

DFO treatment of cells (100 μM, 18 h) followed by H_2O_2 treatment, decreased significantly the H-Ft in both J16 cells and HJ16 cells (i.e. to 11 % and 38 % of the control values, respectively) (see figure 3.31-A1). On the other hand, not a significant change in the L-Ft expression in both cell lines (see figure 3.31-A2). The same relationship between H- and L-Ft was also observed when cells were incubated for another *24 h* in CM following DFO + H_2O_2 treatment; H-Ft was strongly decreased in both J16 cells and HJ16 cells (i.e. to 7 % and 13 % of the control values, respectively) (see figure 3.31-B1). On the other hand, there was a non-significant change in the L-Ft expression was observed in both cell lines (see figure 3.31-B2).

3.4.3.4 Effect of hemin ± H_2O_2 on the Ft levels

The time course experiment following hemin treatment revealed that the increase in H- or L-Ft in the J16 and HJ16 cells was not highly induced in the early hours after treatment (see figure 3.32), presumably because Ft molecules takes time to get synthesized. The latter data are expected as hemin should first be broken down by HO and release its iron which in turn will stimulate *de novo* Ft synthesis. The iron accumulation in HJ16 cells after hemin treatment is only apparent after 2 h post treatment (see table 3.5) with a peak at 6h after which it is reduced, presumably because of sequestration of a portion of it in the newly synthesized Ft molecules. This timing coincides with detection of higher Ft levels presumably as a result of its *de novo* synthesis. The H-Ft in J16 cells decreased up to 4 h and then was strongly induced after 8 h till 24 h after hemin treatment. The L-Ft, on the other hand, did not significantly increase during the time course in J16 cells, except at 18 and 24 h (see figure 3.32).

When J16 cells were treated with 20 μM hemin for 18 h and the Ft levels were measured *immediately,* both the H-Ft and L-Ft were significantly induced (i.e. up to 2.5-fold and 5-fold of the control values, respectively) (see table 3.6-d and figure 3.30-A1,A2). In HJ16 cells, the same treatment strongly increased the levels of H-Ft (i.e. up to 7.3-fold of the control value). On the other hand, there was a non-significant change in the L-Ft expression (see table 3.6-d and figure 3.30-A1,A2). Ferritin biosynthesis also strongly increased in B6 fibroblasts pre-treated with haem arginate (Pantopoulos and Hentze, 1995).

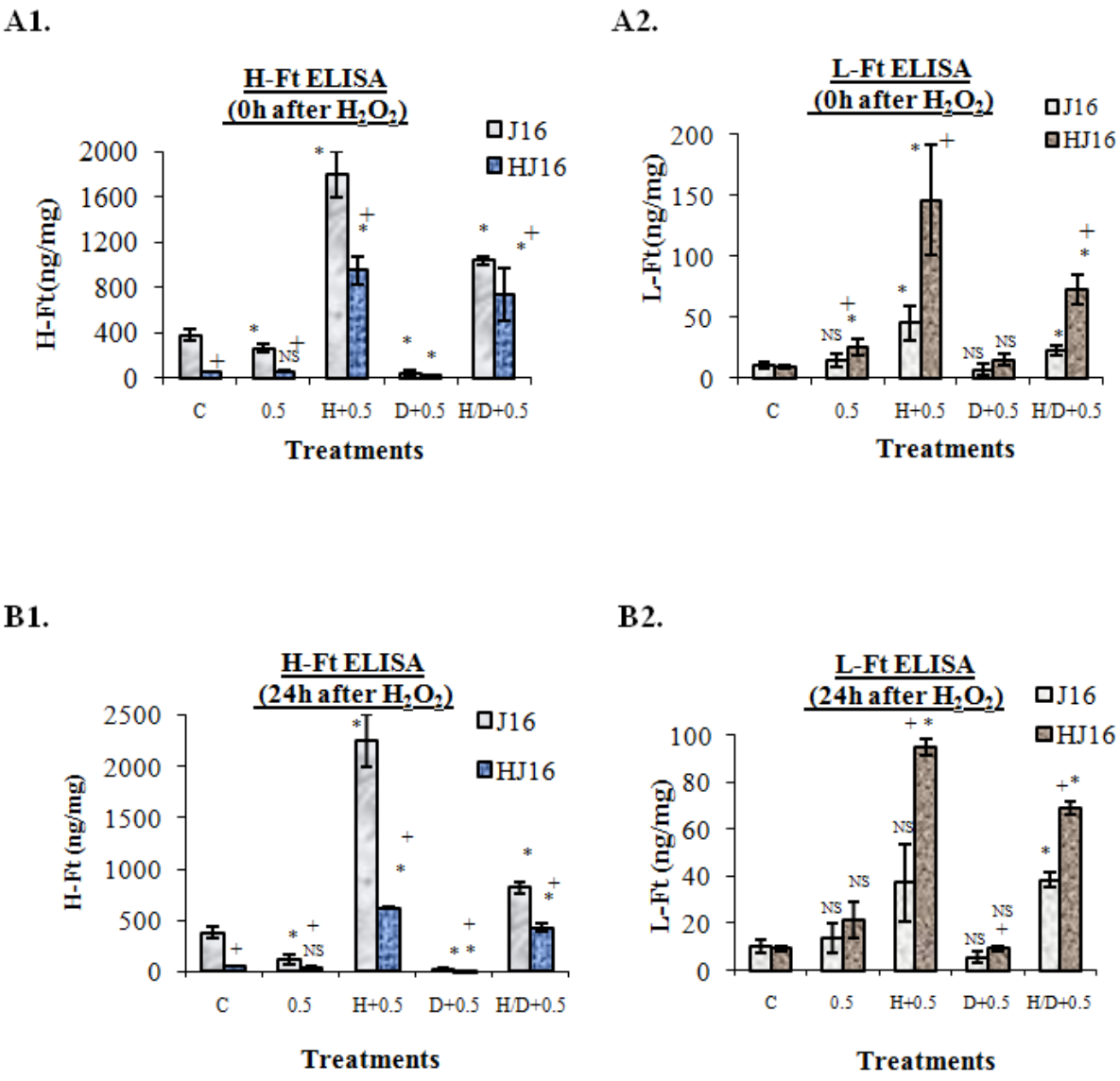

Figure 3.31:

Effect of hemin and/or DFO prior to H_2O_2 treatment on H and L-Ft in J16 and HJ16 cell lines (0, 24h).

J16 and HJ16 cell lines were either treated with 0.5mM H_2O_2 alone (0.5), treated overnight with 20µM hemin and then with 0.5mM H_2O_2 (H+0.5), treated overnight with 100 µM DFO and then with 0.5mM H_2O_2 (D+0.5), or treated with 20 µM hemin for 18 h and then with 1 mM DFO for 2 h and finally with 0.5mM H_2O_2 (H/D+0.5). Cells were either collected *immediately* after the specified treatment (i.e. 0h, A1 and A2) or after incubating them in CM for *24 h* following the specified treatments (i.e. 24 h, B1 and B2) and used to prepare whole cellular extracts for Ferritin ELISA (see section 2.10) to investigate the roles of H and L-Ft (A1 – B1 and A2 – B2, respectively). These results are expressed as mean ± standard deviation (n=3).

* : $p < 0.05$ significant difference between corresponding control.
NS : Non-significant difference between corresponding control.
+ : $p < 0.05$ significantly different when compared with the corresponding J16 cells.

A.

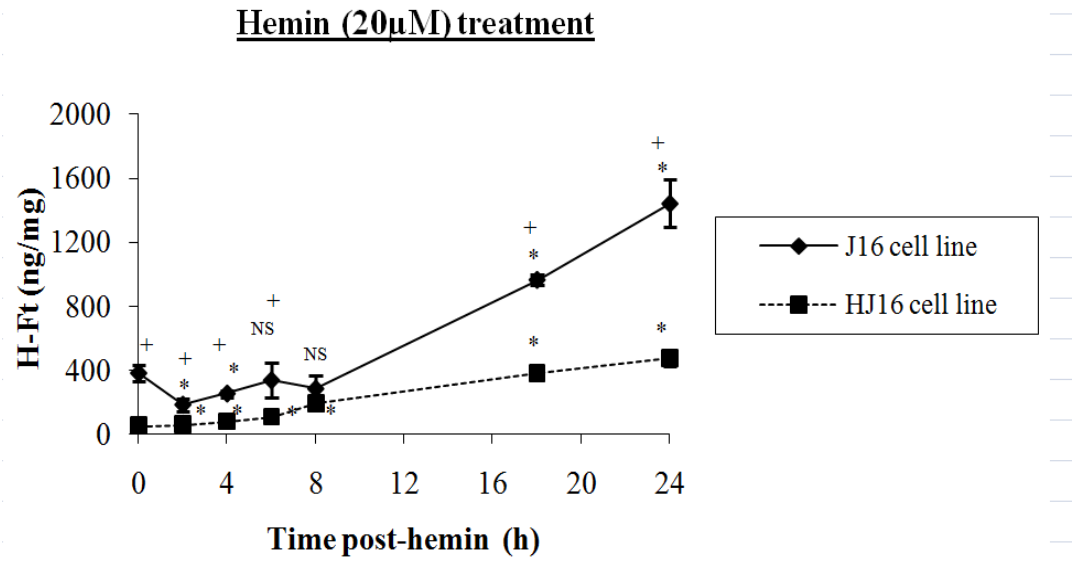

B.

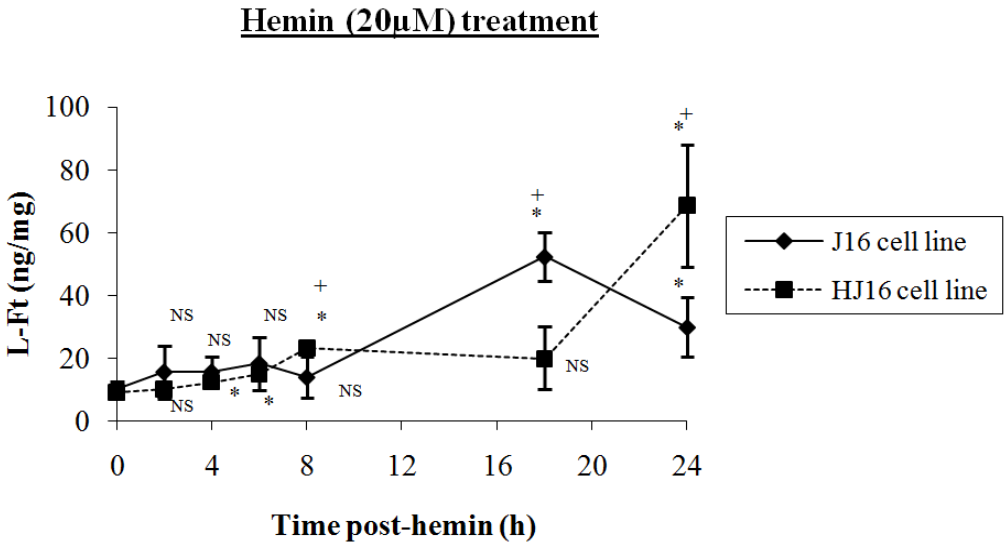

Figure 3.32:

Effect of hemin on H and L-Ft in J16 and HJ16 cell lines.

J16 and HJ16 cell lines were treated with 20 µM hemin and were then collected at various times (i.e. 2, 4, 6, 8, 18, and 24 h). Whole cellular extracts were prepared for Ferritin ELISA (see section 2.10) to investigate the roles of H and L-Ft (A. and B., respectively). These results are expressed as mean ± standard deviation (n=3).

* : $p < 0.05$ significant difference between corresponding control.
NS : Non-significant difference between corresponding control.
+ : $p < 0.05$ significantly different when compared with the other cell line.

Ferritin expression was also increased 6-fold following overnight treatment with hemin in macrophages (Mehlhase *et al,* 2005). A strong up-regulation of both H- and L-Ft chains was reported in HeLa cells after iron administration (Cairo *et al,* 1985). On the contrary, only H-Ft was induced after hemin treatment in bovine artery endothelial cells (Lin *et al,* 1998), L-Ft on the other hand was unaffected. Incubation of cells for *24 h* in CM following 18 h hemin treatment, increased significantly the levels H- and L-Ft in both cell lines (see table 3.7-d figure 3.30-B1,B2).

The time course experiment revealed that iron loading prior to H_2O_2 treatment decreased the H-Ft levels in J16 cells only at early hours following treatment (i.e. 2, 6, and 8 h post- H_2O_2). While in HJ16, significant decrease in H-Ft was only apparent at 4 and 24 h post-H_2O_2 treatment. The L-Ft time course study revealed that the L-Ft levels remain unchanged in HJ16 cells but it was slightly decreased in J16 cells at 4, 8, 18 and 24 h time points (see figure 3.33).

ELISA performed *immediately* after the exposure of hemin-treated cells (20μM, 18 h) to 0.5 mM H_2O_2 revealed an already significant increase in the H-Ft and L-Ft levels in J16 cell line (i.e. up to 5-fold of the control value) (see figure 3.32-A1,A2). Both H-Ft and L-Ft were also induced in HJ16 cells (i.e. up to 18-fold and 5-fold of the control values, respectively) (see figure 3.32 A1,A2). Following *24 h* incubation in CM, H-Ft and L-Ft were also strongly induced in J16 cells (i.e. 6-fold and 4-fold of the control values, respectively). In HJ16 cells, H-Ft and L-Ft were also strongly induced (i.e. up to 12-fold and of the control values) (see figure 3.32 B1,B2).

3.4.3.5 Effect of combined DFO/hemin ± H_2O_2 on the Ft levels

Finally the effect of hemin and DFO treatment with and without H_2O_2 treatment was also investigated. When the ELISA was performed *immediately* in J16 cells, 20 μM hemin (18 h) + 1mM DFO (2 h) significantly increased the H-Ft and L-Ft (i.e. up to 2-fold and 4-fold of the control value, respectively) (see figure 3.32 A1,A2). The levels of H-Ft and L-Ft were also significantly induced in HJ16 cells (i.e. up to 10-fold and 7-fold of the control value, respectively) (see figure 3.30 A1,A2). Following *24 h* incubation in CM, the levels of H-Ft and L-Ft were significantly induced in J16 cells (i.e. up to 2-fold and 3-fold of the control value, respectively) (see figure 3.30-B1,B2).

A.

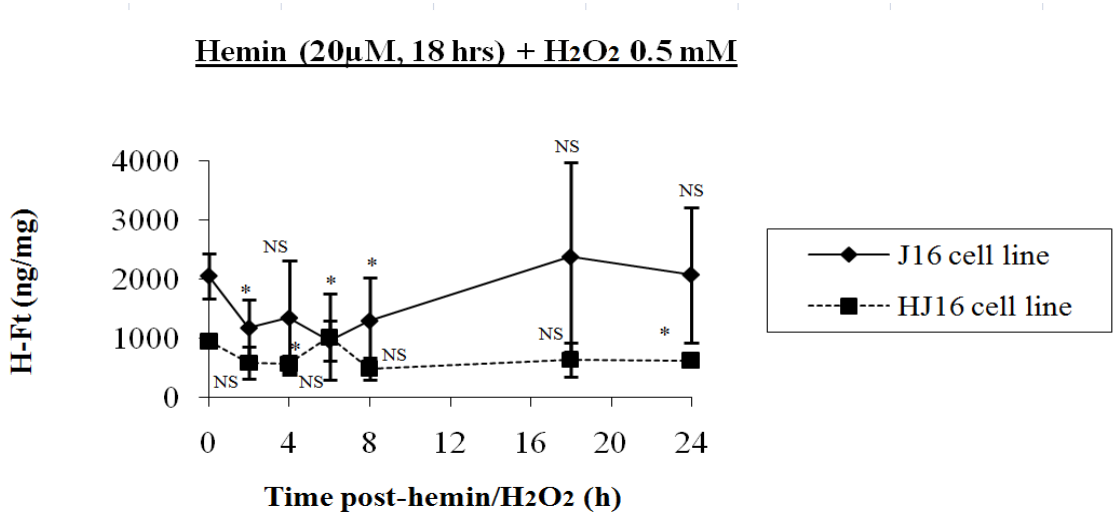

B.

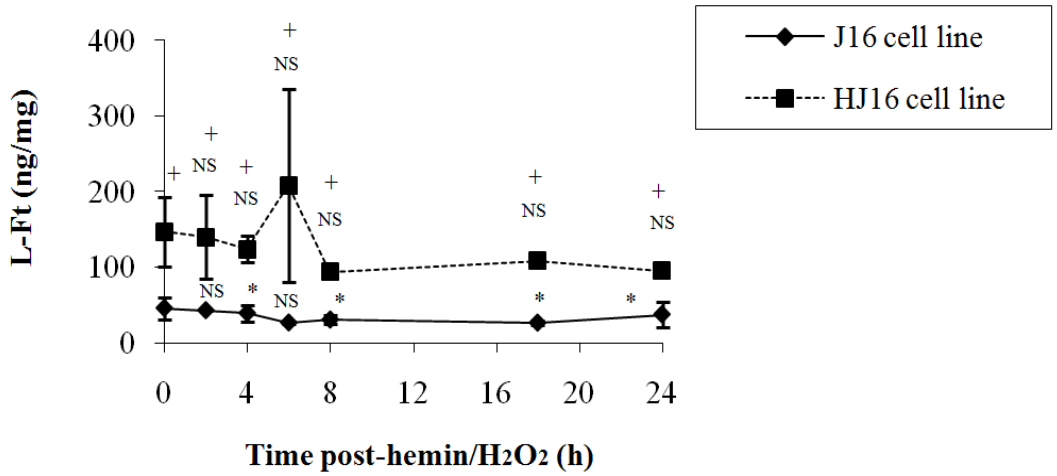

Figure 3.33:

Effect of 20 µM hemin + 0.5 mM H_2O_2 on H and L-Ft in J16 and HJ16 cell lines.

J16 and HJ16 cell lines were treated overnight with 20µM hemin and then with an intermediate dose of H_2O_2 (i.e. 0.5 mM). Cells were collected at various times (i.e. 2, 4, 6, 8, 18, and 24 h) and used to prepare whole cellular extracts for Ferritin ELISA (see section 2.10) to investigate the roles of H and L-Ft (A. and B., respectively). These results are expressed as mean ± standard deviation (n=3).

* : $p < 0.05$ significant difference between corresponding control.
NS : Non-significant difference between corresponding control.
+ : $p < 0.05$ significantly different when compared with the other cell line.

This was also seen in HJ16 cells, levels of H-Ft and L-Ft were also significantly induced in HJ16 cells (i.e. up to 8-fold and 6-fold of the control value, respectively) (see figure 3.30-B1,B2).

ELISA performed *immediately* following H_2O_2 treatment of combined hemin-DFO cells, revealed a significant increase in the levels of H-Ft and L-Ft in J16 cells (i.e. up to 3-fold and 2-fold of the control value, respectively) (see figure 3.32 A1,A2). The levels of both H-Ft and L-Ft were also significantly induced in HJ16 cells (i.e. up to 14-fold and 8-fold of the control values, respectively) (see figure 3.32 A1,A2). Following *24 h* incubation in CM, the levels of H-Ft and L-Ft were also significantly induced in J16 cells (i.e. up to 2-fold and 4-fold of the control values, respectively) (see figure 3.32 B1,B2). This was also seen in HJ16 cells, as levels of H-Ft and L-Ft were also significantly induced following hemin-DFO- H_2O_2 treatment (i.e. up to 8-fold of the control value) (see figure 3.32 B1,B2).

3.4.3.6 Mitochondrial ferritin in the J16 and HJ16 cell line

Mitochondrial ferritin (Mt-Ft) was also measured in both cell lines. In the J16 cell line Mt-Ft basal level was 0.53 ng/mg and 1.52 ng/mg in HJ16 cells. In J16 cell line, Mt-Ft levels following either hemin or DFO treatment prior H_2O_2 treatment or H_2O_2 treatment alone, were negligible. On the other hand, in the HJ16 cell line, Mt-Ft was increased up to 4-fold after 0.5 mM H_2O_2 treatment (measured *24 h* following the treatment), overnight treatment with 20 µM hemin (measured *24 h* following the treatment), and H_2O_2 treatment (0.5 mM) following overnight treatment with 20 µM hemin (measured *immediately* following the treatment). It was also increased up to 5-fold after overnight treatment with 100 µM DFO (measured *24 h* following the treatment). Mitochondrial ferritin (Mt-Ft) is currently under investigation in our cell model.

3.4.4 The role of iron-mediated lysosomal damage in J16 and HJ16 cells

Since lysosomal iron release and necrosis have been related (see section 1.5.1) we wanted to a great extent understand this relationship in our cell model. To investigate the role of iron-mediated lysosomal damage in both acute and chronic oxidative stress conditions, the lysosomal damage was monitored by three

independent assays: (1) Neutral red uptake assay (2) Lysosensor immunofluorescence, and (3) Cathepsin B immunocytochemistry.

3.4.4.1 Neutral red uptake assay

Primarily, the effect of H_2O_2 treatment on lysosomal damage in both J16 and HJ16 cell lines was investigated via Neutral red (NR) uptake assay. Figure 3.34 clearly demonstrates that the lysosomal membranes in the parental J16 cells are very sensitive to H_2O_2 treatment. However, in the HJ16, cells the lysosomal membrane were very resistant to the same treatment.

Using the same approach, in J16 cells, we found that both DFO and hemin protected the cells from lysosomal damage (see figure 3.35). This is in agreement with our previous results showing that these two compounds protected J16 cells from H_2O_2–induced necrosis. In HJ16 cells (see figure 3.36), the scenario was quite different: Interestingly DFO pre-treatment (unlike the necrosis data, see figure 3.15) had no significant protective effect when compared with cells treated with H_2O_2 alone. Hemin, on the other hand, promoted more lysosomal damage in HJ16.

The lysosomal damage was also investigated in both cell lines after combined hemin (i.e. 20 μM for 18 h) - DFO (i.e. 1mM for 2 h) treatment. It was shown that DFO treatment following iron loading for 18 h (see figure 3.37) protected both cell lines from lysosomal damage. These results are in agreement with necrosis data using Flow cytometry (see section 3.4.2).

3.4.4.2 Lysosensor immunofluorescence

The LysoSensor^{TM} Green DND-153 was used to monitor the integrity of lysosomal membranes after relevant treatments. As can be seen in figure 3.38, H_2O_2 damages the lysosomes in J16 cells in a dose-dependent manner (i.e. 0.1, 0.5, and 1mM) as observed by the loss of fluorescence due to the leakage of the dye to the cytosol. However, overnight treatment of J16 cells with either DFO or hemin protected the lysosomes against H_2O_2-induced damage. This is in agreement with the NR assay and the necrosis data using Flow cytometry. In contrast to J16 cells, the lysosomes in HJ16 cells were quite resistant to H_2O_2 treatment (see figure 3.39). Indeed, intact lysosomes could be detected even when cells were exposed to a high dose of H_2O_2 (i.e. 1mM).

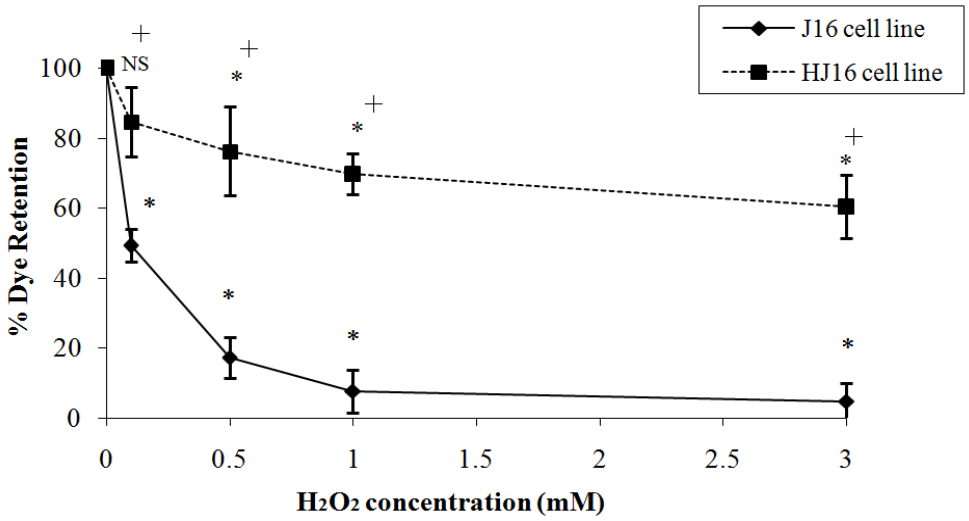

Figure 3.34 :

Effect of different concentrations of H_2O_2 treatment on J16 (parental) and HJ16 (H_2O_2-resistant) cell lines (Analysis : NR assay).

Neutral red assay was performed 24 h following H_2O_2 treatment (see section 2.11). These results are expressed as mean ± standard deviation (n=3)

* : $p < 0.05$ significant difference between corresponding control.
NS : Non-significant difference between corresponding control.
+ : $p < 0.05$ significantly different when compared with the corresponding J16 cells.

A.

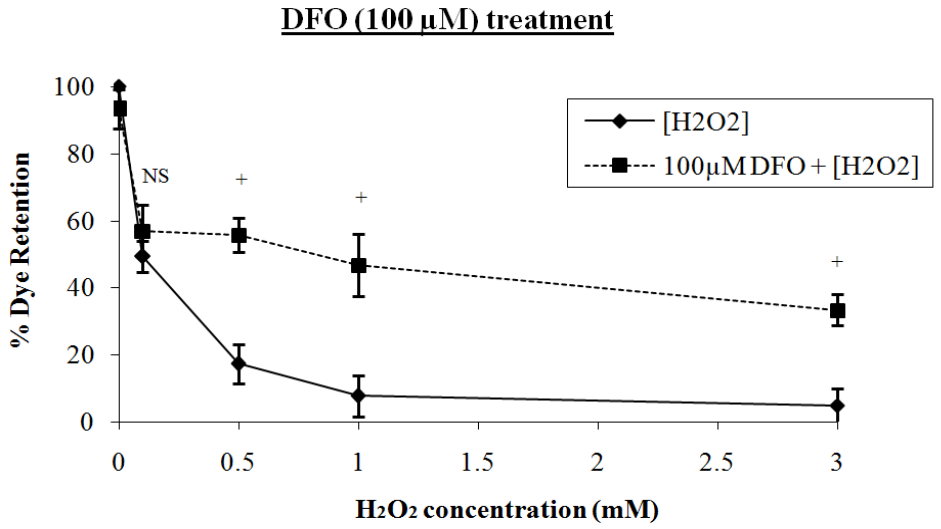

B.

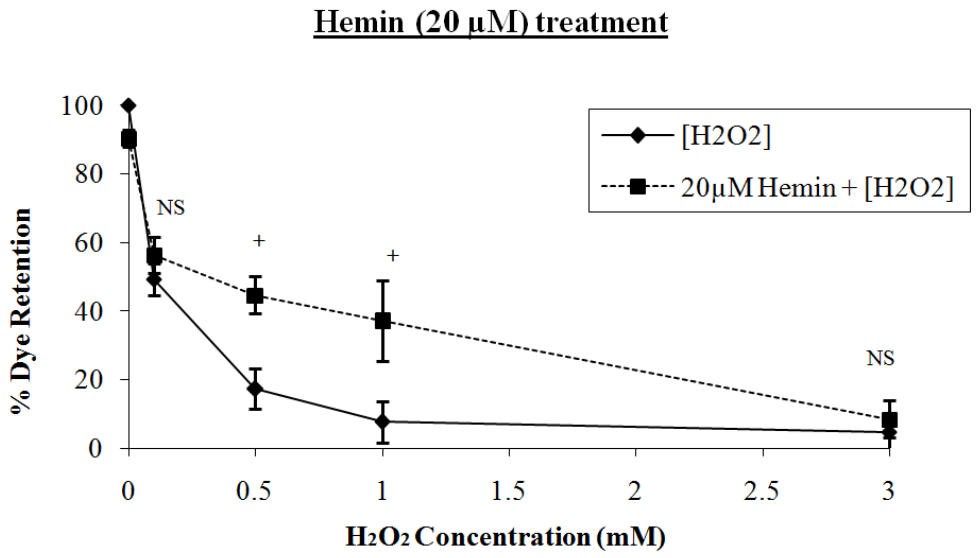

Figure 3.35 :

The assessment of iron chelation and loading on lysosomal damage in J16 cell line (parental cells) - (Analysis : NR assay).

J16 cells were pretreated with either 100 µM DFO (A) or 20 µM hemin (B) for 18 h before H_2O_2 treatment. Neutral red (NR) assay was performed 24 h following H_2O_2 treatment (see section 2.11). These results are expressed as mean ± standard deviation (n=3).

+ : $p < 0.05$ significant difference between DFO (A) or hemin (B) pre-treated cells and cells treated with H_2O_2 alone.
NS : Non-significant difference between DFO (A) or hemin (B) pre-treated cells and cells treated with H_2O_2 alone.

A.

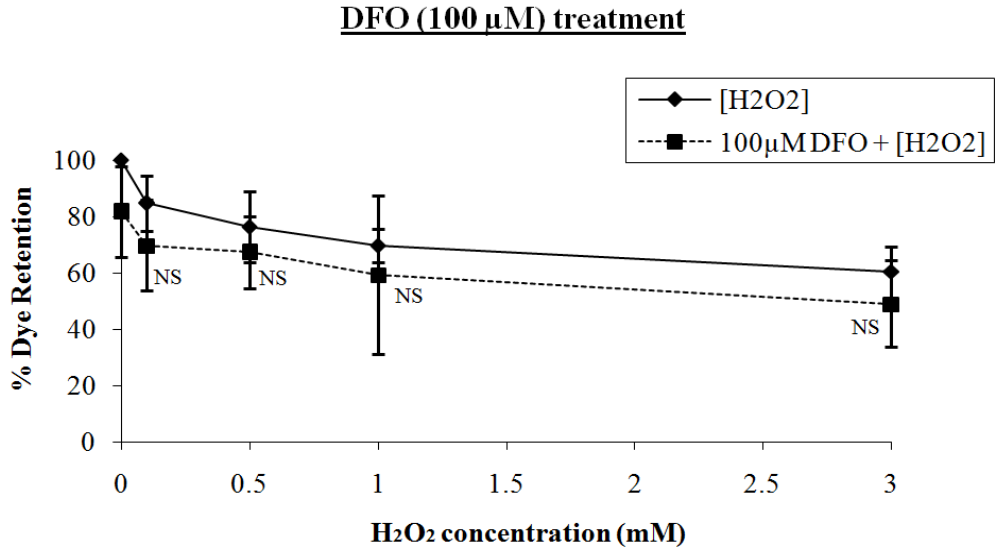

B.

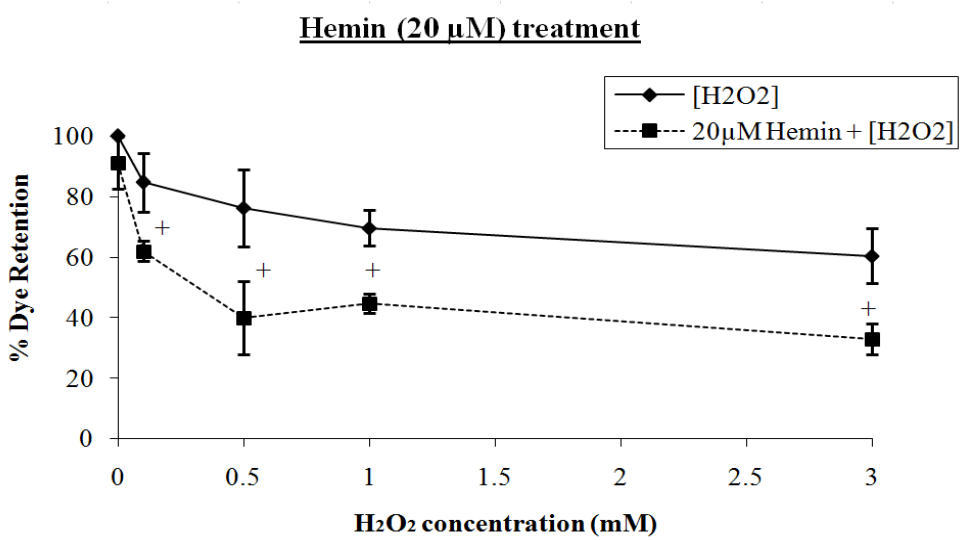

Figure 3.36 :

The assessment of iron chelation and loading on lysosomal damage in HJ16 cell line (H_2O_2-resistant cells) - (Analysis : NR assay).

HJ16 cells were pretreated with either 100 µM DFO (A) or 20 µM hemin (B) for 18 h before H_2O_2 treatment. Neutral red assay was performed 24 h following H_2O_2 treatment (see section 2.11). These results are expressed as mean ± standard deviation (n=3).

+ : $p < 0.05$ significant difference between DFO (A) or hemin (B) pre-treated cells and cells treated with H_2O_2 alone.
NS : Non-significant difference between DFO (A) or hemin (B) pre-treated cells and cells treated with H_2O_2 alone.

A.

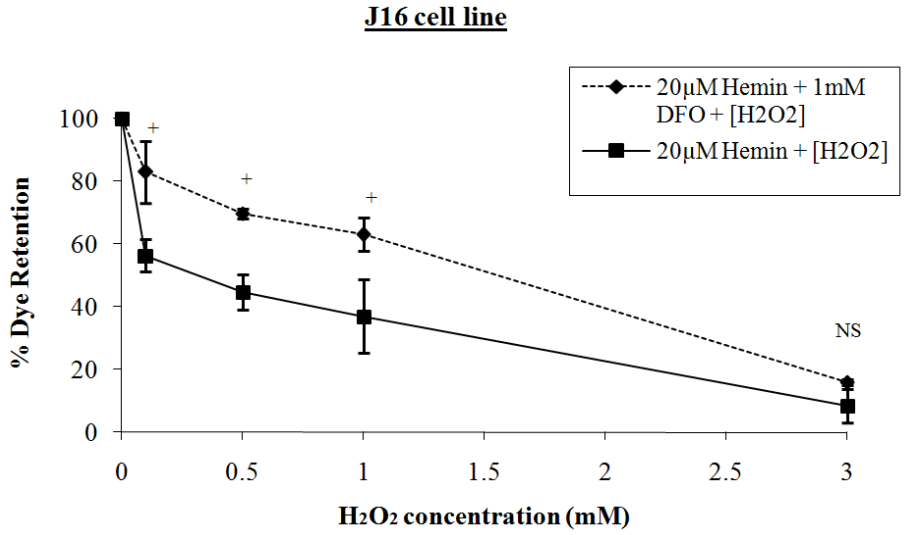

B.

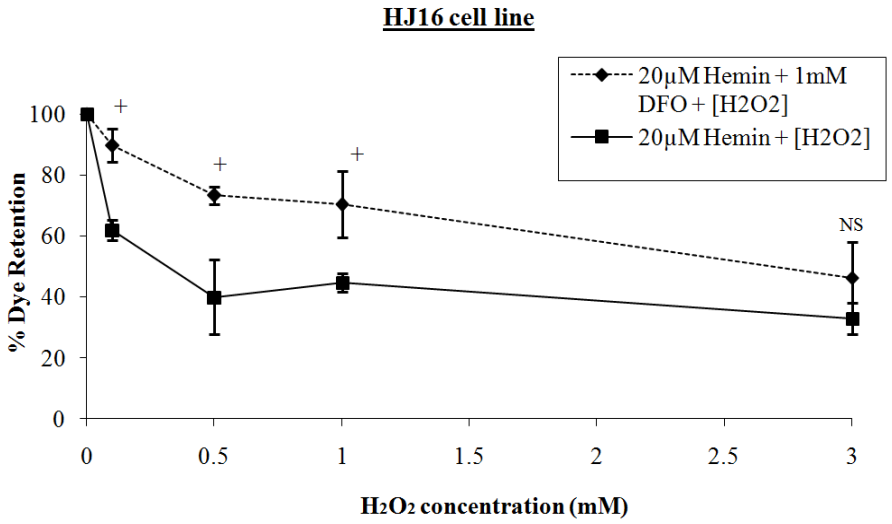

Figure 3.37 :

The assessment of DFO treatment following iron loading prior to H_2O_2 treatment on lysosomal damage in J16 (A) and HJ16 (B) cell lines (Analysis : NR assay).

Both cell lines were pretreated with either 20 µM Hemin for 18 h or 20 µM Hemin for 18 h and then 1mM DFO for 2 h, before H_2O_2 treatment. Neutral red assay was performed 24 h following H_2O_2 treatment (see section 2.11). These results are expressed as mean ± standard deviation (n=3).

+ : $p < 0.05$ significant difference when compared with cells pre-treated with hemin and H_2O_2 alone.
NS : Non-significant difference when compared with cells pre-treated with hemin and H_2O_2 alone.

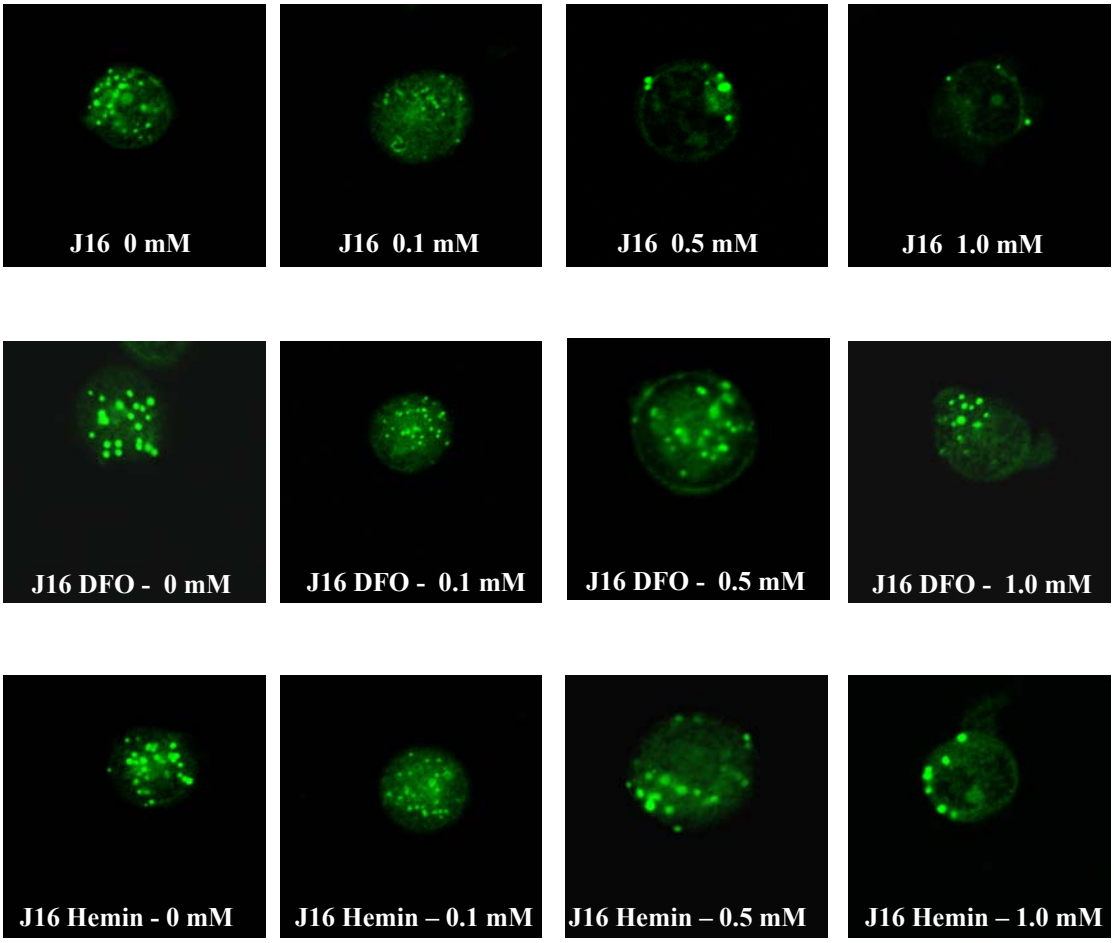

Figure 3.38 :

The effect of iron chelation and loading on the H_2O_2-mediated lysosomal damage in J16 cell line (parental cells).

J16 cells were pre-treated with either 100 μM DFO (second row) or 20 μM hemin (third row) for 18 h before H_2O_2 treatment (i.e. 0.1, 0.5, and 1mM). The Lysosensor assay (see section 2.12) was performed 24 h following H_2O_2 treatment. The photographs are representative of three experiments.

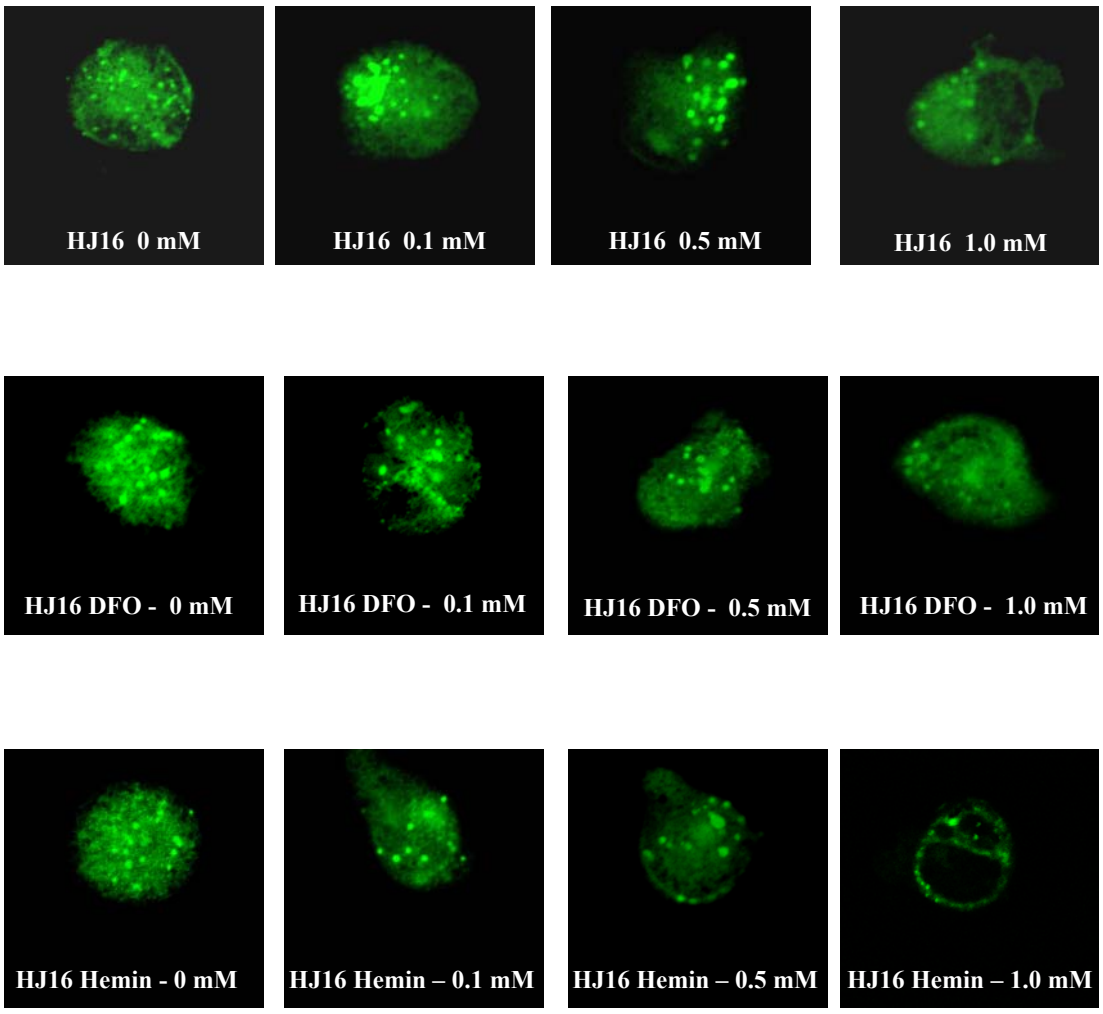

Figure 3.39 :

The effect of iron chelation and loading on the H_2O_2-mediated lysosomal damage in HJ16 cell line (H_2O_2-resistant cells).

HJ16 cells were pre-treated with either 100 µM DFO (second row) or 20 µM hemin (third row) for 18 h before H_2O_2 treatment (i.e. 0.1, 0.5, and 1mM). The Lysosensor assay (see section 2.12) was performed 24 h following H_2O_2 treatment. The photographs are representative of three experiments.

Overnight treatment of HJ16 cells with DFO had no significant effect on the lysosomal integrity. Hemin pre-treatment on the other hand caused dose-dependent damage to the lysosomes following H_2O_2 insult. The latter data are found to be in agreement with the NR assay and the necrosis data by Flow cytometry.

3.4.4.3 Cathepsin B immunocytochemistry

Cathepsin B is a cysteine protease found within the lysosomes. It has been implicated in diseases such as arthritis and cancer. When secreted, it has been shown to degrade the extracellular matrix proteins (Roshy *et al,* 2003). The results obtained from Cathepsin B immunocytochemistry confirmed the results shown with either NR or Lysosensor assays. In J16 cells (see figure 3.40), both DFO and hemin pre-treatments protected the cells against lysosomal membrane damage induced by H_2O_2, whereas in HJ16 cells (see figure 3.41), only hemin pre-treatment was shown to damage the lysosomes following H_2O_2 exposure.

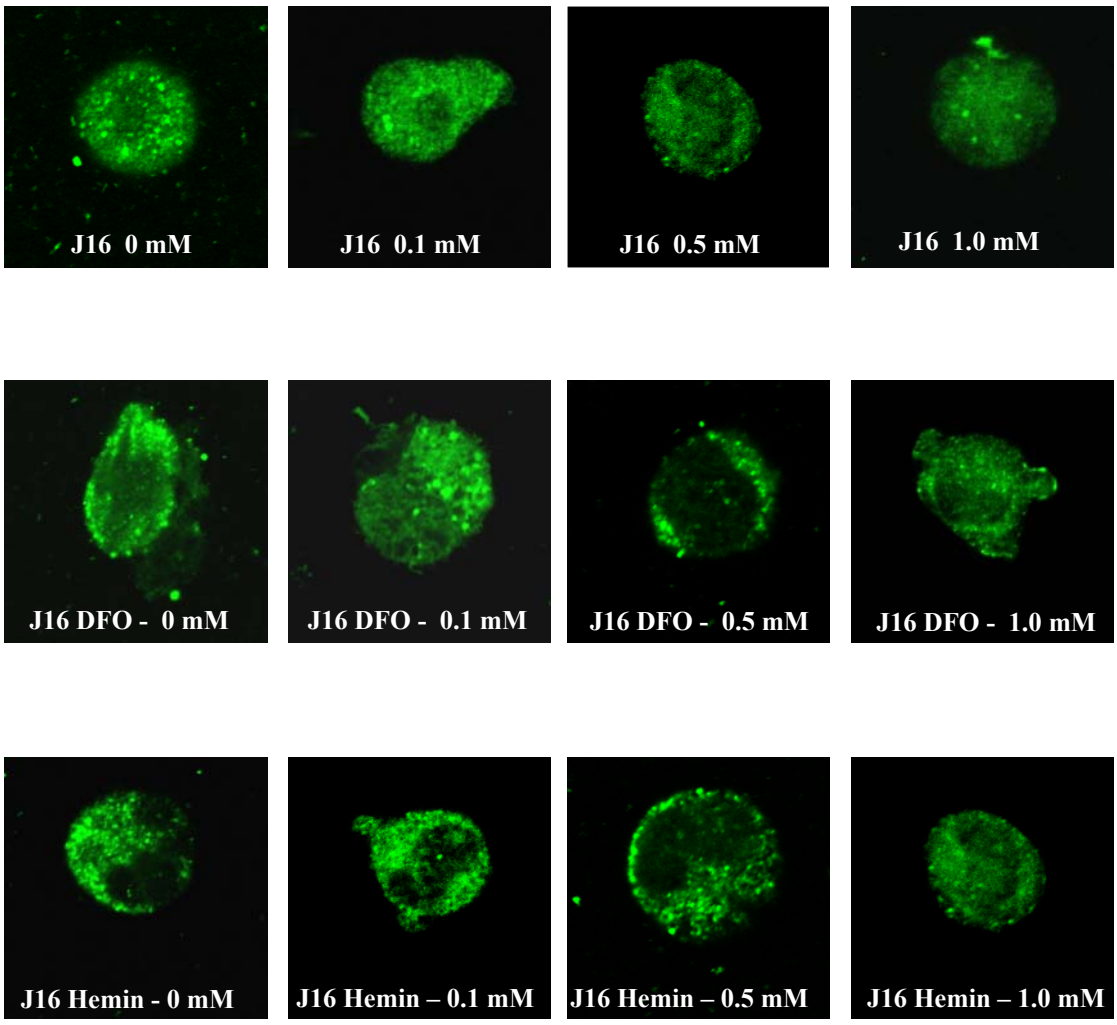

Figure 3.40:

The effect of iron chelation and loading on the H_2O_2-mediated lysosomal damage in J16 cell line (parental cells).

J16 cells were pre-treated with either 100 μM DFO (second row) or 20 μM hemin (third row) for 18 h before H_2O_2 treatment (i.e. 0.1, 0.5, and 1mM). Cathepsin B immunocytochemistry (see section 2.13) was performed 24 h following H_2O_2 treatment**.** The photographs are representative of three experiments.

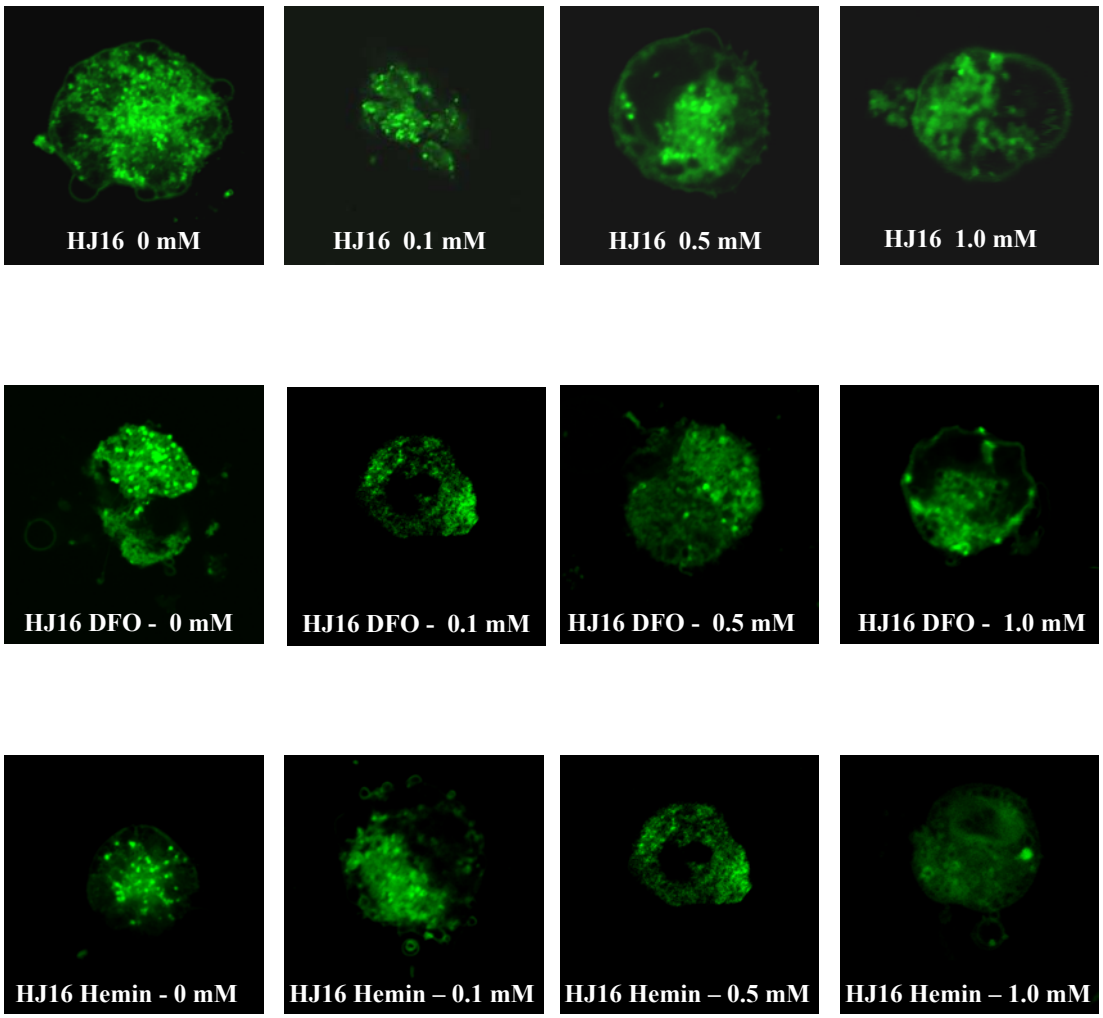

Figure 3.41 :

The effect of iron chelation and loading on the H_2O_2-mediated lysosomal damage in HJ16 cell line (H_2O_2-resistant cells).

HJ16 cells were pre-treated with either 100 µM DFO (second row) or 20 µM hemin (third row) for 18 h before H_2O_2 treatment (i.e. 0.1, 0.5, and 1mM). Cathepsin B immunocytochemistry (see section 2.13) was performed 24 h following H_2O_2 treatment**.** The photographs are representative of three experiments.

3.5 Preliminary clinical data

A preliminary study on human and rat fibroblasts was conducted in parallel with the current study (see section 2.16). In addition to this, LPI measurements of normal, RA and OA synovial fluid (SF) were performed.

3.5.1 MTT assay

Normal (HN-1) and osteoarthritic (HOA-1) human fibroblasts cells were treated with 1, 3, 5, and 7 mM H_2O_2. Unfortunately, MTT studies on the rheumatoid arthritic (HRA-1) cells were not possible due to the difficulty in growing and maintaining these cells. The results (see figure 3.42) revealed that both HN-1 and HOA-1 cells were resistant even to high non-physiological doses of H_2O_2. FEK4 (human fibroblasts cell line, derived from a newborn foreskin explants) and J16 cells were added as controls. The results show that the HN-1 was the most resistant cells. HOA-1 was less resistant than HN-1 and at high doses of H_2O_2, it was even less resistant than human primary fibroblast cell line; FEK4.

Normal (VW-1) and AA (AAVW-1) rat fibroblasts were also treated with the same concentrations of H_2O_2 (i.e. 1, 3, 5, and 7 mM) and it was quite interesting to note (see figure 3.43) that AAVW-1 were very resistant to all the doses used while VW-1 was very sensitive to the same treatment. R6 (the immortalised rat embryo fibroblast cell line) and J16 cells were added as controls.

3.5.2 LIP measurements

The LIP was measured in normal (HN-1), rheumatoid arthritic (HRA-1), and osteoarthritic (HOA-1) human fibroblasts cells. The basal and H_2O_2-induced level of LIP was investigated (see table 3.8). The basal LIP levels of HN-1, HRA-1, and HOA-1 were so low that with this assay were undetectable (i.e. below the threshold). Because of the higher susceptibility of HOA-1 to H_2O_2-mediated damage it was hypothesised that H_2O_2-induced levels of LIP in HOA-1 may be higher than HN-1 following treatment with an intermediate dose of H_2O_2 (i.e. 1mM).

MTT assay with 1mM of H_2O_2 showed a decrease in the percentage of intracellular dehydrogenase activity of HN-1 to 91.5 % of the control value (i.e. 100%) and to 60.8% in HOA-1 cells.

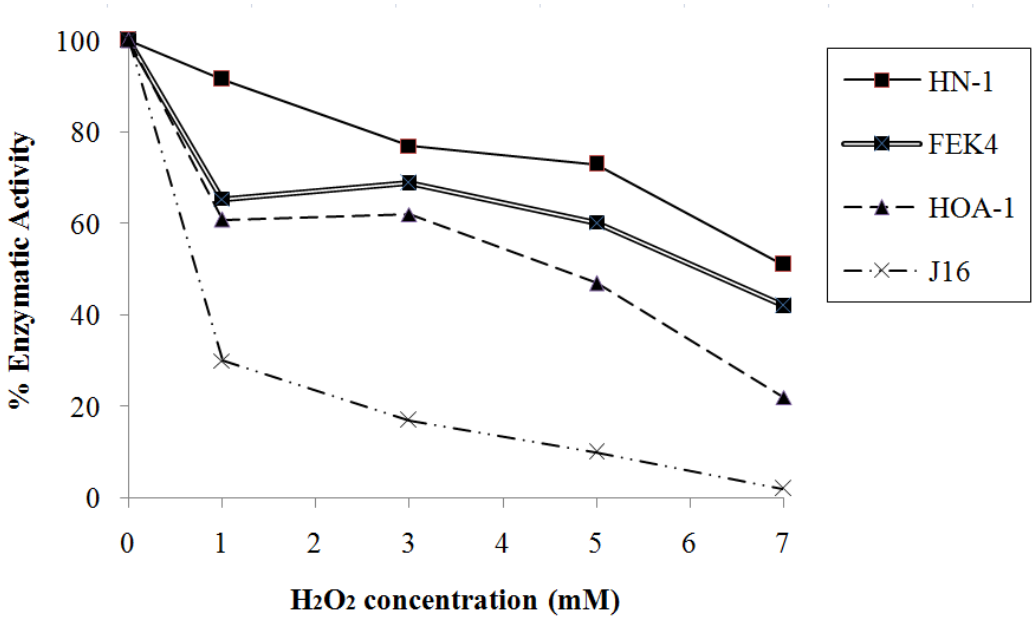

Figure 3.42 :

Effect of different concentrations of H_2O_2 on viable human cells (Analysis : MTT assay).

Normal (HN-1), osteoarthritic (HOA-1) human fibroblasts, FEK4 and J16 cells were treated with 1, 3, 5, and 7 mM H_2O_2. MTT analysis (see section 2.4) was performed 24 h following H_2O_2 treatment (n=1).

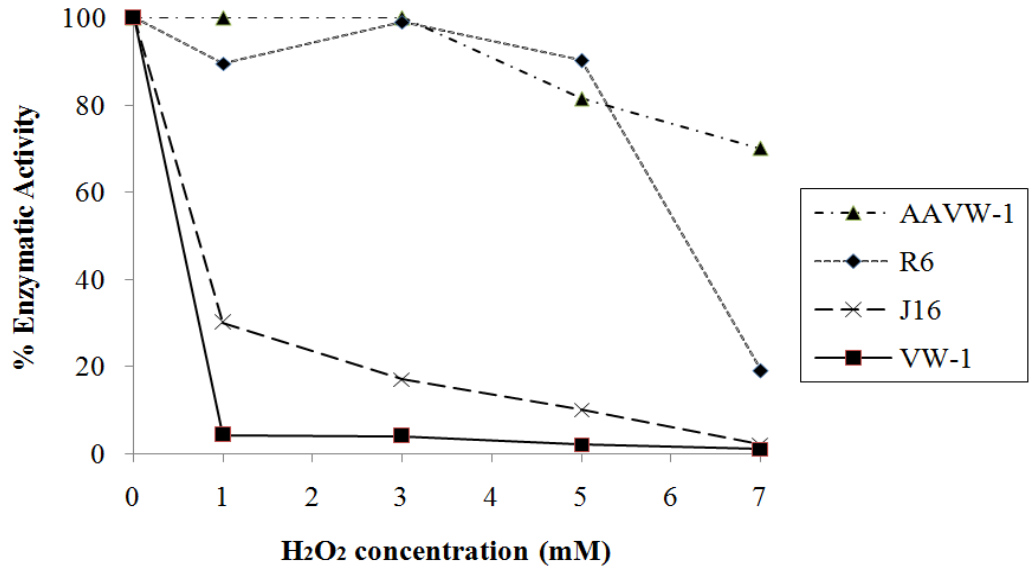

Figure 3.43 :

Effect of different concentrations of H_2O_2 on viable rat cells (Analysis : MTT assay).

Normal (VW-1) and AA (AAVW-1) rat fibroblasts, R6 (rat cell line) and J16 cells were treated with 1, 3, 5, and 7 mM H_2O_2. MTT analysis (see section 2.4) was performed 24 h following H_2O_2 treatment (n=1).

Table 3.8:

Labile iron pool (LIP) basal and H_2O_2-induced (i.e. 1mM) levels of normal (HN-1) and osteoarthritic (HOA-1) human fibroblasts.

Cells	Basal levels (μM/μg)	Post 1mM-H_2O_2 (μM/μg)
HN-1	Undetectable	Undetectable
HRA-1	Undetectable	Undetectable
HOA-1	Undetectable	0.18 ± 0.06

As described in section 2.15, the LIP basal levels and H_2O_2-induced (i.e. 1mM) of both normal (HN-1) and osteoarthritic (HOA-1) human fibroblasts was measured. These results are expressed as mean ± standard deviation (n=3).

These results were in agreement with our hypothesis, since following treatment of cells with an intermediate dose of 1mM H_2O_2, the LIP levels in HOA-1 increased to a detectable level (i.e. 0.18 ± 0.06 μM/μg) while it remained at undectable levels in HN-1. However, more samples are needed to validate our hypothesis. The LIP was also undetectable in HRA-1 cells.

The basal and the H_2O_2-induced (i.e. 1mM) levels of LIP were also investigated in normal (VW-1) and AA (AAVW-1) rat fibroblasts (see table 3.9). The basal levels of the LIP were undetectable in VW-1 but in AAVW-1 cells it was found to be within detectable range of 0.003 ± 1.25 x 10^{-5} μM/μg. Similarly with our rat cell model, it was hypothesised that an increase in LIP will be only seen in the normal (VW-1) cells when compared to AA (AAVW-1) rat fibroblasts after H_2O_2 treatment. The rationale for this hypothesis was that at 1mM of H_2O_2, the intracellular dehydrogenase activity of VW-1 decreased to 4.2 % of the control value (i.e. 100%), and it was not modified in AAVW-1 cells. Following an intermediate dose of 1mM of H_2O_2, the LIP levels of VW-1 increased to the detectable levels and in AAVW-1 cells, the increase was interestingly more than 13-fold.

3.5.3 LPI measurements

Labile plasma iron (LPI) was also measured, as described in section 2.16 in the synovial fluid (SF) of normal, rheumatoid arthritic (RA), and oesteoarthric (OA) patients. Synovial fluid from a normal, two RA, and six OA patients was analysed. The results (see table 3.10) show that there was no consistent pattern in these samples. The LPI of the normal patient was 0.45 ± 0.3 μM, it seems to be slightly higher in RA but it was non-significant (p value > 0.05). In OA samples, some had higher value than the normal sample and others had lower values, but they were all non-significant. Clearly, more samples are needed to complement these observations.

Table 3.9:

Labile iron pool (LIP) basal and H_2O_2-induced (i.e. 1mM) of the normal (VW-1) and AA (AAVW-1) rat fibroblasts.

Cells	Basal levels (µM/µg)	Post 1mM-H_2O_2 (µM/µg)
VW-1	Undetectable	0.02 ± 0.008
AAVW-1	$0.003 \pm 1.25 \times 10^{-5}$	0.04 ± 0.007 *+

As described in section 2.15, the LIP basal levels and H_2O_2-induced (i.e. 1mM) of both of the normal (VW-1) and AA (AAVW-1) rat fibroblasts was measured. These results are expressed as mean ± standard deviation (n=3).

* : $p < 0.05$ significantly different when compared with the basal levels.
+ : $p < 0.05$ significantly different when compared with the corresponding VW-1.

Table 3.10 :

Labile plasma iron (LPI) measurements of synovial fluid from normal, rheumatoid arthritic (RA), and osteoarthritic (OA) patients.

Condition	LPI (μM)
Normal knee	0.45 ± 0.3
RA knee	0.47 ± 0.09 ^{NS}
RA knee	0.54 ± 0.71 ^{NS}
OA knee	1.4 ± 1.06 ^{NS}
OA knee	0.29 ± 0.19 ^{NS}
OA knee	0.76 ± 0.36 ^{NS}
OA knee	0.44 ± 0.2 ^{NS}
OA knee	0.47 ± 0.29 ^{NS}
OA knee	0.04 ± 0.01 ^{NS}

LPI was measured as described in section 2.16. These results are expressed as mean ± standard deviation (n=3).

NS : non significantly different from the normal sample.

CHAPTER FOUR

DISCUSSION

Inflammation is a term used to illustrate the body's complex physiological response, whether acute or chronic, to tissue injury (Underwood, 1996). The role of the acute response is to clear dead cells from the site of the injury, to protect the site against any pathogens, and to permit the immune system to gain access to the site of inflammation (Junqueira *et al,* 1986). It is crucial that inflammatory reactions are self-limited upon e.g. elimination of the triggering factors, if not, they do perpetuate to chronic inflammation (Schett, 2008). The transition between the acute phase and the chronic phase is largely dependent on the persistence of the inflammatory cause. When the cause persists, chronic inflammation follows, which may last for a prolonged duration of time - weeks, months, or even indefinitely, and subsequently the cell population changes (Feghali and Wright, 1997). Lymphocytes and macrophages are the predominant cells in chronic inflammation (Junqueira *et al,* 1986; Underwood, 1996; Stevens and Lowe, 1999). In the inflamed area, these cells engulf the remains of cells and fibres and participate in the production of antibodies against invading microorganisms (Junqueira *et al,* 1986). Lymphocytes are also the key components in the onset and exacerbation of autoimmune diseases and the cytokines produced by them have a great impact on disease progression (Horwood, 2008). Cytokines are the key mediators of inflammation and can be found in abundance in the joints and the blood of patients suffering from rheumatoid arthritis (Christodoulou and Choy, 2006).

Rheumatoid arthritis (RA) is an example of a chronic auto-immune inflammation disease. It primarily affects the joints and ultimately leads to their destruction (Huber *et al,* 2006). Several studies indicate that during an inflammatory response, considerable amounts of ROS are generated that participate in the aetiology and/or the progression of the condition. For example in an inflammatory environment, lymphocytes are exposed to extensive quantities of H_2O_2 produced by macrophages and neutrophils as a result of the inflammatory response. Therefore, oxidative stress has been implicated in several physiological and pathological conditions (Vendemiale

et al, 1999), notably RA. Superoxide anion and H_2O_2 *per se* are not injurious but may become so in the presence of redox active iron or other transition metals. The potentially harmful free 'labile' iron is recognised as an important promoter of oxidative stress through aiding the production of ROS and thus a potential mediator of the inflammatory process in RA.

In addition to UVA (Morliere *et al,* 1997 and Pourzand *et al,* 1999) and visible light irradiation (Ohishi *et al,* 2005), it has already been shown that the exposure of cells to H_2O_2 (see section 1.3.6) provokes an increase in the LIP that correlates with cell damage and necrotic cell death, although the mechanisms involved had not been fully understood. The lysosomal compartment seems to contain the major important cellular pool of labile iron (Petrat *et al,* 2001; Kakhlon and Cabantchik, 2002; Persson *et al,* 2003) since the degradation of many macromolecules that are rich in iron (e.g. ferritin and mitochondrial electron-transport complexes) occurs in the lysosomes (Radisky and Kaplan, 1998 and Kurz *et al,* 2007) making these organelles vulnerable to oxidative stress (Persson *et al,* 2005). Therefore, understanding the link between lysosomal membrane damage and the iron may define pathological mechanisms associated with oxidative stress and lysosomal activity.

In this present study, we have used H_2O_2 as an oxidising agent, since treatment with this agent is commonly used to study the effect of ROS in biochemical pathways and it diffuses easily across cellular compartments (Auntes and Cadenas, 2000). It is known that H_2O_2 is generated during normal metabolism and produced in large quantities by phagocytic cells at inflammatory sites (Hylop *et al,* 1995). Several studies have shown the crucial role iron in inflammatory diseases such as RA; but none, to our knowledge, had differentiated between the role of iron in both acute and chronic phases in the disease and the origin of this 'free' iron. Therefore our primary aim was to investigate the role of iron in both acute and chronic oxidative conditions.

To achieve our aim we have extensively studied two cell lines which were Jurkat cells, human T-cell leukaemia cell line. Our model consisted of two human Jurkat T cell lines of "parental (J16)" and "H_2O_2 adapted/resistant/stressed (HJ16)" types. J16 cells were used to mimic the acute phase of oxidative stress. The HJ16 cell line was used to mimic the chronic phase since unpublished data from N.D Hall's laboratory

(Department of Pharmacy and Pharmacology, University of Bath) have shown that HJ16 cells have characteristics similar to that of rheumatoid synovial T cells.

A. Yiakouvaki from this laboratory (PhD Thesis, 2003 – University of Bath) has already characterised these Jurkat T cell lines in terms of antioxidant defence and modulation of intracellular LIP following H_2O_2. Overall her results provided a link between the amount of H_2O_2-induced labile iron release and the extent of oxidative damage and cell death in Jurkat T cells. Furthermore the study showed that adaptation of Jurkat T cells to H_2O_2 can influence the basal level of antioxidant enzymes that is likely to contribute to resistance of HJ16 cells to H_2O_2 insult.

This thesis has continued the study of Yiakouvaki (2003) by further characterising the differential response of parental J16 and H_2O_2-resistant HJ16 Jurkat T cells to H_2O_2.

The level of resistance of Jurkat T cell lines to H_2O_2-mediated toxicity

Tissues, in different pathological conditions, are confronted with elevated H_2O_2 concentrations derived either extra- or intra-cellularly. Overall the treatment of both cell lines with various concentrations of H_2O_2 revealed that exposure of parental J16 cells to moderate concentrations of H_2O_2 was capable of damaging half of the J16 cell line population since the percentage of live cells was found to be decreased to around 50 % of the control values. On the other hand, the HJ16 cell line showed higher resistance to H_2O_2-mediated oxidative insult, even at doses as high as 3 mM. Flow cytometry analysis further revealed that both cell lines are highly resistant to H_2O_2-mediated apoptotic cell death and that necrosis rather than apoptosis is responsible for H_2O_2-induced cell death.

The ultimate response of cells to oxidative stress is cell death in the form of apoptosis or necrosis. While apoptosis is recognised as a physiological programmed process to eliminate aged, superfluous or superficially damaged cells, necrosis is usually the ultimate response of cells to severe physical- or chemical-induced acute injury. Our results show that J16 parental cells are very sensitive to acute H_2O_2 insult since they die preferentially via necrosis. The gradual adaptation of HJ16 cells to H_2O_2 on the other hand appears to have increased their tolerance to H_2O_2-induced oxidative damage since the percentage of HJ16 cells dying by necrosis is dramatically lower than in parental J16 cells. The higher resistance of HJ16 cells to H_2O_2-induced

necrotic cell death is likely to be related to higher detoxification of H_2O_2 by intracellular antioxidant molecules/enzymes such as catalase, GPx and glutathione. The comparative study carried out by A. Yiakouvaki has already indicated that HJ16 cells have higher intracellular glutathione content and GPx activity when compared to J16 cells. However catalase activity was quite similar between the two cell lines. The study concluded that catalase should have a minor role in detoxifying H_2O_2 as it is located in peroxisomes and its access to cytosolic H_2O_2 is limited. However both GPx and glutathione that is required to complete the catalytic cycle of H_2O_2 are reside in the cytosol.

Interestingly, studies with synovial fluid have shown that RA patients have significantly higher GPx and catalase than normal controls (Biemond *et al,* 1984). GPx was also increased in the serum of patients with RA compared with the healthy control groups (Butkiene *et al,* 2007). It was therefore suggested that oxidative stress occurs in RA because of disturbance of enzymatic and non-enzymatic antioxidants systems.

In the present study it was decided to further characterise the Jurkat T cell lines cells in terms of their antioxidant defence mechanism by comparing the level of glutathione, Ft, HO-1 and HO-2 in presence or absence of H_2O_2 between parental and H_2O_2-resistant cells.

The role of intracellular glutathione

The intracellular glutathione system within the cells acts as a homeostatic redox buffer providing a major constitutive defence against oxidants (Applegate *et al,* 1992). To determine whether the total intracellular levels of glutathione play a role in increased resistance of HJ16 cell line to H_2O_2, the basal glutathione level was monitored in both parental (J16) and H_2O_2–resistant (HJ16) cell lines. Furthermore an attempt was made to deplete the intracellular level of glutathione in both cell lines (i.e. by BSO) to demonstrate the possible link between the intracellular level of glutathione and susceptibility of both cell lines to H_2O_2–mediated cytotoxicity.

The results revealed that in agreement with Yiakouvaki's data, HJ16 cells possess significantly higher (i.e. 3.4-fold) 'basal' levels of intracellular glutathione than J16 cells. However it was important to investigate the fate of glutathione following H_2O_2 treatment in our Jurkat cell models and to check whether the possible

modulation of glutathione levels by H_2O_2 insult could influence the susceptibility of Jurkat cells to necrotic cell death.

Glutathione is believed to be a very important cellular antioxidant compound, as its depletion is used to induce oxidative stress (Recalcati *et al,* 2003 and Tacchini *et al,* 2006). In fact, several studies have shown that the depletion of intracellular glutathione sensitises cell populations to several circumstances e.g. aerobic ionising radiation and cytotoxic drugs. For example glutathione depletion (by BSO) sensitises cultured human lymphoid cells to γ radiation (Dethmers and Meister, 1981), therefore it is regarded as a major protective agent against such radiation. Glutathione not only protects cells from the cytotoxic UVA damage, but also against the damage cause by UVB radiation (Tyrrell and Pidoux, 1988). It was also shown that yeast cells developed an increased sensitivity against H_2O_2 and ionising radiation following the depletion of glutathione (Sipos *et al,* 2002). In the present study we also demonstrated that the susceptibility of both cell lines to H_2O_2-mediated cytotoxicity was substantially increased following the depletion of the intracellular glutathione level. These results are in agreement with the previous observations made by others indicating that intracellular glutathione provides a constitutive mechanism of defence against ROS during oxidative stress conditions.

Oxidative stress in the form of UVA radiation (320 - 380 nm) and H_2O_2 have been shown to deplete intracellular glutathione (Lautier *et al,* 1992; Brunk *et al,* 1995[a]; Hempel *et al,* 1996). Therefore, the levels of total intracellular glutathione were measured following H_2O_2 treatment in J16 and HJ16 cell lines. Our results showed that H_2O_2 doses higher than 0.1 mM depleted significantly the total intracellular glutathione content in J16 cell line. However in HJ16 cells, H_2O_2 treatment only decreased to half the total intracellular level of glutathione. These results strongly suggest that chronic exposure of HJ16 cells to H_2O_2 provokes an adaptive mechanism preventing the total depletion of total intracellular glutathione in these cells. The latter should almost certainly contribute to the resistance of HJ16 cells to the high doses of H_2O_2.

Characterisation of the response of NF-κB to H_2O_2 treatment

The NF-κB complex has been shown to be activated in response to multiple stimuli many of which are possibly mediated by the generation of ROS (Piette *et al,* 1997 and Gilston *et al,* 2001). In response to these stimuli, NF-κB complex

activation has been examined in neutrophils, macrophages, and lymphocytes (reviewed in Makarov, 2001). The inducibility of the NF-κB complex in response to H_2O_2 is cell-specific. Furthermore it is not clear whether this response will be lost if cells are chronically adapted to H_2O_2 treatment, in the case of HJ16 cell line. Therefore the inducibility of NF-κB complex, by Electrophoretic Mobility Shift Assay (EMSA) and immunocytochemistry was investigated in both J16 and HJ16 cell lines following H_2O_2 treatment. Our results demonstrated that NF-κB complex is present and induced by H_2O_2 in both J16 and HJ16 cells, although the induction was higher in HJ16 cells. These findings are in conflict with other studies that have shown that the induction of NF-κB is strongly suppressed in cells pre-exposed to sources of oxidative stress such as H_2O_2 (Lahdenpohja *et al,* 1998).

The NF-κB complex has been shown to be activated in cancer cells and also after chemotherapy or radiotherapy, and therefore it has been associated with the resistance of these cells to apoptosis (reviewed in Piva *et al,* 2006 and Sethi *et al,* 2008). The NF-κB complex therefore plays an important role in cell survival (Habens *et al,* 2005). The higher activation of NF-κB by H_2O_2 in HJ16 cells could be seen as another adaptive mechanism in these cells increasing their survival against H_2O_2-induced oxidative damage and necrotic cell death. To this regard, several recent studies have provided evidence about the existence of a prosurvival pathway initiated by NF-κB that appeared to be responsible for the radioadaptive response (i.e. radioresistance) in all cells (reviewed in Ahmed and Li, 2008). Furthermore it has been speculated that the inducibility of the NF-κB complex in synovial T cells of rheumatoid arthritic patients should be low as these cells are chronically exposed to ROS. *In vitro* studies have proven that this speculation is incorrect (see section 1.6.6).

Studies by Marok *et al* (1996) and Gilston *et al* (1997) have demonstrated that NF-κB complex is highly activated in patients with chronic inflammatory conditions such as rheumatoid arthritis. Our data appears to be in agreement with such studies. As mentioned in section 1.6.3, activation of NF-κB can be divided into two pathways, the 'classical' and the 'alternative' pathway. The classical pathway has been proposed to be responsible for the NF-κB activation in the RA synovium (reviewed Simmonds and Foxwell, 2008). Clearly further studies are necessary to unravel the role of NF-κB in both oxidative stress and inflammatory conditions.

Similarly, in our cell models, further investigations are necessary to understand the mechanism underlying the higher NF-κB activation in HJ16 cells.

The role of LIP in differential sensitivity of the J16 and HJ16 cells to H_2O_2 treatment

Hydrogen peroxide-sensitive (and ionising radiation-resistant) mouse lymphoma cell line has 3-fold higher 'basal' LIP levels than H_2O_2-resistant (and ionising radiation-sensitive) cells (Lipinski *et al,* 2000). However what these authors called 'LIP' levels in their measurements with CA-assay reflects only the CA-bound iron that is usually referred to as chelatable iron pool. The LIP according to Cabantchik and co-workers who developed the CA-assay is operationally defined as the sum of the intracellular level of CA-bound iron (i.e. [CA-Fe]) and free iron (i.e. [Fe] unbound to CA) and requires the determination of the cell-dependent dissociation constant (Kd) for CA-Fe by taking into account the cell volume. These determinations were lacking in the study by Lipinski *et al,* (2000). In our cell volume study we have observed that the HJ16 cells are significantly larger cells than the parental cells (i.e. 3.4-fold bigger than J16), therefore in all our iron studies, it was necessary to first determine the cell-dependent Kd of CA-bound iron in order to calculate the absolute level of LIP. The results demonstrated that the 'basal' LIP levels of both cell lines were quite similar; J16 cells (3.08 μM ± 0.59) and HJ16 cells (3.34 μM ± 0.87). However following H_2O_2 treatment, the LIP was increased by more than 3.2-fold in J16 cells (9.86 μM ± 0.35) and this was correlated with high necrosis. In HJ16 cells, H_2O_2 produced only a moderate increase in the basal LIP level (5.27 μM ± 1.12) when compared with J16 cells and this correlated to lower necrosis than in J16 cells. The lower increase of LIP in HJ16 cells after H_2O_2 treatment is likely to be part of the adaptive mechanism developed in these cells making these cells less susceptible to H_2O_2-induced oxidative iron-damage and necrotic cell death. Interestingly human epidermal keratinocytes that are naturally resistant to UVA-induced damage also show lower LIP levels than the UVA-sensitive dermal fibroblasts following UVA irradiation. The lower UVA-induced LIP levels in keratinocytes has been correlated with their low propensity to UVA-induced necrotic cell death (Zhong *et al*, 2004). It appears that in our cell model, the modulation of the

LIP levels following H_2O_2 treatment also correlates with the extent of cell damage and necrotic cell death.

To ascertain the importance of H_2O_2-induced labile iron release in modulating the susceptibility of cells to H_2O_2-induced necrotic cell death, both J16 and HJ16 were treated with DFO, a strong iron chelator or hemin (i.e. ferric haem) as a source of iron for 18 h prior to H_2O_2 treatment and then the level of LIP was measured following H_2O_2 treatment using the CA assay. The results demonstrated that DFO treatment abolishes both the 'basal' and 'H_2O_2-induced' LIP levels and necrotic cell death in both cell lines, consistent with the notion that iron chelation by DFO protects the cells against H_2O_2-induced necrotic cell death. In the case of hemin treatment, hemin alone (i.e. when not followed by H_2O_2 treatment) did not modulate the level of LIP in J16 cells but upon H_2O_2 treatment it caused a low increase in LIP that correlated with low necrosis. This is in agreement with previews studies by Balla and co-workers showing that the endothelium's susceptibility to H_2O_2-mediated insults decreases following exposure to hemin or haemoglobin (Balla *et al,* 1992 and 1993). It was also demonstrated that extracellular Fe^{2+} and H_2O_2 preserved intracellular glutathione, prostaglandin H synthase, mitochondrial electron transport, and cell calcium entry, and therefore protected endothelial cells from cellular damage (Hempel *et al,* 1996). On the other hand, in HJ16 cell line, hemin treatment modulated both the 'basal' and 'H_2O_2-induced' LIP levels in HJ16 cells. The higher levels of LIP accumulation after overnight hemin treatment of HJ16 cells abolished their resistance to H_2O_2-induced damage since the level of necrosis was significantly increased upon hemin-H_2O_2 treatment. These results strongly suggested that the presence of higher LIP in HJ16 cells following hemin treatment should be responsible for abolishing the resistance of HJ16 cells to H_2O_2–mediated oxidative insult. Hydrogen peroxide can react with Fe^{3+} to form $O_2^{\cdot-}$ and if H_2O_2 is in excess, the Fe^{2+} which is formed can subsequently generate ROS via the Fenton reaction (Henle and Linn, 1997). The iron-mediated damage is very powerful and should almost certainly contribute to severe oxidative damage in HJ16 cells leading to necrotic cell death. Further investigation with time course analysis revealed that in J16 cells, hemin only caused a transient and moderate increase in the LIP levels within the first 2-4 h after treatment, but in HJ16 hemin provoked a higher accumulation of LIP levels that was sustained at least for 18 h. In HJ16 cells, the hemin-mediated increase in LIP was also concentration-dependent. The high accumulation of LIP in HJ16 cells following

hemin treatment increased dramatically the percentage of necrotic cell death, consistent with the notion that the intracellular level of LIP plays an important role in determining the level of sensitivity of these cells to H_2O_2-mediated necrotic cell death.

To further demonstrate the strict dependence of H_2O_2-induced necrotic cell death on LIP level present in the cells, hemin treatment for 18 h was followed by an additional treatment with 1 mM DFO for 2h. The latter treatment was expected to lower the hemin-mediated increase in LIP, leading to decreased necrosis by H_2O_2. The results showed that, in agreement with our hypothesis, in both cell lines DFO treatment of cells pre-treated with hemin, significantly decreases the levels of H_2O_2-induced necrotic cell death when compared to cells treated with hemin alone.

Taken together, from the above results; a picture emerged suggesting that LIP levels must be a key component in determining the extent of the sensitivity of these cells to H_2O_2-induced necrotic cell death. However it was surprising to see how the same treatment provoked two entirely different responses in the cell lines. The hemin treatment increased the resistance of J16 to H_2O_2-induced necrotic cell death but abolished the resistance of HJ16 cells. The hemin overnight treatment increased the levels of LIP in HJ16 cells but not in J16 cells. We hypothesised that the high accumulation of labile iron in HJ16 cells following hemin treatment could either be due to higher HO protein levels or lower intracellular Ft levels in HJ16 cells when compared to parental J16 cells. We therefore investigated the level of these proteins in both J16 and HJ16 cells following various treatments as detailed below.

The role of HO-1 and HO-2 in Jurkat cell lines

The higher expression of HO-1 and/or HO-2 in HJ16 cell line might contribute to accumulation of LIP levels following hemin treatment, since hemin is a known substrate for these enzymes. Previous analysis of the level of *ho-1* mRNA accumulation in J16 and HJ16 cells using the real-time PCR technique (Yiakouvaki, 2003) revealed that the basal level of *ho-1* cDNA is 2-fold higher in the H_2O_2-resistant cells than in the parental cells. Furthermore the basal level of HO-1 protein in H_2O_2 resistant cells was found to be 2-fold higher than in parental cells. So it was concluded that HO-1 expression should play a role in hemin-induced iron accumulation in HJ16 cells. Furthermore when both cell lines were treated with 20 μM hemin at various time points, a significant increase in HO-1 was only observed in

parental cell line. Yiakouvaki (2003) concluded that HO-1 protein is not inducible in HJ16 cells presumably because gradual adaptation of cells to H_2O_2 provokes a refractory response of HO-1 to hemin.

Since hemin is also a known substrate of HO-2 protein, it was important to check in our study the level of its expression in Jurkat T cells. We therefore decided to carry out an in depth study of the expression of HO-1 and HO-2 at protein levels following various treatments using Western blot analysis. Overall, these treatments were (1) Hemin/DFO alone or Hemin/DFO pre-treatment prior to H_2O_2 treatment, (2) Time-course of hemin treatment, (3) Time-course of H_2O_2 treatment, (4), Time-course of hemin pre-treatment prior to H_2O_2 treatment and (5) Hemin pre-treatment followed by with 1 mM DFO for 2 hours and finally H_2O_2 treatment.

The basal level of HO-1 was found to very low in both cell lines and the difference in expression observed by Flow cytometry could not be visualized by Western blot analysis. Furthermore the analysis showed no increase in HO-1 level in these cell lines. Studies with Jurkat T cells performed by others have also shown that HO-1 protein expression is not detectable at basal levels by Western analysis (Pae *et al,* 2004[a]; Choi *et al,* 2004; Pae *et al,* 2004[b]). The basal HO-2 level on the other hand was higher than HO-1 in both cell lines but it was not modulated by any of the above treatments.

To ascertain that HO protein levels were not modulated at early hours following hemin and/or H_2O_2, the HO-1 and HO-2 levels were followed in time course analysis from 0 to 18 and/or 24 h following hemin and/or H_2O_2 treatments. The results revealed that neither HO-1 nor HO-2 levels are modulated by these treatments. To complete the analysis, the levels of HO-1 and HO-2 proteins were also checked after combined hemin+DFO and/or H_2O_2 treatment. Again here, no modulation in protein levels of HO-1 and HO-2 was observed. Taken together these results showed that high iron accumulation after hemin treatment in HJ16 cells might not be related to differential expression of HO proteins in these cells.

Following oxidative stress (UVA and H_2O_2), HO-1 mRNA levels were strongly inducible in dermal fibroblasts and were barely inducible in human epidermal keratinocytes that are known to be naturally resistant to oxidative insults (Applegate *et al,* 1995). HO-2 mRNA levels on the other hand were found to be high in epidermal keratinocytes but low in dermal fibroblasts. The higher resistance of epidermal keratinocytes to UVA-induced necrotic cell death has also been linked to

the LIP, since both 'basal' and 'UVA-induced' levels in keratinocytes were several fold lower than in their matched dermal fibroblasts (Zhong *et al,* 2004).

In eight of the human cancer cells examined (Ding *et al,* 2006); HO-1 expression was not detectable in three, including Jurkat cells. Interestingly, HO-2 was highly expressed in these three cells whereas HO-1 was not present. Si-RNA-mediated knocking down of HO-1 has also been shown to increase HO-2 expression in human skin fibroblasts (Julia Zhong Li and Rex M. Tyrrell, unpublished data). These studies suggested that HO-2 may down regulate the expression of HO-1, thereby directing the co-ordinated expression of HO-1 and HO-2.

Seta *et al,* (2006) were the first to demonstrate that HO-2 is crucial in the regulation of inflammation; in the absence of HO-2, resolution of inflammation was impaired resulting in a continuous influx of inflammatory cells and subsequently, an exacerbation of cellular injury. They have also demonstrated that HO-1 function depends on the activity of HO-2, since the study indicates that in the absence of HO-2, functional HO-1 induction is impaired and HO activity is abrogated.

Both HO-1 and HO-2 break down hemin as their substrate to release its iron. The excess iron is usually sensed by IRP-1 that activates the synthesis of Ft molecules to sequester the iron that would otherwise be potentially harmful to cells especially during an oxidative stress condition. In the present study the high expression of HO-2 appeared to be sufficient to break down hemin to release its iron. But the fate of the released iron appeared to be different in these two cell lines and we speculated that this difference could be related to differential expression of Ft protein in these cell lines.

<u>The role of ferritin in Jurkat cell lines</u>

Ferritin sequesters the potentially harmful labile iron within its shells by H-Ft's ferroxidase activity so that iron could be stored in an inactive form. H-Ft has ferroxidase activity and is required for incorporation of iron *in vivo*. L-Ft (which lacks the ferroxidase centre) on the other hand, promotes nucleation of the metal inside the cavity and stabilizes the ferritin shell; it does not incorporate iron *in vivo*. Several cellular studies have shown that in oxidative stress conditions Ft could have a protective effect against oxidative damage as it removes iron that acts as a catalyst in biological oxidation (reviewed in Arosio and Levi, 2002 and Torti and Torti, 2002).

As mentioned in section 1.4.1.3, in the early stages of oxidative challenge, Ft degradation could be a potential source of iron. Cairo *et al* (1995) have suggested that liver Ft can act as a pro- or an antioxidant in a time dependant manner. An early decrease in Ft has been shown after treatment of Wistar rats with phorone, a glutathione depleting drug that amplifies the effects of ROS. Interestingly, 6-fold induction in Ft synthesis was observed as a late response. In the case of UVA and skin cells, Ft also acts as a pro- and antioxidant in a time dependent manner. Treatment of skin fibroblasts with UVA leads to an immediate degradation of intracellular Ft (Pourzand *et al,* 1999). The consequent iron release played a key role in exacerbating UVA-induced oxidative damage and led to necrotic cell death (Zhong et al, 2004 and Yiakouvaki *et al,* 2006). However 6 h after UVA treatment, Ft levels returned to normal and then increased thereafter up to 3-fold 24-48 hours following UVA treatment. The long term increase in Ft levels was associated with increased resistance of skin fibroblasts to subsequent UVA-induced membrane damage (Vile and Tyrell 1993).

The proteolytic degradation of Ft upon UVA irradiation of skin cells occurs as a result of damage to lysosomal membranes leading to leakage of potentially harmful lysosomal proteases to cytosol which in turn act to degrade cytosolic proteins; notably Ft (Pourzand *et al,* 1999). Studies by Brunk and co-workers (Brunk *et al,* 1995[b]) have demonstrated that acute exposure of macrophage–like J-774 cells to H_2O_2 also triggers lysosomal damage. The irradiation of human fibroblasts with a moderate dose of blue light also resulted in oxidative apoptotic cell death as a result of damage to lysosomal organelles (Brunk *et al,* 1997). Damage to lysosomes was accompanied by leakage of lysosomal contents including hydrolytic enzymes, such as cathepsin D (CATH D) (Roberg and Öllinger, 1998) that should almost certainly lead to proteolytic degradation of Ft as well.

Interestingly epidermal skin keratinocytes that have low basal level of Ft and LIP are naturally resistant to UVA-induced necrotic cell death but overnight hemin treatments renders these cells vulnerable to UVA-induced peroxidative damage and necrotic cell death (Zhong *et al,* 2004). This is because iron loading of cells with hemin increases strongly the level of intracellular Ft which in turn increases the level of UVA-induced LIP upon radiation-mediated proteolysis of Ft molecules.

Since HJ16 cells' resistance to H_2O_2 was abolished after hemin treatment presumably because of high accumulation of labile iron in these cells, it was important to investigate the role of Ft in this phenomenon.

As in HO, in general the conditions for H- and L-Ft levels measurements were: (1) Time-course of H_2O_2 treatment, (2) Time-course of hemin treatment, (3) Time-course of hemin pre-treatment prior to H_2O_2 treatment, (4) Hemin/DFO alone or Hemin/DFO pre-treatment prior to H_2O_2 treatment, and (5) Hemin pre-treatment followed by with 1 mM DFO for 2 hours and finally H_2O_2 treatment.

Our results demonstrated that the 'basal' levels of H-Ft in J16 cell line are 7-fold higher than in HJ16 cell line. The lower H-Ft levels in HJ16 might be part of the adaptive response developed during gradual adaptation of these cells to H_2O_2. As for L-Ft they had the same 'basal' level in both cell lines. However in the study carried out by Lipinski *et al* (2000), both the H- and L-Ft levels were found to be higher in the H_2O_2-resistant cells than in the H_2O_2-sensitive mouse lymphoma cells. The latter results differ from our study, presumably due to difference in cell type or due to difference in the regulation of iron homeostasis or the adaptive mechanism developed following chronic H_2O_2 treatment.

The time course experiment further revealed that following H_2O_2 treatment the levels of H-Ft decreased gradually in J16 cells at 6 h post treatment time point and this level remained lower than control value up to 24 h following treatment. Hydrogen peroxide treatment of cultured fibroblasts and macrophages has also been shown to significantly inhibit the synthesis of Ft (Pantopoulos and Hentze, 1995 and Mehlhase *et al,* 2005, respectively). The decrease in Ft levels has also been shown in rat liver lysates subjected to postischemic reperfusion (Tacchini *et al,* 1997). The L-Ft time course study following H_2O_2 treatment revealed that the L-Ft levels remain unchanged in J16 cells but slightly increase up to 2-fold control value in HJ16 cells at 6 h time point and then return to around control value at 24 h.

When cells were treated with 0.5 mM H_2O_2 and the Ft levels were measured *immediately*, the H-Ft level slightly decreased in J16 cells but did not affect significantly the L-Ft. The H-Ft levels in HJ16 were not significantly affected by H_2O_2 treatment, L-Ft on the other hand increased up to 3-fold of the control value. But when the cells were incubated for an additional *24 h* in CM, the H-Ft decreased more in J16 cells but in HJ16 cells, the H-Ft levels remained unchanged. The H_2O_2-mediated decrease in H-Ft levels in J16 is likely to contribute to their increased

susceptibility to H_2O_2-induced oxidative damage, since the lower Ft levels will not be able to sequester all the iron that is released by H_2O_2. Furthermore since lysosomes are severely damaged after H_2O_2 treatment in J16 cells, it is possible that the decrease in Ft levels is due to its proteolytic degradation by lysosomal proteases leaked in the cytosol. Lysosomes themselves are a known source of iron so their damage should almost certainly increase the pool of potentially harmful iron in the cytosol. It is assumed that a proportion of LIP levels detected in J16 cells following H_2O_2 treatment originates from lysosomal compartments. Similarly, Yiakouvaki (2003) has demonstrated that H_2O_2 also damages the mitochondrial membranes in J16 but not HJ16 cells, leading to intracellular depletion of ATP that contributes to H_2O_2-induced necrotic cell death observed in J16 cells. Damage to mitochondria will release the iron content of these organelles. Indeed in addition to lysosomes, mitochondria are known to contain considerable amount of iron (Petrat *et al,* 2002).

In HJ16 cells, the H-Ft levels remained unchanged following H_2O_2 treatment. Since lysosomal organelles are not significantly damaged by H_2O_2 in this cell line, it is reasonable to assume that Ft molecules remain intact in HJ16 cells and are not subject to proteolytic degradation by lysosomal proteases that leak in the cytosol in the case of J16 cells. Mitochondrial membrane was also more resistant to H_2O_2-induced oxidative damage in HJ16 cells (Yiakouvaki, 2003). The resistance of lysosomal and mitochondrial membranes in HJ16 cells will almost certainly contribute to the observed low LIP levels after H_2O_2 treatment as their compartmental LIP would not release to cytosol as a result of damage. Therefore it is reasonable to suggest that lower Ft levels in HJ16 cells is due to adaptive mechanism developed in these cells, because these cells would only show low LIP levels after H_2O_2 so the presence of high basal levels of H-Ft were redundant for the response of these cells to H_2O_2.

Unlike in our cell model, overexpression of the H-Ft increased the resistance of murine erythroid leukaemia (MEL) cells and HeLa cells to H_2O_2 treatment (Epsztejn *et al,* 1999 and Cozzi *et al,* 2000). Ferritin seems to act as a pro-oxidant molecule in J16 cells and an antioxidant in HJ16 cells following H_2O_2 treatment. The L-Ft on the other hand, was not significantly affected in J16 cells but it was slightly increased in HJ16 cells.

The treatment of cells with 100 μM DFO strongly reduced the level of H-Ft in J16 cells. In HJ16 cells, DFO treatment also decreased the level of H-Ft although to a

lesser extent than in J16 cells. The decrease in H-Ft levels by DFO is consistent with previous observations showing that DFO diminishes Ft biosynthesis in B6 fibroblasts (Pantopoulos and Hentze, 1995) and reduces Ft levels in macrophages (Mehlhase *et al,* 2005). The DFO treatment decreased significantly the L-Ft levels in J16 cells but strongly induced their levels in HJ16 cells. The reason for this increase is not clear. One explanation would be that L-Ft compensates for the strong decrease of H-Ft in HJ16 cells. Indeed Kakhlon *et al,* (2001) have reported that there is an active role of both H- and L-Ft in modulating LIP and that they both balance each other when one of them was repressed. Following the *24 h* incubation in CM after the DFO treatment, H-Ft decreased further in J16 and HJ16 cells. DFO treatment of HeLa cells demonstrated nearly a total repression of Ft (Cairo *et al,* 1985), as it also significantly decreased both subunits in K562 cells (Konijn *et al,* 1999). On the other hand, the L-Ft levels decreased significantly in J16 cells but not in HJ16 cells.

The H_2O_2 treatment of DFO-treated cells, decreased even more the H-Ft levels in J16 cells and HJ16 cells. On the other hand, there was a non-significant change in the L-Ft expression in both cell lines. This was also true following the *24 h* incubation in CM following DFO + H_2O_2 treatment; H-Ft was strongly decreased in J16 cells and HJ16 cells. On the other hand, the L-Ft levels remained unchanged in both cell lines. DFO is known to suppress the Ft synthesis via activation of IRP-1 binding. This has been seen for example with treatment of skin fibroblast cells with DFO (Pourzand *et al*, 1999) and in B6 fibroblasts. In the latter case the IRP/IRE binding activity was increased in B6 cells when pre-treated with DFO alone or prior to H_2O_2 treatment (Pantopoulos and Hentze, 1995).

The time course experiment following hemin treatment revealed that the increase in H-Ft levels in both the J16 and HJ16 cells was not highly induced in the early hours after treatment, presumably because Ft molecules takes time to get synthesized. However this level was increased dramatically from 8 h time point. The latter data is expected as hemin should first be broken down by HO and release its iron which in turn will stimulate *de novo* Ft synthesis. The rate of Ft synthesis in Hela cells increased only 4 h after hemin treatment (Kvam *et al*, 2000). The *de novo* synthesis of Ft in skin fibroblasts following its proteolytic degradation by UVA was also apparent from 4 h post-irradiation time point (Pourzand *et al*, 1999). The iron accumulation in HJ16 cells after hemin treatment was only apparent after 2 h post treatment with a peak at 6 h after which was then reduced, presumably because of

sequestration of a portion of it in the newly synthesized Ft molecules since this timing coincided with detection of higher Ft levels.

Overall the comparison of H-Ft levels between J16 and HJ16 after 18 h hemin treatment shows that J16 has much higher H-Ft levels than HJ16. Ferritin biosynthesis also strongly increased in B6 fibroblasts pre-treated with haem arginate (Pantopoulos and Hentze, 1995). Ferritin expression was highly induced when skin keratinocytes and fibroblasts were treated overnight with hemin (Zhong *et al*, 2004 and Reelfs *et al*, 2004). Ferritin expression was also increased 6-fold following overnight treatment with hemin in macrophages (Mehlhase *et al,* 2005). A strong up-regulation of both H- and L-Ft chains was reported in HeLa cells after iron administration (Cairo *et al,* 1985). On the contrary, only H-Ft was induced after hemin treatment in bovine artery endothelial cells (Lin *et al,* 1998), L-Ft on the other hand was unaffected.

The lower H-Ft level in HJ16 cells after hemin treatment appears to be not sufficient to sequester the excess iron load by hemin, since the level of LIP remains high even after 18 h post-treatment time point. Under conditions of severe macrophage lysosomal iron overload, induction of Ft synthesis is also not enough to completely prevent the H_2O_2-mediated cytotoxicity effects (Garner *et al,* 1997). On the other hand, the higher level of H-Ft in J16 cells appears to be sufficient to incorporate the excess iron from hemin breakdown, since the LIP level were returned to control value 18 h after hemin treatment. Additional incubation of J16 and HJ16 cells for *24 h* in CM following 18 h hemin treatment increased further the H-Ft levels in both cell lines although still to much lower extent in HJ16 cells.

Exposure of hemin treated cells to 0.5 mM H_2O_2 significantly increased the H-Ft and L-Ft levels in both cell lines although to a lesser extent in HJ16 cells. The presence of excess iron in HJ16 cells promoted severe oxidative damage in this cell line that led to high percentage of necrotic cell death. These results indicated that loading of HJ16 cells with iron in the form of hemin abolishes their resistance to H_2O_2. In J16 cells, induction of high H-Ft levels after hemin treatment appeared to protect the cells against H_2O_2-induced oxidative damage and necrotic cell death. So Ft molecules in J16 cells acted as an antioxidant as has been reported in some studies. For example, in endothelial cells, iron loading for 1 h significantly increased the cytotoxicity of H_2O_2 or oxidants from activated inflammatory cells (Balla *et al,* 1992). Interestingly, at 16 hrs the cells became highly resistant to oxidative-mediated injury. This was correlated with 50-fold and 10-fold increase in HO and Ft, respectively.

This has also been demonstrated in murine L1210 lymphocytic leukaemia cells using various types of oxidative insults (Lin and Girotti, 1997). Only after long-term exposure (20-24 hrs) to hemin, cells became significantly resistant to both H_2O_2 and $^1O_2$ toxicity. This observation was correlated with 12 to 15-fold increase in H-Ft. L-Ft, on the other hand, was not modified. This seems to be the case in J16 cells where Ft is acting as an antioxidant, as hemin pre-treatment prior H_2O_2 treatment promoted less necrosis. This could explain the protection that hemin has offered in J16 cells prior to H_2O_2 treatment. In HJ16 cells, the H- and L-Ft induction was highly induced to incorporate the LIP release after hemin pre-treatment, but the absolute level of H-Ft was dramatically lower than that of J16. That is why HJ16 could not cope by excess iron from hemin treatment since Ft induction was not sufficient to sequester extra iron and protect the cells from oxidative damage exerted by H_2O_2 treatment. In the latter case Ft failed to act as an antioxidant.

Finally the effect of hemin and DFO treatment with and without H_2O_2 treatment was investigated. The DFO treatment increased the level of H- and L-Ft induction after hemin treatment in both cell lines. Accordingly the level of necrotic cell death decreased in HJ16 cells after H_2O_2 treatment. The latter data confirmed that the increased susceptibility of HJ16 cells to H_2O_2 was due to high iron accumulation by hemin breakdown that could not be entirely sequestered within low amount of Ft molecules available. But additional DFO treatment cleared excess iron from the cells and therefore decreased the high level of necrotic cell death observed with hemin treatment alone. In at least six different cell lines, DFO exposure to iron pre-loaded cells accelerated Ft protein turnover in the lysosomes and consequently iron release from Ft (Truty *et al,* 2001; Kindane *et al,* 2006; De Domenico *et al,* 2006).

Mitochondrial ferritin (Mt-Ft) was also measured in both cell lines. In J16 cell line Mt-Ft basal level was 0.53 ng/mg and 1.52 ng/mg in HJ16 cells. In J16 cell line, following either hemin or DFO treatment prior H_2O_2 treatment or H_2O_2 treatment alone, Mt-Ft was negligible. On the other hand, in HJ16 cell line, Mt-Ft was increased up to 4-fold after 0.5 mM H_2O_2 treatment (measured 24 h following the treatment), overnight treatment with 20 μM hemin (measured 24 h following the treatment), H_2O_2 treatment (0.5 mM) following overnight treatment with 20 μM hemin (measured immediately following the treatment). It was also increased up to 5-fold after overnight treatment with 100 μM DFO (measured 24 h following the treatment). Mitochondrial ferritin (Mt-Ft) is currently under investigation in our cell model.

The role of iron-mediated lysosomal damage in J16 and HJ16 cells

Lysosomes have been implicated in the turnover of Ft (and consequently, iron release) in K562 cells (human leukaemia cell line) and human fibroblasts (Roberts and Bomford, 1988 and Radisky and Kaplan, 1998). Treatment of human skin fibroblasts with UVA radiation (320 – 380 nm) lead to an immediate release of iron via the proteolysis of Ft (Pourzand *et al,* 1999). This study provided the first evidence that UVA-mediated Ft degradation originates from the destabilization of lysosomal membranes and the subsequent leakage of proteolytic enzymes. Chymotrypsin, a lysosomal protease that is responsible for the degradation of Ft molecules in lysosomes, was around 3-fold higher in UVA-treated cells when compared with unirradiated controls. The degradation of Ft was prevented when cells were pretreated with Chymotrypsin-specific lysosomal protease inhibitors (i.e. Chymostatin and Leupeptin). Delocalisation of CATH B from the lysosomal compartment to the cytosol was observed after UVA radiation in human skin fibroblasts (Basu-Modak *et al,* 2006). When human skin fibroblasts were pre-treated with catechins, flavonoid constituents with protective properties predominantly against oxidative stress, prior to UVA-radiation; iron release was prevented (Basu-Modak *et al,* 2006). De Domenico *et al,* (2006) have suggested that the Ft can be degraded by two mechanisms: lysosomal degradation of Ft and a cytosolic route in which iron is extracted from Ft prior to the degradation by proteasome. It has been also demonstrated that in three different cell types [Rat hepatoma cells, human Caco2 (colonic tumour), and K562 cells] cytosolic Ft is largely degraded in the lysosomes. And that the release of iron from Ft is dependent on the degradation of Ft protein shell by lysosomal proteases (Kidane *et al,* 2006). Therefore it is well known that lysosomes contain high amounts of redox-active iron. Such iron can catalyse Fenton reactions in the presence of H_2O_2, resulting in lysosomal membrane damage and the subsequent efflux of redox-active iron and cathepsins (and other hydrolytic enzymes) into the cytoplasm (Yu *et al,* 2003 and Kurz *et al,* 2004). This efflux can lead to cell damage and ultimately cell death (either apoptotic or necrotic, depending on the magnitude of the insult). Therefore, it was decided to monitor lysosomal membrane damage in the cell model by three independent assays: (1) Neutral red uptake assay (2) Lysosensor immunofluorescence, and (3) Cathepsin B immunocytochemistry.

Overall the results clearly demonstrated that the lysosomal membranes in the parental J16 cells are very sensitive to H_2O_2 treatment, whereas in the HJ16 cells, the

lysosomal membranes were very resistant to the same treatment. In the absence of catalytically active iron neither superoxide radicals nor H_2O_2 induced any lysosomal damage by themselves, in lysosome-enriched mitochondrial fraction of a rat liver homogenate (Zdolsek and Svensson, 1993). Lysosomal rupture may occur within minutes following an oxidative stress insult, however the ultimate leakage of iron may be delayed by hours (reviewed in Kurz *et al,* 2008). In J16 cells, both DFO and hemin protected the cells from lysosomal damage (as discussed previously). This is in agreement with our previous results showing that these two compounds protected J16 cells from H_2O_2-induced necrosis. Since DFO is a hydrophilic molecule, it cannot penetrate cellular membranes very easily. It was therefore proposed that DFO is taken up predominantly via endocytosis and localises almost exclusively within the lysosomal compartment where it seems to remain and makes the iron redox-inactive (Graf *et al,* 1984 and Lloyd *et al,* 1991). Several studies have shown the DFO can protect the cells against H_2O_2-mediated oxidative damage (Doulias *et al,* 2003; Yu *et al,* 2003; Kurz *et al,* 2004). This therefore revealed (1) the importance of redox-active iron in the stability of lysosomes in oxidative stress and (2) H_2O_2 *per se* is not detrimental (reviewed in Kurz *et al,* 2008). In HJ16 cells, the scenario was quite different, interestingly DFO pre-treatment (unlike the necrosis data) had no significant protective effect when compared with cells treated with H_2O_2 alone. Hemin, on the other hand, promoted more lysosomal damage in HJ16. Ferric iron has been shown to be essential for the cell death of hepatocytes by H_2O_2 and the lysosomal pool seems to be the source of this iron (Starke *et al,* 1985). The lysosomal damage was also investigated in both cell lines after combined hemin-DFO treatment. It was shown that DFO treatment following iron loading for 18 h protected both cell lines from lysosomal damage. These results were in agreement with necrosis data using Flow cytometry, since combined hemin-DFO pre-treatment increased significantly the number of live cells.

Cathepsin B is one of the most abundant and widely expressed lysosomal cysteine proteases and is considered necessary for protein turnover in cells (Chapman *et al,* 1997). In the synovial fluid of RA, CATH B may participate in the joint destruction by the degradation of bone collagen (Hashimoto *et al,* 2001). It has been also reported that CATH B contributes to TNF-α-mediated hepatocyte apoptosis by promoting mitochondrial release of cytochrome *c*. Inhibition of CATH B is a mechanism by which NF-κB protects the cells from lysosomal-mediated apoptosis

and necrosis (Liu *et al*, 2003). The results obtained from Cathepsin B immunocytochemistry confirmed the results shown with either NR or Lysosensor assays. In J16 cells, both DFO and hemin pre-treatments protected the cells against lysosomal membrane damage induced by H_2O_2. In contrast, hemin pre-treatment in HJ16 cells significantly damaged the lysosomes following H_2O_2 exposure where DFO pre-treatment had no significant effect.

Preliminary Clinical data

A preliminary study on human and rat fibroblasts were conducted in parallel of the current study. In addition to this, LPI measurements of normal, RA and OA synovial fluid (SF) were measured.

The results revealed that both HN-1 and HOA-1 cells were resistant even to high non-physiological doses of H_2O_2. The basal LIP levels of HN-1, HRA-1, and HOA-1 were very low. Because of the higher susceptibility of HOA-1 to H_2O_2-mediated damage it was hypothesised that H_2O_2-induced levels of LIP in HOA-1 would be higher than HN-1 following treatment with an intermediate dose of H_2O_2 (i.e. 1mM). The results were in agreement with our hypothesis, since following treatment of cells with an intermediate dose of 1mM H_2O_2, the LIP levels in HOA-1 increased to a detectable level (i.e. 0.18 ± 0.06 μM/μg) while it remained at undetectable levels in HN-1. The LIP was also undetectable in HRA-1 cells.

Normal (VW-1) and AA (AAVW-1) rat fibroblasts were also treated with the same concentrations of H_2O_2 and it was quite interesting to note that AAVW-1 cells were very resistant to all the doses used while VW-1 was very sensitive to the same treatment. The basal levels of the LIP were also undetectable in VW-1 but in AAVW-1 cells it was found to be within detectable range of $0.003 \pm 1.25 \times 10^{-5}$ μM/μg. Similarly with our rat cell model, it was hypothesised that an increase in LIP will be only seen in the normal (VW-1) cells when compared to AA (AAVW-1) rat fibroblasts after H_2O_2 treatment. Following an intermediate dose of 1mM of H_2O_2, the LIP levels of VW-1 increased to the detectable levels and in AAVW-1 cells, the increase was interestingly more than 13-fold. From the above results, it seems that the increase in LIP is correlated with H_2O_2-induced cell damage. However, statistically, more clinical samples are needed to draw a proper conclusion. The culture of these synovial fibroblasts was time consuming and difficult and despite receiving appropriate number of biopsies for this thesis, we failed to keep most of

these biopsies in culture. It is therefore necessary to set up in the future new improved culture conditions to be able to provide satisfactory answers to the questions asked in this thesis.

Spectrographic studies showed that synovial fluid (SF) from patients with RA contained elevated concentrations of iron when compared with normal subjects (Niedermeier *et al,* 1962). By emission spectrometric analysis, the mean concentration of iron was higher in the SF of RA patients than normal subjects (Niedermeier and Griggs, 1971). Using a colorimetric method, plasma iron in RA and OA patients were non-significantly lower (p value > 0.05) than healthy subjects (Yazar *et al,* 2005). On the other hand, iron in the SF was significantly higher in OA patients than RA and healthy subjects. Ferritin levels were significantly higher in the SF of RA patients when compared with OA patients (Ahmadzadeh *et al,* 1990).

Labile iron (LI) was measured in the synovial fluid (SF) of normal, rheumatoid arthritic (RA), and osteoarthritic (OA) patients. Synovial fluid from a normal, two RA, and six OA patients was analysed. The results showed that there was no consistent pattern in these fluids. The LPI of the normal patient was 0.45 ± 0.3 μM, it seems to be slightly higher in RA but it was non-significant (p value > 0.05). In OA samples, some had higher value than the normal sample and others had lower values, but they were all non-significant. Clearly, more samples are needed to complement these observations and to draw a proper conclusion.

Concluding Remarks and Limitations of this study

A model of the major findings in this thesis is demonstrated in figures 4.1 and 4.2. Figure 4.1 provides a summary of the effect of H_2O_2 treatment alone or following *iron chelation* in J16 and HJ16 cells in regard to the LIP levels, lysosomal damage, the influence on Ft synthesis/decrease, and the ensuing necrotic cell death. Figure 4.2 provides a summary of the effect of H_2O_2 treatment alone or following *iron loading* in J16 and HJ16 cells in regard to the LIP levels, lysosomal damage, the influence on Ft synthesis/decrease, and the ensuing necrotic cell death. Since the Ft levels were not modulated in HJ16 cells following H_2O_2 treatment, the source of labile iron could generally be from the lysosomal damage shown in HJ16 cells.

Overall the findings of this thesis revealed that the resistance of HJ16 cells to H_2O_2 was mainly related to higher total intracellular glutathione content, higher GPx activity and lower Ft levels than J16 cells. These results strongly suggest that both antioxidants and H_2O_2-induced labile iron are modulated when cells are chronically exposed to H_2O_2. The modulation of intracellular LIP and glutathione content appears to directly influence the susceptibility of cells to H_2O_2-induced oxidative damage and necrotic cell death. These results are consistent with the conclusion that both antioxidant defence mechanisms and labile iron status are important factors to consider in oxidative injuries and in related pathological conditions such as RA. Indeed, during the progression of RA in joints, the synovial cell components notably T-cells and fibroblasts are constantly exposed to high levels of ROS that are generated during ischemia-reperfusion in response to inflammation. The chronic exposure of synovial cells to ROS should almost certainly modulate the intracellular antioxidant defence mechanism of cells; however to our knowledge, no study has investigated this phenomenon in detail. Furthermore, studies carried out by our laboratory and others (e.g. Breuer *et al,* 1997) have clearly demonstrated that acute exposure of cells to oxidising agents such as UVA or H_2O_2, promotes an increase in potentially harmful labile iron in the cells that acts to exacerbate the ongoing peroxidative cell damage, leading to necrotic cell death. However no study has explored this important phenomenon in chronic oxidative conditions such as RA. In order to gain insight into the adaptation of synovial cell components to chronic oxidative exposure in RA, it is necessary to study the behaviour of synovial fibroblast, macrophages and T-cells to both acute and chronic exposure to oxidising agents such as H_2O_2.

A. J16 cell line

In J16 cells, H_2O_2 decreases the ferritin levels and causes damage to the lysosomal membrane. This has been correlated with an increase in LIP levels and the ensuing necrotic cell death. DFO pre-treatment prior to H_2O_2 protects the lysosomal membrane and decreases the ferritin levels. This has been correlated with a decrease in the LIP levels and the ensuing cell death.

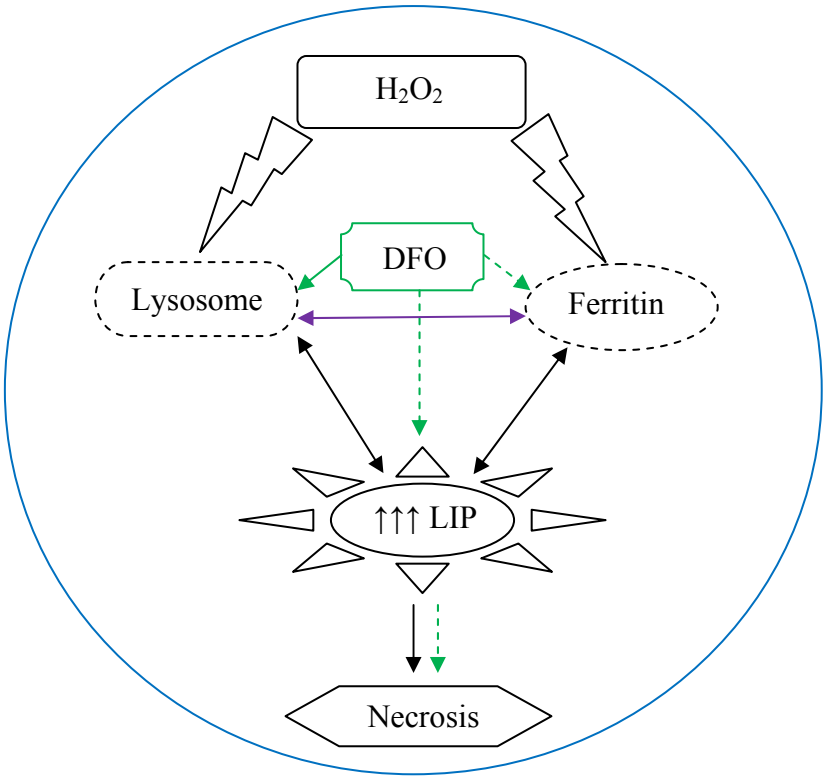

B. HJ16 cell line

In HJ16 cells, H_2O_2 does not significantly modulate the ferritin levels but causes damage to the lysosomal membrane to a lesser extent than in the J16 cells. This has been correlated with an increase in LIP levels and the ensuing necrotic cell death. DFO pre-treatment prior to H_2O_2 has no significant effect on lysosomal membrane but decreases the ferritin levels. This has been correlated with a decrease in the LIP levels and the ensuing cell death.

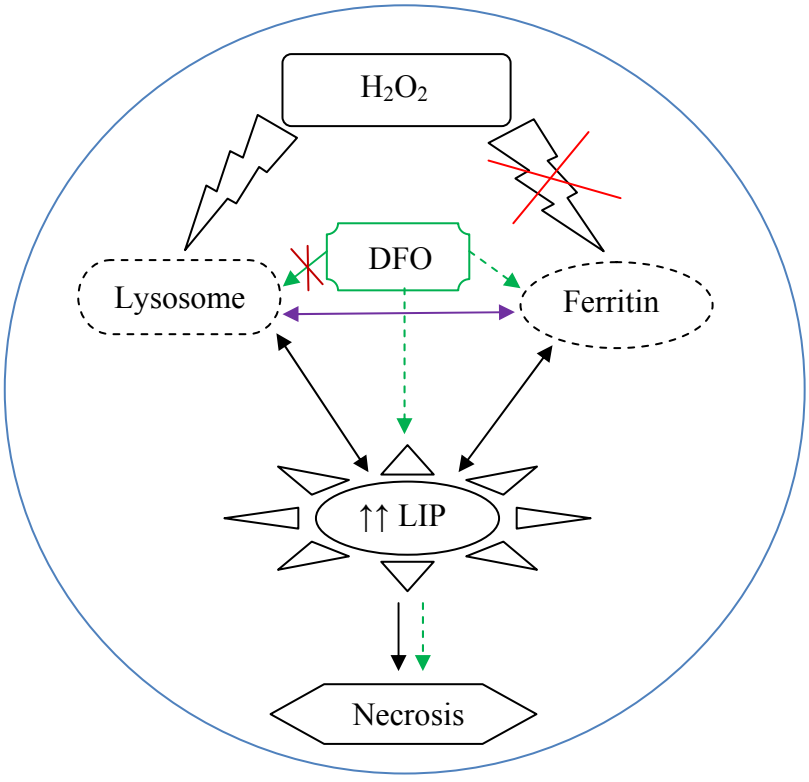

Figure 4.1 : Effect H_2O_2 alone or following iron chelation in J16 and HJ16 cells.

Protection/increase is represented by a solid line - Degradation/decrease is represented by a dashed line, and the upper arrow represents the fold increase of LIP compared with the basal levels). Lysosomes may have been implicated in the degradation of ferritin. The green colour indicates the effect of DFO pre-treatment.

A. J16 cell line

In J16 cells, H_2O_2 decreases the ferritin levels and causes damage to the lysosomal membrane. This has been correlated with an increase in LIP levels and the ensuing necrotic cell death. Hemin pre-treatment prior to H_2O_2 protects the lysosomal membrane and increases the ferritin levels. This has been correlated with a decrease in the LIP levels and the ensuing cell death.

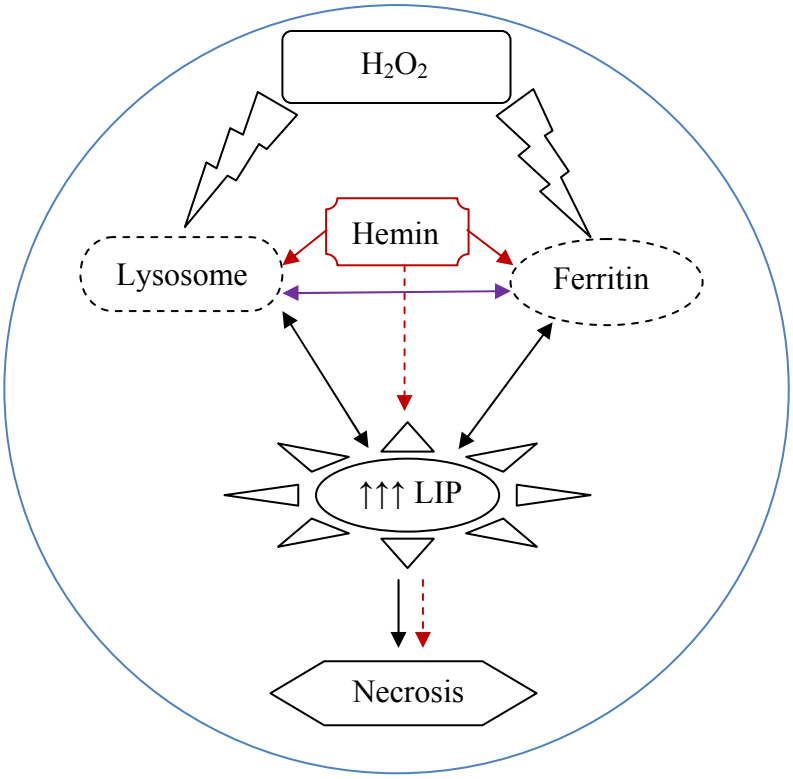

B. HJ16 cell line

In HJ16 cells, H_2O_2 does not significantly modulate the ferritin levels but causes damage to the lysosomal membrane to a lesser extent than in the J16 cells. This has been correlated with an increase in LIP levels and the ensuing necrotic cell death. Hemin pre-treatment prior to H_2O_2 increased the lysosomal membrane damage and the ferritin levels. This has been correlated with an increase in the LIP levels and the ensuing cell death.

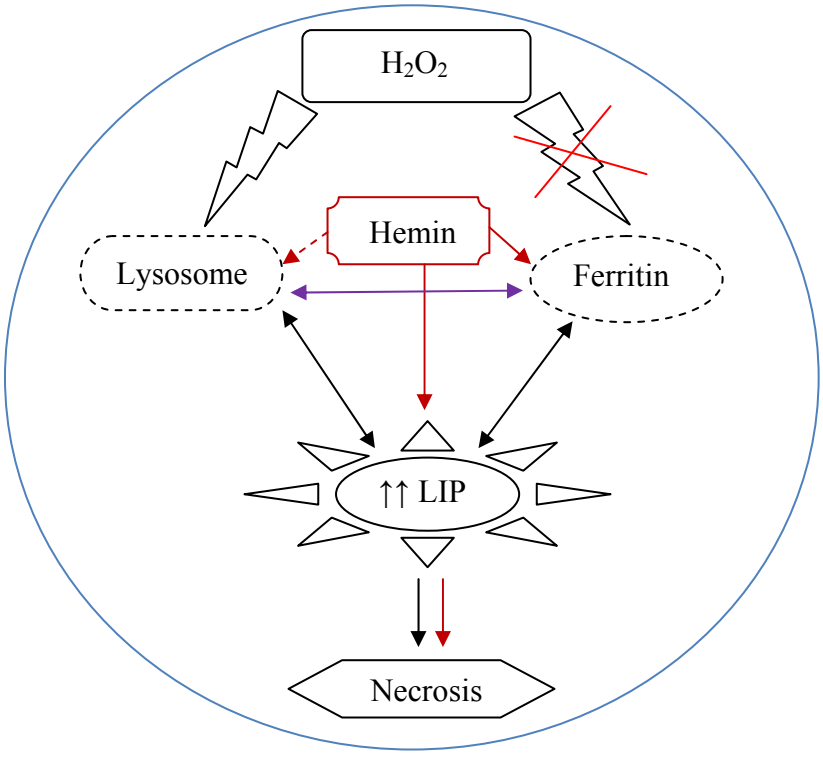

Figure 4.2 : Effect H_2O_2 alone or following iron loading in J16 and HJ16 cells.

(Protection/increase is represented by a solid line - Degradation/decrease is represented by a dashed line, and the upper arrow represents the fold increase of LIP compared with the basal levels). Lysosomes may have been implicated in the degradation of ferritin. The red colour indicates the effect of hemin pre-treatment.

Lymphocytes and macrophages are the predominant cells in chronic inflammation (Junqueira *et al,* 1986; Underwood, 1996; Stevens and Lowe, 1999). Lymphocytes are also the key components in the onset and exacerbation of autoimmune diseases and the cytokines produced by them have a great impact on disease progression (Horwood, 2008). Infiltration of numerous T-cells has been noticed in the RA synovium; T-cells represent 40% of the synovial cellular infiltrate (Ling and Miossec, 2007). Chronic inflammation occurs in an autoimmune disease (e.g. RA) in which self-antigens continually activate T-cells (Goldsby *et al,* 2003). Macrophages, fibroblasts, and T lymphocytes are three cell populations which are found abundantly in the rheumatoid arthritic synovium (Tran *et al,* 2005). T-cells can stimulate both macrophages and fibroblasts to produce more pro-inflammatory cytokines. T-cells can exert potentially pathogenic effects through their ability to modulate the functions of the surrounding cells by cell to cell contact (e.g. macrophages) or through the release of soluble factors (e.g. IL-17 on fibroblasts). Indeed, activated synovial T cells are key initiators and orchestrators of inflammation in RA, and therefore they represent key cellular targets for therapy (Cope *et al,* 2007).

Several studies have attempted to isolate synovial T-cells and macrophages to study e.g. the role of NFκB in rheumatoid arthritis conditions, but these cells have a short half-life in laboratory-based cell culture conditions and as a result can not be used for in-depth long term studies. Furthermore the isolation of these cells in RA is subject to patient to patient differences and most importantly in such studies the lack of a 'proper control' should severely hamper the interpretation of the data obtained. The use of Jurkat parental T-cells (i.e. J16 cell line) in the present study provided us with such 'proper control' for the effects seen in its H_2O_2-adapted counterpart (i.e. HJ16 cell line). Jurkat cells are widely used in the study of T-cell activation processes (Schreck *et al,* 1991) as these cells are considered as critical determinants of the extent and chronicity of an inflammatory response. Furthermore Jurkat T-cells are particularly vulnerable to oxidative stress and therefore could illustrate clearly the nature of oxidative damage in cells upon acute exposure to oxidative stress. On the other hand, the H_2O_2-adapted cell line provides a precious tool to undertake an in-depth long term comparative study in terms of adaptation of T-cells to chronic exposure. Unpublished data from N.D Hall's laboratory (Department of Pharmacy and Pharmacology, University of Bath) have shown that HJ16 cells have characteristics similar to those of rheumatoid synovial T cells. These characteristics

include low CD3 levels, elevated CD69 expression, increased intracellular glutathione levels, and enhanced resistance to apoptosis. They have also noticed that HJ16 cells can stimulate monocytes to secrete pro-inflammatory cytokines (i.e. IL-1β). Although Jurkat cells are not the same as T-cells (otherwise they would not be immortal) in regard to the biochemistry, they are compromised in the study of T-cell function. HJ16 cells were derived by treating the J16 cell line with increasing concentration of H_2O_2 (i.e. from 0.1 mM to 3 mM) at weekly to fortnightly intervals. After each treatment the surviving cells were allowed to recover normal growth characteristics before further exposure to a higher concentration of H_2O_2. Although they were resistant up to a dose of 3mM H_2O_2, at 0.1 mM around 30 % of the cells were dead. The reason may be that the HJ16 cell line is a polyclonal cell line and therefore within its population, it will still contain some fraction of cells with higher susceptibility to H_2O_2 doses used.

The outcome of this study was intended to be checked in synovial fibroblasts obtained from OA and RA patients, so that the study could verify a series of parameters such as the level of antioxidant systems and the labile iron status as well as their level of resistance to H_2O_2 doses applied. As it can be seen in section 3.5, we encountered serious problems in maintaining the synovial fibroblast biopsies in culture and therefore the study lacked a proper end-point for a direct link between the effects observed in the Jurkat cell model and RA/OA cell components. Nevertheless, although our clinical samples were not studied extensively, it appears that synovial fibroblasts were very resistant to H_2O_2 and that iron is implicated in their resistance. Since synovial fibroblasts are the major source of proteases involved in tissue damage in RA, it is expected that an alteration in iron homeostasis would occur and that the potential relevance of iron chelation would be beneficial. The present thesis brings a new dimension to the role of iron in rheumatoid arthritis.

Our results raise the hypothesis that cells chronically exposed to oxidative stress as anticipated in the RA environment can withstand high and continuous levels of free radicals due to the modulation of both the antioxidants and the oxidative stress-induced iron release. It could be predicted that the high iron concentration shown in RA in the cells or in the synovial fluid arises found from the lysosomal membrane damage, and/or degradation of Ft, and/or mitochondrial damage, and/or nuclear damage occurring subsequent to the oxidative stress. However, more

investigations are needed to complement the observations revealed in the Jurkat T cell lines (i.e. J16 and HJ16 cell lines) and to draw a proper conclusion.

Further Directions

The present study provided a potential link between iron, lysosomal-membrane damage and the ensuing necrotic cell death that will almost certainly help to understand their role in progression of iron- related chronic inflammatory disorders such as RA. However it is clear that more in depth investigations are required to unravel the role of Ft in chronic oxidative stress/ inflammatory conditions. Metabolic labelling of Ft and immunoprecipitation with a pulse chase experiment would be very useful in knowing if there was a difference in the half-life of Ft and if there was any difference in its processing in both cell lines. Mitochondrial iron and ferritin would be an important area to look into as Mt-Ft has the potential of being an iron regulator in the cell and to protect the mitochondria from iron-induced damage. Preliminary findings indicate the cells overexpressing Mt-Ft (i.e. HJ16 cells) are more resistant to oxidative damage induced by H_2O_2, but obviously additional studies are required. It would be useful to measure the lysosomal proteases and to use their inhibitors and the lysosomal-membrane stabilisation compounds. Although this study has been useful to unravel some of the mechanisms and factors that might have lead to the resistance of HJ16 cells, more investigations are required: for example, to examine the TfR levels by Western blotting, ferroportin levels, human poly (rC)-binding protein (PCBP1), and the IRP/IRE system in our cell model. It will be important to look at the activity of the ferroxidase site in the H-Ft. This will hopefully lead to a better understanding of the high LIP levels measured after iron loading in HJ16 especially after the study of the radiolabel incorporation of iron. In addition to this, the effect of acute (i.e. 1-2 h) iron loading prior to oxidative stress would be an important area to explore. In the process of this study, iron loading was achieved by using haem iron since it is the most physiological source of iron, however it would be interesting to examine the effects of other sources of iron such as ferric chloride to increase lysosomal iron or ferric ammonium citrate to increase extracellular iron. The use of HO-1 and HO-2 siRNA could also provide more clues as to the role of HO in these cell lines. Moreover, the role of iron in NFκB activation should be interesting to investigate. The role of thioredoxin is ill-defined in our system and it is important in

the future to investigate the role of this key molecule in redox regulation of genes and its role in iron metabolism.

To mimic an inflammatory environment it is necessary i.e. to combine the H_2O_2 treatment with cytokines (e.g. IL-1β and TNF-α) in our cell model so that the effects mimic closely the *in vivo* condition. Measurements of cytokines in these cell lines after relevant treatments would be an interesting area to explore. A completion of the *in vitro* studies is also essential with the human and rat samples to further characterise them in respect to the current findings in our cell lines. It would be also beneficial to harvest and study lymphocytes from RA patients and compare the results obtained from this study. The culture of these synovial fibroblasts from patients were time consuming and difficult and despite receiving appropriate number of biopsies for this thesis, we failed to keep most of these biopsies in culture. It is therefore necessary to set up in the future new improved culture conditions to be able to prevent the contamination of the biopsies and cells. This will hopefully increase our understanding of what is occurring in RA cells.

REFERENCES

Abboud S, Haile DJ (2000) A novel mammalian iron-regulated protein involved in intracellular iron metabolism. *Journal of Biological Chemistry* **275,** 19906-19912.

Agrawal R, Sharma PK, Rao GS (2001) Release of iron from ferritin by metabolites of benzene and superoxide radical generating agents. *Toxicology* **168,** 223-230.

Ahmadzadeh N, Shingu M, Nobunaga M, Yasuda M (1990) Correlation of Metal-Binding Proteins and Proteinase-Inhibitors with Immunological Parameters in Rheumatoid Synovial-Fluids. *Clinical and Experimental Rheumatology* **8,** 547-551.

Ahmed KM, Li JJ (2008) NF-kappa B-mediated adaptive resistance to ionizing radiation. *Free Radical Biology and Medicine* **44,** 1-13.

Aisen P, Listowsky I (1980) Iron Transport and Storage Proteins. *Annual Review of Biochemistry* **49,** 357-393.

Aisen P, Wessling-Resnick M, Leibold EA (1999) Iron metabolism. *Current Opinion in Chemical Biology* **3,** 200-206.

Al-Qenaei A (2004) Redox Regulation of NF-kB in T-cell lines.Master of Philosophy, University of Bath - Department of Pharmacy and Pharmacology.

Alberts B, Johnson A, Lewis J, Raff M, Roberts K, Walter P (2002) 'Molecular Biology of the Cell.' (Garland Science: New York, USA)

Altindag O, Karakoc M, Kocyigit A, Celik H, Soran N (2007) Increased DNA damage and oxidative stress in patients with rheumatoid arthritis. *Clinical Biochemistry* **40,** 167-171.

Alvarezhernandez X, Liceaga J, Mckay IC, Brock JH (1989) Induction of Hypoferremia and Modulation of Macrophage Iron-Metabolism by Tumor Necrosis Factor. *Laboratory Investigation* **61,** 319-322.

Anderson AJ (1970) Lysosomal Enzyme Activity in Rats with Adjuvant-Induced Arthritis. *Annals of the rheumatic diseases* **29** (3)**,** 307-313.

Anderson GJ, Frazer DM, Wilkins SJ, Becker EM, Millard KN, Murphy TL, Mckie AT, Vulpe CD (2002) Relationship between intestinal iron-transporter expression, hepatic hepcidin levels and the control of iron absorption. *Biochemical Society Transactions* **30,** 724-726.

Anderson RGW, Orci L (1988) A View of Acidic Intracellular Compartments. *Journal of Cell Biology* **106,** 539-543.

Andrews FJ, Morris CJ, Kondratowicz G, Blake DR (1987[a]) Effect of Iron Chelation on Inflammatory Joint Disease. *Annals of the rheumatic diseases* **46,** 327-333.

Andrews FJ, Morris CJ, Lewis EJ, Blake DR (1987[b]) Effect of Nutritional Iron-Deficiency on Acute and Chronic Inflammation. *Annals of the rheumatic diseases* **46,** 859-865.

Andrews NC (2000) Iron metabolism: Iron deficiency and iron overload. *Annual Review of Genomics and Human Genetics* **1,** 75-98.

Andrews NC (2004) Probing the iron pool. Focus on " Detection of intracellular iron by its regulatory effect". *American Journal of Physiology-Cell Physiology* **287,** C1537-C1538.

Andrews NC (2005) Molecular control of iron metabolism. *Best Practice & Research Clinical Haematology* **18,** 159-169.

Andriopoulos B, Hegedusch S, Mangin J, Riedel HD, Hebling U, Wang J, Pantopoulos K, Mueller S (2007) Sustained hydrogen peroxide induces iron uptake by transferrin receptor-1 independent of the iron regulatory protein/iron-responsive element network. *Journal of Biological Chemistry* **282,** 20301-20308.

Antunes F, Cadenas E (2000) Estimation of H2O2 gradients across biomembranes. *Febs Letters* **475,** 121-126.

Antunes F, Cadenas E, Brunk UT (2001) Apoptosis induced by exposure to a low steady-state concentration of H2O2 is a consequence of lysosomal rupture. *Biochemical Journal* **356,** 549-555.

Applegate LA, Lautier D, Frenk E, Tyrrell RM (1992) Endogenous Glutathione Levels Modulate the Frequency of Both Spontaneous and Long Wavelength Ultraviolet Induced Mutations in Human-Cells. *Carcinogenesis* **13,** 1557-1560.

Applegate LA, Noel A, Vile G, Frenk E, Tyrrell RM (1995) 2 Genes Contribute to Different Extents to the Heme Oxygenase Enzyme-Activity Measured in Cultured Human Skin Fibroblasts and Keratinocytes - Implications for Protection Against Oxidant Stress. *Photochemistry and Photobiology* **61,** 285-291.

Applegate LA, Scaletta C, Panizzon R, Frenk E (1998) Evidence that ferritin is UV inducible in human skin: Part of a putative defense mechanism. *Journal of Investigative Dermatology* **111,** 159-163.

Arosio P, Levi S (2002) Ferritin, iron homeostasis, and oxidative damage. *Free Radical Biology and Medicine* **33,** 457-463.

Arredondo M, Nunez M (2005) Iron and copper metabolism. *Molecular aspects of medicine* **26,** 313-327.

Arrigo AP (1999) Gene expression and the thiol redox state. *Free Radical Biology and Medicine* **27,** 936-944.

Asahara H, Asanuma M, Ogawa N, Nishibayashi S, Inoue H (1995) High DNA-binding activity of transcription factor NF-kappa B in synovial membranes of patients with rheumatoid arthritis. *Biochemistry and Molecular Biology International* **37,** 827-832.

Atorino L, Silvestri L, Koppen M, Cassina L, Ballabio A, Marconi R, Langer T, Casari G (2003) Loss of m-AAA protease in mitochondria causes complex I deficiency and increased sensitivity to oxidative stress in hereditary spastic paraplegia. *Journal of Cell Biology* **163,** 777-787.

Aya K, Alhawagri M, Hagen-Stapleton A, Kitaura H, Kanagawa O, Novack DV (2005) NF-kappa B-inducing kinase controls lymphocyte and osteoclast activities in inflammatory arthritis. *Journal of Clinical Investigation* **115,** 1848-1854.

Baeuerle PA, Henkel T (1994) Function Amd Activation of Nf-Kappa-B in the Immune-System. *Annual Review of Immunology* **12,** 141-179.

Baldwin AS (2001) The transcription factor NF-kappa B and human disease. *Journal of Clinical Investigation* **107,** 3-6.

Balla G, Jacob HS, Balla J, Rosenberg M, Nath K, Apple F, Eaton JW, Vercellotti GM (1992) Ferritin - A Cytoprotective Antioxidant Strategem of Endothelium. *Journal of Biological Chemistry* **267,** 18148-18153.

Balla J, Jacob HS, Balla G, Nath K, Eaton JW, Vercellotti GM (1993) Endothelial-Cell Heme Uptake from Heme-Proteins - Induction of Sensitization and Desensitization to Oxidant Damage. *Proceedings of the National Academy of Sciences of the United States of America* **90,** 9285-9289.

Basu-Modak S, Ali D, Gordon M, Polte T, Yiakouvaki A, Pourzand C, Rice-evans C, Tyrrell RM (2006) Suppression of UVA-mediated release of labile iron by epicatechin - A link to lysosomal protection. *Free Radical Biology and Medicine* **41,** 1197-1204.

Beaumont C, Leneuve P, Devaux I, Scoazec JY, Berthier M, Loiseau MN, Grandchamp B, Bonneau D (1995) Mutation in the Iron-Responsive Element of the L-Ferritin Messenger-Rna in A Family with Dominant Hyperferritinemia and Cataract. *Nature Genetics* **11,** 444-446.

Berridge M, Tan A, McCoy K, Wang R (1996) The biochemical and cellular basis of cell proliferation assay that use tetrazolium salts. *Biochemica* **4,** 14-19.

Biemond P, Swaak AJG, Koster JF (1984) Protective Factors Against Oxygen Free-Radicals and Hydrogen-Peroxide in Rheumatoid-Arthritis Synovial-Fluid. *Arthritis and rheumatism* **27,** 760-765.

Bissett DL, Chatterjee R, Hannon DP (1991) Chronic Ultraviolet Radiation-Induced Increase in Skin Iron and the Photoprotective Effect of Topically Applied Iron Chelators. *Photochemistry and Photobiology* **54,** 215-223.

Blake DR, Hall ND, Bacon PA, Dieppe PA, Halliwell B, Gutteridge JMC (1981) The Importance of Iron in Rheumatoid Disease. *Lancet* **2,** 1142-1144.

Blake DR, Hall ND, Bacon PA, Dieppe PA, Halliwell B, Gutteridge JMC (1983) Effect of A Specific Iron Chelating Agent on Animal-Models of Inflammation. *Annals of the rheumatic diseases* **42,** 89-93.

Blake DR, Lunec J, Ahern M, Ring EFJ, Bradfield J, Gutteridge JMC (1985) Effect of Intravenous Iron Dextran on Rheumatoid Synovitis. *Annals of the rheumatic diseases* **44,** 183-188.

Bondeson J, Foxwell B, Brennan F, Feldmann M (1999) Defining therapeutic targets by using adenovirus: Blocking NF-kappa B inhibits both inflammatory and destructive mechanisms in rheumatoid synovium but spares anti-inflammatory mediators. *Proceedings of the National Academy of Sciences of the United States of America* **96,** 5668-5673.

Bonizzi G, Karin M (2004) The two NF-kappa B activation pathways and their role in innate and adaptive immunity. *Trends in Immunology* **25,** 280-288.

Bonta I, Bray MA, Parnham MJ (1985) Handbook of Inflammation. In 'The Pharmacology of Inflammation'. (Ed. Elsevier Science Publishers B.V.) pp. 27-43.

Bou-Abdallah F, Santambrogio P, Levi S, Arosio P, Chasteen ND (2005) Unique iron binding and oxidation properties of human mitochondrial ferritin: A comparative analysis with human H-chain ferritin. *Journal of Molecular Biology* **347,** 543-554.

Bowie A, O'Neill LAJ (2000) Oxidative stress and nuclear factor-kappa B activation - A reassessment of the evidence in the light of recent discoveries. *Biochemical Pharmacology* **59,** 13-23.

Bradford MM (1976) Rapid and Sensitive Method for Quantitation of Microgram Quantities of Protein Utilizing Principle of Protein-Dye Binding. *Analytical Biochemistry* **72,** 248-254.

Brambilla L, Cairo G, Sestili P, ODonnel V, Azzi A, Cantoni O (1997) Mitochondrial respiratory chain deficiency leads to overexpression of antioxidant enzymes. *Febs Letters* **418,** 247-250.

Breuer W, Greenberg E, Cabantchik ZI (1997) Newly delivered transferrin iron and oxidative cell injury. *Febs Letters* **403,** 213-219.

Brock J, Alvarez-Hernandez X (1989) Modulation of macrophage iron metabolism by tumour necrosis factor and interleukin 1. *FEMS microbiology immunology* **47,** 309-310.

Brunk UT, Zhang H, Dalen H, Ollinger K (1995[a]) Exposure of Cells to Nonlethal Concentrations of Hydrogen-Peroxide Induces Degeneration-Repair Mechanisms Involving Lysosomal Destabilization. *Free Radical Biology and Medicine* **19,** 813-822.

Brunk UT, Zhang H, Roberg K, Ollinger K (1995[b]) Lethal Hydrogen-Peroxide Toxicity Involves Lysosomal Iron-Catalyzed Reactions with Membrane Damage. *Redox Report* **1,** 267-277.

Brunk UT, Dalen H, Roberg K, Hellquist HB (1997) Photo-oxidative disruption of lysosomal membranes causes apoptosis of cultured human fibroblasts. *Free Radical Biology and Medicine* **23,** 616-626.

Butkiene B, Mieliauskaite D, Serapinas P, Aninkevicius V, Juzikiene V, Stropuviene S, Zabulyte D (2007) Oxidant/antioxidant status and trace elements level in blood of patients suffering from rheumatoid arthritis. *Trace Elements and Electrolytes* **24,** 97-102.

Byun MS, Jeon KI, Choi JW, Shim JY, Jue DM (2002) Dual effect of oxidative stress on NF-kappa B activation in HeLa cells. *Experimental and Molecular Medicine* **34,** 332-339.

Cabantchik ZI, Breuer W, Zanninelli G, Cianciulli R (2005) LPI-labile plasma iron in iron overload. *Best Practice & Research Clinical Haematology* **18,** 277-287.

Cable H, Lloyd JB (1999) Cellular uptake and release of two contrasting iron chelators. *Journal of Pharmacy and Pharmacology* **51,** 131-134.

Cadogan J (1973) 'Principles of free radical chemistry.' (Royal Society of Chemistry: London, UK)

Cairo G, Bardella L, Schiaffonati L, Arosio P, Levi S, Bernellizazzera A (1985) Multiple Mechanisms of Iron-Induced Ferritin Synthesis in Hela-Cells. *Biochemical and Biophysical Research Communications* **133,** 314-321.

Cairo G, Tacchini L, Pogliaghi G, Anzon E, Tomasi A, Bernellizazzera A (1995) Induction of Ferritin Synthesis by Oxidative Stress - Transcriptional and Posttranscriptional Regulation by Expansion of the Free Iron Pool. *Journal of Biological Chemistry* **270,** 700-703.

Cairo G, Castrusini E, Minotti G, Bernellizazzera A (1996) Superoxide and hydrogen peroxide-dependent inhibition of iron regulatory protein activity: A protective stratagem against oxidative injury. *Faseb Journal* **10,** 1326-1335.

Cairo G, Tacchini L, Recalcati S, Azzimonti B, Minotti G, Bernelli-Zazzera A (1998) Effect of reactive oxygen species on iron regulatory protein activity. *Annals of the New York Academy of Sciences* **30,** 179-86.

Cairo G, Pietrangelo A (2000) Iron regulatory proteins in pathobiology. *The Biochemical journal* **352,** 241-250.

Cairo G, Recalcati S, Pietrangelo A, Minotti G (2002) The iron regulatory proteins: Targets and modulators of free radical reactions and oxidative damage. *Free Radical Biology and Medicine* **32,** 1237-1243.

Cairo G, Bernuzzi F, Recalcati S (2006) A precious metal: Iron, an essential nutrient for all cells. *Genes & Nutrition* **1,** 25-40.

Cazzola M, Bergamaschi G, Dezza L, Arosio P (1990) Manipulations of Cellular Iron-Metabolism for Modulating Normal and Malignant-Cell Proliferation - Achievements and Prospects. *Blood* **75,** 1903-1919.

Chapman HA, Riese RJ, Shi GP (1997) Emerging roles for cysteine proteases in human biology. *Annual Review of Physiology* **59,** 63-88.

Cheeseman KH, Slater TF (1993) An Introduction to Free-Radical Biochemistry. *British Medical Bulletin* **49,** 481-493.

Chen ZJ, Hagler J, Palombella VJ, Melandri F, Scherer D, Ballard D, Maniatis T (1995) Signal-Induced Site-Specific Phosphorylation Targets I-Kappa-B-Alpha to the Ubiquitin-Proteasome Pathway. *Genes & Development* **9,** 1586-1597.

Choi BM, Pae HO, Jeong YR, Oh GS, Jun CD, Kim BR, Kim YM, Chung HT (2004) Overexpression of heme oxygenase (HO)-1 renders Jurkat T cells resistant to Fas-mediated apoptosis: Involvement of iron released by HO-1. *Free Radical Biology and Medicine* **36,** 858-871.

Christodoulou C, Choy EH (2006) Joint inflammation and cytokine inhibition in rheumatoid arthritis. *Clinical and Experimental Medicine* **6,** 13-19.

Ciechanover A (2005) Proteolysis: from the lysosome to ubiquitin and the proteasome. *Nature Reviews Molecular Cell Biology* **6,** 79-86.

Cope A (2002) Studies of T-cell activation in chronic inflammation. *Arthritis research* **4,** S197-S211.

Cope AP, Schulze-Koops H, Aringer M (2007) The central role of T cells in rheumatoid arthritis. *Clinical and Experimental Rheumatology* **25,** S4-S11.

Corna G, Santambrogio P, Minotti G, Cairo G (2004) Doxorubicin paradoxically protects cardiomyocytes against iron-mediated toxicity - Role of reactive oxygen species and ferritin. *Journal of Biological Chemistry* **279,** 13738-13745.

Cozzi A, Corsi B, Levi S, Santambrogio P, Albertini A, Arosio P (2000) Overexpression of wild type and mutated human ferritin H-chain in HeLa cells - In vivo role of ferritin ferroxidase activity. *Journal of Biological Chemistry* **275,** 25122-25129.

Cuervo AM, Hu W, Lim B, Dice JF (1998) I kappa B is a substrate for a selective pathway of lysosomal proteolysis. *Molecular Biology of the Cell* **9,** 1995-2010.

Currey HL, Ziff M (1968) Suppression of adjuvant disease in the rat by heterologous antilymphocyte globulin. *J.Exp.Med* **127,** 185-203.

Cuzzocrea S, Thiemermann C, Salvemini D (2004) Potential Therapeutic Effect of Antioxidant Therapy in Shock and Inflammation. *Current Medicinal Chemistry* **11,** 1147-1162.

Darbari D, Loyevsky M, Gordeuk V, Kark JA, Castro O, Rana S, Apprey V, Kurantsin-Mills J (2003) Fluorescence measurements of the labile iron pool of sikle erythrocytes. *Blood* **102,** 357-364.

Dayani PN, Bishop MC, Black K, Zeltzer PM (2004) Desferoxamine (DFO) - mediated iron chelation: rationale for a novel approach to therapy for brain cancer. *Journal of Neuro-Oncology* **67,** 367-377.

De Domenico I, Vaughn MB, Li LT, Bagley D, Musci G, Ward DM, Kaplan J (2006) Ferroportin-mediated mobilization of ferritin iron precedes ferritin degradation by the proteasome. *Embo Journal* **25,** 5396-5404.

De DC, Wattiaux R (1966) Functions of lysosomes. *Annu.Rev.Physiol* **28,** 435-492.

Deng GM, Lenardo M (2006) The role of immune cells and cytokines in the pathogenesis of rheumatoid arthritis. *Drug Discovery Today Disease Mechanisms* **3,** 163-168.

Dethmers JK, Meister A (1981) Glutathione export by human lymphoid cells: depletion of glutathione by inhibition of its synthesis decreases export and increases sensitivity to irradiation. *Proc.Natl.Acad.Sci.U.S.A* **78,** 7492-7496.

Di Rosa M, Giroud J, Willoughby D (1971) Studies on the mediators of the acute inflammatory response induced in rats in different sites by carrageenan and turpentine. *The Journal of pathology* **104,** 15-29.

DiDonato J, Mercurio F, Rosette C, Wuli J, Suyang H, Ghosh S, Karin M (1996) Mapping of the inducible I kappa B phosphorylation sites that signal its ubiquitination and degradation. *Molecular and Cellular Biology* **16,** 1295-1304.

DiDonato JA, Hayakawa M, Rothwarf DM, Zandi E, Karin M (1997) A cytokine-responsive I kappa B kinase that activates the transcription factor NF-kappa B. *Nature* **388,** 548-554.

Ding YY, Zhang YZ, Furuyama K, Ogawa K, Igarashi K, Shibahara S (2006) Down-regulation of heme oxygenase-2 is associated with the increased expression of heme oxygenase-1 in human cell lines. *Febs Journal* **273,** 5333-5346.

Doan T, Massarotti E (2005) Rheumatoid arthritis: An overview of new and emerging therapies. *Journal of Clinical Pharmacology* **45,** 751-762.

Donovan A, Brownlie A, Zhou Y, Shepard J, Pratt SJ, Moynihan J, Paw BH, Drejer A, Barut B, Zapata A, Law TC, Brugnara C, Kingsley PD, Palis J, Fleming MD, Andrews NC, Zon LI (2000) Positional cloning of zebrafish ferroportin1 identifies a conserved vertebrate iron exporter. *Nature* **403,** 776-781.

Donovan A, Andrews NC (2004) The molecular regulation of iron metabolism. *The hematology journal* **5,** 373-380.

Doulias PT, Christoforidis S, Brunk UT, Galaris D (2003) Endosomal and lysosomal effects of desferrioxamine: Protection of HeLa cells from hydrogen peroxide-induced DNA damage and induction of cell-cycle arrest. *Free Radical Biology and Medicine* **35,** 719-728.

Doyle A, Griffiths JB (1998) 'Cell and Tissue Culture Laboratory Procedures in Biotechnology.' (John Wiley and Sons Ltd.: Chichester)

Droge W, Schulze-Osthoff K, Mihm S, Galter D, Schenk H, Eck HP, Roth S, Gmunder H (1994) Functions of glutathione and glutathione disulfide in immunology and immunopathology. *FASEB J.* **8,** 1131-1138.

Duarte TL, Jones GDD (2007) Vitamin C modulation of H2O2-induced damage and iron homeostasis in human cells. *Free Radical Biology and Medicine* **43,** 1165-1175.

Dunn LL, Rahmanto YS, Richardson DR (2007) Iron uptake and metabolism in the new millennium. *Trends in Cell Biology* **17,** 93-100.

Eisenstein RS (2000) Iron regulatory proteins and the molecular control of mammalian iron metabolism. *Annual Review of Nutrition* **20,** 627-662.

Ellis L, Gilston V, Soo CCY, Morris CJ, Kidd BL, Winyard PG (2000) Activation of the transcription factor NF-kappa B in the rat air pouch model of inflammation. *Annals of the rheumatic diseases* **59,** 303-307.

Epinat JC, Gilmore TD (1999) Diverse agents act at multiple levels to inhibit the Rel/NF-kappa B signal transduction pathway. *Oncogene* **18,** 6896-6909.

Epsztejn S, Kakhlon O, Glickstein H, Breuer W, Cabantchik ZI (1997) Fluorescence analysis of the labile iron pool of mammalian cells. *Analytical Biochemistry* **248,** 31-40.

Epsztejn S, Glickstein H, Picard V, Slotki IN, Breuer W, Beaumont C, Cabantchik ZI (1999) H-ferritin subunit overexpression in erythroid cells reduces the oxidative stress response and induces multidrug resistance properties. *Blood* **94,** 3593-3603.

Erdal H, Berndtsson M, Castro J, Brunk U, Shoshan MC, Linder S (2005) Induction of lysosomal membrane permeabilization by compounds that activate p53-independent apoptosis. *Proceedings of the National Academy of Sciences of the United States of America* **102,** 192-197.

Esposito BP, Breuer W, Sirankapracha P, Pootrakul P, Hershko C, Cabantchik ZI (2003) Labile plasma iron in iron overload: redox activity and susceptibility to chelation. *Blood* **102,** 2670-2677.

Ewing JF, Maines MD (1991) Rapid Induction of Heme Oxygenase-1 Messenger-Rna and Protein by Hyperthermia in Rat-Brain - Heme Oxygenase-2 Is Not A Heat-Shock Protein. *Proceedings of the National Academy of Sciences of the United States of America* **88,** 5364-5368.

Fadok VA, Voelker DR, Campbell PA, Cohen JJ, Bratton DL, Henson PM (1992) Exposure of Phosphatidylserine on the Surface of Apoptotic Lymphocytes Triggers Specific Recognition and Removal by Macrophages. *Journal of Immunology* **148,** 2207-2216.

Feghali C, Wright T (1997) Cytokines in acute and chronic inflammation. *Frontiers in bioscience* **2,** 12-26.

Feldmann M, Andreakos E, Smith C, Bondeson J, Yoshimura S, Kiriakidis S, Monaco C, Gasparini C, Sacre S, Lundberg A, Paleolog E, Horwood NJ, Brennan FM, Foxwell BMJ (2002) Is NF-kappa B a useful therapeutic target in rheumatoid arthritis? *Annals of the rheumatic diseases* **61,** 13-18.

Ferris CD, Jaffrey SR, Sawa A, Takahashi M, Brady SD, Barrow RK, Tysoe SA, Wolosker H, Baranano DE, Dore S, Poss KD, Snyder SH (1999) Haem oxygenase-1 prevents cell death by regulating cellular iron. *Nature Cell Biology* **1,** 152-157.

Filomeni G, Aquilano K, Rotilio G, Ciriolo MR (2005) Antiapoptotic response to induced GSH depletion: Involvement of heat shock proteins and NF-kappa B activation. *Antioxidants & Redox Signaling* **7,** 446-455.

Finkel T (2003) Oxidant signals and oxidative stress. *Current Opinion in Cell Biology* **15,** 247-254.

Ganz T (2003) Hepcidin, a key regulator of iron metabolism and mediator of anemia of inflammation. *Blood* **102,** 783-788.

Ganz T (2005) Hepcidin - a regulator of intestinal iron absorption and iron recycling by macrophages. *Best Practice & Research Clinical Haematology* **18,** 171-182.

Ganz T, Nemeth E (2006) Regulation of iron acquisition and iron distribution in mammals. *Biochimica et Biophysica Acta-Molecular Cell Research* **1763,** 690-699.

Ganz T (2007) Molecular control of iron transport. *Journal of the American Society of Nephrology* **18,** 394-400.

Garner B, Roberg K, Brunk UT (1998) Endogenous ferritin protects cells with iron-laden lysosomes against oxidative stress. *Free Radical Research* **29,** 103-114.

Gehring NH, Hentze MW, Pantopoulos K (1999) Inactivation of both RNA binding and aconitase activities of iron regulatory protein-1 by quinone-induced oxidative stress. *Journal of Biological Chemistry* **274,** 6219-6225.

Gerlag DM, Ransone L, Tak PP, Han ZN, Palanki M, Barbosa MS, Boyle D, Manning AM, Firestein GS (2000) The effect of a T cell-specific NF-kappa B inhibitor on in vitro cytokine production and collagen-induced arthritis. *Journal of Immunology* **165,** 1652-1658.

Ghosh S, Karin M (2002) Missing pieces in the NF-kappa B puzzle. *Cell* **109,** S81-S96.

Gilston V, Williams MA, Newland AC, Winyard PG (2001) Hydrogen peroxide and tumour necrosis factor-alpha induce NF-kappa B-DNA binding in primary human T lymphocytes in addition to T cell lines. *Free Radical Research* **35,** 681-691.

Ginn-Pease ME, Whisler RL (1998) Redox signals and NF-kappa B activation in T cells. *Free Radical Biology and Medicine* **25,** 346-361.

Girelli D, Corrocher R, Bisceglia L, Olivieri O, Defranceschi L, Zelante L, Gasparini P (1995) Molecular-Basis for the Recently Described Hereditary Hyperferritinemia Cataract Syndrome - A Mutation in the Iron-Responsive Element of Ferritin L-Subunit Gene (the Verona Mutation). *Blood* **86,** 4050-4053.

Glickstein H, Ben El R, Shvartsman M, Cabantchik ZI (2005) Intracellular labile iron pools as direct targets of iron chelators: a fluorescence study of chelator action in living cells. *Blood* **106,** 3242-3250.

Goldsby R, Kindt T, Osborne B, Kuby J (2003) 'Immunology.' (W. H. Freeman and Company: New York)

Goodson T, Morgan SL, Carlee JR, Baggott JE (2003) The energy cost of adjuvant-induced arthritis in rats. *Arthritis and rheumatism* **48,** 2979-2982.

Graf E, Mahoney JR, Bryant RG, Eaton JW (1984) Iron-Catalyzed Hydroxyl Radical Formation - Stringent Requirement for Free Iron Coordination Site. *Journal of Biological Chemistry* **259,** 3620-3624.

Griffith OW (1980) Determination of Glutathione and Glutathione Disulfide Using Glutathione-Reductase and 2-Vinylpyridine. *Analytical Biochemistry* **106,** 207-212.

Guillen C, McInnes IB, Kruger H, Brock JH (1998) Iron, lactoferrin and iron regulatory protein activity in the synovium; relative importance of iron loading and the inflammatory response. *Annals of the rheumatic diseases* **57,** 309-314.

Habens F, Srinivasan N, Oakley F, Mann DA, Ganesan A, Packham G (2005) Novel sulfasalazine analogues with enhanced NF-kB inhibitory and apoptosis promoting activity. *Apoptosis* **10,** 481-491.

Halliwell B, Gutteridge JMC (1986) Oxygen Free-Radicals and Iron in Relation to Biology and Medicine - Some Problems and Concepts. *Archives of Biochemistry and Biophysics* **246,** 501-514.

Halliwell B, Gutteridge JMC, Cross CE (1992) Free-Radicals, Antioxidants, and Human-Disease - Where Are We Now. *Journal of Laboratory and Clinical Medicine* **119,** 598-620.

Halliwell B (1994) Free-Radicals, Antioxidants, and Human-Disease - Curiosity, Cause, Or Consequence. *Lancet* **344,** 721-724.

Halliwell B, Gutteridge JMC (2003) 'Free Radicals in Biology and Medicine.' (Oxford University Press: Oxford, UK)

Hampton MB, Orrenius S (1997) Dual regulation of caspase activity by hydrogen peroxide: Implications for apoptosis. *Febs Letters* **414,** 552-556.

Han ZN, Boyle DL, Manning AM, Firestein GS (1998) AP-1 and NF-kappa B regulation in rheumatoid arthritis and murine collagen-induced arthritis. *Autoimmunity* **28,** 197-208.

Han MK, Kim JS, Park BH, Kim JR, Hwang BY, Lee HY, Song EK, and Yoo WH (2003) NF-kappaB-dependent lymphocyte hyperadhesiveness to synovial fibroblasts by hypoxia and reoxygenation: potential role in rheumatoid arthritis. *Journal of leukocyte biology* **73,** 525-9.

Handel ML, McMorrow LB, Gravallese EM (1995) Nuclear factor-kappa B in rheumatoid synovium - Localization of p50 and p65. *Arthritis and rheumatism* **38,** 1762-1770.

Harford J, Klausner R (1990) Coordinate post-transcriptional regulation of ferritin and transferrin receptor expression: the role of regulated RNA-protein interaction. *Enzyme* **44,** 28-41.

Harrison PM, Arosio P (1996) Ferritins: Molecular properties, iron storage function and cellular regulation. *Biochimica et Biophysica Acta-Bioenergetics* **1275,** 161-203.

Hashimoto Y, Kakegawa H, Narita Y, Hachiya Y, Hayakawa T, Kos J, Turk V, Katunuma N (2001) Significance of cathepsin B accumulation in synovial fluid of rheumatoid arthritis. *Biochemical and Biophysical Research Communications* **283,** 334-339.

Heeney MM, Andrews NC (2004) Iron homeostasis and inherited iron overload disorders: an overview. *Hematology-Oncology Clinics of North America* **18,** 1379 -1403.

Hempel SL, Buettner GR, Wessels DA, Galvan GM, OMalley YQ (1996) Extracellular iron(II) can protect cells from hydrogen peroxide. *Archives of Biochemistry and Biophysics* **330,** 401-408.

Hentze MW, Kuhn LC (1996) Molecular control of vertebrate iron metabolism: mRNA-based regulatory circuits operated by iron, nitric oxide, and oxidative stress. *Proceedings of the National Academy of Sciences of the United States of America* **93,** 8175-8182.

Hentze MW, Muckenthaler MU, Andrews NC (2004) Balancing acts: Molecular control of mammalian iron metabolism. *Cell* **117,** 285-297.

Hershko C (1975) Study of Chelating Agent Diethylenetriaminepentaacetic Acid Using Selective Radioiron Probes of Reticuloendothelial and Parenchymal Iron Stores. *Journal of Laboratory and Clinical Medicine* **85,** 913-921.

Hintze KJ, Theil EC (2005) DNA and mRNA elements with complementary responses to hemin, antioxidant inducers, and iron control ferritin-L expression. *Proceedings of the National Academy of Sciences of the United States of America* **102,** 15048-15052.

Hirota K, Murata M, Sachi Y, Nakamura H, Takeuchi J, Mori K, Yodoi J (1999) Distinct roles of thioredoxin in the cytoplasm and in the nucleus - A two-step mechanism of redox regulation of transcription factor NF-kappa B. *Journal of Biological Chemistry* **274,** 27891-27897.

Horwood N (2008) Lymphocyte-derived cytokines in inflammatory arthritis. *Autoimmunity* **41,** 230-238.

Huber LC, Distler O, Tarner I, Gay RE, Gay S, Pap T (2006) Synovial fibroblasts: key players in rheumatoid arthritis. *Rheumatology* **45,** 669-675.

Huxford T, Huang DB, Malek S, Ghosh G (1998) The crystal structure of the I kappa B alpha/NF-kappa B complex reveals mechanisms of NF-kappa B inactivation. *Cell* **95,** 759-770.

Hyslop PA, Hinshaw DB, Scraufstatter IU, Cochrane CG, Kunz S, Vosbeck K (1995) Hydrogen-Peroxide As A Potent Bacteriostatic Antibiotic - Implications for Host-Defense. *Free Radical Biology and Medicine* **19,** 31-37.

Imbert V, Rupec RA, Livolsi A, Pahl HL, Traenckner EBM, MuellerDieckmann C, Farahifar D, Rossi B, Auberger P, Baeuerle PA, Peyron JF (1996) Tyrosine phosphorylation of I kappa B-alpha activates NF-kappa B without proteolytic degradation of I kappa B-alpha. *Cell* **86,** 787-798.

Iwai K, Drake SK, Wehr NB, Weissman AM, LaVaute T, Minato N, Klausner RD, Levine RL, Rouault TA (1998) Iron-dependent oxidation, ubiquitination, and degradation of iron regulatory protein 2: Implications for degradation of oxidized proteins. *Proceedings of the National Academy of Sciences of the United States of America* **95,** 4924-4928.

Jacobs A (1977) Low-Molecular Weight Intracellular Iron Transport Compounds. *Blood* **50,** 433-439.

Jones DP, Go YM, Anderson CL, Ziegler TR, Kinkade JM, Kirlin WG (2004) Cysteine/cystine couple is a newly recognized node in the circuitry for biologic redox signaling and control. *Faseb Journal* **18,** 1246-1248.

Jongen-Lavrencic M, Peeters HRM, Vreugdenhil G, Swaak AJG (1995) Interaction of Inflammatory Cytokines and Erythropoeitin in Iron-Metabolism and Eryrhropoiesis in Anemia of Chronic Disease. *Clinical Rheumatology* **14,** 519-525.

Jue DM, Jeon KI, Jeong JY (1999) Nuclear factor kappa B (NF-kappa B) pathway as a therapeutic target in rheumatoid arthritis. *Journal of Korean Medical Science* **14,** 231-238.

Junqueira L, Carneiro J, Long J (1986) 'Basic Histology.' (Appleton-Century-Crofts: Connecticut, USA)

Kakhlon O, Gruenbaum Y, Cabantchik ZL (2001) Repression of ferritin expression increases the labile iron pool, oxidative stress, and short-term growth of human erythroleukemia cells. *Blood* **97,** 2863-2871.

Kakhlon O, Cabantchik ZI (2002) The labile iron pool: Characterization, measurement, and participation in cellular processes. *Free Radical Biology and Medicine* **33,** 1037-1046.

Kamanli A, Naziroglu M, Aydilek N, Hacievhyagil C (2004) Plasma lipid peroxidation and antioxidant levels in patients with rheumatoid arthritis. *Cell Biochemistry and Function* **22,** 53-57.

Karin M (1999) The beginning of the end: I kappa B kinase (IKK) and NF-kappa B activation. *Journal of Biological Chemistry* **274,** 27339-27342.

Karin M, Ben-Neriah Y (2000) Phosphorylation meets ubiquitination: The control of NF-kappa B activity. *Annual Review of Immunology* **18,** 621-663.

Keyse SM, Tyrrell RM (1989) Heme Oxygenase Is the Major 32-Kda Stress Protein-Induced in Human-Skin Fibroblasts by Uva Radiation, Hydrogen-Peroxide, and Sodium Arsenite. *Proceedings of the National Academy of Sciences of the United States of America* **86,** 99-103.

Khurana R, Berney S (2005) Clinical aspects of rheumatoid arthritis. *Pathophysiology* **12,** 153-165.

Kidane TZ, Sauble E, Linder MC (2006) Release of iron from ferritin requires lysosomal activity. *American Journal of Physiology-Cell Physiology* **291,** C445-C455.

Klausner RD, Rouault TA, Harford JB (1993) Regulating the Fate of Messenger-Rna - the Control of Cellular Iron-Metabolism. *Cell* **72,** 19-28.

Kobayashi H, Takeno M, Saito T, Takeda Y, Kirino Y, Noyori K, Hayashi T, Ueda A, Ishigatsubo Y (2006) Regulatory role of heme oxygenase 1 in inflammation of rheumatoid arthritis. *Arthritis and rheumatism* **54,** 1132-1142.

Konijn AM (1994) Iron metabolism in inflammation. *Bailliere's clinical haematology* **7,** 829-849.

Kontou M, Will RD, Adelfalk C, Wittig R, Poustka A, Hirsch-Kauffmann M, Schweiger M (2004) Thioredoxin, a regulator of gene expression. *Oncogene* **23,** 2146-2152.

Koong AC, Chen EY, Giaccia AJ (1994) Hypoxia Causes the Activation of Nuclear Factor Kappa-B Through the Phosphorylation of I-Kappa-B-Alpha on Tyrosine Residues. *Cancer Research* **54,** 1425-1430.

Kuhn L (1994) Molecular regulation of iron proteins. *Bailliere's clinical haematology* **7,** 763-785.

Kunsch C, Sikorski JA, Sundell CL (2005) Oxidative Stress and the Use of Antioxidants for the Treatment of Rheumatoid Arthritis. *Current Medicinal Chemistry Immunology Endocrine and Metabolic Agents* **5,** 249-258.

Kurz T, Leake A, von Zglinicki T, Brunk UT (2004) Lysosomal redox-active iron is important for oxidative stress-induced DNA damage. *Annals of the New York Academy of Sciences* **1019**, 285-288 .

Kurz T, Gustafsson B, Brunk UT (2006) Intralysosomal iron chelation protects against oxidative stress-induced cellular damage. *Febs Journal* **273,** 3106-3117.

Kurz T, Terman A, Brunk UT (2007) Autophagy, ageing and apoptosis: The role of oxidative stress and lysosomal iron. *Archives of Biochemistry and Biophysics* **462,** 220-230.

Kurz T, Terman A, Gustafsson B, Brunk UT (2008) Lysosomes in iron metabolism, ageing and apoptosis. *Histochemistry and Cell Biology* **129,** 389-406.

Kvam E, Hejmadi V, Ryter S, Pourzand C, Tyrrell RM (2000) Heme oxygenase activity causes transient hypersensitivity to oxidative ultraviolet A radiation that depends on release of iron from heme. *Free Radical Biology and Medicine* **28,** 1191-1196.

Lahdenpohja N, Savinainen K, Hurme M (1998) Pre-exposure to oxidative stress decreases the nuclear factor-kappa B-dependent transcription in T lymphocytes. *Journal of Immunology* **160,** 1354-1358.

Langrehr J (1971) 'Oxidation and reduction.' (Jacaranda press: Queensland, Australia)

Lautier D, Luscher P, Tyrrell RM (1992) Endogenous glutathione levels modulate both constitutive and UVA radiation/hydrogen peroxide inducible expression of the human heme oxygenase gene. *Carcinogenesis* **13,** 227-232.

Lawson DM, Treffry A, Artymiuk PJ, Harrison PM, Yewdall SJ, Luzzago A, Cesareni G, Levi S, Arosio P (1989) Identification of the Ferroxidase Center in Ferritin. *Febs Letters* **254,** 207-210.

Le Lan C, Loreal O, Cohen T, Ropert M, Glickstein H, Laine F, Pouchard M, Deugnier Y, Le Treut A, Breuer W, Cabantchik ZI, Brissot P (2005) Redox active plasma iron in C282Y/C282Y hemochromatosis. *Blood* **105,** 4527-4531.

Lee JI, Burckart GJ (1998) Nuclear factor kappa B: Important transcription factor and therapeutic target. *Journal of Clinical Pharmacology* **38,** 981-993.

Levi S, Yewdall SJ, Harrison PM, Santambrogio P, Cozzi A, Rovida E, Albertini A, Arosio P (1992) Evidence That H-Chains and L-Chains Have Cooperative Roles in the Iron-Uptake Mechanism of Human Ferritin. *Biochemical Journal* **288,** 591-596.

Levi S, Corsi B, Bosisio M, Invernizzi R, Volz A, Sanford D, Arosio P, Drysdale J (2001) A human mitochondrial ferritin encoded by an intronless gene. *Journal of Biological Chemistry* **276,** 24437-24440.

Li NX, Karin M (1999) Is NF-kappa B the sensor of oxidative stress? *Faseb Journal* **13,** 1137-1143.

Li W, Yuan XM, Olsson AG, Brunk UT (1998) Uptake of oxidized LDL by macrophages results in partial lysosomal enzyme inactivation and relocation. *Arteriosclerosis Thrombosis and Vascular Biology* **18,** 177-184.

Li ZW, Rickert RC, Karin M (2004) Genetic dissection of antigen receptor induced-NF-kappa B activation. *Molecular Immunology* **41,** 701-714.

Lieu P, Heiskala M, Peterson P, Yang Y (2001) The roles of iron in health and disease. *Molecular aspects of medicine* **22,** 1-87.

Lin F, Bertling CJ, Geiger PG, Girotti AW (1998) Delayed hyperresistance of endothelial cells to photodynamic inactivation after contact with hemin. *Photochemistry and Photobiology* **68,** 211-217.

Lin FB, Girotti AW (1997) Elevated ferritin production, iron containment, and oxidant resistance in hemin-treated leukemia cells. *Archives of Biochemistry and Biophysics* **346,** 131-141.

Lin FB, Girotti AW (1998) Hemin-enhanced resistance of human leukemia cells to oxidative killing: Antisense determination of ferritin involvement. *Archives of Biochemistry and Biophysics* **352,** 51-58.

Ling L, Cao ZD, Goeddel DV (1998) NF-kappa B-inducing kinase activates IKK-alpha by phosphorylation of Ser-176. *Proceedings of the National Academy of Sciences of the United States of America* **95,** 3792-3797.

Link G, Ponka P, Konijn AM, Breuer W, Cabantchik ZL, Hershko C (2003) Effects of combined chelation treatment with pyridoxal isonicotinoyl hydrazone analogs and deferoxamine in hypertransfused rats and in iron-loaded rat heart cells. *Blood* **101,** 4172-4179.

Lipinski P, Drapier JC, Oliveira L, Retmanska H, Sochanowicz B, Kruszewski M (2000) Intracellular iron status as a hallmark of mammalian cell susceptibility to oxidative stress: a study of L5178Y mouse lymphoma cell lines differentially sensitive to H2O2. *Blood* **95,** 2960-2966.

Lipsky PE (2007) Why does rheumatoid arthritis involve the joints? *New England Journal of Medicine* **356,** 2419-2420.

Liu N, Raja SM, Zazzeroni F, Metkar SS, Shah R, Zhang ML, Wang Y, Bromme D, Russin WA, Lee JC, Peter ME, Froelich CJ, Franzoso G, shton-Rickardt PG (2003) NF-kappa B protects from the lysosomal pathway of cell death. *Embo Journal* **22,** 5313-5322.

Lloyd JB, Cable H, Rice-evans C (1991) Evidence That Desferrioxamine Cannot Enter Cells by Passive Diffusion. *Biochemical Pharmacology* **41,** 1361-1363.

Ludwiczek S, Aigner E, Theurl I, Weiss G (2003) Cytokine-mediated regulation of iron transport in human monocytic cells. *Blood* **101,** 4148-4154.

MacKenzie, N (2006) New therapeutics that treat rheumatoid arthritis by blocking T-cell activation. *Drug discovery today* **11**, 952-956.

Maines MD, Trakshel GM, Kutty RK (1986) Characterization of 2 Constitutive Forms of Rat-Liver Microsomal Heme Oxygenase - Only One Molecular-Species of the Enzyme Is Inducible. *Journal of Biological Chemistry* **261,** 411-419.

Makarov SS (2001) NF-kappa B in rheumatoid arthritis: a pivotal regulator of inflammation, hyperplasia, and tissue destruction. *Arthritis research* **3,** 200-206.

Malinin NL, Boldin MP, Kovalenko AV, Wallach D (1997) MAP3K-related kinase involved in NF-kappa B induction by TNF, CD95 and IL-1. *Nature* **385,** 540-544.

Maniatis T (1999) A ubiquitin ligase complex essential for the NF-kappa B, Wnt/Wingless, and Hedgehog signaling pathways. *Genes & Development* **13,** 505-510.

Marok R, Winyard PG, Coumbe A, Kus ML, Gaffney K, Blades S, Mapp PI, Morris CJ, Blake DR, Kaltschmidt C, Baeuerle PA (1996) Activation of the transcription factor nuclear factor-kappa B in human inflamed synovial tissue. *Arthritis and rheumatism* **39,** 583-591.

Martinez-Cayuela M (1995) Oxygen-Free Radicals and Human-Disease. *Biochimie* **77,** 147-161.

Martins EAL, Robalinho RL, Meneghini R (1995) Oxidative Stress Induces Activation of A Cytosolic Protein Responsible for Control of Iron Uptake. *Archives of Biochemistry and Biophysics* **316,** 128-134.

Matthews JR, Wakasugi N, Virelizier JL, Yodoi J, Hay RT (1992) Thioredoxin Regulates the DNA-Binding Activity of Nf-KB by Reduction of A Disulfide Bond Involving Cysteine 62. *Nucleic Acids Research* **20,** 3821-3830.

Maurice MM, Nakamura H, Gringhuis S, Okamoto T, Yoshida S, Kullmann F, Lechner S, van der Voort EAM, Leow A, Versendaal J, Muller-Ladner U, Yodoi J, Tak PP, Breedveld FC, Verweij CL (1999) Expression of the thioredoxin-thioredoxin reductase system in the inflamed joints of patients with rheumatoid arthritis. *Arthritis and rheumatism* **42,** 2430-2439.

McCarty D (1989) 'Arthritis and allied conditions.' (Lea & Febiger: Philadelphia, USA)

McCoubrey WK, Huang TJ, Maines MD (1997) Isolation and characterization of a cDNA from the rat brain that encodes hemoprotein heme oxygenase-3. *European Journal of Biochemistry* **247,** 725-732.

Mckie AT, Marciani P, Rolfs A, Brennan K, Wehr K, Barrow D, Miret S, Bomford A, Peters TJ, Farzaneh F, Hediger MA, Hentze MW, Simpson RJ (2000) A novel duodenal iron-regulated transporter, IREG1, implicated in the basolateral transfer of iron to the circulation. *Molecular Cell* **5,** 299-309.

Mckie AT, Latunde-Dada G, Miret S, McGregor JA, Anderson GJ, Vulpe CD, Wrigglesworth JM, Simpson RJ (2002) Molecular evidence for the role of a ferric reductase in iron transport. *Biochemical Society Transactions* **30,** 722-724.

Mehlhase J, Sandig G, Pantopoulos K, Grune T (2005) Oxidation-induced ferritin turnover in microglial cells: role of proteasome. *Free Radical Biology and Medicine* **38,** 276-285.

Meister A, Anderson ME (1983) Glutathione. *Annu.Rev.Biochem.* **52,** 711-760.

Meneghini R (1997) Iron homeostasis, oxidative stress, and DNA damage. *Free Radical Biology and Medicine* **23,** 783-792.

Menkin V (1940) 'Dynamics of Inflammation.' (Macmillan: New York, USA)

Mercurio F, Manning AM (1999) Multiple signals converging on NF-kappa B. *Current Opinion in Cell Biology* **11,** 226-232.

Merry P, Winyard PG, Morris CJ, Grootveld M, Blake DR (1989) Oxygen Free-Radicals, Inflammation, and Synovitis - the Current Status. *Annals of the rheumatic diseases* **48,** 864-870.

Meyron-Holtz EG, Vaisman B, Cabantchik ZI, Fibach E, Rouault TA, Hershko C, Konijn AM (1999) Regulation of intracellular iron metabolism in human erythroid precursors by internalized extracellular ferritin. *Blood* **94,** 3205-3211.

Miagkov AV, Kovalenko DV, Brown CE, Didsbury JR, Cogswell JP, Stimpson SA, Baldwin AS, Makarov SS (1998) NF-kappa B activation provides the potential link between inflammation and hyperplasia in the arthritic joint. *Proceedings of the National Academy of Sciences of the United States of America* **95,** 13859-13864.

Mihm S, Galter D, Droge W (1995) Modulation of Transcription Factor Nf-Kappa-B Activity by Intracellular Glutathione Levels and by Variations of the Extracellular Cysteine Supply. *Faseb Journal* **9,** 246-252.

Miret S, Simpson RJ, Mckie AT (2003) Physiology and molecular biology of dietary iron absorption. *Annual Review of Nutrition* **23,** 283-301.

Mladenka P, Simunek T, Hubl M, Hrdina R (2006) The role of reactive oxygen and nitrogen species in cellular iron metabolism. *Free Radical Research* **40,** 263-272.

Morel Y, Barouki R (1999) Repression of gene expression by oxidative stress. *Biochemical Journal* **342,** 481-496.

Morliere P, Salmon S, Aubailly M, Risler A, Santus R (1997) Sensitization of skin fibroblasts to UVA by excess iron. *Biochimica et Biophysica Acta-General Subjects* **1334,** 283-290.

Morozova N, Khrapko K, Panee J, Liu WY, Harney JW, Berry MJ (2007) Glutathione depletion in hippocampal cells increases levels of H and L ferritin and glutathione S-transferase mRNAs. *Genes to Cells* **12,** 561-567.

Mosmann T (1983) Rapid Colorimetric Assay for Cellular Growth and Survival - Application to Proliferation and Cyto-Toxicity Assays. *Journal of Immunological Methods* **65,** 55-63.

Muckenthaler M, Galy B, Hentze MW (2008) Systemic Iron Homeostasis and the Iron-Responsive Element/Iron-Regulatory Protein (IRE/IRP) Regulatory Network. *Annual Review of Nutrition* **28,** 3.1-3.17.

Mueller S, Pantopoulos K, Hubner CA, Stremmel W, Hentze MW (2001) IRP1 activation by extracellular oxidative stress in the perfused rat liver. *Journal of Biological Chemistry* **276,** 23192-23196.

Mueller S (2005) Iron regulatory protein 1 as a sensor of reactive oxygen species. *Biofactors* **24,** 171-181.

Muirden K, Senator G (1968) Iron in the synovial membrane in rheumatoid arthritis and other joint diseases. *Annals of the rheumatic diseases* **27,** 38-48.

Muirden KD (1972) Lysosomal Enzymes in Synovial Membrane in Rheumatoid-Arthritis - Relationship to Joint Damage. *Annals of the rheumatic diseases* **31,** 265-&.

Mulvihill M, Zelman M, Holdaway P, Tompary E, Turchany J (2001) 'Human Disease: a Systemic Approach.' (Prentice-Hall: New Jersey, USA)

Nagy G, Clark J, Buzas E, Gorman C, Pasztoi M, Koncz A, Falus A, Cope A (2008) Nitric oxide production of T lymphocytes is increased in rheumatoid arthritis. *Immunology Letters* **118,** 55-58.

Nakayama M, Takahashi K, Kitamuro T, Yasumoto K, Katayose D, Shirato K, Fujii-Kuriyama Y, Shibahara S (2000) Repression of heme oxygenase-1 by hypoxia in vascular endothelial cells. *Biochemical and Biophysical Research Communications* **271,** 665-671.

Narendhirakannan RT, Subramanian S, Kandaswamy A (2007) Anti-inflammatory and lysosomal stability actions of Cleome gynandra L. studied in adjuvant induced arthritic rats. *Food and Chemical Toxicology* **45,** 1001-1012.

Nemes Z, Dietz R, Luth JB, Gomba S, Hackenthal E, Gross F (1979) Pharmacological Relevance of Vital Staining with Neutral Red. *Experientia* **35,** 1475-1476.

Nemeth E, Rivera S, Gabayan V, Keller C, Taudorf S, Pedersen BK, Ganz T (2004[a]) IL-6 mediates hypoferremia of inflammation by inducing the synthesis of the iron regulatory hormone hepcidin. *Journal of Clinical Investigation* **113,** 1271-1276.

Nemeth E, Tuttle MS, Powelson J, Vaughn MB, Donovan A, Ward DM, Ganz T, Kaplan J (2004[b]) Hepcidin regulates cellular iron efflux by binding to ferroportin and inducing its internalization. *Science* **306,** 2090-2093.

Nicolas G, Chauvet C, Viatte L, Danan JL, Bigard X, Devaux I, Beaumont C, Kahn A, Vaulont S (2002) The gene encoding the iron regulatory peptide hepcidin is regulated by anemia, hypoxia, and inflammation. *Journal of Clinical Investigation* **110,** 1037-1044.

Niedermeier W, Creitz E, Holley H (1962) Trace metal composition of synovial fluid from patients with rheumatoid arthritis. *Arthritis and rheumatism* **5,** 439-444.

Niedermeier W, Griggs JH (1971) Trace Metal Composition of Synovial Fluid and Blood Serum of Patients with Rheumatoid Arthritis. *Journal of Chronic Diseases* **23,** 527-&.

Ogawa Y, Kobayashi T, Nishioka A, Kariya S, Ohnishi T, Hamasato S, Seguchi H, Yoshida S (2004) Reactive oxygen species-producing site in radiation and hydrogen peroxide-induced apoptosis of human peripheral T cells: Involvement of lysosomal membrane destabilization. *International Journal of Molecular Medicine* **13,** 655-660.

Ogilvieharris DJ, Fornaiser VL (1980) Synovial Iron Deposition in Osteo-Arthritis and Rheumatoid-Arthritis. *Journal of Rheumatology* **7,** 30-36.

Ohishi K, Zhang XM, Moriwaki S, Hiramitsu T, Matsugo S (2005) Iron release analyses from ferritin by visible light irradiation. *Free Radical Research* **39,** 875-882.

Okazaki Y, Sawada T, Nagatani K, Komagata Y, Inoue T, Muto S, Itai A, Yamamoto K (2005) Effect of nuclear factor-kappa B inhibition on rheumatoid fibroblast-like synoviocytes and collagen induced arthritis. *Journal of Rheumatology* **32,** 1440-1447.

Ollinger K, Brunk UT (1995) Cellular Injury-Induced by Oxidative Stress Is Mediated Through Lysosomal Damage. *Free Radical Biology and Medicine* **19,** 565-574.

Orino K, Lehman L, Tsuji Y, Ayaki H, Torti SV, Torti FM (2001) Ferritin and the response to oxidative stress. *Biochemical Journal* **357,** 241-247.

Ozkan Y, Yardym-Akaydyn S, Sepici A, Keskin E, Sepici V, Simsek B (2007) Oxidative status in rheumatoid arthritis. *Clinical Rheumatology* **26,** 64-68.

Pae HO, Choi BM, Oh GS, Lee MS, Ryu DG, Rhew HY, Kim YM, Chung HT (2004) Roles of heme oxygenase-1 in the antiproliferative and antiapoptotic effects of nitric oxide on Jurkat T cells. *Molecular Pharmacology* **66,** 122-128.

Pae HO, Oh GS, Choi BM, Chae SC, Kim YM, Chung KR, Chung HT (2004) Carbon monoxide produced by heme oxygenase-1 suppresses T cell proliferation via inhibition of IL-2 production. *Journal of Immunology* **172,** 4744-4751.

Pahl HL (1999) Activators and target genes of Rel/NF-kappa B transcription factors. *Oncogene* **18,** 6853-6866.

Panayi GS, Corrigall VM, Pitzalis C (2001) Pathogenesis of rheumatoid arthritis - The role of T cells and other beasts. *Rheumatic Disease Clinics of North America* **27,** 317-334.

Pantopoulos K, Hentze MW (1995) Rapid Responses to Oxidative Stress Mediated by Iron Regulatory Protein. *Embo Journal* **14,** 2917-2924.

Pantopoulos K, Weiss G, Hentze MW (1996) Nitric oxide and oxidative stress (H2O2) control mammalian iron metabolism by different pathways. *Molecular and Cellular Biology* **16,** 3781-3788.

Pantopoulos K, Mueller S, Atzberger A, Ansorge W, Stremmel W, Hentze MW (1997) Differences in the regulation of iron regulatory protein-1 (IRP-1) by extra- and intracellular oxidative stress. *Journal of Biological Chemistry* **272,** 9802-9808.

Papanikolaou G, Pantopoulos K (2005) Iron metabolism and toxicity. *Toxicology and Applied Pharmacology* **202,** 199-211.

Pearson CM (1956) Development of arthritis, periarthritis and periostitis in rats given adjuvants. *Proc.Soc.Exp.Biol.Med* **91,** 95-101.

Persson HL, Yu ZQ, Tirosh O, Eaton JW, Brunk UT (2003) Prevention of oxidant-induced cell death by lysosomotropic iron chelators. *Free Radical Biology and Medicine* **34,** 1295-1305.

Persson HL, Kurz T, Eaton JW, Brunk UT (2005) Radiation-induced cell death: importance of lysosomal destabilization. *Biochemical Journal* **389,** 877-884.

Petrat F, Rauen U, de Groot H (1999) Determination of the chelatable iron pool of isolated rat hepatocytes by digital fluorescence microscopy using the fluorescent probe, phen green SK. *Hepatology* **29,** 1171-1179.

Petrat F, de Groot H, Rauen U (2001) Subcellular distribution of chelatable iron: a laser scanning microscopic study in isolated hepatocytes and liver endothelial cells. *Biochemical Journal* **356,** 61-69.

Petrat F, Weisheit D, Lensen M, de Groot H, Sustmann R, Rauen U (2002) Selective determination of mitochondrial chelatable iron in viable cells with a new fluorescent sensor. *Biochemical Journal* **362,** 137-147.

Pham CG, Bubici C, Zazzeroni F, Papa S, Jones J, Alvarez K, Jayawardena S, De Smaele E, Cong R, Beaumont C, Torti FM, Torti SV, Franzoso G (2004) Ferritin heavy chain upregulation by NF-kappa B inhibits TNF alpha-induced apoptosis by suppressing reactive oxygen species. *Cell* **119,** 529-542.

Piette J, Piret B, Bonizzi G, Schoonbroodt S, Merville MP, LegrandPoels S, Bours V (1997) Multiple redox regulation in NF-kappa B transcription factor activation. *Biological Chemistry* **378,** 1237-1245.

Pigeon C, Ilyin G, Courselaud B, Leroyer P, Turlin B, Brissot P, Loreal O (2001) A new mouse liver-specific gene, encoding a protein homologous to human antimicrobial peptide hepcidin, is overexpressed during iron overload. *Journal of Biological Chemistry* **276,** 7811-7819.

Piva R, Belardo G, Santoro MG (2006) NF-kappa B: A stress-regulated switch for cell survival. *Antioxidants & Redox Signaling* **8,** 478-486.

Potter RF, Wunder C (2003) The Heme Oxygenase System: Its Role in Liver Inflammation. *Current Drug Targets* **3,** 199-208.

Pourzand C, Watkin RD, Brown JE, Tyrrell RM (1999) Ultraviolet A radiation induces immediate release of iron in human primary skin fibroblasts: The role of ferritin. *Proceedings of the National Academy of Sciences of the United States of America* **96,** 6751-6756.

Pourzand C, Reelfs O, Tyrrell RM (2000) Approaches to define the involvement of reactive oxygen species and iron in ultraviolet-A inducible gene expression. *Methods Mol.Biol.* **99,** 257-276.

Radisky DC, Kaplan J (1998) Iron in cytosolic ferritin can be recycled through lysosomal degradation in human fibroblasts. *Biochemical Journal* **336,** 201-205.

Ragno S, Winrow VR, Mascagni P, Lucietto P, DiPierro F, Morris CJ, Blake DR (1996) A synthetic 10-kD heat shock protein (hsp10) from Mycobacterium tuberculosis modulates adjuvant arthritis. *Clinical and Experimental Immunology* **103,** 384-390.

Raha S, Robinson BH (2000) Mitochondria, oxygen free radicals, disease and ageing. *Trends in Biochemical Sciences* **25,** 502-508.

Recalcati S, Tacchini L, Alberghini A, Conte D, Cairo G (2003) Oxidative stress-mediated down-regulation of rat hydroxyacid oxidase 1, a liver-specific peroxisomal enzyme. *Hepatology* **38,** 1159-1166.

Recalcati S, Alberghini A, Campanella A, Gianelli U, De Camilli E, Conte D, Cairo G (2006) Iron regulatory proteins 1 and 2 in human monocytes, macrophages and duodenum: expression and regulation in hereditary hemochromatosis and iron deficiency. *Haematologica-the Hematology Journal* **91,** 303-310.

Reddy GK, Dhar SC (1987) Effect of A New Nonsteroidal Antiinflammatory Agent on Lysosomal Stability in Adjuvant Induced Arthritis. *Italian Journal of Biochemistry* **36,** 205-217.

Reeder BJ, Hider RC, Wilson MT (2008) Iron chelators can protect against oxidative stress through ferryl heme reduction. *Free Radical Biology and Medicine* **44,** 264-273.

Reelfs O, Tyrrell R M and Pourzand C (2004) Ultraviolet a Radiation-Induced Immediate Iron Release Is a Key Modulator of the Activation of NF-Kappa B in Human Skin Fibroblasts. *Journal of Investigative Dermatology* **122**:1440-1447.

Reeve VE, Tyrrell RM (1999) Heme oxygenase induction mediates the photoimmunoprotective activity of UVA radiation in the mouse. *Proceedings of the National Academy of Sciences of the United States of America* **96,** 9317-9321.

Reeve VE, Domanski D (2002) Refractoriness of UVA-induced protection from photoimmunosuppression correlates with heme oxygenase response to repeated UVA exposure. *Photochemistry and Photobiology* **76,** 401-405.

Remans PHJ, van Oosterhout M, Smeets TJM, Sanders M, Frederiks WM, Reedquist KA, Tak PP, Breedveld FC, van Laar JM (2005) Intracellular free radical production in synovial T lymphocytes from patients with rheumatoid arthritis. *Arthritis and rheumatism* **52,** 2003-2009.

Rice-evans C, Baysal E, Singh S, Jones SA, Jones JG (1989) The Interactions of Desferrioxamine and Hydroxypyridone Compounds with Hemoglobin and Erythrocytes. *Febs Letters* **256,** 17-20.

Roberg K, Ollinger K (1998) Oxidative stress causes relocation of the lysosomal enzyme cathepsin D with ensuing apoptosis in neonatal rat cardiomyocytes. *American Journal of Pathology* **152,** 1151-1156.

Roberts S, Bomford A (1988) Ferritin Iron Kinetics and Protein-Turnover in K562 Cells. *Journal of Biological Chemistry* **263,** 19181-19187.

Roff M, Thompson J, Rodriguez MS, Jacque JM, Baleux F, ArenzanaSeisdedos F, Hay RT (1996) Role of I kappa B alpha ubiquitination in signal-induced activation of NF-kappa B in vivo. *Journal of Biological Chemistry* **271,** 7844-7850.

Roshy S, Sloane BF, Moin K (2003) Pericellular cathepsin B and malignant progression. *Cancer and Metastasis Reviews* **22,** 271-286.

Rudeck M, Volk T, Sitte N, Grune T (2000) Ferritin oxidation in vitro: Implication of iron release and degradation by the 20S proteasome. *Iubmb Life* **49,** 451-456.

Ryseck RP, Novotny J, Bravo R (1995) Characterization of Elements Determining the Dimerization Properties of Re1B and P50. *Molecular and Cellular Biology* **15,** 3100-3109.

Ryter SW, Tyrrell RM (2000) The Heme synthesis and degradation pathways: role in oxidant sensitivity - Heme oxygenase has both pro- and antioxidant properties. *Free Radical Biology and Medicine* **28,** 289-309.

Sagara Y, Dargusch R, Chambers D, Davis J, Schubert D, Maher P (1998) Cellular mechanisms of resistance to chronic oxidative stress. *Free Radical Biology and Medicine* **24,** 1375-1389.

Samaniego F, Chin J, Iwai K, Rouault T, Klausner R (1994) Molecular characterization of a second iron-responsive element binding protein, iron regulatory protein 2. Structure, function, and post-translational regulation. *The Journal of biological chemistry* **269,** 30904-30910.

Santambrogio P, Levi S, Cozzi A, Rovida E, Albertini A, Arosio P (1993) Production and Characterization of Recombinant Heteropolymers of Human Ferritin H-Chain and L-Chain. *Journal of Biological Chemistry* **268,** 12744-12748.

Santambrogio P, Cozzi A, Levi S, Rovida E, Magni F, Albertini A, Arosio P (2000) Functional and immunological analysis of recombinant mouse H- and L-ferritins from Escherichia coli. *Protein Expression and Purification* **19,** 212-218.

Santambrogio P, Biasiotto G, Sanvito F, Olivieri S, Arosio P, Levi S (2007) Mitochondrial ferritin expression in adult mouse tissues. *Journal of Histochemistry & Cytochemistry* **55,** 1129-1137.

Saunders EL, Maines MD, Meredith MJ, Freeman ML (1991) Enhancement of Heme Oxygenase-1 Synthesis by Glutathione Depletion in Chinese-Hamster Ovary Cells. *Archives of Biochemistry and Biophysics* **288,** 368-373.

Schenk H, Klein M, Erdbrugger W, Droge W, Schulzeosthoff K (1994) Distinct Effects of Thioredoxin and Antioxidants on the Activation of Transcription Factors Nf-Kappa-B and Ap-1. *Proceedings of the National Academy of Sciences of the United States of America* **91,** 1672-1676.

Scherer DC, Brockman JA, Chen ZJ, Maniatis T, Ballard DW (1995) Signal-Induced Degradation of I-Kappa-B-Alpha Requires Site-Specific Ubiquitination. *Proceedings of the National Academy of Sciences of the United States of America* **92,** 11259-11263.

Schett G (2006) Rheumatoid arthritis: inflammation and bone loss. *Wien Med Wochenschr* **156,** 34-41.

Schett G (2008) Review: Immune cells and mediators of inflammatory arthritis. *Autoimmunity* **41,** 224-229.

Schmidt KN, Amstad P, Cerutti P, Baeuerle PA (1995) The Roles of Hydrogen-Peroxide and Superoxide As Messengers in the Activation of Transcription Factor Nf-Kappa-B. *Chemistry & Biology* **2,** 13-22.

Schoonbroodt S, Ferreira V, Best-Belpomme M, Boelaert JR, Legrand-Poels S, Korner M, Piette J (2000) Crucial role of the amino-terminal tyrosine residue 42 and the

carboxyl-terminal PEST domain of I kappa B alpha in NF-kappa B activation by an oxidative stress. *Journal of Immunology* **164,** 4292-4300.

Schreck R, Rieber P, Baeuerle PA (1991) Reactive Oxygen Intermediates As Apparently Widely Used Messengers in the Activation of the Nf-Kappa-B Transcription Factor and Hiv-1. *Embo Journal* **10,** 2247-2258.

Schreck R, Albermann K, Baeuerle PA (1992) Nuclear Factor Kappa-B - An Oxidative Stress-Responsive Transcription Factor of Eukaryotic Cells (A Review). *Free Radical Research Communications* **17,** 221-237.

Schreck R, Baeuerle PA (1994) Assessing Oxygen Radicals As Mediators in Activation of Inducible Eukaryotic Transcription Factor Nf-Kappa-B. *Methods in Enzymology* **234**, 151-163.

Schreiber E, Matthias P, Muller MM, Schaffner W (1989) Rapid Detection of Octamer Binding-Proteins with Mini-Extracts, Prepared from A Small Number of Cells. *Nucleic Acids Research* **17,** 6419.

Seetharaman R, Mora AL, Nabozny G, Boothby M, Chen J (1999) Essential role of T cell NF-kappa B activation in collagen-induced arthritis. *Journal of Immunology* **163,** 1577-1583.

Sen C, Sies H, Baeuerle PA (2004) 'Antioxidant and Redox Regulation of Genes.' (Academic Press: London, UK)

Sen R, Baltimore D (1986) Multiple Nuclear Factors Interact with the Immunoglobulin Enhancer Sequences. *Cell* **46,** 705-716.

Senftleben U, Cao YX, Xiao GT, Greten FR, Krahn G, Bonizzi G, Chen Y, Hu YL, Fong A, Sun SC, Karin M (2001) Activation by IKK alpha of a second, evolutionary conserved, NF-kappa B signaling pathway. *Science* **293,** 1495-1499.

Seta F, Bellner L, Rezzani R, Regan RF, Dunn MW, Abraham NG, Gronert K, Laniado-Schwartzman M (2006) Heme oxygenase-2 is a critical determinant for execution of an acute inflammatory and reparative response. *American Journal of Pathology* **169,** 1612-1623.

Sethi G, Sung B, Aggarwal BB (2008) Nuclear factor-kB activation: From bench to bedside. *Experimental Biology and Medicine* **233,** 21-31.

Sharp P (2005) Modulation of Gene Expression by Dietary Iron. In 'Oxidative Stress and Disease'. (Eds G Rimbach, J Fuchs, and L Packer) pp. 421-440. (Marcel Dekker Inc: UK)

Shayeghi M, Latunde-Dada GO, Oakhill JS, Laftah AH, Takeuchi K, Halliday N, Khan Y, Warley A, Mccann FE, Hider RC, Frazer DM, Anderson GJ, Vulpe CD, Simpson RJ, Mckie AT (2005) Identification of an intestinal heme transporter. *Cell* **122,** 789-801.

Shi HF, Bencze KZ, Stemmler TL, Philpott CC (2008) A cytosolic iron chaperone that delivers iron to ferritin. *Science* **320,** 1207-1210.

Shin HM, Kim MH, Kim BH, Jung SH, Kim YS, Park HJ, Hong JT, Kyung RM, Kim Y (2004) Inhibitory action of novel aromatic diamine compound on lipopolysaccharide-induced nuclear translocation of NF-kappa B without affecting I kappa B degradation. *Febs Letters* **571,** 50-54.

Siebenlist U, Franzoso G, Brown K (1994) Structure, Regulation and Function of Nf-Kappa-B. *Annual Review of Cell Biology* **10,** 405-455.

Sies H (1997) 'Antioxidants in disease mechanisms and therapy.' (Academic Press)

Simmonds RE, Foxwell BM (2008) Signalling, inflammation and arthritis - NF-kappa B and its relevance to arthritis and inflammation. *Rheumatology* **47,** 584-590.

Sipos K, Lange H, Fekete Z, Ullmann P, Lill R, Kispal G (2002) Maturation of cytosolic iron-sulfur proteins requires glutathione. *Journal of Biological Chemistry* **277,** 26944-26949.

Smith AL (1967) [13] Preparation, properties, and conditions for assay of mitochondria: Slaughterhouse material, small-scale. In 'Methods in EnzymologyOxidation and Phosphorylation', 81-86. (Academic Press)

Snyder SH, Baranano DE (2001) Heme oxygenase: A font of multiple messengers. *Neuropsychopharmacology* **25,** 294-298.

Sohar N, Hammer H, Sohar I (2002) Lysosomal peptidases and glycosidases in rheumatoid arthritis. *Biological Chemistry* **383,** 865-869.

Spector W, Willoughby D (1957) Histamine and 5-hydroxytryptamine in acute experimental pleurisy. *The Journal of Pathology and Bacteriology* **74,** 57-65.

Sriram V, Krishnan KS, Mayor S (2006) Biogenesis and Function of Late Endosomes and Lysosomes. *Proceedings* **72,** 19-42.

Starke PE, Gilbertson JD, Farber JL (1985) Lysosomal Origin of the Ferric Iron Required for Cell Killing by Hydrogen-Peroxide. *Biochemical and Biophysical Research Communications* **133,** 371-379.

Stevens A, Lowe J (1999) 'Pathology.' (Mosby: Barcelona, Spain)

Sun LJ, Chen ZJ (2004) The novel functions of ubiquitination in signaling. *Current Opinion in Cell Biology* **16,** 119-126.

Syed BA, Sargent PJ, Farnaud S, Evans RW (2006) An overview of molecular aspects of iron metabolism. *Hemoglobin* **30,** 69-80.

Tacchini L, Recalcati S, Bernellizazzera A, Cairo G (1997) Induction of ferritin synthesis in ischemic-reperfused rat liver: Analysis of the molecular mechanisms. *Gastroenterology* **113,** 946-953.

Tacchini L, Cairo G, De Ponti C, Massip M, Rosello-Catafau J, Peralta C (2006) Up regulation of IL-6 by ischemic preconditioning in normal and fatty rat livers: Association with reduction of oxidative stress. *Free Radical Research* **40,** 1206-1217.

Tacchini L, Gammella E, De PC, Recalcati S, Cairo G (2008) Role of HIF-1 and NF-kB transcription factors in the modulation of transferrin receptor by inflammatory and anti-inflammatory signals. *Journal of Biological Chemistry*.

Tak PP, Firestein GS (2001) NF-kappa B: a key role in inflammatory diseases. *Journal of Clinical Investigation* **107,** 7-11.

Taramelli D, Recalcati S, Basilico N, Olliaro P, Cairo G (2000) Macrophage Preconditioning with Synthetic Malaria Pigment Reduces Cytokine Production via Heme Iron-Dependent Oxidative Stress. *Laboratory Investigation* **80,** 1781-1788.

Telfer JF, Brock JH (2004) Proinflammatory cytokines increase iron uptake into human monocytes and synovial fibroblasts from patients with rheumatoid arthritis. *Medical Science Monitor* **10,** BR91-BR95.

Tenopoulou M, Kurz T, Doulias PT, Galaris D, Brunk UT (2007) Does the calcein-AM method assay the total cellular 'labile iron pool' or only a fraction of it? *Biochemical Journal* **403,** 261-266.

Tergaonkar V (2006) NF kappa B pathway: A good signaling paradigm and therapeutic target. *International Journal of Biochemistry & Cell Biology* **38,** 1647-1653.

Terman A, Kurz T, Gustafsson B, Brunk UT (2006) Lysosomal labilization. *Iubmb Life* **58,** 531-539.

Thanos D, Maniatis T (1995) Nf-Kappa-B - A Lesson in Family Values. *Cell* **80,** 529-532.

Theil EC (1987) Ferritin - Structure, Gene-Regulation, and Cellular Function in Animals, Plants, and Microorganisms. *Annual Review of Biochemistry* **56,** 289-315.

Theil EC (1990) Regulation of Ferritin and Transferrin Receptor Messenger-Rnas. *Journal of Biological Chemistry* **265,** 4771-4774.

Theil EC (2003) Ferritin: At the crossroads of iron and oxygen metabolism. *Journal of Nutrition* **133,** 1549S-1553S.

Tietze F (1969) Enzymic method for quantitative determination of nanogram amounts of total and oxidized glutathione: applications to mammalian blood and other tissues. *Anal.Biochem.* **27,** 502-522.

Toh ML, Miossec P (2007) The role of T cells in rheumatoid arthritis: new subsets and new targets. *Current Opinion in Rheumatology* **19,** 284-288.

Torti FM, Torti SV (2002) Regulation of ferritin genes and protein. *Blood* **99,** 3505-3516.

Tran C, Lundy S, Fox D (2005) Synovial biology and T cells in rheumatoid arthritis. *Pathophysiology* **12,** 183-189.

Tranter M, Jones WK (2008) Anti-inflammatory effects of HO-1 activity in vascular endothelial cells, commentary on "Carbon monoxide donors or heme oxygenase (HO-1) overexpression blocks interleukin-18-mediated NF-kappa B-PTEN-dependent human cardiac endothelial cell death". *Free Radical Biology and Medicine* **44,** 261-263.

Truty J, Malpe R, Linder MC (2001) Iron prevents ferritin turnover in hepatic cells. *J.Biol.Chem.* **276,** 48775-48780.

Tyrrell RM, Pidoux M (1988) Correlation Between Endogenous Glutathione Content and Sensitivity of Cultured Human-Skin Cells to Radiation at Defined Wavelengths in the Solar Ultraviolet Range. *Photochemistry and Photobiology* **47,** 405-412.

Underwood JCE (1996) 'General and Systematic Pathology.' (Churchill Livingstone: Edinburgh, UK)

Valko M, Leibfritz D, Moncol J, Cronin M, Mazur M, Telser J (2007) Free radicals and antioxidants in normal physiological functions and human disease. *The international journal of biochemistry & cell biology* **39,** 44-84.

Vendemiale G, Grattagliano I, Altomare E (1999) An update on the role of free radicals and antioxidant defense in human disease. *International Journal of Clinical & Laboratory Research* **29,** 49-55.

Vile GF, Tyrrell RM (1993) Oxidative Stress Resulting from Ultraviolet-A Irradiation of Human Skin Fibroblasts Leads to A Heme Oxygenase-Dependent Increase in Ferritin. *Journal of Biological Chemistry* **268,** 14678-14681.

Vile GF, Basumodak S, Waltner C, Tyrrell RM (1994) Heme Oxygenase-1 Mediates An Adaptive Response to Oxidative Stress in Human Skin Fibroblasts. *Proceedings of the National Academy of Sciences of the United States of America* **91,** 2607-2610.

Vile GF, Tanewiliitschew A, Tyrrell RM (1995) Activation of Nf-Kappa-B in Human Skin Fibroblasts by the Oxidative Stress Generated by Uva Radiation. *Photochemistry and Photobiology* **62,** 463-468.

Voulgari PV, Kolios G, Papadopoulos GK, Katsaraki A, Seferiadis K, Drosos AA (1999) Role of cytokines in the pathogenesis of anemia of chronic disease in rheumatoid arthritis. *Clinical Immunology* **92,** 153-160.

Wang ZP, Cai SX, Liu DB, Xu X, Liang HP (2006) Anti-inflammatory effects of a novel peptide designed to bind with NF-kappa B p50 subunit. *Acta Pharmacologica Sinica* **27,** 1474-1478.

Weiss G, Goossen B, Doppler W, Fuchs D, Pantopoulos K, Wernerfelmayer G, Wachter H, Hentze MW (1993) Translational Regulation Via Iron-Responsive Elements by the Nitric-Oxide No-Synthase Pathway. *Embo Journal* **12,** 3651-3657.

Weiss G, Wernerfelmayer G, Werner ER, Grunewald K, Wachter H, Hentze MW (1994) Iron Regulates Nitric-Oxide Synthase Activity by Controlling Nuclear Transcription. *Journal of Experimental Medicine* **180,** 969-976.

Weiss G (2002) Iron and immunity: a double-edged sword. *European Journal of Clinical Investigation* **32,** 70-78.

Weiss G (2005) Modification of iron regulation by the inflammatory response. *Best Practice & Research Clinical Haematology* **18,** 183-201.

Weissman G (1972) Lysosomal Mechanisms of Tissue Injury in Arthritis. *New England Journal of Medicine* **286,** 141-147.

Weng YH, Yang G, Weiss S, Dennery PA (2003) Interaction between heme oxygenase-1 and-2 proteins. *Journal of Biological Chemistry* **278,** 50999-51005.

Wieland HA, Michaelis M, Kirschbaum BJ, Rudolphi KA (2005) Osteoarthritis. An untreatable disease. *Nature Reviews Drug Discovery* **4,** 331-344.

Winrow VR, Winyard PG, Morris CJ, Blake DR (1993) Free-Radicals in Inflammation – 2nd Messengers and Mediators of Tissue Destruction. *British Medical Bulletin* **49,** 506-522.

Winrow VR, Winyard PG, Morris CJ, Blake DR (1993) Free-Radicals in Inflammation - 2Nd Messengers and Mediators of Tissue Destruction. *British Medical Bulletin* **49,** 506-522.

Wong SF, Halliwell B, Richmond R, Skowroneck WR (1981) The Role of Superoxide and Hydroxyl Radicals in the Degradation of Hyaluronic-Acid Induced by Metal-Ions and by Ascorbic-Acid. *Journal of Inorganic Biochemistry* **14,** 127-134.

Worwood M (2005) Inherited iron loading: genetic testing in diagnosis and management. *Blood Reviews* **19,** 69-88.

Xiong SG, She HY, Takeuchi H, Han B, Engelhardt JF, Barton CH, Zandi E, Giulivi C, Tsukamoto H (2003) Signaling role of intracellular iron in NF-kappa B activation. *Journal of Biological Chemistry* **278,** 17646-17654.

Xiong S, She H, Tsukamoto H (2004) Signaling role of iron in NF-kappa B activation in hepatic macrophages. *Comparative Hepatology* **3,** S36.

Xu XY, Pin S, Gathinji M, Fuchs R, Harris ZL (2004) Aceruloplasminemia - An inherited neurodegenerative disease with impairment of iron homeostasis. *The American journal of clinical nutrition* **67**, 972S-977S.

Yamamoto Y, Gaynor RB (2004) I kappa B kinases: key regulators of the NF-kappa B pathway. *Trends in Biochemical Sciences* **29,** 72-79.

Yang X, Chen-Barrett Y, Arosio P, Chasteen N. D, (1998) Reaction Paths of Iron Oxidation and Hydrolysis in Horse Spleen and Recombinant Human Ferritins. *Biochemistry* **37**, 9743-9750.

Yazar M, Sarban S, Kocyigit A, Isikan UE (2005) Synovial fluid and plasma selenium, copper, zinc, and iron concentrations in patients with rheumatoid arthritis and osteoarthritis. *Biological Trace Element Research* **106,** 123-132.

Yiakouvaki A (2003) The link between multidrug resistance and oxidative stress. Doctor of Philosophy,' University of Bath - Department of Pharmacy and Pharmacology.

Yiakouvaki A, Savovic J, Al-Qenaei A, Dowden J, Pourzand (2006) Caged-iron chelators a novel approach towards protecting skin cells against UVA-induced necrotic cell death. *Journal of Investigative Dermatology*. **126**, 2287-95.

Youdim MBH, Grunblatt E, Mandel S (1999) The pivotal role of iron in NF-kappa B activation and nigrostriatal dopaminergic neurodegeneration - Prospects for neuroprotection in Parkinson's disease with iron chelators. *Annals of the New York Academy of Sciences* **890**,7-25.

Yu ZQ, Persson HL, Eaton JW, Brunk UT (2003) Intralysosomal iron: A major determinant of oxidant-induced cell death. *Free Radical Biology and Medicine* **34,** 1243-1252.

Zabel U, Schreck R, Baeuerle PA (1991) DNA-Binding of Purified Transcription Factor Nf-Kappa - Affinity, Specificity, Zn2+ Dependence, and Differential Half-Site Recognition. *Journal of Biological Chemistry* **266,** 252-260.

Zdolsek JM, Svensson I (1993) Effect of Reactive Oxygen Species on Lysosomal Membrane Integrity - A Study on A Lysosomal Fraction. *Virchows Archiv B-Cell Pathology Including Molecular Pathology* **64,** 401-406.

Zhao GH, Arosio P, Chasteen ND (2006) Iron(II) and hydrogen peroxide detoxification by human H-chain ferritin. An EPR spin-trapping study. *Biochemistry* **45,** 3429-3436.

Zhong JL, Yiakouvaki A, Holley P, Tyrrell RM, Pourzand C (2004) Susceptibility of skin cells to UVA-induced necrotic cell death reflects the intracellular level of labile iron. *Journal of Investigative Dermatology* **123,** 771-780.

Zhou YM, Zhong CY, Kennedy IM, Leppert VJ, Pinkerton KE (2003) Oxidative stress and NF kappa B activation in the lungs of rats: a synergistic interaction between soot and iron particles. *Toxicology and Applied Pharmacology* **190,** 157-169.